POLSKIE TOWARZYSTWO MIKROBIOLOGÓW
POLISH SOCIETY OF MICROBIOLOGISTS

Polish Journal of Microbiology

2020

Polish Journal of Microbiology
formerly Acta Microbiologica Polonica
2020, Vol. 69, No 2

CONTENTS

ORIGINAL PAPERS

SHORT COMMUNICATIONS

INSTRUCTIONS FOR AUTHORS
Instructions for authors: https://www.exeley.com/journal/polish_journal_of_microbiology

Polish Journal of Microbiology
2020, Vol. 69, No 2, 133–137
https://doi.org/10.33073/pjm-2020-005

ORIGINAL PAPER

Prevalence of Multi-Drug Resistant Mycobacterium Tuberculosis in Khyber Pakhtunkhwa – A High Tuberculosis Endemic Area of Pakistan

SAJID ALI[1]*, MUHAMMAD TAHIR KHAN[2], ANWAR SHEED KHAN[3], NOOR MOHAMMAD[3], MUHAMMAD MUMTAZ KHAN[4], SAJJAD AHMAD[3], SADIQ NOOR[4], ABDUL JABBAR[4], CANTILLON DAIRE[5] and FARIHA HASSAN[1]

[1] Quaid-i-Azam University, Islamabad, Pakistan
[2] Capital University of Science and Technology, Islamabad, Pakistan
[3] Provincial TB Control Program, Khyber Pakhtunkhwa, Pakistan
[4] University of Haripur, Khyber Pakhtunkhwa, Pakistan
[5] Brighton and Sussex Medical School, University of Sussex, Brighton, United Kingdom

Submitted 24 October 2019, revised 20 December 2019, accepted 8 January 2020

Abstract

Anti-tuberculosis therapy involves the combination of drugs to hamper the growth of *Mycobacterium tuberculosis* (MTB). The emergence of multidrug-resistant tuberculosis (MDR-TB) is a global concern. Pakistan has been ranked 5th position in terms of a high burden of MDR-TB in the world. The aim of the current study was to investigate the prevalence of drug resistance in MTB in Khyber Pakhtunkhwa. Random samples were collected from 25 districts using the simple random sampling formula. All samples were processed in a biosafety level 3 laboratory for culture and drug susceptibility testing. Among 5759 presumptive tuberculosis (TB) cases, 1969 (34%) were positive. The proportion of TB was higher in females (39%) than males (29%), thus it represents a significant association between gender and tuberculosis ($p < 0.05$). People ages between 25 to 34 years were more likely to be infected with MTB (40%). Drug-resistant profile showed 97 (4.9%) patients were infected with MDR-TB. Streptomycin resistance was the highest and was observed in 173 (9%) isolates followed by isoniazid in 119 (6%) isolates. The lowest resistance was observed to pyrazinamide (3%). The prevalence of MDR-TB (10.4%) among patients that previously received anti-tuberculosis treatment is seemingly high. A large-scale drug resistance survey is required to evaluate the drug resistance for better management of tuberculosis.

Key words: tuberculosis, MDR MDR-TB, multi drug-resistant TB

Introduction

Tuberculosis (TB) is a pre-historic disease caused by *Mycobacterium tuberculosis* (MTB) (Daniel 2006). Although there are more than 150 species of *Mycobacterium* sp., MTB is still the most dominant and prevailing member of this genus all over the world, accounting for 10 million deaths in 2019 (WHO 2019).

The World Health Organization (WHO) declared TB as a global emergency in 1993 (Grange and Zumla 2002). Despite significant medical and social interventions, TB consistently affects vulnerable populations across the world and remains a leading global public health problem. Treatment of drug-susceptible TB takes six months while treatment of rifampicin-resistant TB (RR-TB) and multidrug-resistant TB (MDR-TB) requires a long therapy for up to two years (WHO 2019).

Globally, an 85% successful treatment rate has been reported for drug-susceptible MTB. The emergence of drug resistance, however, still poses a threat to global efforts. The WHO estimated 10.4 million new TB cases consist of 490 000 multidrug-resistant TB and 110 000 rifampicin-resistant TB. Five countries such as India, China, Indonesia, Philippines, and Pakistan are accounting for 56% of TB burden. Despite the development of rapid molecular tools, only 37% of MDR-TB were reported globally which shows laboratory gaps. China, India, and Russia reported 47% of the total global MDR/RR-TB cases. Pakistan is a high TB endemic country, standing at 5th position in the list

* Corresponding author: S. Ali, Quaid-i-Azam University, Islamabad, Pakistan; **e-mail: sajidjan@live.com**

of 30 high burden countries (HBC) with an estimated 518 000 TB cases including 15 000 MDR-TB. The estimated proportion of MDR-TB is 4.2% in new patients and 16% in the previously treated patients (WHO 2019). According to the drug resistance survey conducted in 2012, the prevalence of MDR-TB was 3.7% in newly diagnosed TB cases and 18.1% among previously treated TB cases (Tahseen et al. 2016). KPK is one of the four provinces of Pakistan that contributes a proportion of 11.9% in the total national population with an estimated 270 TB cases per 100 000 population (NTP 2014). Patients with drug-susceptible TB receive anti-TB treatment for at least six months while patients with MDR-TB and RR-TB receive longer treatments comprising of second-line drug regimens (NTP 2015). The sputum smear microscopy is used as an initial screening test for TB diagnosis, while GeneXpert assays are employed for the rapid detection of RR-TB at the district level (NTP 2015). In the current study, we analyzed the prevalence of MDR-TB among different lineages prevalent in the Khyber Pakhtunkhwa (KPK) province of Pakistan. MDR-TB is notified after a confirmatory DST test performed at the central BSL-III laboratory.

Experimental

Material and Methods

Study site. Random samples were collected from 25 districts of KPK using a simple random sampling (SRS) formula, which was previously used in a national TB survey of Pakistan:

$$n\,(SRS) = \frac{N \times z^2 \times p \times (1-p)}{d^2 \times (N-1) + z^2 \times p \times (1-p)}$$

where

- SRS – Sample Random Sampling
- N – total number of new smear positive cases registered in the lab
- z – z-value (from the standard normal distribution) that corresponds to the desired confidence level
- d – absolute precision
- p – expected proportion of MDR patient in the target population

Study participants and sample collection. A total of 1969 positive *M. tuberculosis* cases were calculated using this SRS formula. To achieve the target samples a total of 5759 clinical samples were collected from 25 districts and were diagnosed for TB. The patients' data were collected from their parents or the next caretakers.

Sputum processing. All received samples were digested and decontaminated using standard N-acetyl-L-cysteine sodium hydroxide (NALC-NaOH) method (GLI 2014) in a biosafety level 3 laboratory (BSLIII) at the Provincial TB Reference Laboratory, Peshawar. Briefly, one aliquot was inoculated on the Lowenstein Jensen medium (LJ) and in a Mycobacterium growth indicator tube (MGIT). Positive growth in the tubes was confirmed by Tbc ID device (Ref: 245159, Becton, Dickinson).

Drug susceptibility testing (DST). All confirmed mycobacterial isolates were processed for both phenotypic DST and molecular resistance assay. DST was performed using a BD BACTEC MGIT 960 SIRE kit (Ref: 245123, Becton, Dickinson), in which the final drug concentration was 1 μg/ml for RIF, and 0.1 μg/ml for INH. One sample aliquot was processed for acid-fast bacilli (AFB) microscopy using Primostar-LED fluorescent microscopy.

Data analysis. Results were recorded in the local laboratory management information software and analyzed using SPSS V.15 (IBM, USA). Sensitivity and specificity were calculated using Medcalc software (https://www.medcalc.org).

Results

Among 5759 TB suspects, 1969 (34%) were culture-positive, 3121 (54%) were culture-negative, and 344 (6%) were contaminated. The proportion of TB was higher in females (39%) than males (29%), thus, a strong association was observed between the gender and tuberculosis disease (χ (3) = 68.2, p = 0.001). It was observed that the age group of 25–34 years was more likely infected with TB (40%) when compared to other groups (Table I). The susceptibility testing towards the first-line drugs as rifampicin, isoniazid, ethambutol, streptomycin, and pyrazinamide was performed on 1969 culture-positive isolates.

DST results of 1969 isolates showed that 238 (12%) isolates were resistant to at least one drug, while 97 (4.9%) were confirmed to be MDR-TB. The remaining 1731 (88%) isolates were sensitive to all drugs. The drug resistance was the highest to streptomycin in 173 (9%) isolates, followed by isoniazid in 119 (6%), ethambutol in 101 (5%), rifampicin in 99 (5%), and pyrazinamide in 65 (3%) isolates.

The drug resistance found was correlated with different factors from the patient history including age, gender, and treatment history. MDR was observed in 61 (5.2%) males and 36 (4.5%) in female patients. No significant association of MDR with gender (χ (1) = 1, p-value = 0.26) or age group (χ (5.8) = 6, p-value = 0.44) was observed. The prevalence of MDR was higher in the age group of 55–64 years (6.4%), followed by a group of 15–24 years (6%) (Table II). MDR correlation with pulmonary and extra-pulmonary TB was also analyzed and it was found that the prevalence of MDR in pulmonary

Table I
Association of TB with gender, different age groups and treatment history, p-value of < 0.05 shows a statistical significance.

Character	TB Suspects	Positive cases	p-value
Gender			
Male	3189	947 (29%)	$\chi(3) = 68.2$, $p = 0.005$
Female	2570	1022 (39%)	
Age group			
01–14	437	96 (22%)	
15–24	1137	396 (34%)	
25–34	1180	473 (40%)	
35–44	827	298 (26%)	
45–54	732	227 (31%)	
55–64	819	282 (34.4%)	
65–100	627	197 (31.4%)	
Treatment history			
Previously Treated	1024	461 (45%)	$\chi(3) = 68$, p-value = 0.05
Never Treated	3922	1508 (38%)	
Disease type			
Pulmonary	5290	1864 (35%)	$\chi(3) = 68$, p-value < 0.05
Extra Pulmonary	469	105 (22%)	
Sample type			
Ascetic Fluid	91	10 (11%)	$\chi(36) = 259.6$, p-value ≤ 0.05
BAL*	172	45 (26%)	
Bone	20	2 (10%)	
CSF**	44	2 (5%)	
Gastric Lavage	68	5 (7%)	
Lymph Node	10	3 (30%)	
Pericardial fluid	26	3 (12%)	
Pleural Fluid	172	26 (15%)	
Pus	54	9 (17%)	
Sputum	5033	1858 (37%)	
Synovial Fluid	3	0 (0%)	
Tissue	20	5 (25%)	
Urine	46	1 (2%)	

* Bronchoscopy alveolar lavages, ** Cerebrospinal fluid

TB was significantly higher 94 (5.3%) when compared to extra-pulmonary TB (1.5%), $\chi(5.3) = 1$, p-value = 0.009. The resistance of the MTB isolates from the previously treated patients was significantly higher in 48 (10.4%) cases when compared to 49 (3.2%) untreated patients. It can indicate an association of drug resistance with the patient treatment history ($\chi(16) = 2$, p-value = 0.001).

Discussion

MDR-TB is a major threat to public health. Monitoring its trends over time is crucial to prevent further emergence of drug resistance. Surveillance of drug resistance is, therefore, a critical component of any TB control Programme (Zignol et al. 2016). A decade back, only 18 422 laboratory-confirmed MDR-TB cases were reported from 104 countries. It escalated to an estimated 490 000 cases in 2016 (WHO 2019). Even today MDR-TB is a persistent threat to the global community but unfortunately, only 47% of MDR cases could be diagnosed among the global estimates due to limited resources and laboratory gaps. Similarly, among all the registered MDR-TB cases, only 54% could be successfully treated. This study provides preliminary data of MDR-TB in KPK, which contributes to 13% of the national TB burden. In this first large-scale data, we found that MDR-TB was detected among 4.9% of

Table II
Correlation of the MDR-TB prevalence with patient's age, gender, and previous treatment history.

Character	Total DST	Diagnosed with DR-TB	*p*-value
Gender			
Male	1167	61 (5.2%)	$\chi(1)=1, p=0.26$
Female	800	36 (4.5%)	
Age group			
01–14	186	5 (2.6%)	$\chi(5.8)=6, p=0.445$
15–24	333	20 (6%)	
25–34	372	18 (4.8%)	
35–44	279	11 (4%)	
45–54	258	10 (3.8%)	
55–64	294	19 (6.4%)	
65–100	245	14 (5.7%)	
Treatment history			
NT*	1508	49 (3.2%)	$\chi(16)=2$, *p*-value = 0.001
PT**	461	48 (10.4%)	
Disease type			
Pulmonary	1771	94 (5.3%)	$\chi(5.3)=1$, *p*-value = 0.009
Extra Pulmonary	196	3 (1.5%)	

* NT = Never treated; ** PT = previously treated; DST = drug susceptibility testing; DR-TB = drug resistant tuberculosis

newly diagnosed patients. This figure is consistent with the first national DRS of Pakistan where it has been reported 3.7% MDR-TB cases (Tahseen et al. 2016) and 3.6% the global estimates (WHO 2019). Similar findings from Pakistan reported a 2–5% MDR-TB ratio (Javaid et al. 2008; Ejaz et al. 2010). A comparative high ratio of 29% and 9% MDR-TB was reported in early literature from other areas of Pakistan (Javaid et al. 2016; Shah et al. 2016). However, Akhtar et al. demonstrated a much higher MDR ratio of 69% in a study performed in Punjab (Akhtar et al. 2016). Possible differences in these reports might be due to the variance in study design and sample inclusion criteria. People ages 15 to 34 years old were at high risk to develop MDR-TB (Hoa et al. 2015; Akhtar et al. 2016; Khan et al. 2018). The increased drug resistance in previously treated cases (10.4%) was high as compared to newly diagnosed patients. These findings are consistent with previously published data (Tahseen et al. 2016). TB has been found to be more prevalent in males (Neyrolles and Quintana-Murci 2009); however, we did not detect a significant correlation of MDR-TB with gender, extra-pulmonary TB or a sample type (Bhattacherjee and Datta 2014; Wattal et al. 2015). In contrast to this, data from Africa shows a relatively high prevalence of drug-resistant TB in women (O'Donnell et al. 2011).

In conclusion, MDR-TB is an emerging problem in Khyber Pakhtunkhwa, Pakistan. This study has highlighted the MDR surveillance among the population of a geographically distinct area of Pakistan. Knowing the approximate magnitude of MDR-TB, this study will help for better management of drug resistance towards global TB control 2030.

ORCID
Anwar Sheed Khan https://orcid.org/0000-0003-0339-2487

Acknowledgements
We are thankful for the technical support of the Project Director, Dr. Qasim Abbas for his technical support in this study.

Conflict of interest
The authors do not report any financial or personal connections with other persons or organizations, which might negatively affect the contents of this publication and/or claim authorship rights to this publication.

Literature

Akhtar AM, Arif MA, Kanwal S, Majeed S. Prevalence and drug resistance pattern of MDR TB in retreatment cases of Punjab, Pakistan. J Pak Med Assoc. 2016 Aug;66(8):989–993.

Bhattacherjee S, Datta S. Primary multi drug resistant extra-pulmonary tuberculosis presenting as cervical lymphadenitis. J Glob Infect Dis. 2014;6(2):91–92. https://doi.org/10.4103/0974-777X.132066

Ejaz M, Siddiqui AR, Rafiq Y, Malik F, Channa A, Mangi R, Habib F, Hasan R. Prevalence of multi-drug resistant tuberculosis in Karachi, Pakistan: identification of at risk groups. Trans R Soc Trop Med Hyg. 2010 Aug;104(8):511–517. https://doi.org/10.1016/j.trstmh.2010.03.005

GLI. Mycobacteriology Laboratory Manual [Internet]. Global Laboratory Initiative a Working Group of the Stop TB Partnership; 2014 [cited 2019 Oct 3]. Available from http://www.who.int/tb/laboratory/mycobacteriology-laboratory-manual.pdf

Grange JM, Zumla A. The global emergency of tuberculosis: what is the cause? J R Soc Promot Health. 2002 Jun;122(2):78–81. https://doi.org/10.1177/146642400212200206

Hoa NB, Nhung NV, Khanh PH, Hai NV, Quyen BTT. Adverse events in the treatment of MDR-TB patients within and outside the NTP in Pham Ngoc Thach hospital, Ho Chi Minh City, Vietnam. BMC Res Notes. 2015 Dec;8(1):809. https://doi.org/10.1186/s13104-015-1806-4

Javaid A, Hasan R, Zafar A, Ghafoor A, Pathan AJ, Rab A, Sadiq A, Akram CM, Burki I, Shah K, et al. Prevalence of primary multidrug resistance to anti-tuberculosis drugs in Pakistan. Int J Tuberc Lung Dis. 2008 Mar;12(3):326–331.

Khan MT, Malik SI, Ali S, Sheed Khan A, Nadeem T, Zeb MT, Masood N, Afzal MT. Prevalence of pyrazinamide resistance in Khyber Pakhtunkhwa, Pakistan. Microb Drug Resist. 2018 Nov; 24(9):1417–1421. https://doi.org/10.1089/mdr.2017.0234

Neyrolles O, Quintana-Murci L. Sexual inequality in tuberculosis. PLoS Med. 2009 Dec 22;6(12):e1000199. https://doi.org/10.1371/journal.pmed.1000199

NTP. Vision 2020 – National TB Control Strategic Plan [Internet]. Islamabad (Pakistan): National TB Control Program; 2014 [cited 2019 Oct 3]. Available from http://www.ntp.gov.pk/uploads/Vision_2020_National_Strategic_Plan.pdf

NTP. National Guidelines for Diagnosis and Management of Tuberculosis in Pakistan [Internet]. Islamabad (Pakistan): National TB Control Program; 2015 [cited 2019 Oct 3]. Available from http://ntp.gov.pk/uploads/national_guideline_on_tb_case_management_rev_jan_2015.pdf

O'Donnell MR, Zelnick J, Werner L, Master I, Loveday M, Horsburgh CR, Padayatchi N. Extensively drug-resistant tuberculosis in women, KwaZulu-Natal, South Africa. Emerg Infect Dis. 2011 Oct;17(10):1942–1945. https://doi.org/10.3201/eid1710.110105

Wattal C, Raveendran R, Oberoi JK. Multidrug-resistant pulmonary and extrapulmonary tuberculosis: A 13 years retrospective hospital-based analysis. Indian J Med Res. 2015;142(5):575–582. https://doi.org/10.4103/0971-5916.171285

Tahseen S, Qadeer E, Khanzada FM, Rizvi AH, Dean A, Van Deun A, Zignol M. Use of Xpert® MTB/RIF assay in the first national anti-tuberculosis drug resistance survey in Pakistan. Int J Tuberc Lung Dis. 2016 Apr 01;20(4):448–455. https://doi.org/10.5588/ijtld.15.0645

Ullah I, Javaid A, Tahir Z, Ullah O, Shah AA, Hasan F, Ayub N. Pattern of drug resistance and risk factors associated with development of drug resistant *Mycobacterium tuberculosis* in Pakistan. PLoS One. 2016 Jan 25;11(1):e0147529. https://doi.org/10.1371/journal.pone.0147529

Ullah I, Shah AA, Basit A, Ali M, Khan A, Ullah U, Ihtesham M, Mehreen S, Mughal A, Javaid A. Rifampicin resistance mutations in the 81 bp RRDR of rpoB gene in *Mycobacterium tuberculosis* clinical isolates using Xpert® MTB/RIF in Khyber Pakhtunkhwa, Pakistan: a retrospective study. BMC Infect Dis. 2016 Dec;16(1):413. https://doi.org/10.1186/s12879-016-1745-2

WHO. WHO Global tuberculosis report 2019 [Internet]. Genewa (Switzerland): World Health Organization; 2019 [cited 2019 Dec 20]. Available from http://www.who.int/tb/publications/global_report/en/

Zignol M, Dean AS, Falzon D, van Gemert W, Wright A, van Deun A, Portaels F, Laszlo A, Espinal MA, Pablos-Méndez A, et al. Twenty years of global surveillance of antituberculosis-drug resistance. N Engl J Med. 2016 Sep 15;375(11):1081–1089. https://doi.org/10.1056/NEJMsr1512438

Daniel TM. The history of tuberculosis. Respir Med. 2006 Nov; 100(11):1862–1870. https://doi.org/10.1016/j.rmed.2006.08.006

Polish Journal of Microbiology
2020, Vol. 69, No 2, 139–149
https://doi.org/10.33073/pjm-2020-016

ORIGINAL PAPER

PCR-based Screening Approach: A Rapid Method to Detect the Biosynthetic Potential of Antimicrobials in Actinobacterial Strains

NAILA NOUREEN, MOHSIN TASSAWAR CHEEMA, SUMAIRA ANWAR, SHAHIDA HASNAIN and IMRAN SAJID*

Department of Microbiology and Molecular Genetics, University of the Punjab, Quid-i-Azam Campus, Lahore, Pakistan

Submitted 29 November 2019, revised 19 March 2020, accepted 29 March 2020

Abstract

This study aimed to investigate the PCR-based screening strategy for the prediction of the antimicrobial biosynthetic potential of the selected *Streptomyces* strains originated from an extreme environment (Cholistan Desert, Pakistan). The biosynthetic potential was determined by using both molecular and culture-dependent screening approaches. The four biosynthetic genes clusters, including the *pks-1*, *nrps*, cyp P450 hydroxylase (*cyps*), and glycopeptide *oxy b* genes, were investigated in the selected strains by PCR amplification, sequencing, and by subsequent bioinformatics approaches. Among the 40 selected *Streptomyces* strains, 33 strains possessed the *nrps* gene, 17 strains carried the *pks-1* gene, four strains were found to have the *cyps* gene, and none of the strain carried *oxy b* gene. The *Streptomyces* strains including NR-1, NR-10, NR-14, and NR-15 were investigated for *in vitro* antifungal activity against *Fusarium oxysporum*, *Rhizoctonia solani*, and *Aspergillus* sp. The extracts were analyzed for chemical profiling (TLC and HPLC-UV), and a unique pattern of secondary metabolites was observed. The selected strains exhibited pronounced antifungal activity against the fungal test strains with the zone of inhibition up to 17, 18, and 19 mm, respectively. The study depicts that gene-based screening can be successfully applied to identify potentially bioactive strains by usin a single screening process. This PCR-based approach is rapid and can be used for sorting out and selecting the potential candidate among actinobacterial culture collections. Such a preselection or strain prioritization consequently decreases the time and efforts required for selecting the potential bioactive strain, which then can be subjected to the detailed chemical analysis.

Key words: gene-based screening, polyene specific cytochrome P450 hydroxylase (CYP), *nrps*, *pks-1*, *Streptomyces*

Introduction

The gene-based screening allows the rapid detection of biosynthetic gene clusters in the isolated strains (Wood et al. 2007). In the latest years, genome mining has been focused on *Streptomyces* and has become a novel and rapid method to identify the previously unidentified gene clusters (Xu et al. 2019). Genes that are involved in the biosynthesis of secondary metabolites are mainly organized in the secondary metabolism biosynthetic gene clusters. With the progress of genomic sequencing technology, the mining of the organism's secondary metabolism biosynthetic gene clusters becomes possible (Bu et al. 2019; Xu et al. 2019). *Streptomyces* harbor over 20 secondary gene clusters encoding the biosynthesis of many cryptic metabolites that are not expressed under standard laboratory conditions. The genome of *Streptomyces* is genetically engineered to remove the non-essential genes and permit heterologous expression of genes encoding cryptic metabolites (Komatsu et al. 2010; Wu et al. 2017; Bu et al. 2019; Xu et al. 2019). In most of the cases, these gene clusters are silent or ordinarily expressed under the specified laboratory conditions (Ye et al. 2017). One of the essential features of the genome in the genus *Streptomyces* is the occurrence of biosynthetic gene cassettes (Hwang et al. 2014). The *Streptomyces coelicolor* and *Streptomyces avermitilis* contain more than 20 gene clusters for the production of secondary metabolites and innovative antibiotics (Busti et al. 2006). In the genome of

Abbreviations
CYP – cytochrome P450 hydroxylase
NRPS – non-ribosomal peptide synthase
PKS-1 – polyketide synthase

* Corresponding author: I. Sajid, Department of Microbiology and Molecular Genetics, University of the Punjab, Quid-i-Azam Campus, Lahore, Pakistan; **e-mail: imran.mmg@pu.edu.pk**

S. avermitilis there are 25 types of gene clusters for secondary metabolites. From the 25 genes clusters, eight are for type I polyketide, two for type II related polyketide, and eight gene clusters are involved in the biosynthesis of non-ribosomal peptide synthetases (NRPS) compounds (Omura et al. 2001).

The conventional method of natural drug discovery is based on the bioactivity-guided purification of compounds, which is laborious and led to re-discovery of compounds most often. However, most of the biosynthetic potential of microorganisms is not detected under laboratory conditions (Winter et al. 2011).

The biosynthetic gene clusters for polyenes showed the existence of cytochrome P450 hydroxylase. The cytochrome P450 hydroxylase (*cyps*) genes performed different types of oxidation processes in different organisms (Lamb et al. 2003). The polyene-specific cytochrome P450 hydroxylase (*cyps*) has been found in all the earlier categorized polyene gene clusters, such as for nystatin, amphotericin, pimaricin, and candicidin antibiotics (Lee et al. 2006). Glycopeptides are a significant class of antibiotics that inhibit bacterial cell wall synthesis (Sosio et al. 2003). Glycopeptide antibiotics biosynthesis gene cluster of balhimycin encodes the cytochrome P450 monooxygenases such as Oxya, Oxyb, and Oxyc that are responsible for three oxidation steps and convert the linear peptide into cyclized form to make them chemically active. Thus, these three oxygenases act in a stepwise manner in the order Oxyb, then Oxya, and Oxyc for the formation of glycopeptide antibiotics (Bischoff et al. 2001).

The genomic studies of actinomycetes indicated that non-ribosomal peptide synthetases and type I polyketide synthases (PKS-1) contribute about half of the biosynthetic systems that encode the genes for the biosynthesis of the secondary metabolites (Komaki et al. 2016). The PKS type I catalyzes the synthesis of macrolide antibiotics including erythromycin and tylosin (Le et al. 2014). The *pks-1* gene codes for at least three domains equivalent to a ketosynthase (KS), acyltransferase (AT), and an acyl carrier protein (ACP) that enable the condensation of different subunits. All the PKS I domains collaborate to form a new polyketide chain (Ayuso-Sacido and Genilloud 2005). The non-ribosomal peptide includes clinically essential antibiotics, such as cyclosporins, bleomycin, vancomycin, and penicillins. A representative NRPS unit consists of three essential domains, such as an adenylation (A) domain, a peptidyl carrier protein (PCP), and a condensation (C) domain. New domains are continually evolving, as novel gene clusters for peptide biosynthesis are being categorized (Du et al. 2000).

The PCR-based screening approach sets the stage for the discovery of novel metabolites. This method helped to meet the medical severe demand for new drug candidates and enhance the acceptance of natural metabolic products as suitable drug candidates.

In this study, a PCR-based genome screening method was used for 40 independently isolated *Streptomyces* strains, and the detection of CYP specific polyene (cytochrome P450 hydroxylase), the glycopeptide *oxy b* gene (cytochrome P450 monooxygenase), type I polyketide synthase (PKS-1), and the non-ribosomal peptide synthase (NRPS) gene, based on the presence of the expected size of the PCR amplified DNA fragments, was performed. These results suggest that the PCR-based genome screening method is an efficient method for the detection of potentially valuable *Streptomyces*. The bioinformatics studies were also applied to confirm the presence of glycopeptide Oxyb, NRPS, and PKS-1 proteins, which play an important role in the antibiotics biosynthesis pathways. The functional analysis of the sequenced strains was performed by using different bioinformatics tools including BLASTn, BLASTp, EMBOSS TRANSq, and MEGA 6.0. The biological and chemical analyses were performed to confirm that the selected *Streptomyces* strains can produce the antifungal compounds (*cyps* genes) under the culture condition.

Experimental

Materials and Methods

***Streptomyces* strains and genomic DNA extraction.** A total of 40 *Streptomyces* strains were obtained from the collection of the Department of Microbiology and Molecular Genetics, University of the Punjab, Lahore, Pakistan. The selected strains were previously isolated from Cholistan desert of Pakistan. The GYM-broth (glucose 10 g, yeast extract 5 g, malt extract 5 g, distilled water 1,000 ml) was prepared, and 40 ml broth was taken in a 100 ml flask and was inoculated with the fresh culture of *Streptomyces* strains in each case. The flasks were incubated at 28°C on a rotatory shaker for about 7 days. The culture broth was taken in the Eppendorf tube and centrifuged at 10,000 rpm for 2 minutes to get the cell pellet or mycelial mass. The cell pellet was further utilized for DNA extraction by using the tissue Genomic DNA Extraction Mini Kit (FavorPrep™).

PCR amplification of antibiotics biosynthesis genes. The PCR was performed (Primus 96 (PeqLab) thermal cycler). All amplifications contained a total volume of 50 µl with 0.5 × Master Mix (25 µl) (Thermo Scientific), 10 pmol of each primer (3 µl) (1 st BASE laboratories), 100 ng of DNA template (3 µl) and 19 µl of deionized water. The gradient PCR was performed to identify the optimum annealing temperatures for each pair of primers. The PCR based screening of the non-ribosomal peptide synthase, polyketide synthase

Table I
PCR primers for the *nrps*, *pks-1, cyps*, and *oxy b* genes.

Genes	Primers	Sequence (5'-3')	Length	Tm	Product size	References
cyps	CYP-F	TGGATCGGCGACGACCGSVYCGT	23 bp	63.8	350 bp	Ayuso-Sacido and Genilloud 2005
	CYP-R	CCGWASAGSAYSCCGTCGTACTT	23 bp	56.6		
oxy b	GLY-F	CTGGTCGGCAACCTGATGGAC	21 bp	61.7	560 bp	Ayuso-Sacido and Genilloud 2005
	GLY-R	CAGGTACCGGATCAGCTCGTC	21 bp	61.7		
pks1	K1F	TSAAGTCSAACATCGGBCA	19 bp	48.4	1200–1500 bp	Ayuso-Sacido and Genilloud 2005
	M6R	CGCAGGTTSCSGTACCAGTA	20 bp	55.4		
nrps	A3F	GCSTACSYSATSTACACSTCSGG	23 bp	53.1	700 bp	Wood et al. 2007
	A7R	SASGTCVCCSGTSCGGTAS	19 bp	50.6		

1 (*pks-1*), polyene specific *cyp* P450 hydroxylase, and glycopeptide *oxy b* genes was accomplished using the primers given in Table I.

Sequencing of the amplified PCR product. The PCR products were purified by using MicroElute gel extraction kit (Favorgen) and sequenced by dye terminator chemistry using an automated sequencer, using the commercial facility of 1st BASE laboratories. The sequences were analyzed using the BLASTn search program at The National Center for Biotechnology Information (NCBI): http://www.ncbi.nlm.nih.gov/BLAST/. The BLASTn was performed to estimate the percentage homology with the reported gene clusters, and the sequences were submitted to NCBI, GenBank, to get the accession numbers.

Sequence analysis by bioinformatics tools. The sequences were analyzed by using various bioinformatics tools, such as the nucleotide sequence was translated by using EMBOSS transq (https://www.ebi.ac.uk/Tools/st/emboss_transeq/) into their resulted peptides sequence. The BLASTP (https://blast.ncbi.nlm.nih.gov/Blast.cgi?PAGE=Proteins) of all the resultant translated frames was performed, to find the similarity index of the peptides based on the percentage similarity, the functional protein with the highest similarity, was selected from all the 6 reading frame. The translated sequence of *Streptomyces* proteins were selected for multiple sequence alignment by using the Clustal_W alignment tool built-in MEGA 6 (https://www.megasoftware.net/). The partial 16S rRNA sequences of the selected actinobacterial strains were compared using the BLAST tool available on NCBI. The sequences of closely related species were obtained from NCBI and aligned using the CLUSTAL_W program. The neighbor-joining phylogenetic tree was inferred using a Kimura's 2-parameters in software MEGA 6.0. Tree topologies were evaluated for branch support using 1,000 replications Fig. 1.

Preparation of cell extracts for biological and chemical screening. The cell extracts of actinomycetes were prepared by inoculating the actinomycetes cultures, in the 200 ml GYM-broth, the inoculated flasks were incubated for 6–7 days at 28°C on the rotatory shaker. The cultures were sonicated in the sonicating

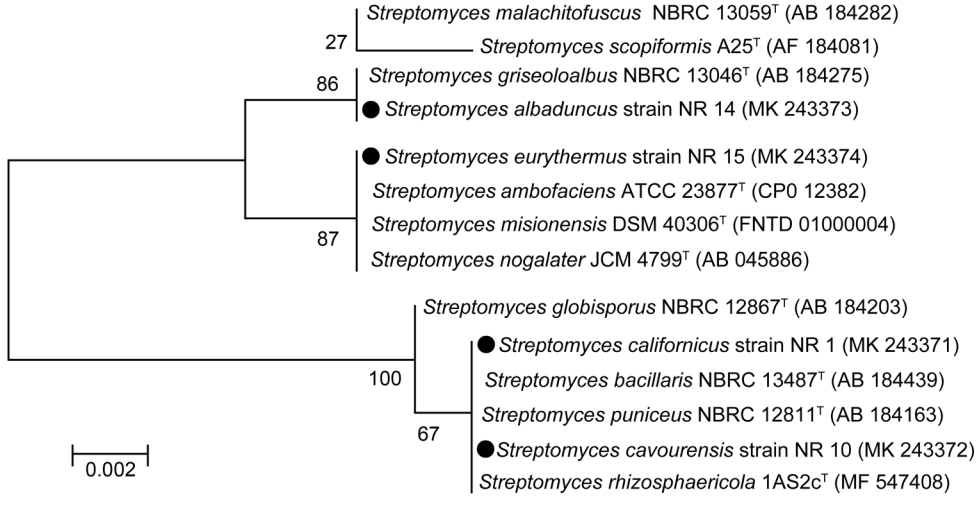

Fig. 1. Neighbor-joining tree based on 16S rRNA gene sequences of closely related type strains. Evolutionary distance was calculated using Kimura 2-parameters with 1000 bootstrap value.

bath to break the cells, an equal volume of ethyl acetate was added, and the mixture was taken in a separating funnel and was vigorously shaken for 5–10 minutes. The separating funnel was kept un-disturbed; after some time, two distinctive layers appeared. The aqueous layer was separated from the organic layer carefully. The ethyl acetate was recycled on a rotary evaporator, and the extracts were obtained in methanol, and stored in clean vials at 4°C. These methanolic extracts were further used for *in vitro* antifungal activity and for chemical profiling, using TLC and HPLC/UV (Fatima et al. 2019).

Determination of the antifungal activity. The PDA (potato dextrose agar) plates were prepared, and the inverted side of the plate was marked from edge to about 2 cm from both sides. After marking, agar plugs were cut from well-grown cultures of selected actinomycetes, and were placed on PDA plates about 2 cm from the edge, and the plates were incubated for about 2 days. After 2 days of incubation, similarly, agar plugs were cut from the fungal cultures, and were placed on the opposite side of the same plate that contained the actinomycetes agar plug. The plates were incubated for further 4 to 5 days at 27°C. After that the incubation zone of inhibition was measured.

In another method, the fungal test strains, including *F. oxysporum* (FO), *R. solani* (RS), and *Aspergillus* sp. (FN2) were streaked on SDA (Sabourad dextrose agar). The fresh cultures of fungal strains were swabbed with the help of a cotton swab on SDA plates, and the wells were made with the help of a sterile cork borer in the plates. Further, 60 µl of methanolic extracts were loaded on each well, and the plates were incubated at 28°C for 4–5 days. After incubation, the inhibition zones were measured in mm (Silambarasan et al. 2012).

Thin-layer chromatography (TLC). The methanolic extracts were spotted on the TLC plate with the help of a capillary tube. The spots were air-dried, before developing the plate with CH_2Cl_2/MeOH (10%) solvent system. The developed air-dried TLC plates were visualized under UV at 254 nm and 366 nm. The TLC plates were stained, by spraying with anisaldehyde/H_2SO_4, and Ehrlich's reagents, (Merck) individually.

High-performance liquid chromatography (HPLC-UV) analysis. The methanolic extracts of actinomycetes were analyzed, on the HPLC (Sykum HPLC system) by using the software clarity. The column used was Rp C18 with a 30 cm length. The Mobile phase was methanol and water (95:5), and the flow rate was adjusted to 1 ml/minute. The methanolic extracts were dissolved in HPLC grade methanol, and 20 µl of each extract were injected and were run for 20 minutes, the UV absorbance was measured at 254 nm. The peaks of each component were measured and were compared at different retention times (t_R) with standard UV absorption data of secondary metabolites.

Results

About 40 selected *Streptomyces* strains were screened for the presence of cytochrome P450 hydroxylase (*cyps*) gene. Out of 40 strains (Table II), only four showed the presence of the *cyp* P450 hydroxylase gene, with the

Table II
Streptomyces sp. GenBank accession numbers of 16S rRNA genes.

S. No. Given Code of Strain	GenBank Accession No.	Identified as
NR-1	MK243371	*Streptomyces* sp.
NR-10	MK243372	*Streptomyces* sp.
NR14	MK243373	*Streptomyces* sp.
NR15	MK243374	*Streptomyces* sp.
NR11	MN912434	*Streptomyces* sp.
C2	MN912435	*Streptomyces pseudovenezuelae*
D6-3	MN912436	*Streptomyces flavogriseus*
H34A	MN912437	*Streptomyces* sp.
H34B	MN912438	*Streptomyces* sp.
NR28	MN912439	*Streptomyces flavoviridis*
NR1	MN912440	*Streptomyces* sp.
NR5	MN912441	*Streptomyces werraensis*
10M	MN912442	*Streptomyces* sp.
C3	MN912443	*Streptomyces fenghuangensis*
H32B	MN912444	*Streptomyces* sp.
B5K	MN912445	*Streptomyces fimbriatus*
H31A	MN912446	*Nocardioides* sp.
M19	MN912447	*Streptomyces albogriseolus*
MM5	MN912448	*Streptomyces Streptomyces griseus*
NR3	MN912449	*Streptomyces* sp.
M63	MN912450	*Streptomyces misionensis*
M32	MN912451	*Streptomyces* sp.
M12	MN912452	*Streptomyces steffisburgensis.*
MM7	MN912453	*Streptomyces fimbriatus.*
M13	MN912454	*Streptomyces niveoruber*
D3-1	MN912455	*Streptomyces bambusae*
M29	MN912456	*Streptomyces* sp.
M28	MN912457	*Streptomyces coerulescens*
NR24	MN912458	*Streptomyces silaceus*
NR22	MN912459	*Streptomyces* sp.
H26	MN912460	*Streptomyces steffisburgensis*
M43	MN912461	*Streptomyces rubrolavendulae*
NR12	MN912462	*Streptomyces neopeptinius*
NR6	MN912463	*Streptomyces coeruleoprunus*
D3-3	MN912464	*Streptomyces* sp.
D3-2	MN912465	*Streptomyces* sp.
M93	KM062032	*Streptomyces laurentii*
M71	KM062033	*Streptomyces vitaminophilus*
M54	KM062034	*Streptomyces hypolithicus*
M51	KM062035	*Streptomyces chartreusis*

Table III
Streptomyces sp. GenBank accession numbers of the genes sequences.

S. No.	Isolates	Nucleotide length	GenBank Accession No.	% age homology	Genes encoding for
1.	NR-1	350 bp	98	CYP	MF279145
2.	NR-10	350 bp	100	CYP	MF279146
3.	NR14	350 bp	98	CYP	MK272790
4.	NR15	350 bp	98	CYP	MK272791
5.	NR-16	700 bp	100	NRPS	MF279147
6.	M13	700 bp	99	NRPS	MF279148
7.	NR-12	700 bp	98	NRPS	MF279150
8.	NR-6	1500 bp	98	PKS-1	MF279149

amplicon size of 350 bp. The strains NR10, NR15, NR14, and NR1 were detected for the presence of the *cyp* P450 hydroxylase gene. Out of 40 strains, about 33 strains showed the presence of the *nrps* gene. The *nrps* primer pair A3F/A7R amplified the band of approximately 700 bp. The strains including NR11, C2, D6-3, H34A, H34B, NR28, NR1, NR5, 10M, C3, H32B, B5K, H31A, M19, MM5, MM63, NR3, M12, MM7, M13, NR6, M29, M28, NR24, NR22, H26, M43, NR12, NR6, M29, M28, and NR24 were found to have the *nrps* gene. To determine the presence of the glycopeptide *oxy b* (P450 monooxygenase) gene in selected *Streptomyces* strains the PCR utilizing the primer pair Gly-F/Gly-R, which amplified the 560 bp fragment was carried out. Out of 40 strains, none of the strains exhibited the presence of the glycopeptide *oxy b* gene. The gene-specific PCR for *pks-1* utilized the KI-F/M6-R primer set; the amplified product of the primer was about 1200–1500 bp gene fragment. 40 strains were screened for the *pks-1* gene; among them 17 strains were found positive for the *pks-1* gene (Table III).

The PCR amplified gene fragments were sequenced, and sequence data was analyzed with the BLAST to check the percentage homology of the given genes such as the cytochrome P450 hydroxylase (*cyps*), glycopeptide *oxy b*, *pks-1*, and non-ribosomal peptide synthase (*nrps*) genes with the other genes that are present in NCBI GenBank. The percentage homology of the amplified gene fragments in different *Streptomyces* strains with the cytochrome P450 hydroxylase (*cyps*) gene was as follows: NR-1, NR-10, and NR14 (98%, 100%, and 100%). The percentage homology of the amplified genes in *Streptomyces* strains with non-ribosomal peptide synthase (*nrps*) gene are given as: NR-6, M13, M29, and NR-12 (100%, 99%, 100%, and 98%). The percentage homologies of *Streptomyces* strains with type 1 polyketide synthase (*pks-1*) were 98% for the strain NR-6 (Table III).

The sequences were submitted to NCBI GenBank (BANKit) as follows: strain NR-1 Accession No. MF279145, strain NR-10 Accession No. MF279146, strain NR-6 Accession No. MF279147, strain M13 Accession No. MF279148, strain NR-12 Accession No. MF279150, strain NR-6 Accession No. MF27914, strain NR-14 Accession No. MK272790, and strain NR-15 Accession No. MK272791 (Table II). The 16S rRNA gene accession numbers are given as follows: NR-1 Accession No. MK243371, NR-10 Accession No. MK243372, NR-14 Accession No. MK243373, and NR-15 Accession No. MK243374.

The nucleic acid sequence of strains NR-1, NR-10, NR-14, and NR-15 with the cytochrome P450 hydroxylase gene was translated using EMBOSS Transq. The similarity index of the translated nucleotide of strain NR-1, with cytochrome P450 hydroxylase protein from all six reading frames, were mentioned in Table IV. The EMBOSS_001_1 showed the highest percentage similarity of 98% with cytochrome P450 hydroxylase (CYP) protein, while the EMBOSS_001_4 indicated the lowest similarity with cytochrome P450 hydroxylase (CYP) protein. The EMBOSS_001_5 and EMBOSS_001_6 are non-functional proteins, and no significant similarity was found. The protein sequence that showed highest similarity index were further selected for alignment by using the MEGA 6.0. It might be possible the given antifungal activity of the *Streptomyces* strains, including NR-1, NR-10, NR14, and NR-15, was due to the different amino acid residues within the protein sequence. The bioinformatic studies confirmed the presence of cytochrome P450 hydroxylase), cytochrome P450 monooxygenase, non-ribosomal peptide synthase, and type I polyketide synthase proteins that plays a vital role in the antibiotics biosynthesis pathways. The biological and chemical screening results showed that the selected *Streptomyces* strains NR-1, NR-10, NR-14, and NR-15 can produce the polyene compounds under laboratory conditions.

The results of the agar plug method indicated that all the four strains carrying the *cyp* gene showed an

Table IV
The translated DNA sequence of NR-1 based on six reading frames and their percentage similarity with cytochrome P450 hydroxylase (CYP) protein.

Sequence translation (EMBOSS Transq)	% similarity with cytochrome P450 hydroxylase protein
EMBOSS_001_1	98
EMBOSS_001_2	50
EMBOSS_001_3	No significant similarity found
EMBOSS_001_4	45
EMBOSS_001_5	No significant similarity found
EMBOSS_001_6	No significant similarity found

Table V
Antifungal activity of the selected polyene producing *Streptomyces* sp. against different fungal strains (*Fusarium oxysporum*, *Rhizoctonia solani,* and *Aspergillus* sp.).

The fungus strain tested	Zone of inhibition in mm					
	NR-1	NR-10	NR-14	NR-15	MM7	CHX
Fusarium oxysporum	17.0 ± 0.11	17.8 ± 0.18	14.7 ± 0.22	16.0 ± 0.25	5.1 ± 0.121	9.9 ± 0.26
Rhizoctonia solani	18.0 ± 0.32	12.2 ± 0.41	13.8 ± 0.45	16.6 ± 0.45	0.2 ± 0.11	10.9 ± 0.53
Aspergillus sp.	22.1 ± 0.40	19.0 ± 0.12	18.8 ± 0.27	18.3 ± 0.38	1.7 ± 0.42	14.0 ± 0.18

inhibitory effect toward the tested fungal strains (Table V). The strain NR1 showed the most remarkable inhibitory effect on the tested fungal strains. The strains NR-1 and NR-14 have the most prominent inhibitory effect on the test strain FN2 (Fig. 2). While in the well-diffusion method cycloheximide (2 mg/ml) was used as standard, and the MM7 methanolic crude extract was used as the negative control. The crude extracts of strains NR-1, NR-10, NR-14, NR-15, and MM7 showed 17.0 ± 0.11 mm, 17.8 ± 0.18 mm, 14.7 ± 0.22 mm, 16.0 ± 0.25 mm, 5.1 ± 0.121 mm zone of inhibition, while CHX (cycloheximide) showed 9.9 ± 0.26 mm inhibitory zone against the *F. oxysporum* (FO). The selected crude extract showed the following zones of inhibition against the *R. solani* (RS): 18.0 ± 0.32 mm, 12.2 ± 0.41 mm, 13.8 ± 0.45 mm, and 16.6 ± 0.45 mm. The fungal strain *Aspergillus* (FN2) against which the antifungal activity was determined by

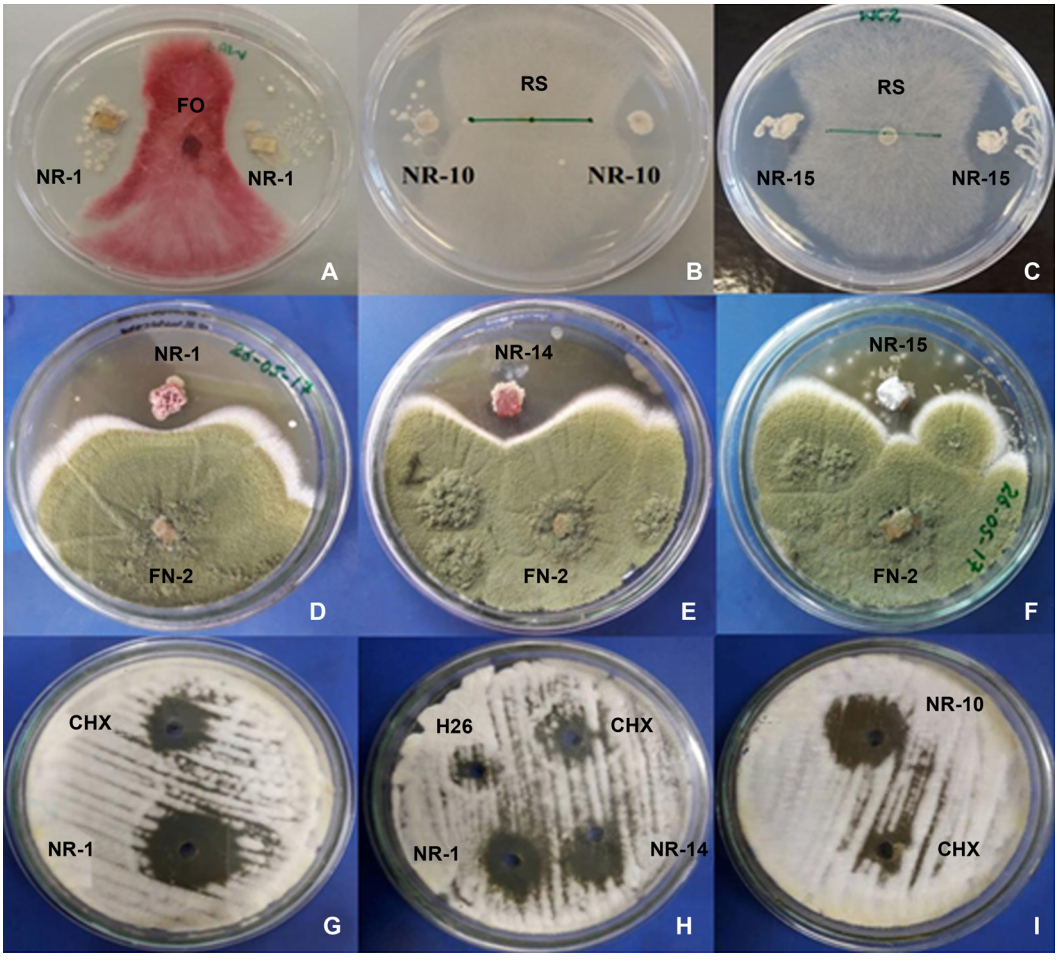

Fig. 2. Antifungal activity of the selected polyene producing *Streptomyces* sp. against different fungal strains tested (*Fusarium oxysporum* (FO), *Rhizoctonia solani* (RS), and *Aspergillus* sp. (FN2). (A), (B), (C) Anti fungal activity of NR-1, NR-10, and NR-15 by the agar plug method against *Fusarium oxysporum* (FO), *Rhizoctonia solani* (RS). (D), (E), (F) Activity of NR-1, NR-14, and NR-15 by the agar plug method against *Aspergillus* sp. (FN2). (G), (H), (I) Activity of NR-1, NR-14, NR-10, H26, and CHX (cycloheximide) by the well diffusion method against *Aspergillus* sp.

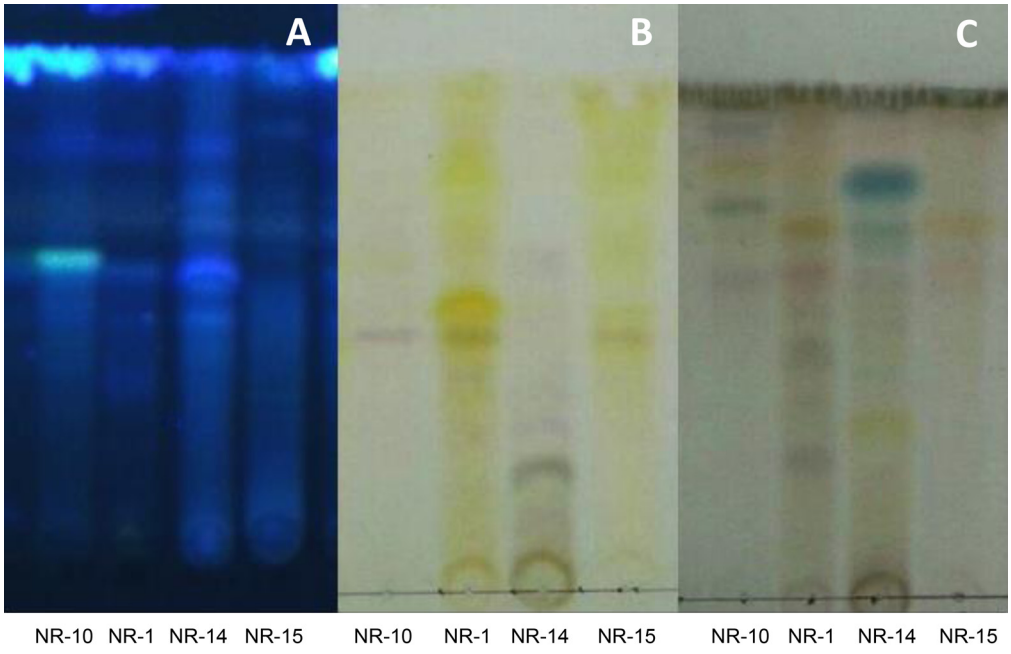

Fig. 3. Chemical profile of the selected Actinomycetes strains. (A) TLC plate at 366 nm. (B) TLC plate after spraying with Ehrlich's reagent. (C) TLC plate after spraying with anisaldehyde reagent.

utilizing the crude extracts of NR-1, NR-10, NR-14, and NR-15 strains. The strain NR-1 showed the most prominent zone of inhibition which was 22.1 ± 0.40 mm, while NR-10, NR14, and NR-15 indicated 19.0 ± 0.12 mm, 18.8 ± 0.27 mm, and 18.3 ± 0.38 mm zone of inhibition, respectively. The MM7 (control) did not show any significant zone of inhibition compared to the tested *Streptomyces* extracts (Table V).

In a thin-layer chromatography, different biologically active components were analyzed in the crude extracts. The *Streptomyces* strains indicated various bands, which were of unique color. Many components of the crude extract displayed UV absorbance: however, most noticeable bands were observed in crude extracts of strains NR-14 and NR-1 (Fig. 3). NR-14 and NR-1 showed red, pink, and the most important green color band after spraying with anisaldehyde/H_2SO_4. The NR-10, NR15, NR 14, and NR-1 exhibited bands of yellowish, pink, and purple after staining with Ehrlich's reagent.

The biologically active strains, including NR-1, NR10, NR14, and NR-15 that showed the presence of polyene specific the cytochrome P450 hydroxylase (*cyps*) gene, were further analyzed on HPLC to indicate either these strains had peaks related to any polyene compounds when grown in culture. The strain NR-1 showed three peaks at different retention times; the most prominent peak was observed at t_R 2.95 minutes. The strain NR-10 showed two peaks, but the most prominent peak was detected at t_R 3.22 minutes. The other strains, which were analyzed on the HPLC chromatogram, included NR-14, which displayed two prominent bands at 2.94 minutes and 3.20 minutes retention time (t_R). The strain NR-15 showed the most prominent peak at t_R 3.02 minutes (Fig. 4).

Each of the HPLC/UV chromatogram of methanolic extract of selected *Streptomyces* were compared with the standard nystatin HPLC/UV chromatogram (Hwang et al. 2007). The standard nystatin displayed the peak at a retention time of 3.03 minutes. After that comparison, it was confirmed that all the strains that showed the presence of polyene specific CYP P450, produced some polyene like antifungal metabolites.

Discussion

The current advances in the field of genomics, metagenomics, and high-throughput screening is beneficial for the natural product's detection (Genilloud et al. 2011). Due to the rediscovery of the already known metabolites, there is a strong need to explore the unique habitats and ecological niches, so that the probability of the discovery of novel metabolites with appropriate bioactivities could increase (Dhaneesha et al. 2017). The genome mining has thus delivered a comprehensive innovative tool, for the discovery of already identified, as well as previously unidentified natural metabolites, and the explanation of new biochemical revolutions and biosynthetic pathways (Chou et al. 2010).

Among the 40 tested *Streptomyces* strains only four strains indicated the presence of a predictable 350 bp PCR product for the polyene specific cytochrome P450 hydroxylase gene. The results indicated that polyene gene is a rare gene because only a low hit rate was found.

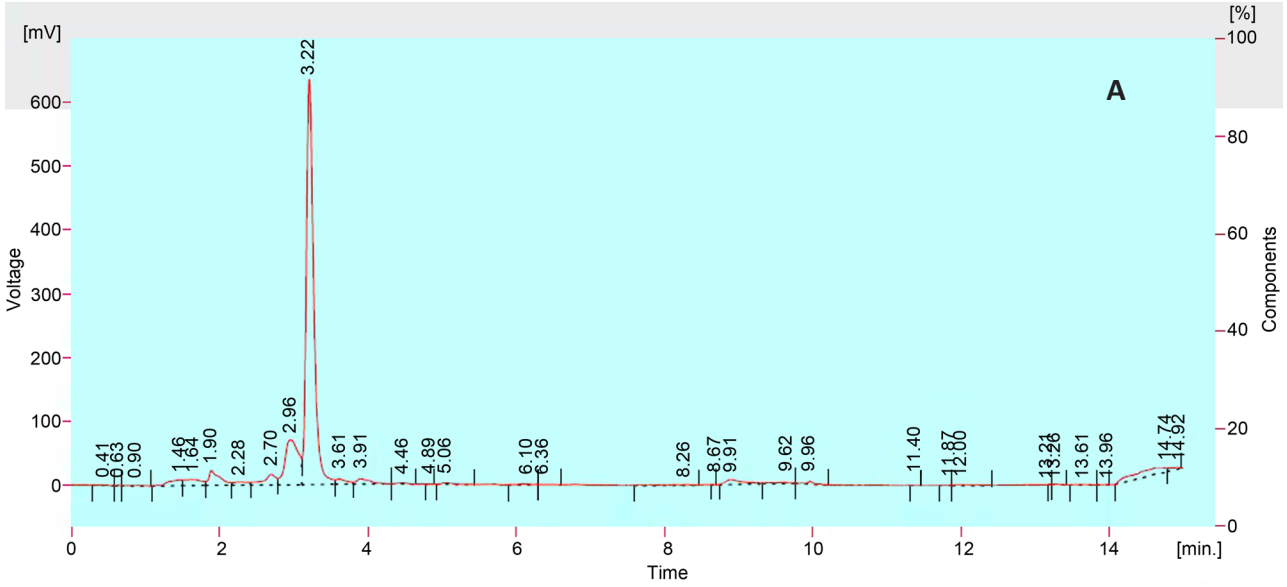
A
[mV]
[%]
Voltage
Components
Time
[min.]
3.22
2.96
2.70
2.28
1.90
1.64
1.46
0.90
0.63
0.41
3.61
3.91
4.46
4.89
5.06
6.10
6.36
8.26
8.67
9.91
9.62
9.96
11.40
11.87
12.00
13.21
13.28
13.61
13.96
14.74
14.92

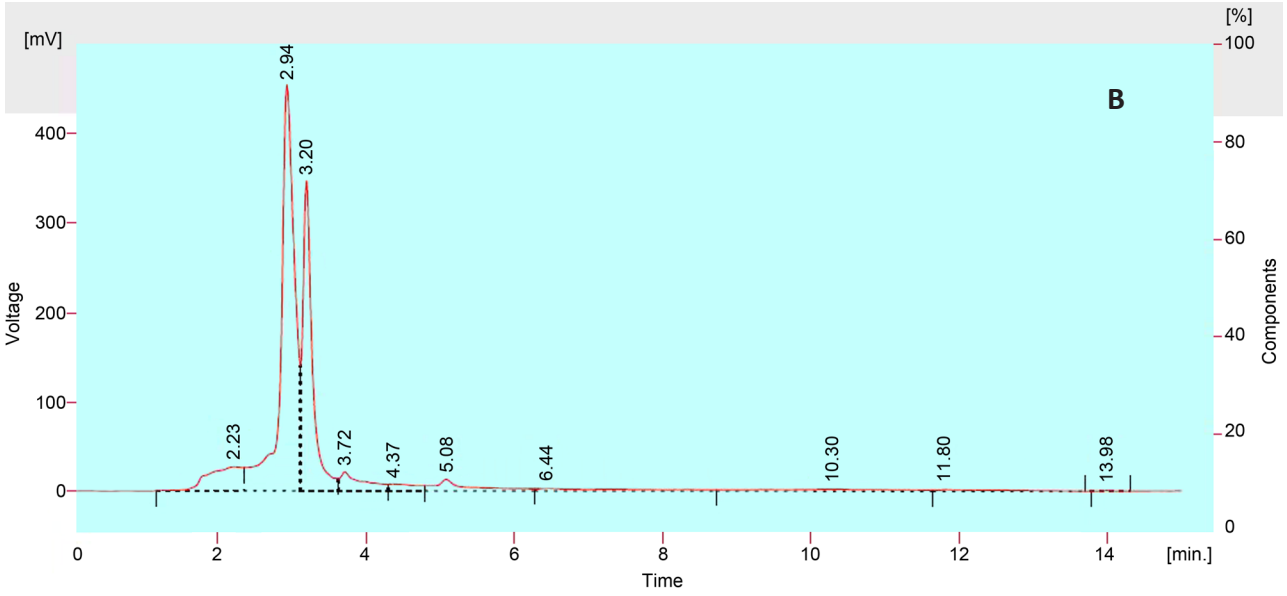
B
[mV]
[%]
Voltage
Components
Time
[min.]
2.94
3.20
2.23
3.72
4.37
5.08
6.44
10.30
11.80
13.98

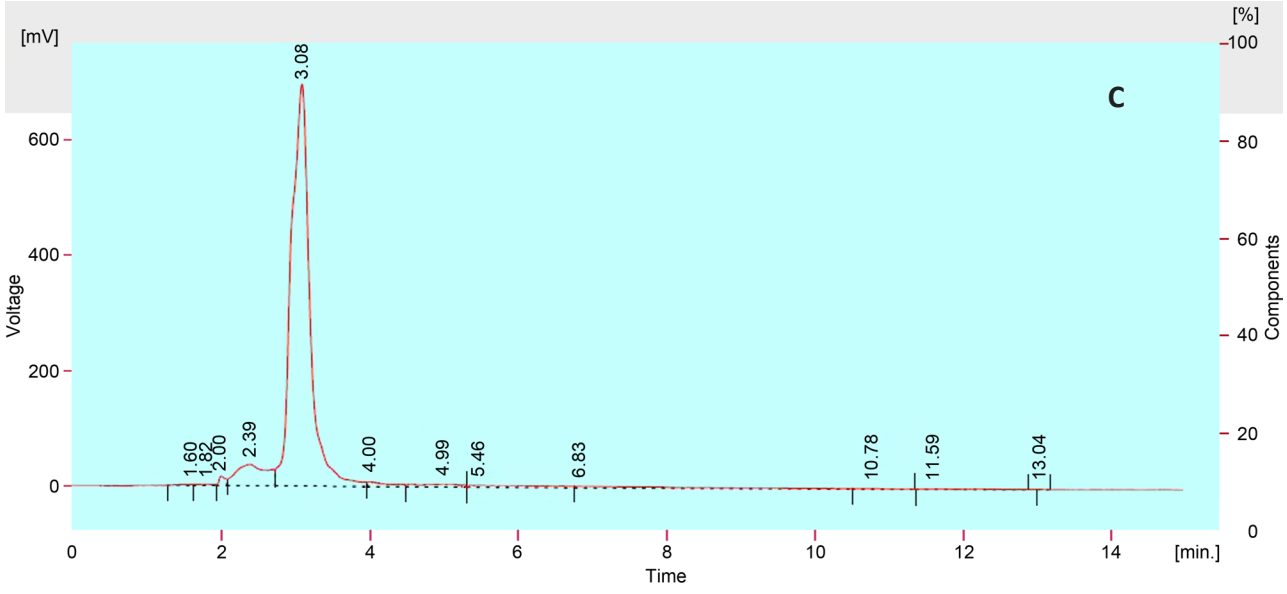
C
[mV]
[%]
Voltage
Components
Time
[min.]
3.08
2.39
1.80
2.00
1.60
4.00
4.99
5.46
6.83
10.78
11.59
13.04

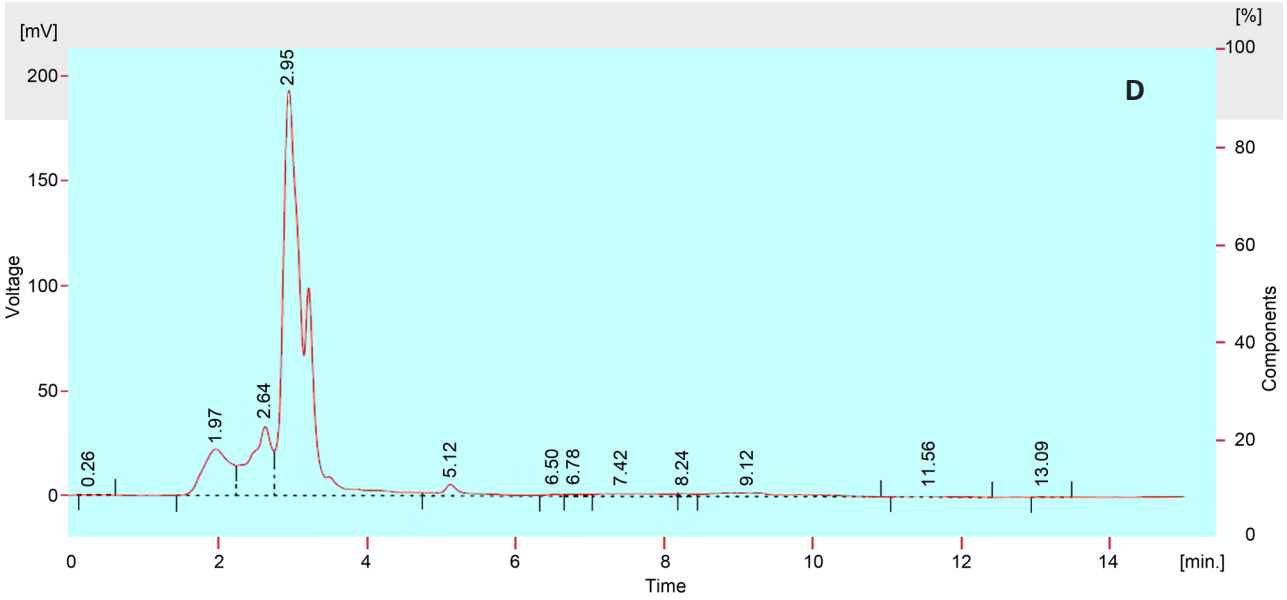

Fig 4. HPLC analysis of crude extracts of the polyene producing *Streptomyces* sp. (A) HPLC chromatogram of strain NR-1, (B) HPLC chromatogram of strain NR-10, (C) HPLC chromatogram of strain NR-14, (D) HPLC chromatogram of strain NR-15.

The use of fungal antibiotics is limited because of its high toxicity, so the genome-guided screening approach for the detection of new polyene antibiotics like compounds having improved pharmacological ability and less cytotoxicity is welcomed (Brautaset et al. 2002).

To screen the selected *Streptomyces* strains for the detection of the glycopeptide *oxy b* gene a PCR was performed. After optimization, not a single strain could be found positive for the desired gene; it might be because the glycopeptide gene cluster is rare. Encheva-Malinova et al. (2014) reported that almost all the strains possessed *pks-II* gene, and among the 11 strains screened for the *nrps* gene, six were positive for polyene, and four were positive for glycopeptide gene. The study confirmed that the glycopeptide antibiotics gene is rare among all four genes screened. In this study, for 33 strains amplification of the 700 bp fragment was successful that indicated the presence of the non-ribosomal peptide synthase gene. Gontang et al. (2010) reported that three primer sets for different domains of the *nrps* gene utilized for PCR based screening. The results of study showed that all domains were amplified in the isolated *Streptomyces*, and the biosynthetic domains were involved in the production of secondary metabolites. For the *pks-1* gene, the annealing temperature utilized in gradient PCR was 55 ± 0.5°C for 2 minutes. The most appropriate PCR product of 1200–1500 bp was visualized at temperature 53°C.

The *in vitro* antifungal assays indicated that the selected *Streptomyces* have the potential to synthesize the polyene specific CYPs proteins when grown in culture conditions. The published literature also indicated that most of the secondary metabolites from *Streptomyces* are extracellular when grown under certain cultural conditions (Arasu et al. 2013).

Overall, this study revealed that a PCR-based screening approach that targets novel genes from biosynthetic gene clusters is a powerful tool for the rapid detection and identification of bioactive strains within the large culture collections. Moreover, in the recent past, the screening of large culture collections has led to the rediscovery of already known compounds; this greatly increases the usefulness of the PCR-based screening approach. Furthermore, in this study, a phylogenetic analysis of the amplified PCR products showed the exact prediction of the structural class of secondary metabolites being synthesized by an individual strain. The gene-based screening approach is helpful and can act as an additional pre-screening strategy for the selection of promising *Streptomyces* strains in a collection before cultivating the strains on a large scale for the purification and identification of the compounds. The relative abundance of the selected genes is shown in Fig. 5.

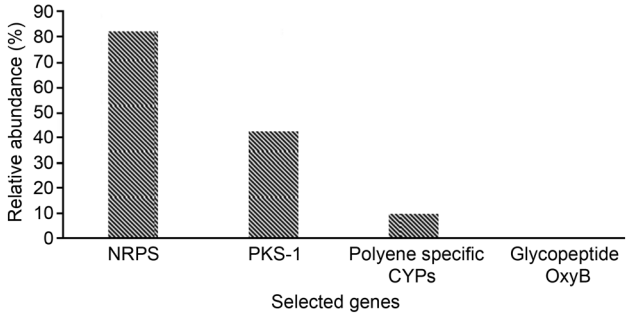

Fig. 5. The relative abundance of the *nrps*, *pks-1, cyps*, *oxy b* genes in the selected *Streptomyces* strains.

Acknowledgments

The financial support for this work by the Higher Education Commission of Pakistan (HEC) through the HEC-NRPU Project No. 2121 is gratefully acknowledged. The results reported in this manuscript belong to the Master's thesis of the author Naila Noureen.

Conflict of interest

The authors do not report any financial or personal connections with other persons or organizations, which might negatively affect the contents of this publication and/or claim authorship rights to this publication.

Literature

Arasu MV, Duraipandiyan V, Ignacimuthu S. Antibacterial and antifungal activities of polyketide metabolite from marine *Streptomyces* sp. AP-123 and its cytotoxic effect. Chemosphere. 2013 Jan; 90(2):479–487. https://doi.org/10.1016/j.chemosphere.2012.08.006

Ayuso-Sacido A, Genilloud O. New PCR primers for the screening of NRPS and PKS-I systems in actinomycetes: detection and distribution of these biosynthetic gene sequences in major taxonomic groups. Microb Ecol. 2005 Jan;49(1):10–24. https://doi.org/10.1007/s00248-004-0249-6

Bischoff D, Pelzer S, Bister B, Nicholson GJ, Stockert S, Schirle M, Wohlleben W, Jung G, Süssmuth RD. The biosynthesis of vancomycin-type glycopeptide antibiotics – the order of the cyclization steps. Angew Chem Int Ed. 2001 Dec 17; 40(24): 4688–4691. https://doi.org/10.1002/1521-3773(20011217)40:24<4688::AID-ANIE4688>3.0.CO;2-M

Brautaset T, Bruheim P, Sletta H, Hagen L, Ellingsen TE, Strøm AR, Valla S, Zotchev SB. Hexaene derivatives of nystatin produced as a result of an induced rearrangement within the nysC polyketide synthase gene in *S. noursei* ATCC 11455. Chem Biol. 2002 Mar;9(3):367–373. https://doi.org/10.1016/S1074-5521(02)00108-4

Bu QT, Yu P, Wang J, Li ZY, Chen XA, Mao XM, Li YQ. Rational construction of genome-reduced and high-efficient industrial Streptomyces chassis based on multiple comparative genomic approaches. Microb Cell Fact. 2019 Dec;18(1):16. https://doi.org/10.1186/s12934-019-1055-7

Busti E, Monciardini P, Cavaletti L, Bamonte R, Lazzarini A, Sosio M, Donadio S. Antibiotic-producing ability by representatives of a newly discovered lineage of actinomycetes. Microbiology. 2006 Mar 01;152(3):675–683. https://doi.org/10.1099/mic.0.28335-0

Chou WKW, Fanizza I, Uchiyama T, Komatsu M, Ikeda H, Cane DE. Genome mining in *Streptomyces avermitilis*: cloning and characterization of SAV_76, the synthase for a new sesquiterpene, avermitilol. J Am Chem Soc. 2010 Jul 07;132(26):8850–8851. https://doi.org/10.1021/ja103087w

Dhaneesha M, Benjamin Naman C, Krishnan KP, Sinha RK, Jayesh P, Joseph V, Bright Singh IS, Gerwick WH, Sajeevan TP. *Streptomyces artemisiae* MCCB 248 isolated from Arctic fjord sediments has unique PKS and NRPS biosynthetic genes and produces potential new anticancer natural products. 3 Biotech. 2017 May;7(1):32. https://doi.org/10.1007/s13205-017-0610-3

Du L, Chen M, Sánchez C, Shen B. An oxidation domain in the BlmIII non-ribosomal peptide synthetase probably catalyzing thiazole formation in the biosynthesis of the anti-tumor drug bleomycin in *Streptomyces verticillus* ATCC15003. FEMS Microbiol Lett. 2000;189(2):171–175. https://doi.org/10.1111/j.1574-6968.2000.tb09225.x

Encheva-Malinova M, Stoyanova M, Avramova H, Pavlova Y, Gocheva B, Ivanova I, Moncheva P. Antibacterial potential of streptomycete strains from Antarctic soils. Biotechnol Biotechnol Equip. 2014 Jul 04;28(4):721–727. https://doi.org/10.1080/13102818.2014.947066

Fatima A, Aftab U, Shaaban KA, Thorson JS, Sajid I. Spore forming Actinobacterial diversity of Cholistan Desert Pakistan: polyphasic taxonomy, antimicrobial potential and chemical profiling. BMC Microbiol. 2019 Dec;19(1):49. https://doi.org/10.1186/s12866-019-1414-x

Genilloud O, González I, Salazar O, Martín J, Tormo JR, Vicente F. Current approaches to exploit actinomycetes as a source of novel natural products. J Ind Microbiol Biotechnol. 2011 Mar; 38(3):375–389. https://doi.org/10.1007/s10295-010-0882-7

Gontang EA, Gaudêncio SP, Fenical W, Jensen PR. Sequence-based analysis of secondary-metabolite biosynthesis in marine actinobacteria. Appl Environ Microbiol. 2010;76(8):2487–2499. https://doi.org/10.1128/AEM.02852-09

Hwang KS, Kim HU, Charusanti P, Palsson BØ, Lee SY. Systems biology and biotechnology of *Streptomyces* species for the production of secondary metabolites. Biotechnol Adv. 2014 Mar;32(2):255–268. https://doi.org/10.1016/j.biotechadv.2013.10.008

Hwang YB, Lee MY, Park HJ, Han K, Kim ES. Isolation of putative polyene-producing actinomycetes strains via PCR-based genome screening for polyene-specific hydroxylase genes. Process Biochem. 2007 Jan;42(1):102–107. https://doi.org/10.1016/j.procbio.2006.06.031

Komaki H, Ichikawa N, Tamura T, Oguchi A, Hamada M, Fujita N. Genome-based survey of nonribosomal peptide synthetase and polyketide synthase gene clusters in type strains of the genus Microtetraspora. J Antibiot (Tokyo). 2016 Sep;69(9):712–718. https://doi.org/10.1038/ja.2015.139

Komatsu M, Uchiyama T, Ōmura S, Cane DE, Ikeda H. Genome-minimized Streptomyces host for the heterologous expression of secondary metabolism. Proc Natl Acad Sci USA. 2010 Feb 09; 107(6):2646–2651. https://doi.org/10.1073/pnas.0914833107

Lamb DC, Ikeda H, Nelson DR, Ishikawa J, Skaug T, Jackson C, Omura S, Waterman MR, Kelly SL. Cytochrome P450 complement (CYPome) of the avermectin-producer Streptomyces avermitilis and comparison to that of Streptomyces coelicolor A3(2). Biochem Biophys Res Commun. 2003 Aug;307(3):610–619. https://doi.org/10.1016/S0006-291X(03)01231-2

Le TH, Sivachidambaram V, Yi X, Li X, Zhou Z. Quantification of polyketide synthase genes in tropical urban soils using real-time PCR. J Microbiol Methods. 2014 Nov;106:135–142. https://doi.org/10.1016/j.mimet.2014.08.010

Lee MY, Myeong JS, Park HJ, Han K, Kim ES. Isolation and partial characterization of a cryptic polyene gene cluster in *Pseudonocardia autotrophica*. J Ind Microbiol Biotechnol. 2006 Feb;33(2):84–87. https://doi.org/10.1007/s10295-005-0018-7

Omura S, Ikeda H, Ishikawa J, Hanamoto A, Takahashi C, Shinose M, Takahashi Y, Horikawa H, Nakazawa H, Osonoe T, et al. Genome sequence of an industrial microorganism *Streptomyces avermitilis*: deducing the ability of producing secondary metabolites. Proc Natl Acad Sci USA. 2001 Oct 09;98(21): 12215–12220. https://doi.org/10.1073/pnas.211433198

Silambarasan S, Murugan T, Saravanan D, Balagurunathan R. Antibacterial and antifungal activities of Actinobacteria isolated from Rathnagiri hills. J Appl Pharm Sci. 2012 Oct 28;2:99. https://doi.org/10.7324/JAPS.2012.21020

Sosio M, Stinchi S, Beltrametti F, Lazzarini A, Donadio S. The gene cluster for the biosynthesis of the glycopeptide antibiotic A40926 by nonomuraea species. Chem Biol. 2003 Jun;10(6):541–549. https://doi.org/10.1016/S1074-5521(03)00120-0

Winter JM, Behnken S, Hertweck C. Genomics-inspired discovery of natural products. Curr Opin Chem Biol. 2011 Feb;15(1):22–31. https://doi.org/10.1016/j.cbpa.2010.10.020

Wood SA, Kirby BM, Goodwin CM, Le Roes M, Meyers PR. PCR screening reveals unexpected antibiotic biosynthetic potential in *Amycolatopsis* sp. strain UM16. J Appl Microbiol. 2007 Jan; 102(1):245–253. https://doi.org/10.1111/j.1365-2672.2006.03043.x

Wu L, Chen G, Feng G. Complete genome sequence of *Streptomyces griseochromogenes* ATCC 14511^T, a producer of nucleoside compounds and diverse secondary metabolites. J Biotechnol. 2017 May; 249:16–19. https://doi.org/10.1016/j.jbiotec.2017.03.017

Xu L, Ye K-X, Dai W-H, Sun C, Xu L-H, Han B-N. Comparative genomic insights into secondary metabolism biosynthetic gene cluster distributions of marine *Streptomyces*. Mar Drugs. 2019 Aug 26;17(9):E498. https://doi.org/10.3390/md17090498

Ye S, Molloy B, Braña AF, Zabala D, Olano C, Cortés J, Morís F, Salas JA, Méndez C. Identification by genome mining of a type I polyketide gene cluster from *Streptomyces argillaceus* involved in the biosynthesis of pyridine and piperidine alkaloids argimycins P. Front Microbiol. 2017 Feb 10;8:194. https://doi.org/10.3389/fmicb.2017.00194

Polish Journal of Microbiology
2020, Vol. 69, No 2, 151–164
https://doi.org/10.33073/pjm-2020-018

ORIGINAL PAPER

Characterization of Microbial Diversity and Community Structure in Fermentation Pit Mud of Different Ages for Production of Strong-Aroma Baijiu

XU-JIA WANG[2], HONG-MEI ZHU[2], ZHI-QIANG REN[1, 3], ZHI-GUO HUANG[1, 3], CHUN-HUI WEI[1, 3] and JIE DENG[1, 3]*

[1] Liquor Making Biotechnology and Application Key Laboratory of Sichuan Province, Sichuan University of Science and Engineering, Yibin, P.R. China
[2] Sichuan C-Luminary Biotech Company, Chengdu, P.R. China
[3] School of Bioengineering, Sichuan University of Science and Engineering, Yibin, P.R. China

Submitted 6 January 2020, revised 25 March 2020, accepted 29 March 2020

Abstract

In the traditional fermentation process of strong-aroma Baijiu, a fermentation pit mud (FPM) provides many genera of microorganisms for fermentation. However, the functional microorganisms that have an important effect on the quality of Baijiu and their changes with the age of fermentation pit (FP) are poorly understood. Herein, the Roche 454 pyrosequencing technique and a phospholipid fatty-acid analysis were employed to reveal the structure and diversity of prokaryotic communities in FPM samples that have been aged for 5, 30, and 100 years. The results revealed an increase in total prokaryotic biomass with an FP age; however, Shannon's diversity index decreased significantly ($p < 0.01$). These results suggested that a unique microbial community structure evolved with uninterrupted use of the FP. The number of functional microorganisms, which could produce the flavor compounds of strong-aroma Baijiu, increased with the FP age. Among them, *Clostridium* and *Ruminococcaceae* are microorganisms that directly produce caproic acid. The increase of their relative abundance in the FPM might have improved the quality of strong-aroma Baijiu. *Syntrophomonas*, *Methanobacterium*, and *Methanocorpusculum* might also be beneficial to caproic acid production. They are not directly involved but provide possible environmental factors for caproic acid production. Overall, our study results indicated that an uninterrupted use of the FP shapes the particular microbial community structure in the FPM. This research provides scientific support for the concept that the aged FP yields a high-quality Baijiu.

Key words: strong-aroma Baijiu, fermentation pit mud, microbial community, Roche 454 pyrosequencing, PLFAs

Introduction

Strong-aroma Baijiu is a unique liquor that is clear and transparent and comprises of water, ethanol, and flavor compounds. The flavor compounds include acids, alcohols, esters, carbonyl, and phenolic compounds, etc. (Liu and Sun 2018; Wu et al. 2019; Zhao et al. 2019). Although the content of flavor compounds is less than 2%, it determines the consumers' acceptance and preference of Baijiu (Zhao et al. 2018). Microorganisms produce most flavor compounds during fermentation. Strong-aroma Baijiu has a unique production process and fermentation vessels (Fig. 1). The fermentation vessel is called a mud pit (Li et al. 2017; Liu and Sun 2018). The mud pit is a similar cuboid pond (Ding et al. 2015), just below the horizon and surrounded by special mud that is called a fermentation pit mud (FPM). The fresh FPM is produced via a complicated process using natural yellow soil that contains the abundance of iron oxide and aluminum oxide, Daqu, the fermented exudate that is called Huangshui, and Baijiu (Sun et al. 2017; Liu et al. 2019). During the fermentation process, the FPM interacts with Huangshui and fermentation grain (Li et al. 2017). The fermentation grain was called Zaopei, and it is composed of sorghum, rice husks, and Daqu. The FPM gradually matures when the fermentation process is carried out round after round. The content of flavor substances in the produced liquor is gradually increasing until it becomes relatively stable (Tao et al. 2014; Zheng et al. 2015; Wang et al. 2017). In general

* Corresponding author: J. Deng, School of Bioengineering, Sichuan University of Science & Engineering, Yibin, Sichuan, P.R. China; **e-mail: jiedeng1988@foxmail.com**

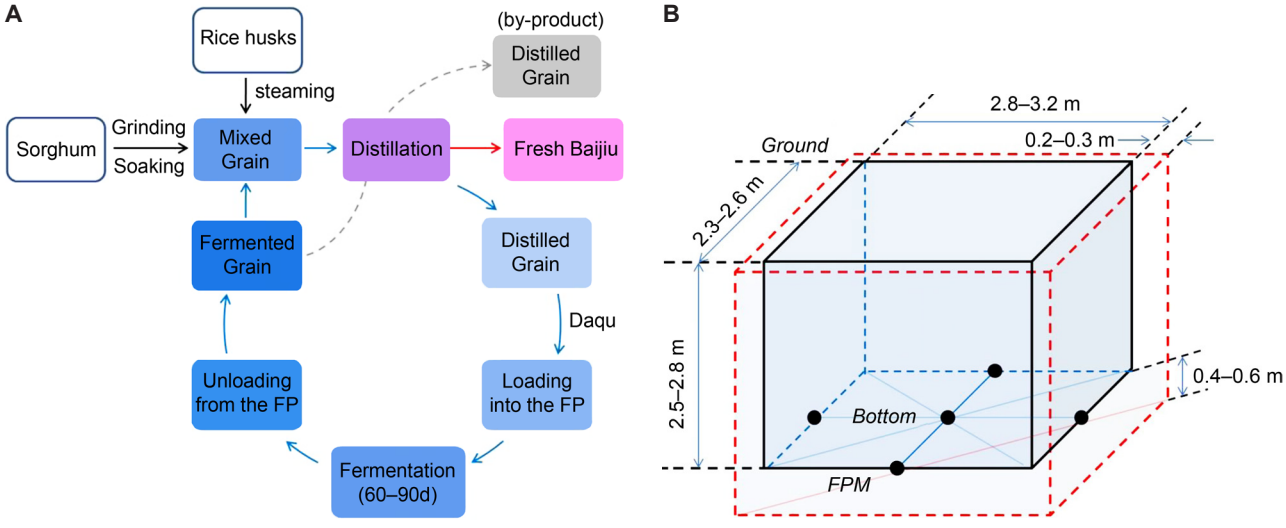

Fig. 1. The production (A) and the FP (B) of strong-aroma Baijiu.

A: The concentration of rice husks is about 20% of sorghum (dry weight); the main chemical composition of the fresh grain (sorghum and rice husks) are starch (48.1–50.4%), protein (5.3–8.3%), fat (3.2–3.7%), cellulose (8.3–10.2%), lignin (4.8–6.4%), pentosan (3.2–3.4%), tannin (0.1–0.5%), etc; the concentration of fresh grain is about 20% of mixed grain (dry weight); the concentration of Daqu is about 20% of sorghum; during fermentation, the moisture content of the grain is about 55–60%. B: The solid circle (●) represent sampling sites of FPM, the FP is surrounded by FPM.

the quality of Baijiu is improved when the fermentation pit (FP) age is more than five years (Zhao et al. 2012), and becomes relatively stable when the FP age is about 30 years (Tao et al. 2014).

During strong-aroma Baijiu brewing, multiple of microorganisms co-exist in the FP. The FPM contained plentiful of microbes that can produce the flavoring compounds (Deng et al. 2012; Zhao et al. 2012; Liu et al. 2014; Luo et al. 2014). Therefore, the quality of Baijiu partly depends on the microbes from the FPM (Tao et al. 2014; Li et al. 2017; Xu et al. 2017). In general, the PFM in the aged PF contains more microbes that can produce the flavoring compounds. (Hu et al. 2016; Liu et al. 2017; Zhang et al. 2017). In China, the people regard the aged FP as a living artifact, and it can apply for urban or national cultural heritage to protect when the FP age is more than 30 or 100 years. The most famous is *Luzhou Laojiao* national cultural heritage FP group, especially the 1573 FP group that began construction in 1573 AD (Liu et al. 2017). The aged FP can produce high-quality Baijiu (Ding et al. 2014; Tao et al. 2014; Yao et al. 2015; Xu et al. 2017). However, the key factors to produce high-quality Baijiu are microorganisms that are more conducive to the yielding of the flavor compound in the FPM (Ding et al. 2014; Hu et al. 2015; Liu et al. 2017; Chai et al. 2019). Therefore, analysis of the microbial community in the FPM of different ages is intentional and may detect the significant functional microorganisms.

With the techniques of molecular biology and the detection methods developed, the unveiling of microbial communities in environmental samples become quite an easy task. The composition of microbial communities in samples such as soils (Torsvik and Øvreås 2002), ocean water (DeLong 2009), hot springs (Chapelle et al. 2002), gut (Chapelle et al. 2002), and FPM (Tao et al. 2014; Li et al. 2017; Chai et al. 2019) has been reported in succession. High-throughput sequencing technology is one of the most used techniques for analyzing of microbial communities. It could be used widely in the studies of Baijiu, such as analysis of the microbial communities of fermentation starters (Wang et al. 2017) or fermented grains (Chai et al. 2019), FPM (Tao et al. 2017). The determination of the content of phospholipid fatty acid (PLFA) is one of the most popular techniques for analyzing of total biomass in a sample (Green and Scow 2000; Zheng et al. 2013; Ding et al. 2015). Therefore, pyrosequencing and PLFAs were employed to assess the structure of prokaryotic communities within the FPM and to reveal the changes within these communities with age during the FPM maturation. In addition, the relationship between environmental factor variables and prokaryotic community structure and diversity in the FPM was revealed. It would be promising to find out the functional microorganisms that produced the flavor compounds of strong-aroma Baijiu.

Experimental

Materials and Methods

Materials. UltraClean Soil DNA Isolation Kit was purchased from MOBIO (USA). QIAquick Gel Extraction Kit was purchased from QIAGEN (USA).

Quant-iT™ PicoGreen™ dsDNA Assay Kit was acquired from Invitrogen (China). DNA polymerase, dNTPs, and DNA Marker were purchased from Takara (Japan). DNA sequencing was carried out at the Roche GS Junior sequencing platform.

Samples collection. The FPM samples were obtained from the renowned strong-aroma Baijiu producer from Luzhou, Sichuan province, China. Samples of the FP that had been utilized for 5, 30, and 100 years were sampled in triplicate, with five FP samples being collected in each FP when a round of fermentation process is just over. The sampling points were located at the bottom of the FP in the midpoint of the four sides and the intersection of the diagonal (Fig. 1). Each sample (20 g) was frozen at –20°C and shipped to the Sichuan University of Science and Engineering, Yibin, China on dry ice for analysis of the microbiome.

Chemical analysis. A gravimetric approach was used to measure the FPM moisture, with soil being collected and immediately dried at 60°C for 48 h. A method previously detailed by Mehlich was used for the humic acid measurements (Mehlich 1984), while the Kjeldahl method was used to quantify total nitrogen content (Tao et al. 2014). The levels of NH_4^+ in samples were measured via a sodium salicylate approach (Tao et al. 2014). Ammonium fluoride and hydrochloric acid were used to extract phosphorus (Sun et al. 2017), which was measured by SpectraMax 190 Microplate Reader (Molecular Devices, USA). Total acidity was measured via 0.1 M NaOH titration, as previously described (Wherry 1920; Zhang et al. 2017). Primary organic acids (the levels of caproic, acetic, butyric, and lactic acids) were measured with an ion chromatograph (Metrohm 761 Compact IC, Switzerland) that had a conductivity detector as well as an ion exclusion column (Metrosep Organic Acids 6.1005.200, Switzerland), as previously detailed (Rozendal et al. 2006). The available calcium was determined using ICP-OES (Agilent, USA) (Górecka et al. 2006).

DNA extraction and PCR amplification. The samples of the FPM were homogenized by mixing. DNA within a ~0.5 g oven-dried mud samples were extracted with the UltraClean Soil DNA Isolation Kit following the manufacturer's instructions. Extraction was conducted on ice with a 200 µl elution volume, after which a Nanodrop ND-2000 spectrophotometer (Nanodrop, USA) was used to quantify DNA levels. Also, 0.8% agarose gel electrophoresis was used to assess the DNA sample integrity, with 0.5 × TBE (45 mM Tris-borate, 1 mM EDTA, pH 8.0) being used as a buffer.

The community of the FP was prepared via a combination of equally sized 10 µl samples of five sampling isolates from the same pit. The DNA mixture from each FP was amplified, respectively, using the two-primer pairs specific for the V2-V3 and V6-V8 regions of the 16S rRNA gene. For V2-V3, 109F (Großkopf et al. 1998) was a forward primer: 5'-ACK GCT CAG TAA CAC GT-3' and 518R (Ovreås et al. 1997): 5'-ATT ACC GCG GCT GCT GG-3' was a reverse primer. For V6-V8, 968F: 5'-AAC GCG AAG AAC CTT AC-3' was a forward primer, and 1401R: 5'-CGG TGT GTA CAA GAC CC-3' (Sánchez et al. 2007) was a reverse primer. In addition, forward primers contained the Titanium A adapter sequence together with sample-specific 9-bp sample barcodes. Amplification reactions were conducted in a 50 µl volume containing 50 ng DNA together with 0.4 µM of specific primers, 5 U *Ex Taq*™ DNA polymerase, 1 × Ex Taq Buffer, and 0.2 mM dNTP. Thermocycler settings were as follows: 4 min at 94°C; 25 cycles of 94°C for 30 s, 56°C for 30 s, and 68°C for 80 s, and 10 min at 72°C. The amplified PCR products were separated via 1% agarose gel electrophoresis, then, their purification via QIAquick Gel Extraction Kit (QIAGEN, USA) was performed based on the directions provided.

Pyrosequencing and data analysis. The amplified sequences of the 16s rRNA gene prepared as above were then sequenced with a Roche 454 FLX Titanium sequencing platform. The QIIME pipeline was then used to process the raw read sequences, as in previous studies (Wang J et al. 2017). Briefly, those sequences that were either < 200 bp or > 600 bp long were excluded from analyses, after which all high-quality sequences underwent operational taxonomic unit (OTU) clustering via USEARCH (v7.0.1090) (Edgar 2013), with a 97% similarity threshold. The sequences representatives for each OTU were obtained. An OTU was only considered valid if a minimum of five reads in the present study were associated with it. The UCHIME (v4.2.40) algorithm (Edgar et al. 2011) was used for chimera filtration. The optimized sequences were used for OTU alignment, and OTU abundance in each sample was then analyzed. The SILVA web-based tools (http://www.arb-silva.de) were used for representative OTU sequence taxonomic classification (Quast et al. 2012).

PLFA extraction and analysis. The FPM samples were freeze-dried and grounded using a ball mill to a particle size of fewer than 10 µm prior to analysis. A modified version of a three-step protocol was then used for PLFA extraction (Bligh and Dyer 1959). Briefly, methanol, chloroform, and water were used to extract lipids from the soil, after which a silicic acid column was used to separate out phospholipids, neutral lipids, and glycolipids. A gas chromatograph (Agilent 6890) equipped with a 19091B-102 column (25.0 m × 200 µm × 0.33 µm, Agilent Technology, USA) and a flame ionization detector (FID) was then used for the alkaline methanolysis of phopholipids. GC settings for this analysis were: a 250°C inlet temperature, a 10:1 split ratio, and a 1 ml/minute flow of hydrogen

Table I
PLFA markers used for taxonomic groups.

Taxonomic group	PLFA group	Specific PLFA markers	Reference
Bacteria	Multiple groups	Sum of i15:0, a15:0, i16:0, i17:0, a17:0, cy17:0, cy19:0, 16:1ω7, 18:1ω7, and 17:1ω9	(Frostegård and Bååth 1996)
Gram-positive bacteria	Branched PLFAs	Sum of i15:0, a15:0, i16:0, i17:0, and a17:0	(O'Leary 1988)
Gram-negative bacteria	Cyclopropyl and mono PLFAs	Sum of cy17:0, 16:1ω7, 18:1ω7, and 17:1ω9	(Moore-Kucera and Dick 2008)
Actinomycetes	10Me-PLFAs	Sum of 10Me16:0, 10Me17:0, and 10Me18:0	(Moore-Kucera and Dick 2008)
Anaerobes	Cyclopropyl	Sum of cy17:0, cy19:0ω7, cy19:0ω9	(Li et al. 2017)

as a carrier gas. The oven was warmed for 2 minutes at 140°C, and the temperature was then raised by 5°C per minute up to a final 250°C temperature where it was maintained for 5 minutes. Peak areas were then compared to those of an internal C19:0 reference standard (Fluka, Switzerland) in order to quantify PLFAs. Fatty acids that had a < 0.5% overall relative abundance were omitted from this data set. Besides, PLFA nomenclature was designated according to a previous report (Moore and Dick 2008). The abundance of certain microbial groups was assessed by using specific PLFAs as biomarkers (O'Leary 1988; Frostegård and Bååth 1996; Moore-Kucera and Dick 2008; Li et al. 2017) (Table I), whereas PLFA 16:0 is present within all species of bacteria, plants, and fungi, and was therefore not considered to be a group-specific PLFA (Ding et al. 2015).

Data analysis. All data were means ± standard deviation from triplicate analyses, and were compared via ANOVAs. $P < 0.05$ was the significance threshold. SPSS 17.0 was used for all statistical analyses. The redundancy analysis (RDA) and microbial community analysis were performed using a program of RStudio (v1.0.136).

Results and Discussion

Chemical properties of the FPM. The physicochemical properties of the FPM are shown in Table II. The moisture increased in the FPM with age, and it may imply that there were differences in the microbial metabolic activity. The samples containing higher moisture might represent higher microbial metabolic activity. The available phosphorus can be an indirect indicator of biomass; it increased from 5 to 30 years and then stabilized. This pattern could also represent changes in biomass. There was no significant difference in total acidity; however, the content of caproic acid increased, and the content of lactic acid significantly declined with the FP age ($p < 0.05$). Caproic acid is produced by microbial fermentation. The high caproic acid content indicated that the FPM contained more numerous microorganisms producing caproic acid. Lactic acid mainly comes from Huangshui, and it was produced during fermentation, and its content was similar in FP of different ages. The content of lactic acid in the FPM was variable, indicating that there was a different abundance of microorganisms that could use lactic

Table II
Basic physiocochemical properties of fermentation pit mud.

Variable	Values for fermentation pit age (yr)[a]		
	5	30	100
Moisture(%)	35.15 ± 6.42	39.62 ± 1.11	44.97 ± 2.83
Humic matter (%)	10.54 ± 1.59	13.82 ± 0.09	10.90 ± 0.52
Total acidity(%)	1.54 ± 0.09	1.81 ± 0.05	1.13 ± 0.15
Acetic acid(mg/g)	3.98 ± 0.36	3.44 ± 0.46	4.21 ± 0.67
Lactic acid(mg/g)	94.22 ± 1.30	28.81 ± 7.05	21.33 ± 3.15
Butyric acid(mg/g)	2.87 ± 0.34	2.36 ± 0.26	2.79 ± 0.38
Caproic acid(mg/g)	15.15 ± 5.12	29.62 ± 4.19	45.97 ± 5.13
Total nitrogen(%)	0.94 ± 0.09	1.41 ± 0.08	2.16 ± 0.11
NH_4^+(mg/g)	14.12 ± 1.77	21.02 ± 2.03	25.32 ± 1.66
Available phosphorus(mg/g)	4.91 ± 0.52	9.15 ± 0.78	9.15 ± 0.41
Available calcium(mg/g)	9.51 ± 1.02	8.18 ± 1.91	7.41 ± 0.52

[a]All data are presented as means ± standard deviations (n = 3)

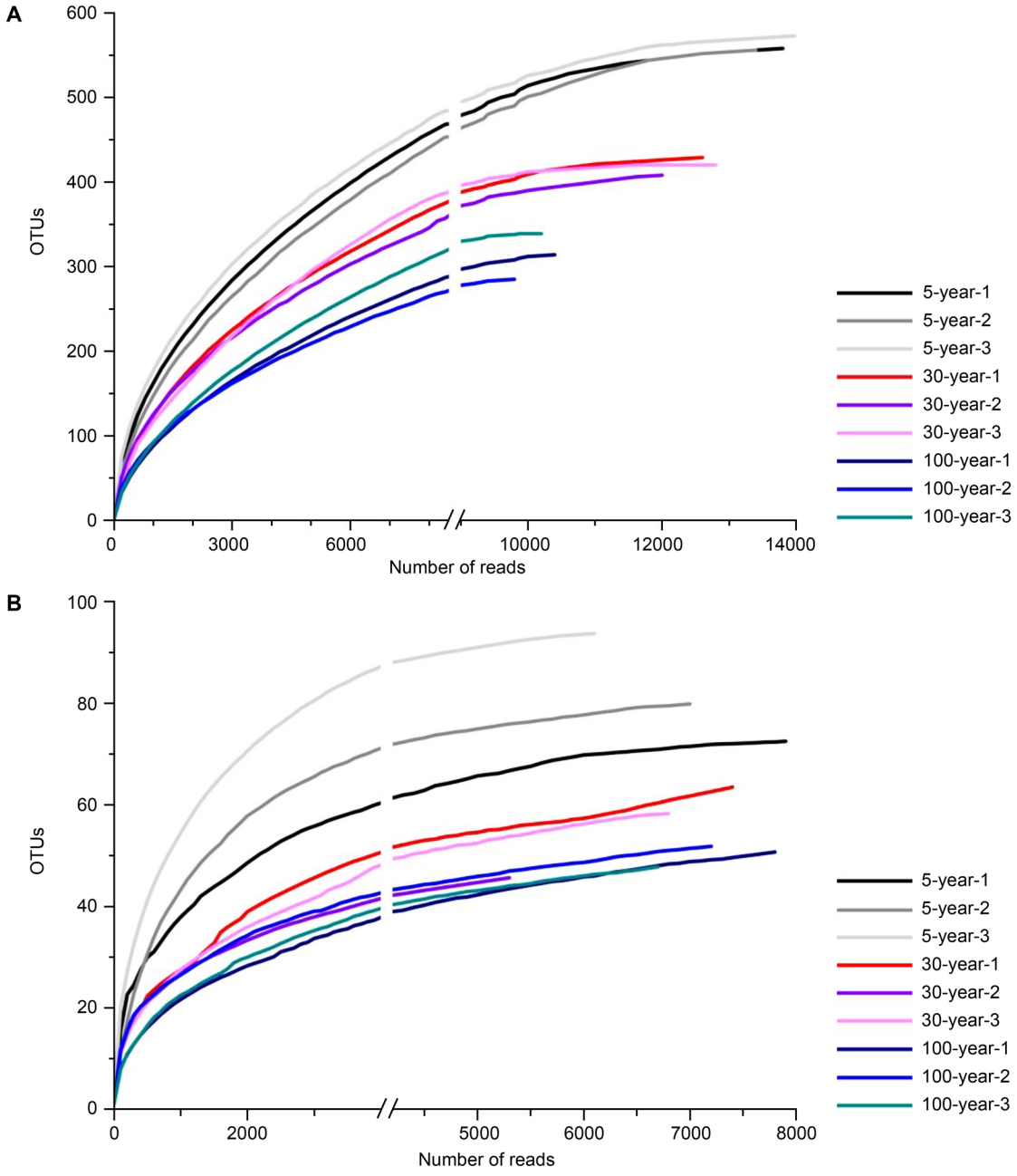

Fig. 2. OTUs rarefaction curves at a 97% sequence similarity cutoff. OTUs from the amplicon libraries of bacteria (A), and archaea (B).

acid. The content of NH_4^+ increased in the FPM with age; it may imply that old FPM might contain more microorganisms metabolizing amino acids to produce NH_4^+. Total nitrogen increase could be understood as an accumulation process that included a dynamic balance of nitrification and nitrogen loss. The available calcium decrease could be considered as a gradual loss process when compared to Huangshui.

The prokaryotic community structure and diversity. Each of the FP samples generates two amplicon libraries by amplification of V2-V3 and V6-V8 regions. Eighteen amplicon libraries were sequenced using the Roche 454 Junior platform, yielding 2.2 Gb of data, of which 34% passed Q30. After quality control, denoising, and chimera removal, we obtained 211,740 reads, with an average 377.4 bp read length. A total of 1,089 OTUs (952 OTUs belong to bacteria, 137 OTUs belong to archaea) were obtained based on a 3% dissimilarity in the sequences of the 16S rRNA gene, considering those OTUs with ≥5 sequences to be valid ones. Rarefaction analyses revealed a good representation of all prokaryotic communities within these samples, as all the curves approached a saturation plateau (Fig. 2).

Compared with archaea, the bacteria occupy an absolute advantage on OTUs. As the age of the FPM increases, the diversity of microorganisms decreases.

Table III
Prokaryotic diversity indices based on a cutoff of 97% similarity of the 16S rRNA gene sequences[a].

FPM age (yr)	Bacteria			Archaea		
	Chao1	Observed OTU	Shannon	Chao1	Observed OTU	Shannon
5	634.0 ± 84.4	583 ± 13	2.49 ± 0.56	97.3 ± 12.2	75 ± 7	1.374 ± 0.049
30	501.6 ± 64.6	419 ± 11	2.16 ± 0.31	78.5 ± 6.3	53 ± 5	1.159 ± 0.068
100	435.8 ± 62.1	312 ± 27	1.93 ± 0.34	74.2 ± 4.7	48 ± 4	1.068 ± 0.087

[a]All data are presented as means ± standard deviations (n = 3)

Table IV
The preference of sequencing results based on different variable regions V2-V3 and V6-V8[a] of the 16S rRNA gene.

Variable region	FPM age (yr)	Total		Bacteria		Archaea	
		reads	OTU	reads	OTU	reads	OTU
V2-V3	5	10977 ± 684	126 ± 12	1267 ± 104	51 ± 9	9710 ± 562	75 ± 7
	30	10562 ± 513	100 ± 11	1009 ± 84	47 ± 8	9553 ± 410	53 ± 5
	100	11172 ± 751	75 ± 6	938 ± 53	27 ± 5	10233 ± 720	48 ± 4
V6-V8	5	18893 ± 886	594 ± 17	17826 ± 844	583 ± 13	1067 ± 89	11 ± 3
	30	17409 ± 395	428 ± 15	16543 ± 354	419 ± 11	866 ± 68	9 ± 2
	100	16894 ± 806	319 ± 24	15537 ± 758	312 ± 20	1357 ± 133	7 ± 2

[a] All data are presented as means ± standard deviations (n = 3)

This result reflected in the rarefaction curve that the total number of OTUs in the sample decreases (Fig. 2). The lowest diversity was observed in the 100-year samples. Shannon's diversity index decreased significantly with the FP age ($p < 0.05$) from 5- to 30-year old FPM, and it became constant in the 30- to 100-year old FPM. Richness levels (OTUs) of bacteria significantly decreased in the 5-, 30-, and 100-year samples ($p < 0.05$). For archaea, it decreased in the 5-year to 30-year aged samples and were similar in the 30-year to 100-year aged samples (Table III). In general, the microbial community structure changed in both periods, but the change was faster in the period from 5 to 30 years than from 30 to 100 years. Although the variable of the number was similar, the latter period takes more time (70 years). These results indicated that the microbial community decreases rapidly and then gradually stabilizes. It could be the adaptation pattern of microorganisms to this unique habitat of the FP (the enriched organic matter, acidity, and lack of oxygen). The adaptive microorganisms enriched gradually, and formed the dominant species, and eventually shaped a stable community structure.

Phylogenetic composition of the FPM community. The significant differences were observed in sequencing results using different variable regions (V2-V3, V6-V8) of the 16S rRNA gene (Table IV). The results showed that most of the reads (about 90.2%) belonged to archaea when sequencing was performed with the V2-V3. However, most of the reads (about 93.8%) belonged to bacteria when sequencing was performed within the V6-V8. These results indicate that the variable regions have a preference for some types of microorganisms. The variable region V2-V3 is more suitable than V6-V8 for analyzing community of archaea, and V6-V8 is more suitable than V2-V3 for analyzing community of bacteria in the FPM samples. Thus, different primers may lead to different results. Therefore, the choice of suitable primers based on the characteristics of the microbial structure is essential to obtain the objective results. There are abundant microbial species in the FPM, including bacteria and archaea. What kind of primers is most suitable for the particular environment samples? This issue requires further research.

There were 952 OTUs that belonged to bacteria, of which 95.9% were relative of low abundance (< 1%), and 21.8% (208) OTUs were present in all samples. 137 OTUs belonged to archaea, of which 93.4% were relative of low abundance (< 1%), and 20.4% (28) OTUs were present in all samples. These results showed that although there were many types of microorganisms, there were also the dominant microorganisms in the FPM. These dominant microorganisms may be functional microorganisms of the FPM.

Most bacteria belonged to five phyla *Firmicutes Bacteroidetes*, *Chloroflexi*, *Actinobacteria*, and *Synergistetes*. The two most dominant phyla of bacteria were *Firmicutes* (75.8%), and *Bacteroidetes* (5.6%) (Fig. 3). Only *Euryarchaeota* was observed within archaea in all FPM samples (data not show).

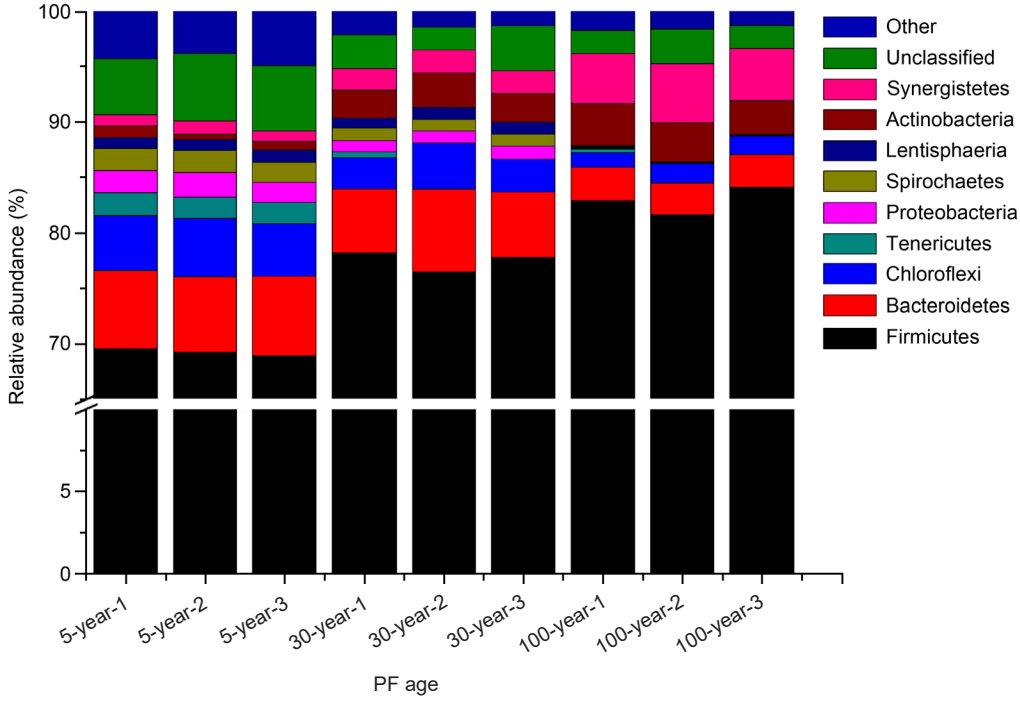

Fig. 3. Phylum level prokaryotes taxonomic classification in the FPM samples as determined with the RDP classifier using an 85% confidence threshold.

At the genus level, most bacteria belonged to 29 genera (Fig. 4A), 11 of them are core genera. The core genera were those present within all samples and had a relative abundance of more than 1.0%. The core genera belonged to *Firmicutes* (*Lactobacillus*, *Ruminococcaceae*, *Bacillus*, *Syntrophomonas*, *Clostridium*, *Carnobacterium*, and *Sporanaerobacter*), *Bacteroidetes* (*Petrimonas* and *Proteiniphilum*) *Actinobacteria* (*Cellulomonadaceae*) and *Chloroflexi* (*Anaerolineaceae*). Most archaea belonged to seven genera (Fig. 4B); six of them were core genera: *Methanobacterium*, *Thermoplasmatales*, *Methanoculleus*, *Methanosata*, *Methanobrevibacter*, and *Methanocorpusculum*. These core genera constituted 53–77% of total abundance.

Microbial community structure changes with the FP age. *Firmicutes* were the dominant phyla; its relative abundance increased with the FP age. It is worth noting that all the seven core genera of *Firmicutes* increased in number with the FP age. This result showed that Firmicutes could adapt to the special environment of the FP. This adaptation may benefit from their special stress-resistant structure, such as thick cell walls. It may also advantage from their diverse metabolic patterns. *Actinobacteria* relative abundance increases with the FP age. The core genus of Acinetobacter, *Cellulomonadaceae*, may be involved in cellulose metabolism (Stackebrandt and Schumann 2015). Although there was cellulose in the FP, the harmful environmental factors such as acidity and lack of oxygen may be the reasons for hindering its rapid increase. *Synergistetes* did not contain core genera, but its relative abundance had increased significantly. It also contained only one genus, *Aminobacterium*, which might be involved in amino acid metabolism (Baena et al. 2015). The abundant amino acids in the environment provided favorable conditions for the increase of its relative abundance. *Bacteroidetes* includes two core genera, *Proteiniphilum* and *Petrimonas*; their relative abundance decreases with the PF age. *Proteiniphilum* might be involved in protein metabolism (Whitman et al. 2015b), *Petrimonas* could metabolize glucose through fermentation (Whitman et al. 2015a), and the reason for their reduction needs further study. *Chloroflexi* contained a core genus, its relative abundance decreased with the FP age. The core genus, *Anaerolineaceae*, might be involved in carbohydrate and protein metabolism (Yamada and Sekiguchi 2020), the product included hydrogen. The high partial hydrogen pressure in the FP might be the reason for its reduction. The relative abundance of the other four phyla decreased with age. All speculations about metabolism mentioned above were based on the Bergey's Manual of Systematics of Archaea and Bacteria.

Regarding archaea, the relative abundance of two core genera *Methanobacterium* and *Methanocorpusccum* increased with the FP age, and the other four core genera, *Methanoculleus*, *Methanobrevibacter*, *Methanosata,* and *Thermoplasmatales*, decreased with the FP age. *Methanobacterium* and *Thermoplasmatales* had the highest relative abundance. However, their trends of change were in the opposite. This change might be the result of competition among microbial genera.

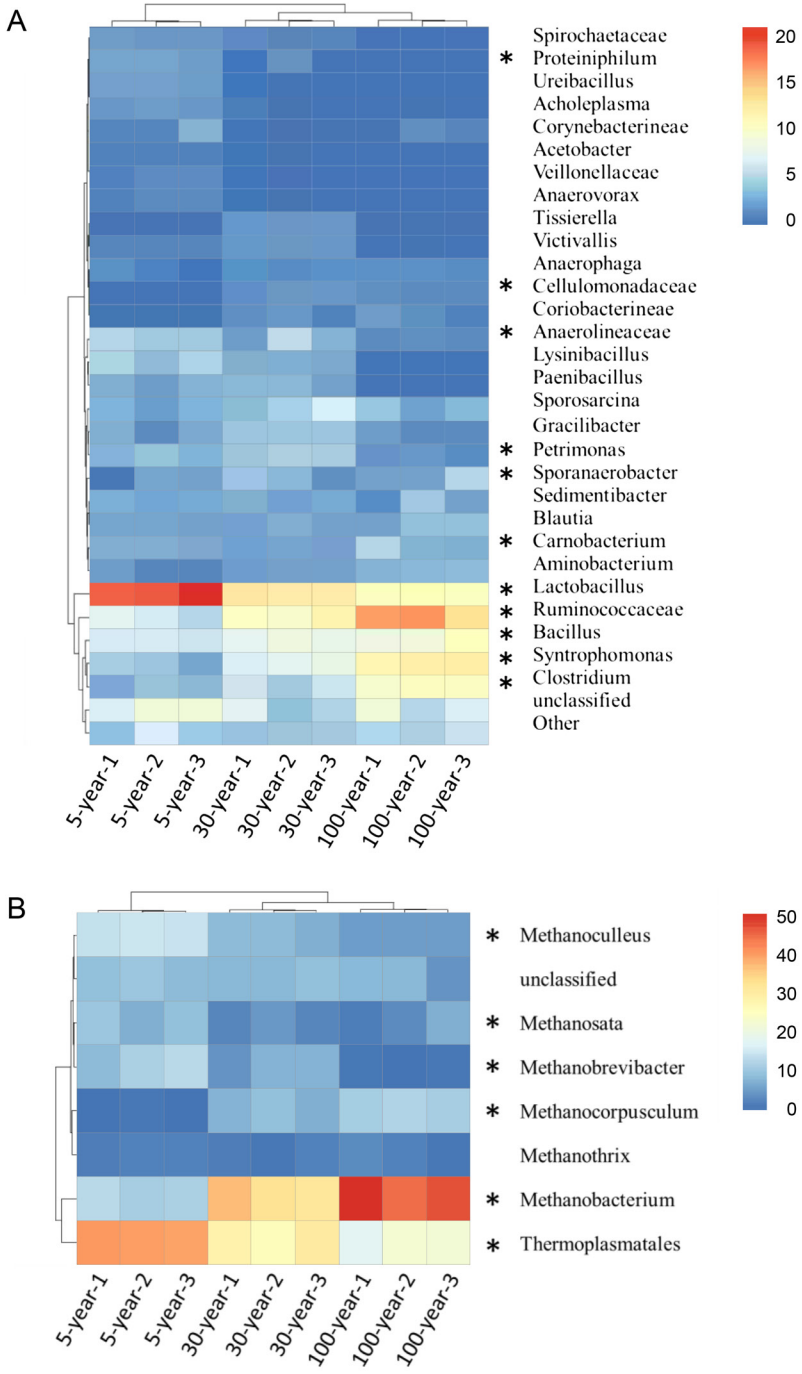

Fig. 4. The relative FPM prokaryotic genera abundance, based on Roche 454 pyrosequencing. It includes the genera of bacteria (A) and genera of archaea (B). Variations in $\log_2$ scale-based genera abundance are shown by the scale bar, with "*" indicating the genera shared among all FPM samples that had the relative abundance >1%.

Thermoplasmatales might be inferior in the competition because it lacks a true cell wall (Langworthy 2015).

Quantitative Analysis of Specific Microbial Groups Based on PLFAs Detection. Microbial biomass was assessed based on PLFAs concentrations in the FPM. A total of 30 PLFAs were identified (Fig. 5). The results show that the concentrations of most PLFAs in the FPM were different in the samples of different ages. It indicates that there was a difference in the microbial community structure in the FPM of different ages. This result is a validation of the sequencing results and once again shows that the community structure changes with FP age.

The concentrations of total PLFAs increased with the pit age (Fig. 6). This result suggested that the total biomass increased with age. However, microbial diversity decreased with age (Table III). These results suggested that the number of specific microbial species had increased. The changes in the contents of microbes, such as Gram-positive bacteria, anaerobes, and actinomy-

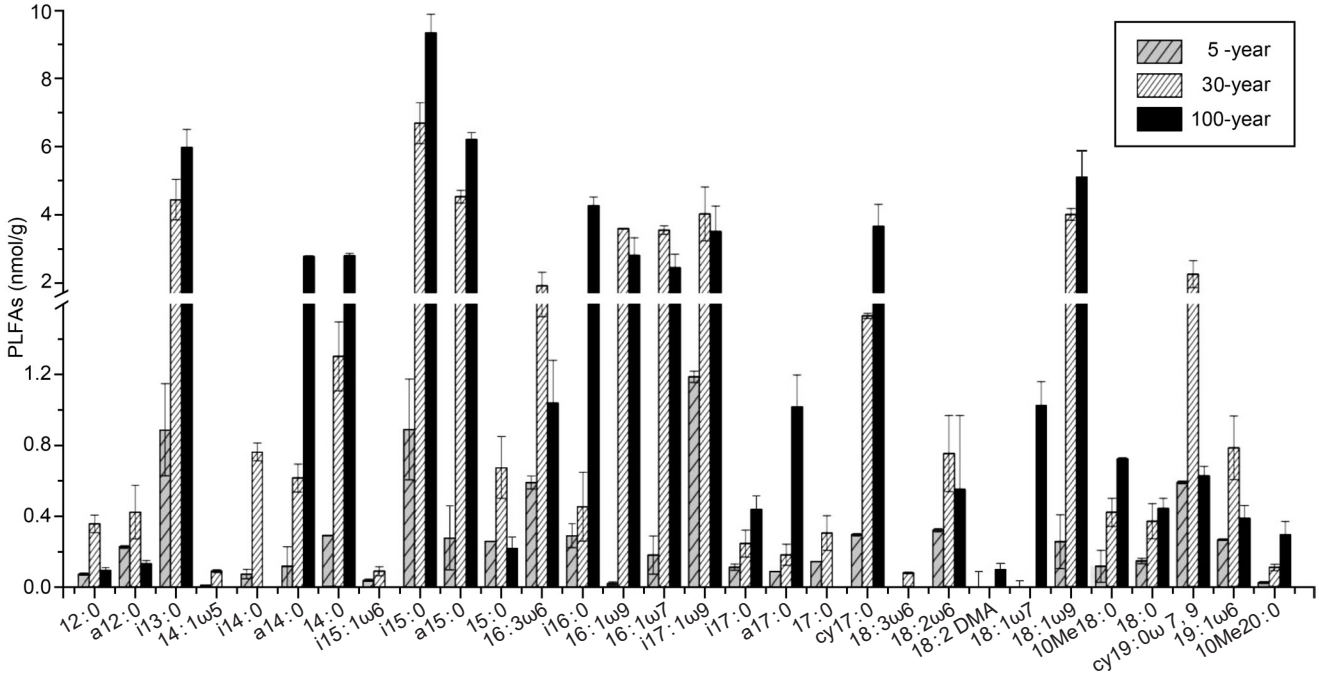

Fig. 5. Concentration of phospholipid fatty acids (PLFAs) in different FPM samples. The concentration of each sample was determined by an internal standard (19:0). Error bars indicate standard deviations (n = 3).

cetes were similar to the changes of total PLFA (Fig. 6). The probable reason that the biomass of Gram-positive bacteria increased with the FP age is that these groups of microorganisms have thick cell walls and strong resistance to stress. This result is consistent with changes in the structure of the microbial community. There are 11 core bacterial genera, six of them belong to Gram-positive, and five of them belong to Gram-negative (Ezaki 2015; Hammes and Hertel 2015a; Hammes and Hertel 2015b; Hernandez-Eugenio et al. 2015; Logan and Vos 2015; Rainey et al. 2015; Sekiguchi 2015; Stackebrandt and Schumann 2015; Whitman 2015a; Whitman 2015b; Yamada and Sekiguchi 2020). The relative abundance of the seven core bacterial genera increased with the FP age, there were five genera belonging to Gram-positive and two genera belonging to Gram-negative. The relative abundance of four core bacterial genera decreases with age; there were three genera of Gram-negative and one genus of Gram-positive. Environmental screening may be responsible for the relative abundance of the

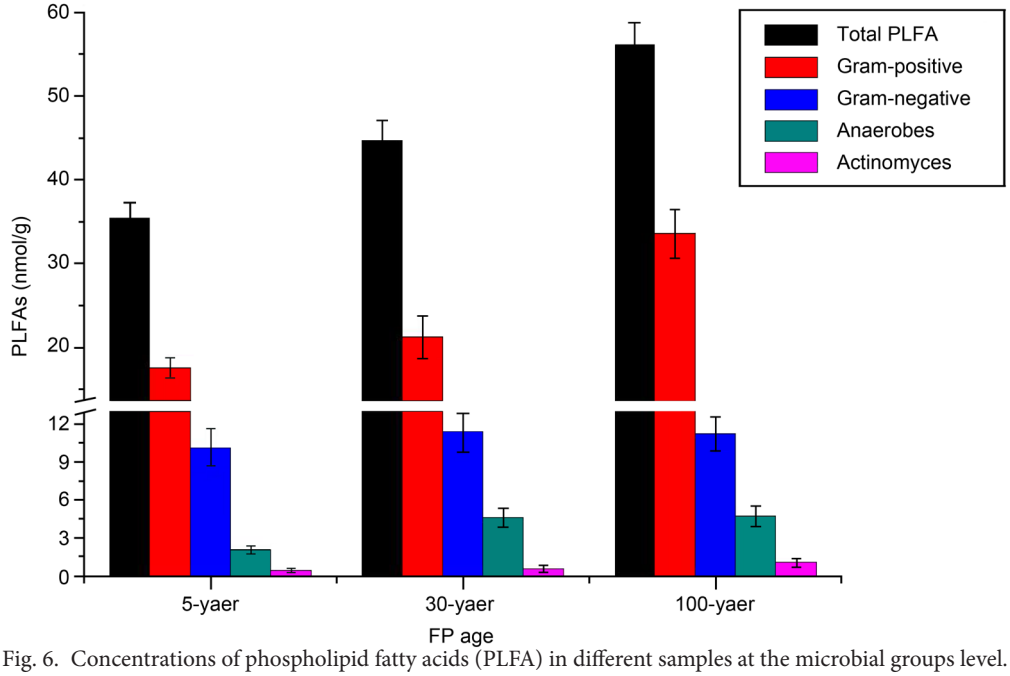

Fig. 6. Concentrations of phospholipid fatty acids (PLFA) in different samples at the microbial groups level. Error bars show standard deviations (n = 3).

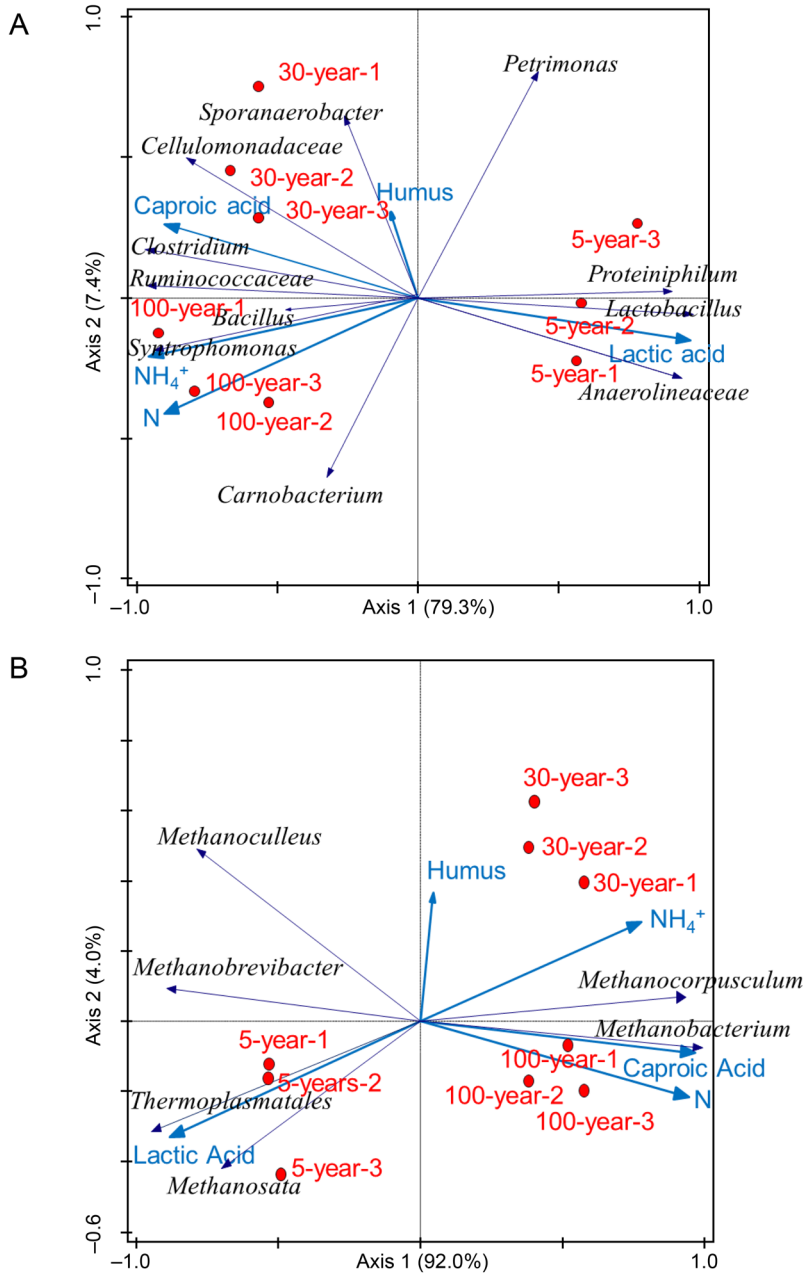

Fig. 7. Prokaryotic community redundancy analysis (RDA) based upon Roche 454 pyrosequencing and chemical properties. The dominant community structure-related genera and the direction/magnitude of chemical properties are represented by arrows. It includes the genera of bacteria (A) and genera of archaea (B).

anaerobic group. During long-term fermentation, in the FP, an anaerobic environment occurs. The reason that the relative abundance of actinomycetes increases with the FP age needs further stud, and the relative abundance of core genus, *Cellulomonadaceae*, increased in with the FP age, and it might be a key factor.

Relationships between prokaryotic communities and environmental variables. Redundancy analysis (RDA) was performed to discern the possible relationship between prokaryotic community structure and environmental parameters (Fig. 7). The two axes with respect to bacteria community differentiation explained 86.7% of the variation, while these two axes explained 96% of the archaeal variation, suggesting the remarkable correlation between prokaryotic community structure and environmental factors. Lactic acid levels mainly correlated positively with prokaryotic communities in the 5-year samples. However, caproic acid and NH_4^+ levels mainly correlated with those in the 30- and 100-year samples. Humic acid and TN levels mainly correlated with those in the 30- and 100-year samples, respectively.

The content of lactic acid correlated positively with *Lactobacillus*, and negatively correlated with *Clostridium*, *Ruminococcaceae,* and *Syntrophomonas*. These results suggested that lactic acid might be produced by *Lactobacillus*, and *Clostridium*. *Ruminococcaceae* and

Syntrophomonas may be involved in the process of lactic acid consumption. The content of caproic acid correlated positively with *Clostridium*, *Ruminococcaceae*, *Syntrophomonas*, *Methanobacterium,* and *Methanocorpusculum* abundance, and negatively correlated with *Lactobacillus* and *Thermoplasmatales* levels. *Clostridium* is a classic microorganism that produces caproic acid using ethanol (Rainey et al. 2015). *Ruminococcaceae* can produce caproic acid from lactic acid, such as *Ruminococcaceae bacterium* CPB6 (Yin et al. 2016). *Syntrophomonas* can use carboxylic acid to produce acetic acid and hydrogen. *Syntrophomonas* dependence on caproic acid may be the reason for its positive correlation with caproic acid content. A high partial pressure of hydrogen accompanied The production of caproic acid. This condition is also beneficial to *Methanobacterium* (Boone 2015), and *Methanocorpusculum* (Chong and Boone 2015). The symbiotic interactions between them need further study. The content of humic acid correlated positively with *Cellulomonadaceae*. Humus produced via the degradation of lignin and cellulose, and its content in the 30-year samples was significantly higher than that those in the 5-year and 100-year (Table II). It is worth noting that the trend of changes in the number of *Cellulomonadaceae* is similar to that of humus level. *Cellulomonadaceae* may be involved in cellulose metabolism (Stackebrandt and Schumann 2015). The content of TN and NH_4^+ affected the relative abundance of various microbial genera; they involved amino acid metabolism, nitrification, and denitrification. In addition, the nitrogen source, as the main nutrient element for microbial growth and development is closely related to the microbial community.

The FPM provides a large number of microorganisms for the fermentation of strong-aroma Baijiu. It involved protein and amino acid, carbohydrate, lignin and cellulose metabolism, as well as hydrogen, acid and methane production, etc. The most relevant to the quality of strong-aroma Baijiu is the production of caproic acid. *Clostridium* and *Ruminococcaceae* are microbes that directly produce caproic acid. Increasing their relative abundance in the FPM could improve the quality of strong-aroma Baijiu. In addition, the simplest way to increase the relative abundance of these two genera of microorganisms is to inoculate them in large quantities into the FPM. Nevertheless, this may not necessarily be an effective method. Although inoculation with microorganisms can temporarily increase relative abundance, there is a risk of decline. The strict monitoring of ecological factors makes the evolution of microorganisms beneficial to these two groups; thus, forming the dominant populations can provide better results. What ecological factors do they need? This issue needs further study. *Syntrophomonas*, *Methanobacterium,* and *Methanocorpusculum* may also be beneficial to caproic acid production. These genera are not directly involved, but provide possible environmental factors for caproic acid production.

Conclusions

These results offer insight into microbial community structural diversity within the FPM used for producing strong-aroma Baijiu as determined via Roche 454 pyrosequencing and PLFA. Our results demonstrate that the variable regions have a preference for the specific groups of microorganisms in the FPM, and sequencing with the appropriate variable region can make the results more objective. The complex functional populations of microorganisms inhabit the FPM ecosystem, and the microbial community structure in the FPM changes with the FP age. The total prokaryotic biomass in the FPM increased with the FP age; however, Shannon's diversity index decreased significantly ($p < 0.01$). These results suggested that a unique microbial community structure evolved with uninterrupted use of the FP. The results of RDA correlations indicate that *Clostridium* and *Ruminococcaceae* are genera that directly produce caproic acid. Increasing their relative abundance in the FPM could improve the quality of strong-aroma Baijiu. The control of ecological factors makes the community succession of microorganisms beneficial to these two groups, which could promote the quality of strong-aroma Baijiu. However, the way of control of these ecological factors requires further research.

Acknowledgment

This work was supported by the Key R&D projects of Sichuan Province Science and Technology Department (2016SZ0074), Open Foundation of Liquor Making Biotechnology and Application Key Laboratory of Sichuan Province (NJ2016-05 and NJ2018-04), Open Foundation of China Light Industry Key Laboratory of Strong-aroma Baijiu Solid State Fermentation (2018JJ007).

Authors' contributions

Jie Deng conceived and designed the experiments; Xu-Jia Wang performed the experiments; Hong-Mei Zhu analyzed the data; Zhi-Qiang Ren completed the manuscript; Zhi-Guo Huang and Chun-Hui Wei gave important suggestions.

Conflict of interest

The authors do not report any financial or personal connections with other persons or organizations, which might negatively affect the contents of this publication and/or claim authorship rights to this publication.

Literature

Baena S, Garcia JL, Cayol JL, Ollivier B. *Aminobacterium*. In: Whitman WB, Rainey F. Kämpfer P. Trujillo M, Chun J, DeVos P, Hedlund B, Dedysh S, editors. Bergey's Manual of Systematics of

Archaea and Bacteria. Hoboken (USA): John Wiley & Sons, Inc., in association with Bergey's Manual Trust. 2015; p. 1–5. https://doi.org/10.1002/9781118960608.gbm01253

Bligh EG, Dyer WJ. A rapid method of total lipid extraction and purification. Can J Biochem. Physiol. 1959 Aug;37:911–917. https://doi.org/10.1139/y59-099

Boone DR. *Methanobacterium*. In: Whitman WB, Rainey F. Kämpfer P. Trujillo M, Chun J, DeVos P, Hedlund B, Dedysh S, editors. Bergey's Manual of Systematics of Archaea and Bacteria. Hoboken (USA): John Wiley & Sons, Inc., in association with Bergey's Manual Trust. 2015; p. 1–8. https://doi.org/10.1002/9781118960608.gbm00495

Chai LJ, Lu ZM, Zhang XJ, Ma J, Xu PX, Qian W, Xiao C, Wang ST, Shen CH, Shi JS, Xu ZH. Zooming in on butyrate-producing Clostridial consortia in the fermented grains of baijiu via gene sequence-guided microbial isolation. Front Microbiol. 2019 Jun 21;10:1397. https://doi.org/10.3389/fmicb.2019.01397

Chai LJ, Xu PX, Qian W, Zhang XJ, Ma J, Lu ZM, Wang ST, Shen CH, Shi JS, Xu ZH. Profiling the Clostridia with butyrate-producing potential in the mud of Chinese liquor fermentation cellar. Int J Food Microbiol. 2019 May 16;297:41–50. https://doi.org/10.1016/j.ijfoodmicro.2019.02.023

Chapelle FH, O'Neill K, Bradley PM, Methé BA, Ciufo SA, Knobel LL, Lovley DR. A hydrogen-based subsurface microbial community dominated by methanogens. Nature. 2002 Jan 17; 415(6869):312–315. https://doi.org/10.1038/415312a

Chong SC, Boone DR. *Methanocorpusculum*. In: Whitman WB, Rainey F. Kämpfer P. Trujillo M, Chun J, DeVos P, Hedlund B, Dedysh S, editors. Bergey's Manual of Systematics of Archaea and Bacteria. Hoboken (USA): John Wiley & Sons, Inc., in association with Bergey's Manual Trust. 2015; p. 1–4. https://doi.org/10.1002/9781118960608.gbm00504

DeLong EF. The microbial ocean from genomes to biomes. Nature. 2009 May 13;459(7244):200–206. https://doi.org/10.1038/nature08059

Deng B, Shen CH, Shan XH, Ao ZH, Zhao JS, Shen XJ, Huang ZG. PCR-DGGE analysis on microbial communities in pit mud of cellars used for different periods of time. J Inst Brew. 2012 May 23;118(1):120–126. https://doi.org/10.1002/jib.2

Ding XF, Wu CD, Huang J, Li H, Zhou RQ. Eubacterial and archaeal community characteristics in the man-made pit mud revealed by combined PCR-DGGE and FISH analyses. Food Res Int. 2014 Aug;62:1047–1053. https://doi.org/10.1016/j.foodres.2014.05.045

Ding XF, Wu CD, Huang J, Li H, Zhou RQ. Interphase microbial community characteristics in the fermentation cellar of Chinese Luzhou-flavor liquor determined by PLFA and DGGE profiles. Food Res Int. 2015 Jun;72:16–24. https://doi.org/10.1016/j.foodres.2015.03.018

Edgar RC, Haas BJ, Clemente JC, Quince C, Knight R. UCHIME improves sensitivity and speed of chimera detection. Bioinformatics. 2011 Jun 23;27(16):2194–2200. https://doi.org/10.1093/bioinformatics/btr381

Edgar RC. UPARSE: highly accurate OTU sequences from microbial amplicon reads. Nat methods. 2013 Aug 18;10(10):996. https://doi.org/10.1038/nmeth.2604

Ezaki T. *Ruminococcus*. In: Whitman WB, Rainey F. Kämpfer P. Trujillo M, Chun J, DeVos P, Hedlund B, Dedysh S, editors. Bergey's Manual of Systematics of Archaea and Bacteria. Hoboken (USA): John Wiley & Sons, Inc., in association with Bergey's Manual Trust. 2015; p. 1–5. https://doi.org/10.1002/9781118960608.gbm00678

Frostegård Å, Bååth E. The use of phospholipid fatty acid analysis to estimate bacterial and fungal biomass in soil. Biol Fertil Soils. 1996 Apr;22(1-2):59–65. https://doi.org/10.1007/BF00384433

Górecka H, Chojnacka K, Górecki H. The application of ICP-MS and ICP-OES in determination of micronutrients in wood ashes used as soil conditioners. Talanta. 2006 Dec 15;70(5):950–956. https://doi.org/10.1016/j.talanta.2006.05.061

Green CT, Scow KM. Analysis of phospholipid fatty acids (PLFA) to characterize microbial communities in aquifers. Hydrogeol J. 2000 Mar;8(1):126–141. https://doi.org/10.1007/s100400050013

Großkopf R, Janssen PH, Liesack W. Diversity and structure of the methanogenic community in anoxic rice paddy soil microcosms as examined by cultivation and direct 16S rRNA gene sequence retrieval. Appl Environ Microbiol. 1998 May 1;64(3):960.

Hammes WP, Hertel C. *Carnobacterium*. In: Whitman WB, Rainey F. Kämpfer P. Trujillo M, Chun J, DeVos P, Hedlund B, Dedysh S, editors. Bergey's Manual of Systematics of Archaea and Bacteria. Hoboken (USA): John Wiley & Sons, Inc., in association with Bergey's Manual Trust. 2015a; p. 1–14. https://doi.org/10.1002/9781118960608.gbm00593

Hammes WP, Hertel C. *Lactobacillus*. In: Whitman WB, Rainey F. Kämpfer P. Trujillo M, Chun J, DeVos P, Hedlund B, Dedysh S, editors. Bergey's Manual of Systematics of Archaea and Bacteria. Hoboken (USA): John Wiley & Sons, Inc., in association with Bergey's Manual Trust. 2015b; p. 1–76. https://doi.org/10.1002/9781118960608.gbm00604

Hernandez-Eugenio G, Fardeau ML, Garcia JL, Ollivier B. *Sporanaerobacter*. In: Whitman WB, Rainey F. Kämpfer P. Trujillo M, Chun J, DeVos P, Hedlund B, Dedysh S, editors. Bergey's Manual of Systematics of Archaea and Bacteria. Hoboken (USA): John Wiley & Sons, Inc., in association with Bergey's Manual Trust. 2015; p. 1–6. https://doi.org/10.1002/9781118960608.gbm00720

Hu XL, Du H, Ren C, Xu Y. Illuminating anaerobic microbial community and cooccurrence patterns across a quality gradient in Chinese liquor fermentation pit muds. Appl Environ Microbiol. 2016 Apr 4;82(8):2506–2515. https://doi.org/10.1128/AEM.03409-15

Hu XL, Du H, Xu Y. Identification and quantification of the caproic acid-producing bacterium Clostridium kluyveri in the fermentation of pit mud used for Chinese strong-aroma type liquor production. Int J Food Microbiol. 2015 Dec 2;214:116–122. https://doi.org/10.1016/j.ijfoodmicro.2015.07.032

Langworthy TA. *Thermoplasma*. In: Whitman WB, Rainey F. Kämpfer P. Trujillo M, Chun J, DeVos P, Hedlund B, Dedysh S, editors. Bergey's Manual of Systematics of Archaea and Bacteria. Hoboken (USA): John Wiley & Sons, Inc., in association with Bergey's Manual Trust. 2015; p. 1–8. https://doi.org/10.1002/9781118960608.gbm00524

Li H, Huang J, Liu XP, Zhou RQ, Ding XF, Xiang QY, Zhang LQ, Wu CD. Characterization of Interphase Microbial Community in Luzhou-Flavored liquor manufacturing pits of various ages by polyphasic detection methods. J Microbiol Biotechnol. 2016 Oct 6;27(1):130–140. https://doi.org/10.4014/jmb.1605.05036

Liu CL, Huang D, Liu LY, Zhang J, Deng Y, Chen L, Zhang WX, Wu ZY, Fan A, Lai DY, Dai LR. *Clostridium swellfunianum* sp. nov., a novel anaerobic bacterium isolated from the pit mud of Chinese Luzhou-flavor liquor production. Antonie van Leeuwenhoek. 2014 May 31;106(4):817–825. https://doi.org/10.1007/s10482-014-0251-z

Liu HL, Sun BG. Effect of fermentation processing on the flavor of Baijiu. J Agric Food Chem. 2018 May 11;66(22):5425–5432. https://doi.org/10.1021/acs.jafc.8b00692

Liu MK, Tang YM, Guo XJ, Zhao K, Tian XH, Liu Y, Yao WC, Deng B, Ren DQ, Zhang XP. Deep sequencing reveals high bacterial diversity and phylogenetic novelty in pit mud from Luzhou Laojiao cellars for Chinese strong-flavor Baijiu. Food Res Int. 2017 Dec;102:68–76. https://doi.org/10.1016/j.foodres.2017.09.075

Liu MK, Tang YM, Zhao K, Liu Y, Guo XJ, Ren DQ, Yao WC, Tian XH, Gu YF, Yi B, Zhang XP. Determination of the fungal community of pit mud in fermentation cellars for Chinese strong-

flavor liquor, using DGGE and Illumina MiSeq sequencing. Food Res Int. 2017 Jan;91:80–87. https://doi.org/10.1016/j.foodres.2016.11.037

Liu MK, Tang YM, Zhao K, Liu Y, Guo XJ, Tian XH, Ren DQ, Yao WC. Contrasting bacterial community structure in artificial pit mud-starter cultures of different qualities: a complex biological mixture for Chinese strong-flavor Baijiu production. 3 Biotech. 2019 Feb 18;9(3):89. https://doi.org/10.1007/s13205-019-1622-y

Logan NA, Vos PD. *Bacillus*. In: Whitman WB, Rainey F. Kämpfer P. Trujillo M, Chun J, DeVos P, Hedlund B, Dedysh S, editors. Bergey's Manual of Systematics of Archaea and Bacteria. Hoboken (USA): John Wiley & Sons, Inc., in association with Bergey's Manual Trust. 2015; p. 1–163. https://doi.org/10.1002/9781118960608.gbm00530

Luo QC, Liu CL, Wu ZY, Wang HY, Li WF, Zhang KZ, Huang D, Zhang J, Zhang WX. Monitoring of the prokaryotic diversity in pit mud from a Luzhou-flavour liquor distillery and evaluation of two predominant archaea using qPCR assays. J Inst Brew. 2014 Apr 15;120(3):253–261. https://doi.org/10.1002/jib.132

Mehlich A. Photometric determination of humic matter in soils, a proposed method. Commun Soil Sci Plant Anal. 1984;15(12): 1417–1422. https://doi.org/10.1080/00103628409367569

Moore-Kucera J, Dick RP. PLFA profiling of microbial community structure and seasonal shifts in soils of a Douglas-fir chronosequence. Microb Ecol. 2007 Aug 31;55(3):500–511. https://doi.org/10.1007/s00248-007-9295-1

O'Leary MH. Carbon isotopes in photosynthesis. Bioscience. 1988 May;38(5):328–336. https://doi.org/10.2307/1310735

Ovreås L, Forney L, Daae FL, Torsvik V. Distribution of bacterioplankton in meromictic Lake Saelenvannet, as determined by denaturing gradient gel electrophoresis of PCR-amplified gene fragments coding for 16S rRNA. Appl Environ Microbiol. 1997 Sep;63(9):3367.

Quast C, Pruesse E, Yilmaz P, Gerken J, Schweer T, Yarza P, Peplies J, Glöckner FO. The SILVA ribosomal RNA gene database project: improved data processing and web-based tools. Nucleic Acids Res. 2013 Jan 1;41(D1):D590–D596. https://doi.org/10.1093/nar/gks1219

Rainey FA, Hollen BJ, Small AM. *Clostridium*. In: Whitman WB, Rainey F. Kämpfer P. Trujillo M, Chun J, DeVos P, Hedlund B, Dedysh S, editors. Bergey's Manual of Systematics of Archaea and Bacteria. Hoboken (USA): John Wiley & Sons, Inc., in association with Bergey's Manual Trust. 2015; p. 1–122. https://doi.org/10.1002/9781118960608.gbm00619

Rozendal RA, Hamelers HVM, Euverink GJW, Metz SJ, Buisman CJN. Principle and perspectives of hydrogen production through biocatalyzed electrolysis. Int J Hydrogen Energy. 2006 Sep;31(12):1632–1640. https://doi.org/10.1016/j.ijhydene.2005.12.006

Sánchez O, Gasol JM, Massana R, Mas J, Pedrós-Alió C. Comparison of different Denaturing Gradient Gel Electrophoresis primer sets for the study of marine bacterioplankton communities. Appl Environ Microbiol. 2007 Sep 11;73(18):5962. https://doi.org/10.1128/AEM.00817-07

Sekiguchi Y. *Syntrophomonas*. In: Whitman WB, Rainey F. Kämpfer P. Trujillo M, Chun J, DeVos P, Hedlund B, Dedysh S, editors. Bergey's Manual of Systematics of Archaea and Bacteria. Hoboken (USA): John Wiley & Sons, Inc., in association with Bergey's Manual Trust. 2015; p. 1–11. https://doi.org/10.1002/9781118960608.gbm00682

Stackebrandt E, Schumann P. *Cellulomonas*. In: Whitman WB, Rainey F. Kämpfer P. Trujillo M, Chun J, DeVos P, Hedlund B, Dedysh S, editors. Bergey's Manual of Systematics of Archaea and Bacteria. Hoboken (USA): John Wiley & Sons, Inc., in association with Bergey's Manual Trust. 2015; p. 1–14. https://doi.org/10.1002/9781118960608.gbm00063

Sun ZK, Chen C, Hou XG, Zhang J, Tian FS, Li CW. Prokaryotic diversity and biochemical properties in aging artificial pit mud used for the production of Chinese strong flavor liquor. 3 Biotech. 2019 Sep 19;7(5):335. https://doi.org/10.1007/s13205-017-0978-0

Tao Y, Li JB, Rui JP, Xu ZC, Zhou Y, Hu XH, Wang X, Liu MH, Li DP, Li XZ. Prokaryotic communities in pit mud from different-aged cellars used for the production of Chinese strong-flavored liquor. Appl Environ Microbiol. 2014 Mar 11;80(7):2254. https://doi.org/10.1128/AEM.04070-13

Tao Y, Wang X, Li XZ, Wei N, Jin H, Xu ZC, Tang QL, Zhu XY. The functional potential and active populations of the pit mud microbiome for the production of Chinese strong-flavour liquor. Microb Biotechnol. 2017 Jul 13;10(6):1603–1615. https://doi.org/10.1111/1751-7915.12729

Torsvik V, Øvreås L. Microbial diversity and function in soil: from genes to ecosystems. Curr Opin Microbiol. 2002 Jun 1;5(3):240–245. https://doi.org/10.1016/S1369-5274(02)00324-7

Wang J, Fan H, Han Y, Zhao JZ, Zhou ZJ. Characterization of the microbial communities along the gastrointestinal tract of sheep by 454 pyrosequencing analysis. Asian-Australas J Anim Sci. 2017 Jun 30;30(1):100. https://doi.org/10.5713/ajas.16.0166

Wang XD, Ban SD, Hu BD, Qiu SY, Zhou HX. Bacterial diversity of Moutai-flavour Daqu based on high-throughput sequencing method. J Inst Brew. 2017 Mar 28;123(1):138–143. https://doi.org/10.1002/jib.391

Wang XS, Du H, Xu Y. Source tracking of prokaryotic communities in fermented grain of Chinese strong-flavor liquor. Int J Food Microbiol. 2017 Mar 6;244:27–35. https://doi.org/10.1016/j.ijfoodmicro.2016.12.018

Wherry ET. Soil acidity and a field method for its measurement. Ecology. 1920 Jul;1(3):160–173. https://doi.org/10.2307/1929133

Whitman WB, Rainey F. Kämpfer P. Trujillo M, Chun J, DeVos P, Hedlund B, Dedysh S. *Petrimonas*. In: Whitman WB, Rainey F. Kämpfer P. Trujillo M, Chun J, DeVos P, Hedlund B, Dedysh S, editors. Bergey's Manual of Systematics of Archaea and Bacteria. Hoboken (USA): John Wiley & Sons, Inc., in association with Bergey's Manual Trust. 2015a; p. 1–2. https://doi.org/10.1002/9781118960608.gbm00245

Whitman WB, Rainey F. Kämpfer P. Trujillo M, Chun J, DeVos P, Hedlund B, Dedysh S. *Proteiniphilum*. In: Whitman WB, Rainey F. Kämpfer P. Trujillo M, Chun J, DeVos P, Hedlund B, Dedysh S, editors. Bergey's Manual of Systematics of Archaea and Bacteria. Hoboken (USA): John Wiley & Sons, Inc., in association with Bergey's Manual Trust. 2015b; p. 1–2. https://doi.org/10.1002/9781118960608.gbm00247

Wu ZY, He F, Qin D, Li HH, Sun JY, Sun XT, Sun BG. Determination of phenolic compounds in alcoholic fermentation materials and spent grains by ultrasound-assisted alkali alcohol extraction coupled with HPLC. Anal Methods. 2019 Sep 27;11(42): 5366–5375. https://doi.org/10.1039/C9AY01739A

Xu ML, Yu Y, Ramaswamy HS, Zhu SM. Characterization of Chinese liquor aroma components during aging process and liquor age discrimination using gas chromatography combined with multivariable statistics. Sci Rep. 2017 Jan 6;7:39671. https://doi.org/10.1038/srep39671

Yamada T, Sekiguchi Y. *Anaerolineaceae*. In: Whitman WB, Rainey F. Kämpfer P. Trujillo M, Chun J, DeVos P, Hedlund B, Dedysh S, editors. Bergey's Manual of Systematics of Archaea and Bacteria. Hoboken (USA): John Wiley & Sons, Inc., in association with Bergey's Manual Trust. 2020; p. 1–5. https://doi.org/10.1002/9781118960608.fbm00301

Yao F, Yi B, Shen CH, Tao F, Liu YM, Lin ZX, Xu P. Chemical analysis of the Chinese liquor Luzhoulaojiao by comprehensive

two-dimensional gas chromatography/time-of-flight mass spectrometry.SciRep.2015Apr10;5:9553.https://doi.org/10.1038/srep09553
Yin Q, Tao Y, Zhu XY, Zhou Y, He XH, Cheng L, Huang Y, Li DP. *Clostridium liquoris* sp. nov., isolated from a fermentation pit used for the production of Chinese strong-flavoured liquor. Int J Syst Evol Microbiol. 2016 Feb 1;66(2):749–754.
https://doi.org/10.1099/ijsem.0.000787
Zhang QY, Yuan YJ, Liao ZM, Zhang WX. Use of microbial indicators combined with environmental factors coupled with metrology tools for discrimination and classification of Luzhou-flavoured pit muds. J Appl Microbiol. 2017 Jul 23;123(4):933–943.
https://doi.org/10.1111/jam.13544
Zhao DR, Jiang YS, Sun JY, Li HH, Luo XL, Zhao MM. Anti-inflammatory mechanism involved in 4-ethylguaiacol-mediated inhibition of LPS-induced inflammation in THP-1 cells. J Agric Food Chem. 2019 Jan 7;67(4):1230–1243.
https://doi.org/10.1021/acs.jafc.8b06263
Zhao DR, Shi DM, Sun JY, Li AJ, Sun BG, Zhao MM, Chen F, Sun XT, Li HH, Huang MQ, Zheng F. Characterization of key aroma compounds in Gujinggong Chinese Baijiu by gas chromatography – olfactometry, quantitative measurements, and sensory evaluation. Food Res Int. 2018 Mar;105:616–627.
https://doi.org/10.1016/j.foodres.2017.11.074
Zhao JS, Zheng J, Zhou RQ, Shi B. Microbial community structure of pit mud in a Chinese strong aromatic liquor fermentation pit. J Inst Brew. 2012 Jan 28;118(4):356–360.
https://doi.org/10.1002/jib.52
Zheng J, Liang R, Zhang LQ, Wu CD, Zhou RQ, Liao XP. Characterization of microbial communities in strong aromatic liquor fermentation pit muds of different ages assessed by combined DGGE and PLFA analyses. Food Res Int. 2013 Nov;54(1):660–666.
https://doi.org/10.1016/j.foodres.2013.07.058
Zheng Q, Lin BR, Wang YB, Zhang QP, He XX, Yang P, Zhou J, Guan X, Huang XH. Proteomic and high-throughput analysis of protein expression and microbial diversity of microbes from 30- and 300-year pit muds of Chinese Luzhou-flavor liquor. Food Res Int. 2015 Sep;75:305–314.
https://doi.org/10.1016/j.foodres.2015.06.029

Polish Journal of Microbiology
2020, Vol. 69, No 2, 165–176
https://doi.org/10.33073/pjm-2020-019

ORIGINAL PAPER

Comparison of Rapid and Routine Methods of Identification and Antibiotic Susceptibility Testing of Microorganisms from Blood Culture Bottles

SADIK AKGUN[1] and HAKAN SEZGIN SAYINER[2]

[1] Adiyaman University, Faculty of Medicine, Department of Medical Microbiology, Adiyaman, Turkey
[2] Adiyaman University, Faculty of Medicine, Department of Infectious Diseases and Clinical Microbiology, Adiyaman, Turkey

Submitted 13 February 2020, revised 15 March 2020, accepted 29 March 2020

Abstract

Reporting of the results of routine laboratory blood culture tests to clinicians is vital to the patients' early treatment. This study aimed to perform identification and antibiotic susceptibility tests of the blood cultures showing positive signals of microbial growth in the first 12 hours of incubation by using centrifugation and Gram staining of 5 ml of liquid from the vial, thus achieving faster results. This study included 152 consecutively incubated blood culture samples showing positive microbial growth signals in the first 12 hours. The samples were centrifuged and then categorized into two groups (Gram-positive and Gram-negative) using Gram staining. Identification and antibiotic susceptibility tests were performed using an automated culture antibiogram device. For routine processing, media inoculated with positive blood culture were kept in the incubator for at least 24 hours. To compare the two methods in terms of the bacteria identification, matrix-assisted laser desorption/ionization time-of-flight mass spectrometry (MALDI-TOF MS) of the growing colony was studied. By Gram staining, the same bacterial strains were obtained for 138 (92%) of the 152 samples, similar to the results of the procedures mentioned earlier. With the samples tested with both methods, the antibiotic susceptibility profiles were compared using the antibiogram results for 1,984 samples that underwent the antibiotic testing. A 97.4% (for 1,934 antibiotic susceptibility assays) agreement was observed between the two methods. Comparing the results of the post-centrifugation Gram staining to those obtained for the specimens using routine procedures, the clinicians reported a high success rate (approximately 97%).

Key words: blood culture, Gram staining, antibiotic susceptibility test, rapid reporting, MALDI-TOF MS

Introduction

Bloodstream infections, especially in intensive care units, are among the most important causes of morbidity and mortality despite the antimicrobial treatment. The early diagnosis and treatment of these infections is clinically vital (Durmaz et al. 2003; Ferreira et al. 2011). For the proper identification and antibiotic susceptibility testing, the bacteria grown in blood culture bottles are sent to laboratories; the detection of bloodstream infections under the appropriate growth conditions, at the appropriate periods, and using the appropriate conventional methods constitute a significant portion of microbiological testing. The recently developed automated systems have been shown to be suitable for bacterial culture, and upon detection of a growth signal, clinicians can remove the bottles from the device and inoculate the sample into media. These media generally include resins or coal particles that absorb antimicrobial agents or other substances that inhibit bacterial growth and may be present in the patient's blood sample (Morrell et al. 2005; Kirn et al. 2014; Nataraj et al. 2016; Jacobs et al. 2017). Early and correct treatment of patients is essential for reducing morbidity and mortality.

For this reason, rapid identification of microorganisms and antibiotic susceptibility testing is crucial. Due to Gram staining of microorganisms in blood cultures, their identification and antibiotic sensitivity results are obtained early, clinicians are informed quickly, and the patient is given the opportunity to start early antibiotic treatment. Continuous monitoring of automated blood

* Corresponding author: S. Akgun, Adiyaman University, Faculty of Medicine, Department of Medical Microbiology, Adiyaman, Turkey; **e-mail: sakgungizem@hotmail.com**

culture systems allows a positive blood culture to be detected within 6 to 24 hours of incubation (Morrell et al. 2005; Behera et al. 2010; Ferreira et al. 2011; Kirn et al. 2014; Nataraj et al. 2016).

In recent years, advances in the methods involving polymerase chain reaction and DNA sequencing have changed the nature of clinical microbiology laboratories. However, the lack of diagnostic tests that are fast, reliable, easy to use, and inexpensive, as well as applicable for use as diagnostic checkpoints is a significant limitation (Tuite et al. 2014; Yis 2015; Caliendo and Hodinka 2017). Although several molecular or proteomic methods (e.g., Matrix-Assisted Laser Desorption/Ionization Time-of-Flight Mass Spectrometry [MALDI-TOF MS]) exist that can be used to direct evaluation of specimens or colonies, the gold-standard methods with the highest sensitivity and safety still remain blood culture-based methods (Mamishi et al. 2005; Behera et al. 2010; Tuite et al. 2014; Yis 2015; Nataraj et al. 2016; Caliendo and Hodinka 2017; Jacobs et al. 2017).

This study aimed to use a different, faster-than-usual method, which involves centrifugation at 12 hours of bacterial culture to allow clinicians to rapidly (in less than 12 hours) complete the antibiotic susceptibility testing. It may be due to more accurate information about the Gram-staining characteristics of growing microorganisms via a positive signal of microbial growth in the incubator.

Experimental

Materials and Methods

Clinical samples. The study included 152 bottles of blood culture (aerobic, pediatric blood culture vials, BD, USA), which gave positive signals in the first 12 hours in the incubator (Bactec FX, BD, USA) out of 2,455 blood culture samples sent from different clinics of our hospital to the Medical Microbiology Laboratory between August 2018 and July 2019. Of these 152 blood culture bottles, 102 were sent from intensive care units, 31 from internal sciences clinics, and 19 from surgical sciences clinics. Of these, 130 belonged to adult patients (≥ 18 years old), and 22 belonged to pediatric patients (< 18 years old).

The rapid method. Centrifugation. Five ml of the inoculating fluid was taken from the positive blood culture vials, and, unlike in the routine procedure, the centrifugation was conducted in a standard blood collection tube (BD Vacutainer 5.0 ml, BD, USA) at 2,000 rpm for 10 minutes. After centrifugation, the blood components (erythrocytes, etc.) were placed under a gel, and the bacteria in the serum adhered to the gel to provide a gelatinous coating that formed a film layer. Then, the supernatant liquid remaining on the gel in the collection tube was slowly discharged. A small number of the bacteria collected in the form of a layer on the gel in the collection tube was removed with a cotton swab and spread on a sterile microscope slide for Gram staining.

Gram staining. After the serum fraction was removed, a few bacteria were taken from the bacterial film layer just above the gel. Then, a small volume of this layer was spread and air-dried on a slide. The air-dried preparations were subjected to Gram staining (Becerra et al. 2016) using a Gram-staining set (Moslab, Ankara, Turkey). For this, crystal violet was poured onto the slide, left for 2 minutes, and washed with water. Then, the Lugol solution was poured, left for 2 minutes, washed with water, then decolorized with alcohol and washed with water. Finally, diluted fuchsin was poured onto the slide, and after 30 seconds, the preparation was washed with water and allowed to air-dry. The preparations were then examined with a microscope with a 100× objective. Based on the results of the study, the strains were defined as Gram-positive or Gram-negative (Figs. 1–4).

Identification and antibiotic susceptibility testing using the rapid method. After Gram staining, the strains of Gram-positive and Gram-negative bacteria or yeast were picked from the gel with a cotton-tipped extruder. Bacteria of a concentration equivalent to a McFarland standard of 0.5–0.63 (for yeasts, 1.8–2.2) were diluted with the manufacturer's identification solution (ID broth, BD, USA). Then, 0.5 µl of the dilution was transferred to the antibiotic susceptibility test solution (AST broth, BD, USA), and identification and antibiotic susceptibility tests were conducted using an automated identification and susceptibility testing system (Phoenix 100, BD, USA) and the appropriate kits (GP ID/AST, GN ID/AST or YEAST ID, BD, USA). The tests run for an average of 8–12 hours, depending on the type of microorganism. The results were reported quickly within 24 hours by the clinician involved.

The routine procedures. For comparison, the microorganisms from bottled blood samples were also cultured on sheep blood agar (SBA), eosin methylene blue (EMB) agar, and some other media without centrifugation and routinely incubated at 37°C for 18–24 hours. The next day, when sufficient growth was observed, routine Gram-staining and antibiotic susceptibility testing were performed. With the help of a sterile loop, a small volume of the colonies grown on the medium was taken and mixed in the identification broth (ID broth, BD, USA). Then, 0.5 µl of the dilution was transferred to the solution for antibiotic susceptibility testing (AST broth, BD, USA). Both solutions were transferred to the appropriate kits. Identification and antibiotic susceptibility tests were conducted using the automated identification and susceptibility testing system (Phoenix 100, BD, USA), and the appropriate

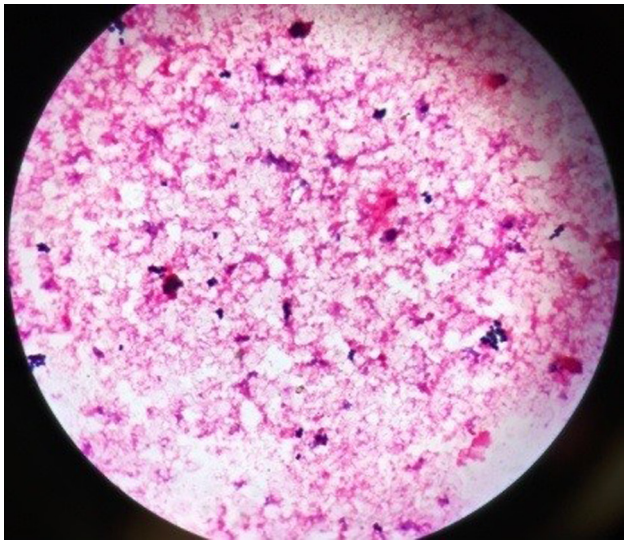

Fig. 1. Microscopic appearance of Gram-positive bacteria after Gram staining with the routine method at a magnification of 1000×.

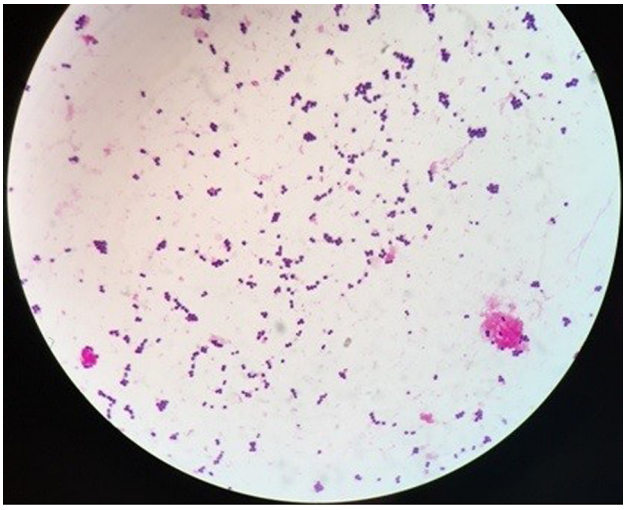

Fig. 2. Microscopic appearance of Gram-positive bacteria after Gram staining with the rapid method at a magnification of 1000×.

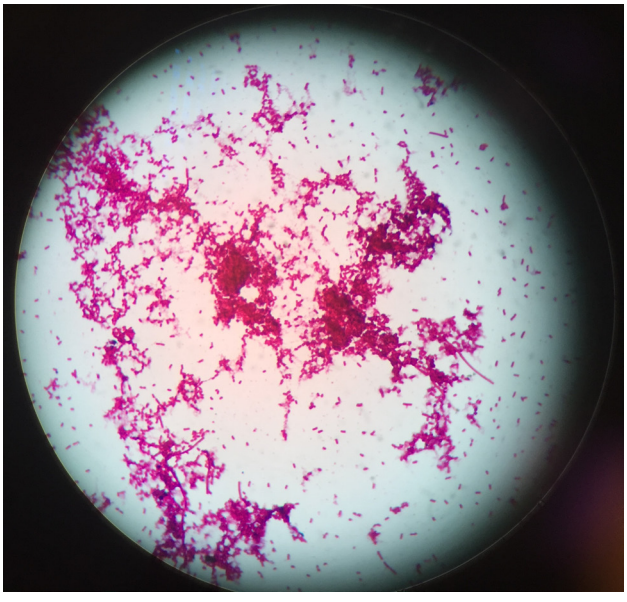

Fig. 3. Microscopic appearance of Gram-negative bacteria after Gram staining with the routine method at a magnification of 1000×.

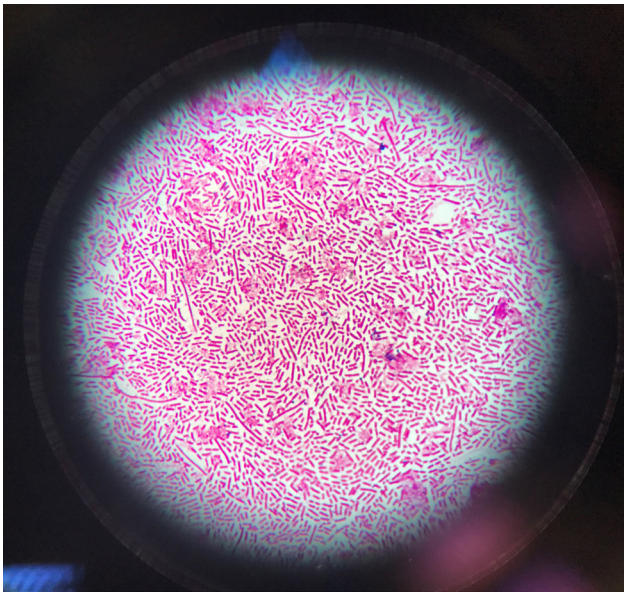

Fig. 4. Microscopic appearance of Gram-negative bacteria after Gram staining with the rapid method at a magnification of 1000×.

kits (GP ID/AST or GN ID/AST, BD, USA). The tests were run for an average of 8–12 hours, depending on the type of microorganism. The results were reported quickly, within 24 hours, by the clinician involved.

MALDI-TOF MS Analysis. The samples were collected with the aid of a sterile loop from colonies of microorganisms grown on the appropriate medium using a routine method, and each bacterial or yeast isolate was transferred to a separate well on a distinct plate in the MALDI-TOF system. One microliter of 70% formic acid (FA) (FA extraction solution, Bruker Daltonik GmbH, Germany) was added to the plate, and after drying at room temperature, 1 µl of α-cyano-4-hydroxycinnamic acid matrix solution (HCCA) (IVD Matrix HCCA, Bruker Daltonik GmbH, Germany) was again dried at room temperature (20–25°C). The dried plates were placed in the instrument (MSP 96 target polished steel, Bruker Daltonik GmbH, Germany) and loaded onto the MALDI-TOF MS (Bruker, Germany) for analysis. At the end of the analysis, the reported microorganisms were recorded using a particular software system (IVD MALDI Biotyper, Bruker Daltonik GmbH, Germany) (Schulthess et al. 2014). For the scoring used in the identification, values were in the range from 0 to 3. Microorganisms with a score ≥ 2 were evaluated as correctly identified at the genus and

species level. A score of 1.7–2 given to organisms indicated a correct identification at the genus level. Organisms with a score of < 1.7 were identified as those that required testing again.

Data analysis. In terms of identification, in the Phoenix 100 Expert System's interpretation, organisms with a reliability > 90 were accepted as being correctly identified. Those with a value of < 90 were considered incorrectly identified. In terms of susceptibility, the minimum inhibitory concentration (MIC) values of the bacteria against the antimicrobials evaluated by both the rapid and routine method were translated into clinical categories (susceptible [S], intermediate [I], or resistant [R]) according to the Phoenix 100 Expert System's interpretive criteria.

For comparison of the results of both methods, the Clinical and Laboratory Standards Institute (CLSI) M52 Verification of Commercial Microbial Identification and Antimicrobial Susceptibility Testing System (Campigotto et al. 2018) was used. According to this methodology, the identification results were divided into three categories: not identified, misidentified (organism was incorrectly identified at the genus or species level [discrepancy]), and full consistency (accurate identification at the same genus and species level by both methods). For the antibiotic susceptibility results, the discrepancies were classified as minor errors (mEs: susceptible/resistant versus intermediate susceptibility), major errors (MEs: false resistant, considered as resistant susceptibility by one method but susceptible by the other method), and very major errors (VMEs: false susceptibility).

Statistical analysis. The statistical analyses were performed using software (SPSS 15.0, IBM, USA). The results of the continuous data analyses were given as minimum, maximum, median, and mean values, and the results of some categorical variables were given as frequencies and percentages.

Results

A positive signal, which was a bacterial growth marker, was recorded for 152 bottles of blood culture included in the study. They were sent from 102 (67.1%) intensive care units (84 internal intensive care, nine coronary intensive care, and nine pediatric intensive care), 31 (20.4%) from internal clinics (15 internal medicine clinics, ten oncology/hematology clinics, and six pediatric clinics), and 19 (12.5%) from surgical clinics (10 general surgery clinics, seven pediatric surgery clinics, and two gynecology clinics). Of the 152 samples, 130 (85.5%) came from adult patients and 22 (14.5%) from pediatric patients. Of the patients, 82 (54%) were female, 70 (46%) were male, and the youngest patient was one year old, while the oldest was 89 years old (their mean age was 57.5). Because of the lack of blood-based elements in the bacterial layer and the presence of a more significant number of microorganisms than usual, the images of the microorganisms obtained by microscopic examination following Gram staining after centrifugation were more satisfactory in terms of their quality and quantity than those obtained following Gram staining without centrifugation.

According to the results obtained, of the 152 samples included in the study, 150 (98.7%) contained only one type of bacteria. While 116 (77.3%) of these 150 strains stained as Gram-positive (107 cocci and nine bacilli), and 30 (20%) stained as Gram-negative bacilli. The remaining four strains (2.7%) stained as Gram-positive, but they were placed in a separate category because they were yeast. In the other two (1.3%) samples, two bacterial species (*Escherichia coli* and *Staphylococcus aureus*), one Gram-positive and one Gram-negative were detected. In the microscopic examination of the stained cells, these two specimens, that contained more than one type of microorganism, were not evaluated because these bacteria could not be separately tested for antibiotic susceptibility and because the bacteria must be inoculated onto appropriate media. In other words, these two samples were passaged and terminated 18–24 hours after incubation according to routine procedures.

For the identification and antibiotic susceptibility testing, 116 (77.3%) of the 150 microbial strains were analyzed using GP ID/AST kits because these strains were detected as being Gram-positive by Gram staining, and 30 (20%) strains evaluated using GN ID/AST kits because these strains were detected as being Gram-negative by Gram staining. Furthermore, four samples were determined using a YEAST/ID kit because they were observed as yeast in the Gram staining (Table I).

According to the results obtained the following morning, of the 116 Gram-positive strains studied by MALDI-TOF MS analysis, 71 (61.2%) were identified as coagulase-negative *Staphylococcus* (CoNS), and seven (6.0%) were identified as *Staphylococcus aureus*

Table I
Distribution of microorganisms detected by Gram staining after centrifugation according to the rapid method procedure.

Gram-staining result	n (%)
Gram-positive cocci	107 (70.4)
Gram-negative bacilli	30 (19.7)
Gram-positive bacilli	9 (5.3)
Gram-positive cocci + Gram-negative bacilli	2 (1.3)
Yeast (*Candida* spp.)	4 (2.6)
Total number of samples	152 (100)

n – number

Table II
Distribution of bacteria identified by both methods at the genus and species level.

Rapid method	n (%)	Routine method	n (%)
Gram-positive bacteria (total)	**116**	**Gram-positive bacteria (total)**	**116**
Staphylococcus aureus	7 (6.0)	***Staphylococcus aureus***	8 (6.9)
MRSA: 2, MSSA: 5		MRSA: 3, MSSA: 5	
Coagulase-negative Staphylococci	**71 (61.2)**	***Coagulase-negative Staphylococci***	
Staphylococcus epidermidis: 45		*Staphylococcus epidermidis: 48*	**76 (65.5)**
Staphylococcus hominis: 16		*Staphylococcus hominis: 18*	
Staphylococcusschleiferi: 4		*Staphylococcusschleiferi: 4*	
Staphylococcus haemolyticus: 2		*Staphylococcus haemolyticus: 2*	
Staphylococcus capitis: 2		*Staphylococcus capitis: 2*	
Staphylococcus warneri: 2		*Staphylococcus warneri: 2*	
Enterococci	**20 (17.2)**	***Enterococci***	**20 (17.2)**
Enterococcus faecalis: 18		*Enterococcus faecalis: 18*	
Enterococcus faecium: 2	3 (2.6)	*Enterococcus faecium:* 2	2 (1.8)
Arcanobacterium haemolyticum	3 (2.6)	*Arcanobacterium haemolyticum*	2 (1.8)
Bacillus cereus/subtilis	2 (1.8)	*Bacillus subtilis*	2 (1.8)
Dermacoccus nishinomiyaensis	4 (3.5)	*Dermacoccus nishinomiyaensis*	2 (1.8)
Micrococcus luteus/lylae	3 (2.6)	*Micrococcus luteus/lylae*	2 (1.8)
Corynebacterium amycolatum	3 (2.6)	*Corynebacterium amycolatum*	2 (1.8)
Corynebacterium jeikeium		*Corynebacterium jeikeium*	
Gram-negative bacteria (total)	**30**	**Gram-negative bacteria (total)**	**30**
Escherichia coli	15 (50)	*Escherichia coli*	15 (50)
Pseudomonas aeruginosa	5 (16.7)	*Pseudomonas aeruginosa*	5 (16.7)
Klebsiella pneumoniae	5 (16.7)	*Klebsiella pneumoniae*	5 (16.7)
Stenotrophomonas maltophilia	3 (10.0)	*Stenotrophomonas maltophilia*	3 (10.0)
Acinetobacter baumannii	2 (6.7)	*Acinetobacter baumannii*	2 (6.7)
Yeasts	**4**	**Yeasts**	**4**
Candida parapsilosis	2 (50)	*Candida parapsilosis*	2 (50)
Candida tropicalis	2 (50)	*Candida tropicalis*	2 (50)

MRSA – methicillin-resistant *Staphylococcus aureus*; MSSA – methicillin-susceptible *Staphylococcus aureus*; n – number

(one isolate, identified as *S. epidermidis*, was, in fact, methicillin-resistant *S. aureus* [MRSA] as demonstrated with both the routine method and the MALDI-TOF system), while 20 (17.2%) were *Enterococcus* species. These values, when studied by the routine method, were as follows: 76 (65.5%), 8 (6.9%), and 20 (17.2%), respectively. No isolates of vancomycin-resistant enterococci (VRE) were found in this study. In addition, 15 (50%) of Gram-negative isolates were identified as *E. coli*, five as *P. aeruginosa*, five as *Klebsiella pneumoniae,* three as *Stenotrophomonas maltophilia,* and two as *Acinetobacter baumannii*. When the yeast isolates were analyzed using the appropriate kit (YEAST/ID, BD, USA) and the appropriate McFarland (1.8–2.2) standard (BD PhoenixSpec, BD, USA), the results obtained by both methods were found to be fully compatible (two of the four specimens were identified as *Candida parapsilosis* and the other two as *Candida tropicalis*) (Table II).

Two of the three strains identified as *S. epidermidis* were identified by MALDI-TOF as *Micrococcus luteus/lylae,* and one was identified as *Arcanobacterium haemolyticum.* One isolate was identified as *Corynebacterium amycolatum,* which should have been identified as *S. aureus.* One of the two isolates, which should have been identified as *Staphylococcus hominis*, was identified as *Bacillus cereus/subtilis*, and the other was identified as *Corynebacterium jeikeium*. As a result, 138 (92%) out of 150 isolates were correctly identified, while the number misidentified was only 12. In fact, all false identifications at the genus or species level were also associated with Gram-positive bacteria (Table III).

These values were compared with the identification and antibiotic susceptibility results obtained by the routine procedures. According to this comparison, for 138 (92%) of the 150 strains studied, the same results for the identification testing were obtained using

Table III
Distribution of the identified species according to MALDI-TOF MS results when working with both methods.

Organisms	MALDI-TOF Biotyper scores < 1.7; 1.7–2.0; ≥ 2 n n n Total	Rapid method n	Routine method n
Gram-positive bacteria	**116**	**116**	**116**
Staphylococcus aureus	0 0 8 8	7	8
Staphylococcus epidermidis	0 12 36 48	45	48
Staphylococcus hominis	0 2 16 18	16	18
Staphylococcusschleiferi	0 0 4 4	4	4
Staphylococcus haemolyticus	0 0 2 2	2	2
Staphylococcus capitis	0 0 2 2	2	2
Staphylococcus warneri	0 0 2 2	2	2
Enterococcus faecalis	0 0 18 18	18	18
Enterococcus faecium	0 0 2 2	2	2
Arcanobacterium haemolyticum	0 1 1 2	3	2
Bacillus cereus/subtilis	0 0 0 0	1	0
Bacillus subtilis	0 0 2 2	2	2
Dermacoccus nishinomiyaensis	0 0 2 2	2	2
Micrococcus luteus/lylae	0 1 1 2	4	2
Corynebacterium amycolatum	0 1 1 2	3	2
Corynebacterium jeikeium	0 1 1 2	3	2
Gram-negative bacteria	**30**	**30**	**30**
Escherichia coli	0 0 15 15	15	15
Pseudomonas aeruginosa	0 1 4 5	5	5
Klebsiella pneumoniae	0 0 5 5	5	5
Stenotrophomonas maltophilia	0 0 3 3	3	3
Acinetobacter baumannii	0 0 2 2	2	2
Yeasts	**4**	**4**	**4**
Candida parapsilosis	0 0 2 2	2	2
Candida tropicalis	0 0 2 2	2	
Total	0 19 131 150	150	150

MALDI-TOF MS – matrix-assisted laser desorption/ionization time-of-flight mass spectrometry; n – number

both methods, demonstrating complete consistency between the two methods. However, a discrepancy was detected between the two methods for 12 (8%) strains, with small differences observed in only Gram-positive bacteria. Conversely, for the 30 Gram-negative strains, 100% consistency was observed between the rapid method and the MALDI-TOF MS system. Two samples were terminated without processing because they contained more than one type of microorganism (polymicrobial) and were not evaluated. Therefore, when the identification and antibiotic susceptibility tests of all the Gram-negative bacteria were compared, no discrepancy occurred between the results from either method (of the 150 strains, 30 [20%] Gram-negative bacilli continued to be studied; the same identification and antibiotic susceptibility results were obtained with both methods). No difference was observed between the results obtained by both methods for all strains of enterococci belonging to Gram-positive bacteria (20 [13.3%] of the 150 strains). However, when other Gram-positive bacteria were evaluated, a small inconsistency (identification of different microorganisms at the genus or species level using each method) equal to 8% was observed between these methods. In addition, this inconsistency was also observed in the results obtained for the Gram-positive strains, which can be regarded as indicative of contamination (Table IV).

The agreement for the AST results performed by both methods are the same in terms of the MIC values (100% of similarity) for most of the antimicrobials (e.g.,

Table IV
Analysis of the compatibility between the identification results of the rapid method when compared with the MALDI-TOF MS.

Bacteria	Full consistency n (%)	Misidentified n (%)	Not identified n (%)
Gram-positive bacteria	104 (89.7)	12 (10.3)	0
Gram-negative bacteria	30 (100)	0	0
Yeasts	4 (100)	0	0
Total	138 (92)	12 (8)	0

MALDI-TOF MS – matrix-assisted laser desorption/ionization time-of-flight mass spectrometry; n – number

vancomycin, teicoplanin, ampicillin, and linezolid), whereas the lowest agreement value was obtained for the piperacillin/tazobactam combination (Table V). However, when all the antibiotic susceptibility results between the two methods were examined, the ratio of the full agreement was 97.4%, the VME ratio (0.8%) was slightly higher than the ME ratio (0.1%), and the mE value was found as expected: 33 (1.7%) (Table VI).

Table V
Distribution of the resistance profiles for Gram-positive and Gram-negative bacteria as a result of the antibiotic susceptibility testing when both methods were applied.

Antibiotics	The rapid method, n (%)			The routine method, n (%)		
	S	I	R	S	I	R
Amikacin	28 (93.3)	–	2 (6.7)	28 (93.3)	–	2 (6.7)
Ampicillin	18 (19.1)	–	76 (80.9)	18 (19.1)	–	76 (80.9)
Amoxicillin/Clavulanic acid	18 (15.8)	–	96 (84.2)	18 (15.8)	–	96 (84.2)
Aztreonam	18 (60)	1 (3.3)	11 (36.7)	15 (50)	–	15 (50)
Cefepime	20 (66.7)	–	10 (33.3)	14 (46.7)	–	16 (53.3)
Cefoxitin	–	36 (41.9)	50 (58.1)	–	35 (40.7)	51 (59.3)
Ceftazidime	10 (33.3)	10 (33.3)	10 (33.3)	10 (33.3)	10 (33.3)	10 (33.3)
Ceftriaxone	18 (60)	–	12 (40)	18 (60)	–	12 (40)
Ciprofloxacin	82 (66.1)	–	42 (33.9)	66 (53.2)	10 (8.1)	48 (38.7)
Colistin	30 (100)	–	–	30 (100)	–	–
Clindamycin	50 (53.2)	1 (1.1)	43 (45.7)	51 (554.3)	–	43 (45.7)
Daptomycin	71 (75.5)	23 (24.5)	–	65 (69.1)	29 (30.9)	–
Ertapenem	28 (93.3)	–	2 (6.7)	28 (93.3)	–	2 (6.7)
Erythromycin	14 (14.9)	–	80 (85.1)	14 (14.9)	–	80 (85.1)
Fusidic acid	35 (40.7)	–	51 (59.3)	36 (41.9)	–	50 (58.1)
Gentamicin	66 (53.2)	–	58 (46.8)	66 (53.2)	1 (0.8)	57 (50)
Imipenem	28 (93.3)	–	2 (6.7)	28 (93.3)	–	2 (6.7)
Meropenem	28 (93.3)	–	2 (6.7)	28 (93.3)	–	2 (6.7)
Linezolid	94 (100)	–	–	94 (100)	–	–
Oxacillin	12 (12.8)	–	82 (87.2)	12 (12.8)	–	82 (87.2)
Piperacillin/Tazobactam	10 (33.3)	10 (33.3)	10 (33.3)	16 (53.3)	2 (6.7)	12 (40)
Rifampin	62 (66)	–	32 (34)	62 (66)	–	32 (34)
Teicoplanin	94 (100)	–	–	94 (100)	–	–
Tetracycline	35 (40.7)	–	51 (59.3)	35 (40.7)	–	51 (59.3)
Tigecycline	84 (89.4)	8 (8.5)	2 (2.1)	86 (91.5)	6 (6.4)	2 (2.1)
TMP/SX	55 (44.4)	–	69 (55.6)	51 (41.1)	3 (2.4)	70 (56.5)
Vancomycin	94(100)	–	–	94 (100)	–	–
Total	1102 (55.5)	89 (4.5)	793 (40)	1077 (54.3)	96 (4.8)	811 (40.9)

n – number; I – intermediate; R – resistant; S – susceptible; TMP/SX – Trimethoprim/Sulfamethoxazole

Table VI
Categorical distribution of discrepancies in the antibiotic susceptibility results of the rapid method compared to the routine method.

Antibiotics	Agreement n (%)	mEs n (%)	MEs n (%)	VMEs n (%)	Total n
Amikacin	30 (100)				30
Ampicillin	94 (100)				94
Amoxicillin/Clavulanic acid	114 (100)				114
Aztreonam	26 (86.7)	1 (3.3)		3 (10)	30
Cefepime	24 (80)			6 (20)	30
Cefoxitin	85 (98.8)	1 (1.2)			86
Ceftazidime	30 (100)				30
Ceftriaxone	30 (100)				30
Ciprofloxacin	108 (87.1)	10 (8.1)		6 (4.8)	124
Colistin	30 (100)				30
Clindamycin	93 (98.9)	1 (1.1)			94
Daptomycin	88 (93.6)	6 (6.4)			94
Ertapenem	30 (100)				30
Erythromycin	94 (100)				94
Fusidic acid	85 (98.8)		1 (1.2)		86
Gentamicin	123 (99.2)	1 (0.8)			124
Imipenem	30 (100)				30
Meropenem	30 (100)				30
Linezolid	94 (100)				94
Oxacillin	94 (100)				94
Piperacillin/Tazobactam	22 (73.3)	8 (26.7)			30
Rifampin	94 (100)				94
Teicoplanin	94 (100)				94
Tetracycline	86 (100)				86
Tigecycline	92 (97.9)	2 (2.1)			94
TMP/SX	120 (96.8)	3 (2.4)		1 (0.8)	124
Vancomycin	94 (100)				94
Total	1934 (97.4)	33 (1.7)	1 (0.1)	16 (0.8)	1984

n – number; mEs – minor errors; MEs – major errors; TMP/SX – Trimethoprim/Sulfamethoxazole; VMEs – very major errors

Discussion

To date, a limited number of studies have been conducted to use rapid methods to determine the type of organisms that grow in blood cultures and evaluate their antibiotic susceptibility. However, the rapid identification of infectious agents circulating in patients' blood and the determination of the species and the correct antibiotic to be used will shorten the treatment time by 12 hours, and reduce the cost. The early identification of bloodstream infections allows for the early modification of antimicrobial treatment and a diminished need for other diagnostic tests. Thus, patients' hospital stay can be shortened, and expenditures on patients can be reduced (Beekmann et al. 2003).

In a study conducted by a group of researchers, 501 microorganisms from blood-circulating infections were detected in the patients with bacteremia or candidiasis with MALDI-TOF with the Antimicrobial Stewardship Team test. MALDI-TOF analysis of 245 patients in the intervention group and 256 patients in the preintervention group showed reductions in the identification times (84 hours to 56 hours), effective antibiotic treatment times (30 to 20 hours), and optimal antibiotic treatment times (90 to 47 hours) for the organism (Huang et al. 2013). Our study reports the identification and antibiotic susceptibility tests that are much shorter (< 24 hours) than conventional tests (routinely > 72 hours). In contrast to routine tests, this study achieved 97% success without having to use any expensive methods.

In a study (Dodemont et al. 2014), nucleic acid-based tests were performed on Gram-positive and Gram-negative bacteria from blood cultures; the test

was designed to rapidly identify multiple bacterial strains and the resistance associated with these strains. This method was compared with the routine method for 117 isolates, and the identification and antibiotic resistance markers were reported as correct and accurate, achieving 97% and 92% rates of detection of pathogens from the blood cultures and reduced laboratory times. In our study, the observed 92% accurate identification and 97% antibiotic susceptibility compliance results were similar.

In another study (Mancini et al. 2014), a total of 102 positive blood cultures were tested with the Verigene BC-GN test, which detected certain Gram-negative bacteria and selected resistance genes. Ninety-eight percent of the isolates were correctly identified, and 29% were identified as those carrying the resistance genes (CTX-M, KPC, VIM, and OXA genes). The other researchers (Hill et al. 2014) included 54 blood culture samples that gave positive signals between 7 and 23 hours using the Verigene BC-GN test, and correctly identified 51 of these samples as Gram-negative bacilli, whereas Mancini et al. (2014)) reported that they correctly identified the full-length carbapenemase enzyme. In a test run, the identification of the organisms was reported to be faster than the conventional method by an average of 24 hours. The other group (Sothoron et al. 2015) studied the blood cultures of 126 patients with Gram-negative bacteremia using an antimicrobial stewardship program test. In a study evaluating the VITEK 2 system with the Verigene BC-GN test, the mean survival rate in the optimal treatment was shorter in the post-intervention group than in the pre-intervention group (38 to 49 hours, respectively). The rapid method in our study does not require any additional costs, systems, or devices, and it is 24 hours shorter than the method in the abovementioned study. We believe our method can be used for all bacteria instead of only certain bacteria.

The MALDI-TOF and a VITEK 2 system were used together in a study by Machen and coworkers (Machen et al. 2014) performed to the same-day identification and the full panel antimicrobial susceptibility testing of bacteria from a total of 100 positive blood culture bottles. Compared to conventional methods, the direct results were 94% correctly identified with the VITEK system, and the identification and antibiograms were concluded on the same day. In our study, direct results were also reported, with a high success rate of 94% being achieved (without 24 hours of incubation) using 5 ml of liquid from the blood culture fluid and without the need for a device that adds costs to the conventional method.

In a study conducted by another group of researchers (Banerjee et al. 2015), the detection of bacterial and fungal resistance genes in the strains directly identified in 617 positive blood cultures was performed using a direct rapid multiplex PCR (rmPCR). It was followed by the evaluation of the treatment duration and mortality. The shortest period after Gram staining needed to appropriate evaluation of antimicrobial susceptibility was achieved by rmPCR. These results allowed for the reduction of mortality and the use of antibiotics. Because we were working with fewer samples in our study (which would not significantly change the results), the rapid delivery of blood culture results was critical to the patient; in terms of cost, the centrifugation of blood culture bottles with positive signals required no extra cost, and this method was used to obtain faster results (< 24 hours).

In a study by Stevenson et al. (2010), a total of 212 patient samples, 179 of which were positive blood cultures and 33 of which were isolated broth species, were prepared and processed for MALDI-TOF analysis. In this study, 42 strains (12 *Propionibacterium acnes* and seven *S. epidermidis*) with spectral scores < 1.7 could not be identified. Twenty-four strains with scores between 1.7 and 1.9 were correctly identified (six were *S. epidermidis*). The strains with scores of 1.9 were correctly identified at the species level. Similarly, in our study, the species determination and antibiotic susceptibility testing of strains from a single-species culture in the blood cultures were performed using a rapid method. Alternatively, for rapid reporting (97% success) of the antibiotic susceptibility results, we used a direct analysis with a centrifugation process. Notably, the use of mass spectrometry technology can only be established in large laboratories.

The other researchers (Lupetti et al. 2010) studied 57 blood cultures that were collected from different clinics and found to be a single-species culture of Gram-positive cocci by Gram staining. The addition of saponin in the new procedure was compared with the routine method. Discrepancies between the two methods were resolved by ID32 Staph or by Rapid ID32 Strep and E-test. With the new method, 44 (80%) of the Gram-positive cocci were detected as CoNS (34 [62%] *S. epidermidis*). In our study, unlike the one above, not only Gram-positive bacteria but also other bacteria and yeasts were studied. In addition, saponin or a similar substance was not used in this study. Among the identification values obtained by the rapid method, the CoNS rate was slightly lower (62%). Although our antibiotic susceptibility findings were similar, we notably had few VMEs, which maybe because of the presence of gel in the tubes.

In another study (Chen et al. 2015), Gram staining was performed after samples were cultured on blood; this method was performed on 400 positive-signal blood cultures on weekdays between 8:00 am and 3:00 pm. Samples that were a single species culture after the Gram staining were included in the study. While

358 (89.5%) isolates were identified correctly by VITEK MS, 343 (85.8%) were identified correctly at the species level, and 15 (3.7%) were identified correctly at the genus level. Of these definitions, 146 (96.1%) isolates of 152 Gram-negative bacilli (78 *E. coli* and 25 *Klebsiella* species isolates) were correctly identified, while 197 (79.4%) isolates of 248 Gram-positive organisms (76 of 95 CoNS and 56 of 58 *S. aureus*) were correctly identified. In our study, Gram-negative bacilli and yeasts were correctly identified in 100%, and Gram--positive bacteria were correctly identified in approximately 90%. These identifications were obtained without any culturing on media or incubation after centrifugation; instead, the identification occurred by loading directly into the culture antibiogram device. In addition, enterococci were also completely identified when compared with MALDI-TOF MS.

In one study (Tian et al. 2016), 485 positive specimens were evaluated by injecting various body fluids into blood culture bottles. Then, the researchers combined MALDI-TOF MS with a VITEK AST system and conducted rapid microbial identification (RMI), and rapid multiple AST (RMAST). Then, the RMAST results were compared with the standard method results. Discrepancies in the MIC values were resolved by broth dilution, according to CLSI (2015) guidelines. RMI correctly identified Gram-negative and Gram-positive bacteria (98.9%, and 87.2%, respectively), and fungi (75.7%). As a result, the RMI and RMAST were completed 18–36 hours in advance of the report notification. In our study, only blood cultures were evaluated. A longer centrifugation time with a lower speed was utilized. After comparable identification and antibiotic susceptibility testing procedures, similar results were obtained. Our report notifications were made within 24 hours.

Recently, in a study conducted by Campigottoa et al. (2018), MALDI-TOF MS analysis was used for the identification of bacteria directly from blood cultures, followed by antibiotic susceptibility tests and rapid determination of methicillin-resistance and beta-lactam-resistance status. A total of 125 positive blood cultures sent from various intensive care units were included in the study. The VITEK 2 system and appropriate AST cards were used to determine the antibiotic susceptibility, and standard procedures were applied. When compared with the routine method, 91.2% were correctly identified at the genus level, 82.4% had species-level compatibility, and eight unidentified isolates at the genus level were Gram-positive organisms. Gram-negative bacteria were detected at a high species level of 100% and 93%, respectively. All four fungal isolates *C. albicans*, *C. parapsilosis,* and *C. tropicalis* were correctly identified at the species level. In contrast to the above study, in our study, the centrifugation time was longer, the rpm was lower, and the bacterial suspension was prepared and loaded directly onto the Phoenix 100 instrument. Similar error rates (2.6% in total) and agreement (97%) were observed. Furthermore, in our study, the goal of reporting results in 24 hours was successfully achieved.

Conclusions

The search for methods that do not require additional financing and are widely available is on-going. In this study, 5 ml of blood samples were taken directly from blood cultures with positive signals, and the results were obtained within 24 hours. It was achieved with centrifugation, Gram staining, and an appropriate antimicrobial panel (Gram-positive or Gram-negative). The Gram-negative strains were reported with 100% consistency, and the Gram-positive strains were reported with 90% consistency among the new and routine methods. For the Gram-positive bacteria that were inconsistently identified with these methods, we believe that further studies in this area will help to distinguish pathogenic and nonpathogenic strains. In particular, we believe that unnecessary antibiotic treatments can be avoided for patients infected with Gram-positive bacteria, which can be identified as contaminants sooner than Gram-negative bacteria. Due to the rapid culture antimicrobial susceptibility testing used in this study, antibiotic therapies could begin early, since the patients' blood culture results will be reported very quickly (in about 12 hours) without the need for extra costs. In addition, since this can shorten the length of hospital stay of patients, medical and economic benefits will be achieved at the national level. We also believe that the volume of the sample taken directly from the bottles should be increased (to at least 10 ml) and that employees should have sufficient experience; then, the efficiency of this method can be higher. However, the most crucial limitation of this method is the presence of more than one species in the blood cultures (polymicrobial cultures). Finally, the rapid method used in the study allows obtaining the diagnosis of bloodstream infections in a short span of 12 hours and with an accuracy of 97% (100% for Gram-negative bacteria).

List of abbreviations

AST – antibiotic susceptibility test
BC-GN – Gram-negative blood culture
CLSI – Clinical and Laboratory Standards Institute
CoNS – coagulase-negative *Staphylococcus*
EMB – eosin methylene blue
FA – formic acid
GN – Gram-negative
GP – Gram-positive
HCCA – α-cyano-4-hydroxycinnamic acid matrix solution

ID – identification
MALDI-TOF MS – matrix-assisted laser desorption/ionization time-of-flight mass spectrometry
ME – major error
mE – minor error
MIC – minimum inhibitory concentration
MRSA: methicillin-resistant *Staphylococcus aureus*
RMAST – rapid multiple AST
RMI – rapid microbial identification
rmPCR – rapid multiplex PCR
SBA – sheep blood agar
VME – very major error

Authors' contributions

SA and HSS participated in the study design and coordination and conducted the data analyses. SA participated in and performed the measurements, laboratory testing, and data collection. All authors read and approved the final manuscript. All authors contributed to the draft of the manuscript and discussed the results. All authors gave final approval for publication.

ORCID
Sadik Akgun: https://orcid.org/0000-0002-1413-0450
Hakan Sezgin Sayiner: https://orcid.org/0000-0002-4693-3784

Acknowledgments

Thanks to the staff of our hospital's culture laboratory for their contributions.

Conflict of interest

The authors do not report any financial or personal connections with other persons or organizations, which might negatively affect the contents of this publication and/or claim authorship rights to this publication.

Literature

Banerjee R, Teng CB, Cunningham SA, Ihde SM, Steckelberg JM, Moriarty JP, Shah ND, Mandrekar JN, Patel R. Randomized trial of rapid multiplex polymerase chain reaction-based blood culture identification and susceptibility testing. Clin Infect Dis. 2015 Oct 01;61(7):1071–1080. https://doi.org/10.1093/cid/civ447

Becerra SC, Roy DC, Sanchez CJ, Christy RJ, Burmeister DM. An optimized staining technique for the detection of Gram positive and Gram negative bacteria within tissue. BMC Res Notes. 2016 Dec;9(1):216. https://doi.org/10.1186/s13104-016-1902-0

Beekmann SE, Diekema DJ, Chapin KC, Doern GV. Effects of rapid detection of blood stream infections on length of hospitalization and hospital charges. J Clin Microbiol. 2003;41(7):3119–3125. https://doi.org/10.1128/JCM.41.7.3119-3125.2003

Behera B, Mathur P, Gupta B. Blood culture gram stain, acridine orange stain and direct sensitivity-based antimicrobial therapy of bloodstream infection in patients with trauma. Indian J Med Microbiol. 2010;28(2):138–142. https://doi.org/10.4103/0255-0857.62491

Caliendo AM, Hodinka RL. A CRISPR way to diagnose infectious diseases. N Engl J Med. 2017 Oct 26;377(17):1685–1687. https://doi.org/10.1056/NEJMcibr1704902

Campigotto A, Goneau L, Matukas LM. Direct identification and antimicrobial susceptibility testing of microorganisms from positive blood cultures following isolation by lysis-centrifugation. Diagn Microbiol Infect Dis. 2018 Nov;92(3):189–193. https://doi.org/10.1016/j.diagmicrobio.2018.06.010

Chen Y, Porter V, Mubareka S, Kotowich L, Simor AE. Rapid identification of bacteria directly from positive blood cultures by use of a serum separator tube, smudge plate preparation, and matrix-assisted laser desorption ionization–time of flight mass spectrometry. J Clin Microbiol. 2015 Oct;53(10):3349–3352. https://doi.org/10.1128/JCM.01493-15

Dodémont M, De Mendonça R, Nonhoff C, Roisin S, Denis O. Performance of the Verigene Gram-negative blood culture assay for rapid detection of bacteria and resistance determinants. J Clin Microbiol. 2014 Aug 01;52(8):3085–3087. https://doi.org/10.1128/JCM.01099-14

Durmaz G, Us T, Aydinli A, Kiremitci A, Kiraz N, Akgün Y. Optimum detection times for bacteria and yeast species with the BACTEC 9120 aerobic blood culture system: evaluation for a 5-year period in a Turkish university hospital. J Clin Microbiol. 2003 Feb 01;41(2):819–821. https://doi.org/10.1128/JCM.41.2.819-821.2003

Ferreira L, Sánchez-Juanes F, Porras-Guerra I, García-García MI, García-Sánchez JE, González-Buitrago JM, Muñoz-Bellido JL. Microorganisms direct identification from blood culture by matrix-assisted laser desorption/ionization time-of-flight mass spectrometry. Clin Microbiol Infect. 2011 Apr;17(4):546–551. https://doi.org/10.1111/j.1469-0691.2010.03257.x

Hill JT, Tran KDT, Barton KL, Labreche MJ, Sharp SE. Evaluation of the nanosphere Verigene BC-GN assay for direct identification of Gram-negative bacilli and antibiotic resistance markers from positive blood cultures and potential impact for more-rapid antibiotic interventions. J Clin Microbiol. 2014 Oct 01;52(10):3805–3807. https://doi.org/10.1128/JCM.01537-14

Huang AM, Newton D, Kunapuli A, Gandhi TN, Washer LL, Isip J, Collins CD, Nagel JL. Impact of rapid organism identification via matrix-assisted laser desorption/ionization time-of-flight combined with antimicrobial stewardship team intervention in adult patients with bacteremia and candidemia. Clin Infect Dis. 2013 Nov 1;57(9):1237–1245. https://doi.org/10.1093/cid/cit498

Jacobs MR, Mazzulli T, Hazen KC, Good CE, Abdelhamed AM, Lo P, Shum B, Roman KP, Robinson DC. Multicenter clinical evaluation of BacT/Alert virtuo blood culture system. J Clin Microbiol. 2017 Aug;55(8):2413–2421. https://doi.org/10.1128/JCM.00307-17

Kirn TJ, Mirrett S, Reller LB, Weinstein MP. Controlled clinical comparison of BacT/alert FA plus and FN plus blood culture media with BacT/alert FA and FN blood culture media. J Clin Microbiol. 2014 Mar 01;52(3):839–843. https://doi.org/10.1128/JCM.03063-13

Lupetti A, Barnini S, Castagna B, Capria AL, Nibbering PH. Rapid identification and antimicrobial susceptibility profiling of Gram-positive cocci in blood cultures with the Vitek 2 system. Eur J Clin Microbiol Infect Dis. 2010 Jan;29(1):89–95. https://doi.org/10.1007/s10096-009-0825-2

Machen A, Drake T, Wang YF. Same day identification and full panel antimicrobial susceptibility testing of bacteria from positive blood culture bottles made possible by a combined lysis-filtration method with MALDI-TOF VITEK mass spectrometry and the VITEK2 system. PLoS One. 2014;9(2):e87870. https://doi.org/10.1371/journal.pone.0087870

Mamishi S, Pourakbari B, Ashtiani MH, Hashemi FB. Frequency of isolation and antimicrobial susceptibility of bacteria isolated from bloodstream infections at Children's Medical Center, Tehran, Iran, 1996–2000. Int J Antimicrob Agents. 2005 Nov;26(5):373–379. https://doi.org/10.1016/j.ijantimicag.2005.08.004

Mancini N, Infurnari L, Ghidoli N, Valzano G, Clementi N, Burioni R, Clementi M. Potential impact of a microarray-based

nucleic acid assay for rapid detection of Gram-negative bacteria and resistance markers in positive blood cultures. J Clin Microbiol. 2014 Apr 01;52(4):1242–1245.
https://doi.org/10.1128/JCM.00142-14

Morrell M, Fraser VJ, Kollef MH. Delaying the empiric treatment of candida bloodstream infection until positive blood culture results are obtained: a potential risk factor for hospital mortality. Antimicrob Agents Chemother. 2005 Sep 01;49(9):3640–3645.
https://doi.org/10.1128/AAC.49.9.3640-3645.2005

Nataraj G, Surase PV, Pattamadai K, Mehta PR, Pazare AR, Agarwal MC, Nanavati RN. An appropriately performed conventional blood culture can facilitate choice of therapy in resource-constrained settings-comparison with BACTEC 9050. J Postgrad Med. 2016;62(4):228–234.
https://doi.org/10.4103/0022-3859.184958

Schulthess B, Bloemberg GV, Zbinden R, Böttger EC, Hombach M. Evaluation of the Bruker MALDI Biotyper for Identification of Gram-Positive Rods: Development of a Diagnostic Algorithm for the Clinical Laboratory. J Clin Microbiol. 2014;52(4):1089–1097.
https://doi.org/10.1128/JCM.02399-13

Sothoron C, Ferreira J, Guzman N, Aldridge P, McCarter YS, Jankowski CA. A stewardship approach to optimize antimicrobial therapy through use of a rapid microarray assay on blood cultures positive for gram-negative bacteria. J Clin Microbiol. 2015 Nov; 53(11):3627–3629.
https://doi.org/10.1128/JCM.02161-15

Stevenson LG, Drake SK, Murray PR. Rapid identification of bacteria in positive blood culture broths by matrix-assisted laser desorption ionization-time of flight mass spectrometry. J Clin Microbiol. 2010 Feb 01;48(2):444–447.
https://doi.org/10.1128/JCM.01541-09

Tian Y, Zheng B, Wang B, Lin Y, Li M. Rapid identification and multiple susceptibility testing of pathogens from positive-culture sterile body fluids by a combined MALDI-TOF mass spectrometry and Vitek susceptibility system. Front Microbiol. 2016 Apr 20;7:523.
https://doi.org/10.3389/fmicb.2016.00523

Tuite N, Reddington K, Barry T, Zumla A, Enne V. Rapid nucleic acid diagnostics for the detection of antimicrobial resistance in Gram-negative bacteria: is it time for a paradigm shift? J Antimicrob Chemother. 2014 Jul 01;69(7):1729–1733.
https://doi.org/10.1093/jac/dku083

Yiş R. Evaluation of blood cultures in a children's hospital located in Southeastern Anatolia. Turk Pediatri Ars. 2015 Jul 20;50(2):102–107.
https://doi.org/10.5152/tpa.2015.2593

Polish Journal of Microbiology
2020, Vol. 69, No 2, 177–184
https://doi.org/10.33073/pjm-2020-020

ORIGINAL PAPER

The Resurgence of Measles Infection and its Associated Complications in Early Childhood at a Tertiary Care Hospital in Peshawar, Pakistan

MUHAMMAD ILYAS[1]*, SUMERA AFZAL[1], JAMSHAID AHMAD[1], SAAD ALGHAMDI[2] and MUHAMMAD KHURRAM[3]

[1] Centre of Biotechnology and Microbiology, University of Peshawar KP, Pakistan
[2] Laboratory Medicine Department, Faculty of Applied Medical Sciences, Umm Al-Qura University Makkah Saudi Arabia
[3] Department of Pharmacy, Abasyn University, Peshawar KP, Pakistan

Submitted 1 February 2020, revised 31 March 2020, accepted 31 March 2020

Abstract

Measles infection is of substantial interest to immunologists due to its paradoxical interaction with the immune system. After the acquisition of the measles infection, secondary infection plays a pivotal role in measles-related deaths. A cross-sectional study conducted between December 2018 and July 2019 is presented here. A total of one hundred children of both genders presented with measles complications were included following WHO criteria. Measles confirmation was done by quantitative determination of anti-measles antibodies (IgM) in patients' sera while patient-related demographic data, vaccination status, and other clinical information were obtained on a separate form. The number of female patients (52%) slightly exceeded the number of males (48%). 43% of patients' parents were illiterate, and half of the patients (50%) were from a poor background. The majority of children (76%) who presented with the complications did not receive a measles vaccine. 56% of children were breastfed while 58% received vitamin A supplements but developed complications. The elevated levels of anti-measles IgM were observed in 77% of cases. In both genders, the major complications were pneumonia, lower respiratory tract infection (LRTI), acute diarrhea, diarrhea and LRTI, pneumonia and diarrhea, otitis media and pneumonia, myocarditis and LRTI, and pneumothorax. The majority of the infected children (n = 48) under 12 months of age had associated complications. It has been observed that the measles virus strikes early age children in the northwestern region of Pakistan, which is an alarming situation and is associated with the aforementioned complications, especially in unvaccinated children. Anti-measles IgM is an important serological parameter for early diagnosis of measles infection.

Key words: measles, pneumonia, subacute-sclerosing panencephalitis, IgM, myocarditis, pneumothorax

Introduction

Measles is a highly contagious systemic viral infection caused by the Measles virus (MeV). This virus belongs to the Paramyxoviridae family, has ssRNA genome and a lipid envelope. It spreads through respiratory droplets and also through conjunctiva contact (Khan et al. 2013). Its diagnostic criteria include high-grade fever (38°C lasting for > 3 days), generalized maculopapular rashes, cough, coryza, and conjunctivitis (WHO 2018a). Measles viral infection is the leading cause of morbidity and mortality worldwide among children, even though there is a safe and effective live attenuated viral vaccine (Wolfson et al. 2009). In 2010, there were about 20 million measles infections reported with 0.14 million deaths (Simons et al. 2012). The death toll surged to approximately 0.16 million in 2011, with 95% of deaths reported from developing countries (WHO 2013). Presently, 45 million new measles cases were recorded, with one million deaths per year (Li et al. 2015). In 2011, measles hit 4386 people in Pakistan, with 64 deaths reported. In 2012, 2,676 laboratory-confirmed cases, and 310 deaths were reported in this country (Khan and Qazi 2014; CDC 2018). Measles viral infection is of substantial interest to immunologists due to its paradoxical interaction with the immune system. Many manifestations of the disease like rashes, conjunctivitis, and stomatitis are tagged with the immune response to

* Corresponding author: M. Ilyas, Centre of Biotechnology and Microbiology, University of Peshawar KP, Pakistan;
e-mail: milyas_1978@hotmail.com

infection. This immune response clears the virus from the body, providing lifelong immunity. After the acute phase of measles infection, the presence of the viral genome and its proteins in the lymphatic tissues leads to a suppressed immune system. Furthermore, as the immune suppression spans to several weeks, there is an opportunity for secondary microbial infections, which increase the mortality rate among children (Beckford et al. 1985; De Vries et al. 2012).

After measles infection, secondary infections play a crucial role in measles-related deaths. Lower respiratory tract infections (LRTI) like bronchial pneumonia, are the leading cause of death in measles cases, particularly among children under 5 years of age (Li et al. 2015). Other serious complications, particularly among immunocompromised and malnourished children, include blindness, acute diarrhea, otitis media, encephalitis, and myocarditis (WHO 2016). One of the fatal complications related to measles is sub-acute sclerosing panencephalitis (SSPE), which is a progressive, disabling, and deadly brain disorder of the central nervous system, usually developed between 7 and 10 years after a person is infected by the measles virus (Bellini et al. 2005). In a recent study conducted in Pakistan, complications like pneumonia, oral lesions, and acute diarrhea were reported due to measles infection among unvaccinated children (Hussain et al. 2016). Associated factors that are instrumental in the generation of complications include vitamin A deficiency, weakened immunity, living in congested environments, and poor access to health care facilities (Sultana et al. 2015).

Developed countries were successful in the reduction of measles infections through effective immunization. Under the auspices of the WHO, a campaign of immunization against communicable diseases started in Pakistan in 1978 (Bugvi et al. 2006). However, like other developing countries, the coverage of measles vaccination is below 60% in Pakistan (Mere et al. 2019). In preventing and reduction of measles infection and associated complications, the only hope is effective measles vaccination, which can significantly reduce the incidence of measles infection and related deaths among children (Gafaar et al. 2003). Unfortunately, recent outbreaks of measles infection (in 2018) in Pakistan occurred in different regions of the country (WHO 2019). The primary reasons for these measles episodes are lack of awareness regarding vaccination among the general population due to reduced literacy rate, lack of motivation among health care staff, and poor health care infrastructure.

Keeping in view the current scenario, this study was designed to investigate the measles incidence and its associated complications among the children of Khyber Pakhtunkhwa (KP) located in the northwestern region of Pakistan.

Experimental

Materials and Methods

The present study is a cross-sectional study conducted in the pediatric unit of the Lady Reading Hospital (LRH), a tertiary care hospital in District Peshawar, KP. Measles cases were defined in accordance with WHO criteria (2018), i.e., fever (38°C lasting for more than three days) and maculopapular rash, cough, coryza, or conjunctivitis. Measles cases were confirmed by detecting measles-specific IgM antibodies (anti-MeV IgM) in a patient serum through enzyme-linked immunosorbent assays (ELISA). A total of one hundred measles cases were studied for anti-MeV IgM confirmation. Venereal blood samples were collected aseptically between December 2018 and July 2019 from measles-infected children of both genders, above four months of age but under ten years, with measles complications and having been admitted to the pediatric unit of LRH Peshawar. Children aged less than 4 months or over ten years old or having congenital heart disease, thalassemia, or other congenital diseases were excluded from the study. Measles complications were diagnosed by physicians based on clinical findings with the support of laboratory and radiological findings, like X-ray chest, electrocardiogram, serum electrolytes, and complete blood count.

Patient demographic data and clinical information like age, sex, socio-economic status, educational level of parents, feeding history, vitamin A intake, and complications were recorded on a separate predesigned form. The measles vaccination status of a patient was established either through a vaccination card or through verbal confirmation with parents (if vaccination card not available). A written consent form was given to the parents, explaining the use of their data for research and publication.

Detection of measles-specific IgM antibodies. For the detection of measles-specific IgM antibodies, a fresh blood sample of about 2 ml from measles-infected children was collected by the vein puncture method in a gel tube. All the samples were centrifuged at 8,000 rpm in order to obtain a clear serum and to send for estimation of measles-specific IgM antibodies (ORGENTEC Diagnostka Alegria Anti Measles IgM Assay). The measuring range of Alegria assay was 0–200 U/ml. The cut-off value for the assay was 25 U/ml. Interpretation of the result was as follows: patient value less than 20 U/ml was considered negative, while a value between 20–25 U/ml was considered borderline, and a value > 25 U/ml was considered positive (Alegria Orgentec).

Principle of the assay. Detection of measles-specific IgM antibodies was done using Alegria®, a fully automated random access analyzer. The Alegria® Test Strip is designed for a single determination of one patient

sample, which holds a complete set of reagents, including enzyme conjugate (Anti-human IgM HRP labeled), enzyme substrate (Tetramethyle benzidin), sample buffer, and a test specific control (Test specific antibodies). Antibodies quantification is based on an indirect enzyme-linked immune reaction in which purified particles of inactivated measles virus coated on a well surface interact with the corresponding anti-measles antibodies present in patient serum. After subsequent washing, an enzyme conjugate that binds to the immobilized antibody-antigen complex is added. After incubation, the addition of the enzyme substrate results in the development of a blue color, which is proportional to the concentration of the antibody-antigen complex measured at $\lambda = 650$ nm.

Results

Patients' demographic data (Table I) shows that out of 100 patients, 52 (52%) were females with a mean age of 15.06 (±9.42), while 48 (48%) were males aged 15.94 (±9.70). As far as the educational status of the parents was concerned, a high percentage (43%) were uneducated, while 28% had Grade 10 (Secondary education level), and 22% had Grade 5 level (Primary education) educational competence. Only 7% of parents were found to have beyond Grade 10 level education (Higher education).

As far as the socio-economic position is concerned, half (50%) of the patients belonged to low-income families (≤ $1,700 per annum), while 38% were from middle-class families (≥ $1,701 and ≤ $4,300 per annum). Only 7% of patients were from the upper class (≥ $4,301 per annum). Criteria of income per annum of the parents were sited, according to Hussain et al. (2016) with little modification.

Breast-feeding of babies in this region of Pakistan is a common practice in early childhood, although trends are changing. It was observed that 56% of children were breastfed while 32% were given formula milk. A comparatively small group of babies (12%) was found to be on formula as well as being breast-fed. It was also observed that 58% of measles-infected children had received vitamin A drops during the routine vaccination schedule.

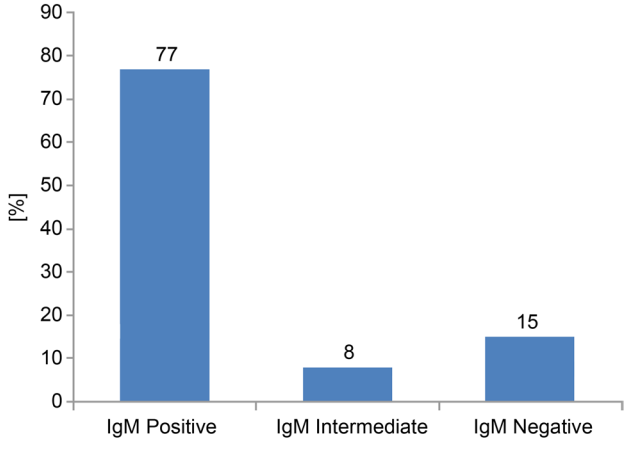

Fig. 1. The overall distribution of anti-measles antibody (IgM) in patients' sera (n = 100).

Table I
Demographic and related data of the patients.

Parameters	Patient
Patient-related	
Total Number	100
Male	48 (48%)
Female	52 (52%)
Age-wise (in months)	
Male	15.06 (±9.42)
Female	15.94 (±9.42)
Feeding history (%)	
Breastfeed	56%
Formula feed	32%
Breast + Formula	12%
Measles vaccination status (%)	
Vaccinated (Total) < 12 months 12–24 months > 24 months	24% (n = 2) (n = 17) (n = 5)
Unvaccinated (Total) < 12 months 12–24 months > 24 months	76% (n = 42) (n = 23) (n = 11)
Vitamin A intake (*both genders*)	58%
Parents-related	
Socio-economic status (%)	
High (≥ $4,301 per annum)	12%
Middle (≥ $1,701 and ≤ $4,300 per annum)	38%
Lower (≤ $1,700 per annum)	50%
Educational status (%)	
Higher	7%
Secondary	28%
Primary	22%
Uneducated	43%

The antibody (IgM) levels (Fig. 1) were found to be elevated in a majority (77%) of cases, while 8% of cases indicated intermediate levels, and 15% were found negative for the IgM presence. The measles infection was found in 76% of children who did not receive the vaccination, but 24% of cases were resurgence, where children had received one dose of measles vaccination (Table I).

The gender distributions of measles-associated complications are given in Fig. 2. In male patients major complications were pneumonia (n = 20; 41.7%) followed

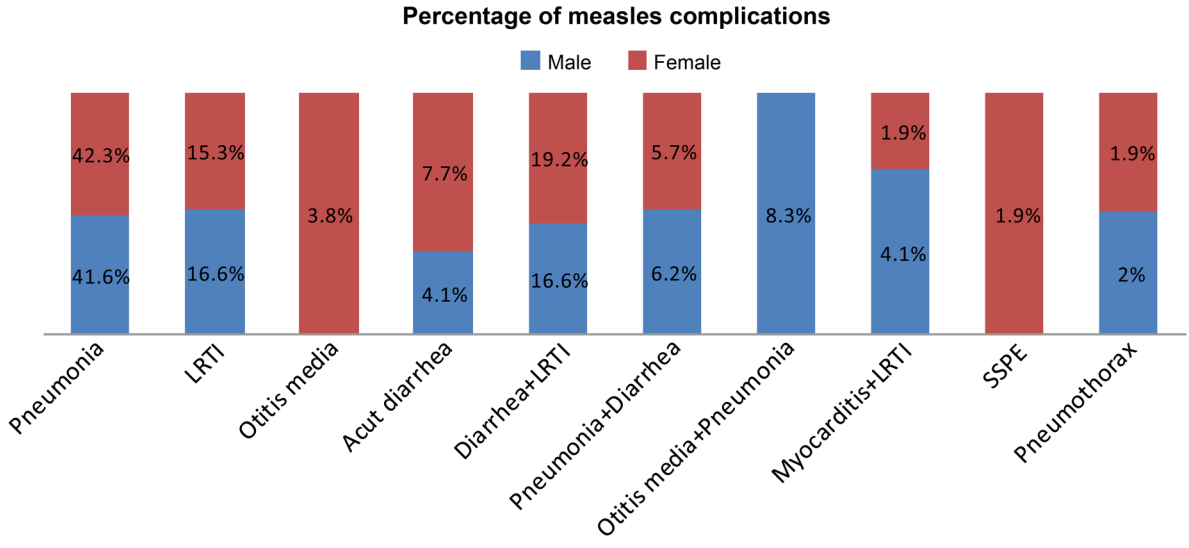

Fig. 2. Gender distribution of measles complications (Percentage).

by LRTI (n = 8; 16.7%), acute diarrhea (n = 2; 4.2%), diarrhea and LRTI (n = 8; 16.6%), pneumonia and diarrhea (n = 3; 6.2%), otitis media and pneumonia (n = 4; 8.3%), myocarditis and LRTI (n = 2; 4.1%), and pneumothorax (n = 1; 2.0%), respectively. In female patients, pneumonia (n = 21; 42.4%) was the major complication followed by LRTI (n = 10: 19.2%), otitis media (n = 2; 3.8%), acute diarrhea (n = 4; 7.7%), diarrhea and LRTI (n = 10; 19.2%), pneumonia and diarrhea (n = 3; 5.7%), myocarditis and LRTI (n = 1; 1.9%), SSPE (n = 1; 1.9%), and pneumothorax (n = 1; 1.9%).

The age distribution (Table II) of clinical complications showed a high frequency of pneumonia (n = 23; 47.9%), followed by LRTI (n = 8; 16.7%), acute diarrhea (n = 4; 8.3%), diarrhea and LRTI (n = 6; 12.5%), pneumonia and diarrhea (n = 3; 6.25%), otitis media and pneumonia (n = 2; 4.1%), myocarditis and LRTI (n = 1; 2%), and pneumothorax (n = 1; 2%) in patients less than 12 months old. While for the age group 12–24 months, pneumonia (n = 15; 37.5%) was the major complication, followed by LRTI (n = 8; 20%), otitis media (n = 1; 2.5%), acute diarrhea (n = 1; 2.5%), diarrhea and LRTI (n = 8; 20.0%), pneumonia and diarrhea (n = 2; 5%), otitis media and pneumonia (n = 1; 2.5%), myocarditis and LRTI (n = 2; 5%), SSPE (n = 1; 2.5%) and pneumothorax 1 (2.5%). Complications presentation for the age group > 24 months were predominated by pneumonia (n = 3; 25%) and diarrhea + LRTI (n = 3; 25%), followed by LRTI (n = 2; 16.7%), otitis media (n = 1; 8.3%), acute diarrhea (n = 1; 8.3%), pneumonia and diarrhea (n = 1; 8.3%) and otitis media and pneumonia (n = 1; 8.3%). In the current study, the majority of the children (n = 76)

Table II
Frequency and distribution of measles complications in different age groups of patients

Clinical complications	Age-wise distribution			
	< 12 months	12–24 months	> 24 months	Total
Pneumonia	23 (47.9%)	15 (37.5%)	3 (25%)	41
LRTI	8 (16.7)	8 (20)%	2 (16.7%)	18
Otitis media	–	1 (2.5%)	1 (8.3%)	2
Acute diarrhea	4 (8.3%)	1 (2.5%)	1 (8.3%)	6
Diarrhea + LRTI*	6 (12.5%)	8 (20%)	3 (25%)	17
Pneumonia + Diarrhea	3 (6.25%)	2 (5%)	1 (8.3%)	6
Otitis media + Pneumonia	2 (4.1%)	1 (2.5%)	1 (8.3%)	4
Myocarditis + LRTI	1 (2.0%)	2 (5%)	–	3
SSPE†	–	1 (2.5%)	–	1
Pneumothorax	1 (2.0%)	1 (2.5%)	–	2
Total	48	40	12	100

* LRTI – Lower respiratory tract infection
† SSPE – Subacute sclerosing panencephalitis

suffering from measles complications were unvaccinated, while only 24 children who had received one dose of measles vaccination were shown in Fig. 4.

Discussion

Measles is a highly contagious viral disease that leads to increased morbidity and mortality among children, especially in developing countries. Measles infection has the potential to lead to life-threatening complications (Filia et al. 2013).

Eradication of measles is an crucial section of Millennium Development Goal 4 of the WHO. Pakistan, as a member of the Eastern Mediterranean Region, agreed in 1997 to eliminate measles infection by 2010 (Gafaar et al. 2003). Unfortunately, the resurgence of measles is continuously reported from different regions of Pakistan over the last decade. According to a WHO 2019 report, during 2011, 2012, and 2013, the number of confirmed measles cases in Pakistan was 2,676, 8,048, and 8,030, respectively. More recently, in 2017 and 2018, significant measles episodes were reported throughout the country (Fig. 3). According to the Pakistan demographic health survey and social living standard measurement, the Expanded Program on Immunization (EPI) coverage is currently 65% and each year about 2 million Pakistani children do not receive their first dose of measles vaccination, while the coverage of the second dose of measles is lower (< 60%) (CDC 2018).

The upsurge of measles in Pakistan could be attributed to several factors. Graft in the healthcare system, which encompasses illicit allocation of funds, poor attitude of healthcare workers, quackery, fake vaccination campaigns, and marketing of expired drugs, plays a central role. Another hurdle is dissatisfactory health infrastructure in the country contributes to the resurgence of measles outbreaks (Islam et al. 2019).

Detection of measles-specific immunoglobulin (IgM), produced as a result of the primary immune response, serves as the gold standard in accurate diagnosis of measles infection. These antibodies are easily detected in patient serum within a few days after the onset of the rashes through an enzyme-linked immunosorbent-based assay (Xavier et al. 2019). In the current study, the WHO-recommended ELISA technique was used for the detection of serum antibodies with 77% positive results (Patient value > 25 IU). Grey zone or borderline titers, i.e., values between 20–25 IU, were observed in 8% cases, while 15% of cases were negative (Patient value < 20 IU). The borderline titers or seronegative results may be attributed to inadequate immune responses of the host or maybe due to early blood sample collection before elevated IgM level in the serum of the respective patients. IgM may also be negative in a true measles case if the specimen is collected too early or too late in the course of the illness. In the first 72 hours after rash onset, a negative result for measles IgM may be obtained from up to 30% of measles cases. The sensitivity of the test is lower ≤ three days after rash onset (WHO 2018b). The vitamin A deficiency often leads to increase in the risk of blindness among the measles-infected children. In the present study, vitamin A had been administered in 58% of measles-infected

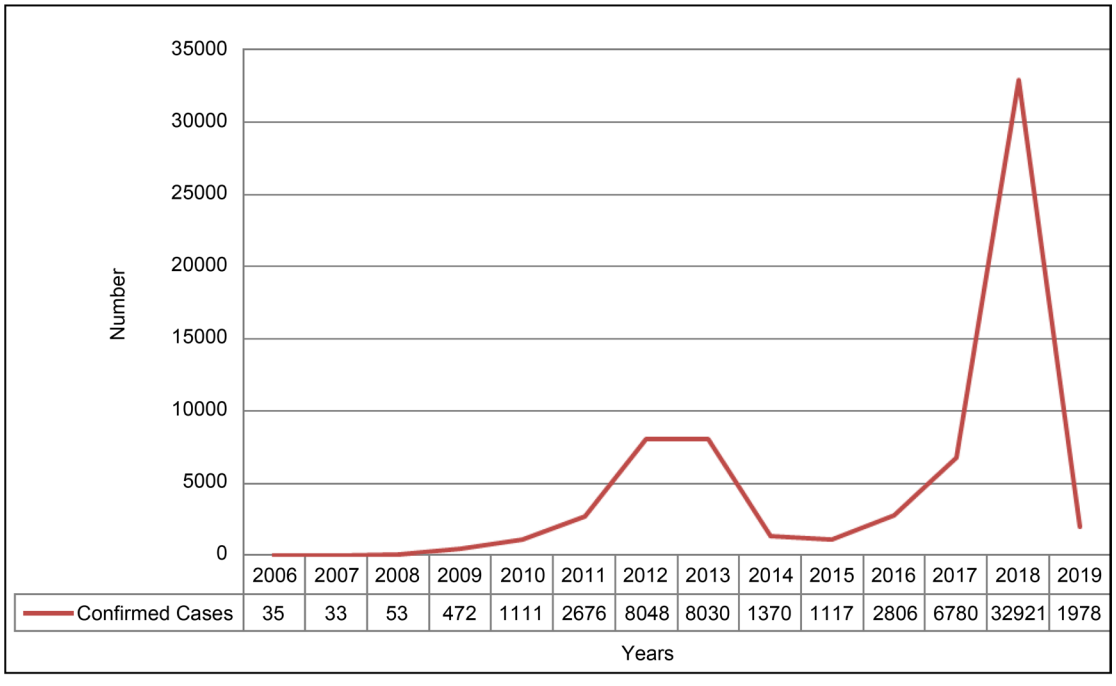

Fig. 3. Number of confirmed measles cases from 2006 to 2019 in Pakistan (WHO 2019; updates).

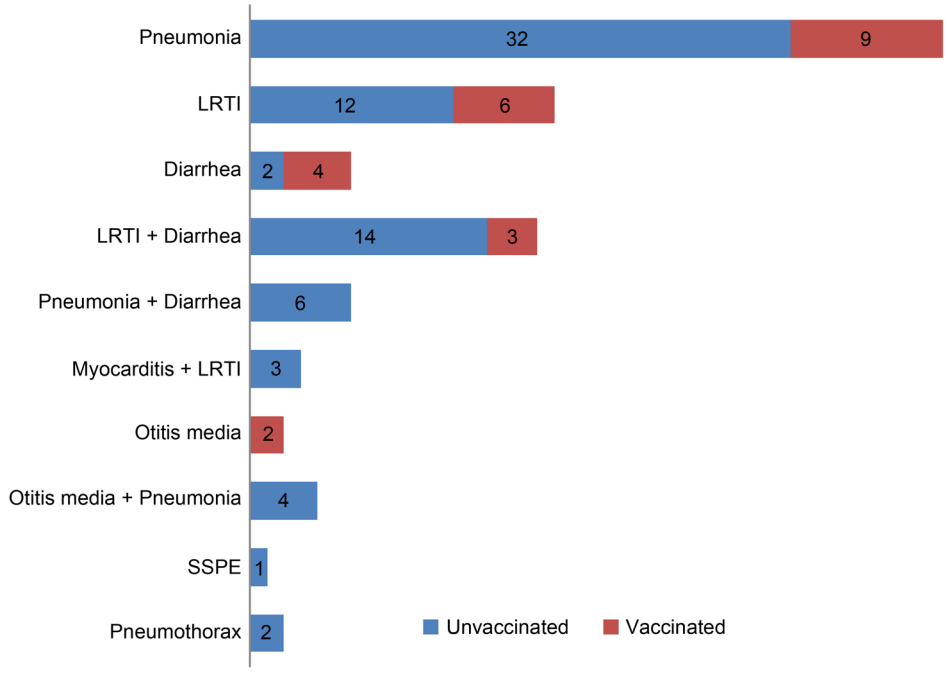

Fig. 4. Distribution of measles complications among measles-vaccinated and unvaccinated children.

children, although vitamin A administration is not a regular part of the vaccine schedule followed in Pakistan. Poor immune response, improper maintenance of cold chain during transportation, and neglectful attitude of health care staff may be factors leading to the development of complications. In the present study, vitamin A intake information was made through verbal communication with the parents of the children.

The age-wise distribution, status of vaccination, and incidence of measles infection for the period September 2018 to August 2019 in Pakistan was given in 2019 WHO report. The findings suggest an emergency and the need for quick intervention. Furthermore, prompt education on the awareness and benefits of immunization among the population of this region is needed.

In the present study, pneumonia (41%) and diarrhea were the major complications associated with measles infection, and these observations are similar to a report by Khan et al. (2013), while in a separate study conducted by Rashid et al. (2016), a slightly high frequency for the complications mentioned above was reported. In the present study, co-infections like diarrhea with LRTI, pneumonia and diarrhea, otitis media and pneumonia, and myocarditis and LRTI were observed. In the present study, the vaccination status of the measles-infected children was established through vaccination cards issued by EPI Health department KP, Pakistan. The vaccination status of the patients was confirmed through a vaccination card in more than 80 children. Only for a few children was vaccination status confirmed by parents through verbal communication. Negligence, low education status, and less awareness about vaccination schedules among the parents determine their mindset regarding the prevention of measles in this region. It is evident from the present study that significant factors that may contribute to the resurgence of measles infections include low vaccination (24 vaccinated babies versus 76 unvaccinated) that may be due to lack of vaccination awareness, poor health infrastructure, malnutrition, and missing of a booster dose. Malnutrition is a significant risk factor in measles-infected children around acquiring complications that lead to increased mortality among unvaccinated children. Furthermore, the majority of the infected children (76%) were not vaccinated, which highlights the higher risk of acquiring infection and resultant complications. In a report by Husain et al. (2016), 75% of children with pneumonia were malnourished, while 83.3% of such children also had diarrhea. In the present study, children under one year of age, particularly between 7–8 months, developed measles complications. The principal reason behind this may be the underdeveloped immune system that makes children more prone to this disease and its subsequent complications.

In Pakistan, the vaccination schedule for measles vaccination is nine months, while the booster dose is at 14 or 15 months (Table III). For this disease, it has been recommended that the administration of booster dose be made at 14 to 15 months of age, increasing the vaccine efficacy up to 99% and providing more protection compared to a single dose (De Serres et al. 2012). However, in the present research, we did not observe any booster dose administration for the children infected by measles. It is an alarming finding that necessitates

Table III
Vaccination schedule for children in Pakistan.

Age of vaccine administration	Name of vaccine
Immediate after birth	1. BCG
	2. OPV
	3. Hepatitis-B
After 6 weeks	1. OPV-1
	2. Penta-1
	3. Pneumo-1
After 10 weeks	1. OPV-2
	2. Penta-2
	3. Pneumo-2
After 14 weeks	1. OPV-3
	2. Penta-3
	3. Pneumo-3
	4. IPV
After 9 months	Measles-1
After 15 months	Measles-2

http://www.epi.gov.pk/immunisation-schedule/

a mandatory administration of the primary as well as the booster dose among children.

Measles remains a leading cause of death among young children worldwide despite the availability of a live attenuated effective vaccine. In the present study, severe complications like pneumonia, acute diarrhea, myocarditis, and pneumothorax were observed in children under one year of age. Only one case of SSPE was observed that was confirmed through the detection of anti-measles antibodies in cerebrospinal fluid (CSF) of the patient. The number of children with SSPE may be underestimated; generally, it is developed 7–10 years after a person has measles, even though the person seems to have fully recovered from the illness.

Multiple outbreaks of measles have been reported from different parts of the world (Wolfson et al. 2009) and particularly from this region of Pakistan. It is not only worrisome but needs an effective strategy in the health care system to devise a national strategy for measles vaccinations. Combined efforts of the health care staff, awareness through social media, and related health professionals are required to augment awareness among the general public regarding the vaccination program and clinical consequences of measles infection in order to prevent the disease from resurging as endemic.

Conclusions

The measles virus has potentially fatal consequences at an early age of childhood, not only in Pakistan but worldwide, which is alarming. Major complications observed in the present case included pneumonia, LRTI, diarrhea, otitis media, myocarditis, and SSPE, with some patients presenting more than one complication. Primarily, the complications were observed among unvaccinated and among children vaccinated only with one dose of vaccine, which illustrates the importance of the measles vaccination. Moreover, the booster dose administration can be made mandatory in order to achieve better immunization. Furthermore, the workhorse method proved to be significant and can be effectively utilized in the early diagnosis of measles infection.

Authors' contributions

MI carried out samples collection, participated in the experimental work, and wrote the manuscript. SA designed the overall study and critically reviewed the manuscript. JA, SAG, and MK helped in manuscript writing, drafting of tables of figures, and funds arrangement. All the authors edited and approved the final manuscript.

Acknowledgments

The authors are very grateful for the lab facilities of the Centre of Biotechnology and Microbiology University of Peshawar and Sarhad University of Science and Information Technology, Peshawar KP, Pakistan.

Conflict of interest

The authors do not report any financial or personal connections with other persons or organizations, which might negatively affect the contents of this publication and/or claim authorship rights to this publication.

Literature

Beckford AP, Kaschula ROC, Stephen C. Factors associated with fatal cases of measles. A retrospective autopsy study. S Afr Med J. 1985 Dec 7;68(12):858–863.

Bellini WJ, Rota JS, Lowe LE, Katz RS, Dyken PR, Zaki SR, Shieh WJ, Rota PA. Subacute sclerosing panencephalitis: more cases of this fatal disease are prevented by measles immunization than was previously recognized. J Infect Dis. 2005 Nov 15;192(10):1686–1693. https://doi.org/10.1086/497169

Bugvi AS, Rahat R, Zakar R, Zakar MZ, Fischer F, Nasrullah M, Manawar R. Factors associated with non-utilization of child immunization in Pakistan: evidence from the Demographic and Health Survey 2006–07. BMC Public Health. 2014 Dec;14(1):232. https://doi.org/10.1186/1471-2458-14-232

CDC. Progress toward regional measles elimination-worldwide 2000–2017. Atlanta (USA): Centers for Disease Control and Prevention; 2018.

De Serres G, Boulianne N, Defay F, Brousseau N, Benoît M, Lacoursière S, Guillemette F, Soto J, Ouakki M, Ward BJ, et al. Higher risk of measles when the first dose of a 2-dose schedule of measles vaccine is given at 12–14 months versus 15 months of age. Clin Infect Dis. 2012 Aug 1;55(3):394–402. https://doi.org/10.1093/cid/cis439

de Vries RD, McQuaid S, van Amerongen G, Yüksel S, Verburgh RJ, Osterhaus ADME, Duprex WP, de Swart RL. Measles immune suppression: lessons from the macaque model. PLoS Pathog. 2012 Aug 30;8(8):e1002885. https://doi.org/10.1371/journal.ppat.1002885

Filia A, Bella A, Rota M, Tavilla A, Magurano F, Baggieri M, Nicoletti L, Iannazzo S, Pompa M, Declich S. Analysis of national measles surveillance data in Italy from October 2010 to December 2011 and priorities for reaching the 2015 measles elimination goal. Euro Surveill. 2013 May 16;18(20):20480.

Gaafar T, Moshni E, Lievano F. The challenge of achieving measles elimination in the Eastern Mediterranean Region by 2010. J Infect Dis. 2003;187(Supplement_1):S164–S171. https://doi.org/10.1086/368035

Hussain S, Yasir M, Tarar SH, Sabir MUD. Measles: demographic profile and associated morbidities of measles cases admitted in a teaching hospital. Pak Armed Forces Med J. 2016;66(1):92–97.

Islam A, Younas Z, Qadri KFI, Alelwani W, Rauf M, Qadri I. The Battle against measles in Pakistan – the current scenario. 1–2. New York (USA): Crimson Publisher; 2019.

Khan I, Khattak AA, Muhammad A. Complications of measles in hospitalized children. KMUJ-Khyber Med Univ J. 2013;5(1):27–30.

Khan T, Qazi J. Measles outbreaks in Pakistan: causes of the tragedy and future implications. Epidemiol Rev. 2014;2(1):1.

Li J, Zhao Y, Liu Z, Zhang T, Liu C, Liu X. Clinical report of serious complications associated with measles pneumonia in children hospitalized at Shengjing hospital, China. J Infect Dev Ctries. 2015 Oct 29;9(10):1139–1146. https://doi.org/10.3855/jidc.6534

Mere MO, Goodson JL, Chandio AK, Rana MS, Hasan Q, Teleb N, Alexander JP Jr. Progress toward measles elimination – Pakistan, 2000–2018. MMWR Morb Mortal Wkly Rep. 2019 Jun 07;68(22): 505–510. https://doi.org/10.15585/mmwr.mm6822a4

Rashid MA, Afridi MI, urRehman MA. Frequency of complications in measles patients at Peshawar. Gomal J Med Sci. 2016;14(2): 112–116.

Saeed A, Butt ZA, Malik T. Investigation of measles outbreak in a district of Balochistan province, Pakistan. J Ayub Med Coll Abbottabad. 2015 Oct-Dec;27(4):900–903.

Simons E, Ferrari M, Fricks J, Wannemuehler K, Anand A, Burton A, Strebel P. Assessment of the 2010 global measles mortality reduction goal: results from a model of surveillance data. Lancet. 2012 Jun;379(9832):2173–2178. https://doi.org/10.1016/S0140-6736(12)60522-4

Sultana A, Sabir SA, Awan A. Characteristics of patients with measles admitted to Allied hospital Rawalpindi. J Ayub Med Coll Abbottabad. 2015;27(2):318–322.

WHO. Measles fact sheet. WHO Updated. No. 286. Geneva (Switzerland): World Health Organization; 2013. [cited 2020 Jan 20]. Available from: http://www.who.int/mediacentre/factsheets/fs286/en/index.html

WHO. Measles fact sheet. Geneva (Switzerland): World Health Organization; 2016. [cited 2020 Jan 20]. Available from: http://www.who.int/topics/measles/en/

WHO. Manual for the laboratory-based surveillance of measles, rubella, and congenital rubella syndrome, 3rd edition. Geneva (Switzerland): World Health Organization; 2018a. [cited 2020 Jan 20]. Available from: http://www.who.int/immunization/monitoring_surveillance/burden/laboratory/manual/en/

WHO. Vaccine preventable disease surveillance standards. Measles. Geneva (Switzerland): World Health Organization; 2018b. p. 1–30.

WHO. Measles and rubella surveillance data, latest updates. Geneva (Switzerland): World Health Organization; 2019. [cited 2020 Jan 20]. Available from: https://www.who.int/immunization/monitoring_surveillance/burden/vpd/surveillance_type/active/measles_monthlydata/en/

Wolfson LJ, Grais RF, Luquero FJ, Birmingham ME, Strebel PM. Estimates of measles case fatality ratios: a comprehensive review of community-based studies. Int J Epidemiol. 2009 Feb 01;38(1): 192–205. https://doi.org/10.1093/ije/dyn224

Xavier AR, Rodrigues TS, Santos LS, Lacerda GS, Kanaan S. Clinical, laboratorial diagnosis and prophylaxis of measles in Brazil. J Bras Patol Med Lab. 2019;55(4):390–401. https://doi.org/10.5935/1676-2444.20190035

Polish Journal of Microbiology
2020, Vol. 69, No 2, 185–191
https://doi.org/10.33073/pjm-2020-021

ORIGINAL PAPER

A Current Microbiological Picture of *Mycobacterium* Isolates from Istanbul, Turkey

BILGE SUMBUL[1]* and MEHMET ZIYA DOYMAZ[2]

[1] Department of Medical Microbiology, Faculty of Medicine, Bezmialem Vakıf University, Istanbul, Turkey
[2] Beykoz Institute of Life Sciences and Biotechnology, Bezmialem Vakıf University, Istanbul, Turkey

Submitted 13 January 2020, revised 3 April 2020, accepted 3 April 2020

Abstract

Despite advances in diagnosis and treatment, tuberculosis (TB) continues to be one of the essential health problems throughout the world. Turkey is considered to be endemic for TB. In this study, we analyzed the distribution of *Mycobacterium* species, compare the diagnostic methods, and susceptibilities to anti-tuberculosis drugs of TB isolates. The aim was to document the current status and to provide a frame of reference for future studies. In this study, 278 *Mycobacterium* species isolated from 7,480 patients between September 2015 and June 2019 were included. Löwenstein-Jensen medium (LJ) and MGIT 960 were used for the isolation of strains. Susceptibility to 1st-line anti-tuberculosis drugs was determined. Positivity rates in clinical samples were as follows: 1.4% for direct microscopic acid-fast bacilli (AFB) detection, 3.4% for growth on the LJ, and 3.7% for growth on MGIT-960. Two hundred thirty-three isolates were identified as *Mycobacterium tuberculosis* complex (MTBC) and 45 were non-tuberculous mycobacteria (NTMs). Eleven of the NTMs (24.4%) were *Mycobacterium fortuitum* group isolates, and eight NTMs (17.7%) were *Mycobacterium abscessus* complex isolates. A number of patients diagnosed with tuberculosis peaked twice between the ages of 20–31 and 60–71. A hundred and eighty-two MTBC isolates (78.1%) were susceptible to all 1st-line anti-tuberculosis drugs, while 51 isolates (21.9%) were resistant to at least one drug tested. The multidrug-resistant tuberculosis rate was 13.7% among resistant strains and 3% in all strains. The liquid cultures were better for detection of both MTBC and NTMs isolates. The data demonstrate that MTBC continues to be challenge for this country and indicates the need for continued surveillance and full-spectrum services of mycobacteriology laboratory and infectious diseases.

Key words: tuberculosis, *Mycobacterium* species, *Mycobacterium tuberculosis* complex, culture, drug resistance

Introduction

Tuberculosis (TB), as an infectious disease is caused by *Mycobacterium* species in humans (Miotto et al. 2018). The etiological agent of the disease is most often *Mycobacterium tuberculosis* (MTB), and less commonly other species in the *Mycobacterium tuberculosis* complex (MTBC). *Mycobacterium* species other than these species are classified as non-tuberculosis mycobacteria (NTMs) (Waters and Ratjen 2016). In recent years, the incidence of diseases caused by NTMs has increased due to the increasing number of immunosuppressed patients (Samli and Ilki 2016).

Members of MTBC are usually transmitted to susceptible persons through airborne means such as coughing, sneezing, or speaking by patients suffering from infectious tuberculosis (Churchyard et al. 2016). The successful establishment of an infection in the lungs is influenced by various factors such as phagocytosis of the bacilli, their intracellular multiplication, latency, and active lung infection (Banuls et al. 2015). However, there is no clear evidence that NTMs are transmitted from either person to person or from animals to people. Therefore, the transmission of NTMs is probably through individual contacts with the source of infection (Churchyard et al. 2016).

Since the treatment of *Mycobacterium* species depends on the correct identification of the isolate, mycobacteriological tests that are leading to the identification are crucial. Methods that include direct microscopic acid-fast bacilli detection (AFB), growth on the solid or liquid media, and biochemical tests continue to play significant roles in the identification of mycobacteria (Kurtoglu et al. 2011).

* Corresponding author: B. Sumbul, Department of Medical Microbiology, Faculty of Medicine, Bezmialem Vakıf University, Istanbul, Turkey; **e-mail: bilgesumbul@hotmail.com, bsumbul@bezmialem.edu.tr**

Treatment and prophylaxis of tuberculosis differ from most other bacterial infections. In general, patients should receive multiple antibiotic treatments for at least 6 to 9 months (Ozmen et al. 2017). The World Health Organization (WHO) recommends the combined use of 1st-line drugs in the initial treatment of tuberculosis. However, anti-tuberculosis drug resistance remains a significant problem. Of the primary anti-tuberculosis drugs, isolates showing at least isoniazid (INH) and rifampin (RIF) resistance are defined as Multiple Drug-Resistant Tuberculosis (MDR-TB) (WHO 2019).

In this study, we aimed to document *Mycobacterium* species isolated in a large metropolitan tertiary care hospital in Turkey. The laboratory procedures used to isolate the organisms were also compared. Similarly, the resistance rates to the 1st-line anti-tuberculosis drugs were determined. The ultimate aim was to compare these data with the earlier studies and to provide the frame of reference for future studies.

Experimental

Materials and Methods

Ethical approval was provided from the Ethics Committee of Medical School, Bezmialem University, Istanbul, Turkey (10.09.2019/16–302).

Our facility is a 700-bed academic hospital providing tertiary health care in Istanbul city centre, and 7,480 patients with pre-diagnosis of tuberculosis admitted to Bezmialem University Medical Faculty Hospital between September 2015 and June 2019 were included in the study. Between the dates indicated, 7,480 clinical specimens were sent to the Clinical Microbiology Laboratory with a preliminary diagnosis of tuberculosis. Two hundred seventy-eights of these samples were positive for *Mycobacterium* species in at least one of the methods studied. Only the first positive isolates from the same patient were included in the study.

Homogenization and decontamination of sputum, bronchoalveolar lavage (BAL), fasting gastric juice, urine, and abscess materials were performed according to published guidelines. Sterile body fluids such as cerebrospinal fluid (CSF), peritoneal and pleural fluid, and tissue samples were tested without decontamination. N-acetyl-L-cysteine-4% sodium hydroxide-1.47% sodium citrate (NALC-NaOH) method was used for decontamination and homogenization of the samples. Five to ten ml of each clinical sample was mixed with an equal volume of NALC-NaOH solution. The mixture was transferred to tubes and vortexed for not more than 30 seconds. The tubes containing the mixture were allowed to stand at room temperature for 15 minutes. Fifty ml of phosphate buffer (0.067 M, pH = 6.8) was added to each tube containing the mixture, and the tubes were centrifuged at 3,000 g for 15 minutes. The resulting precipitates were diluted with 1–2 ml of phosphate buffer (pH = 6.8), and smears were prepared from these precipitates. The smears were stained by Erlich-Ziehl-Neelsen (EZN) (GBL Rose Biology Laboratory, Istanbul) method and examined microscopically under immersion oil.

Isolation of *Mycobacterium* species. For all the samples, both liquid and solid media are used for culture. Therefore, any isolate growing either on one of these media were used in identification studies. In some patients, multiple specimens were submitted for culture, and multiple cultures were positive for growth. In those patients, the very first isolate was used in the study.

For the liquid culture of mycobacteria, a *Mycobacterium* Growth Indicator Tube (BD MGIT-960, BD, Sparks, MD, USA) system was utilized, and the procedure suggested by the manufacturer was followed. Briefly, oleic acid-albumin-dextrose-catalase (OAOC) was added to the culture medium and as antimicrobial agents, polymyxin B (50 U/ml), azlocillin (10 mcg/ml), nalidixic acid (20 mcg/ml), trimethoprim antibiotic mixture (PANTA, Becton Dickinson, Sparks, MD, USA; 5.0 mcg/ml), and amphotericin B (5.0 mcg/ml) were added. 0.5 ml of the samples from decontaminated clinical mixtures was inoculated into the culture medium, and the culture bottles were incubated for six weeks at 37°C. Samples were considered negative if no growth signal was obtained by the end of this incubation period.

Simultaneous cultivation of the samples on solid media was carried out on Löwenstein-Jensen (LJ) slants (Becton Dickinson, USA). LJ tubes were evaluated daily for 42 days, and the cultures were terminated by 42nd day if no colonies observed. The presence of acid-resistant bacilli was screened by EZN staining from positive cultures.

Identification of *Mycobacterium* species. When MGIT-960 instrument signaled positivity, firstly, an EZN stain was performed to screen for AFB, and the positive tubes were inoculated on blood agar medium (Becton Dickinson, USA) containing 5% sheep blood, and the growth was examined to rule out a contaminating bacterial species. Samples were also inoculated onto the LJ medium for future susceptibility testing. After the growth on either solid or liquid media, the identification was performed using the MPT64 immunochromatographic test (BD MGIT TBc Identification Test, Becton Dickinson, Sparks, USA).

In the study, *M. tuberculosis* isolates were identified at the 'complex' level, and no further identification was performed, and therefore, isolates were designated as *M. tuberculosis* complex (MTBC). Non-tuberculous mycobacteria (NTMs) species were identified by the

Turkish Public Health Laboratory through a commercial molecular assay (GenoType *Mycobacterium* CM, Hain Lifescience GmbH, Nehren, Germany).

Antimycobacterial susceptibility tests. The susceptibilities of MTBC strains to isoniazid (INH), Streptomycin (SM), Rifampicin (RIF), and Ethambutol (ETM) were investigated. For this aim, a commercial susceptibility test method (BD BACTEC MGIT-960 SIRE) was used. The concentrations of the drugs in the testing kit were as follows: SM at 1.0 μg/ml, INH at 0.1 μg/ml, RIF at 1.0 μg/ml, ETM at 5.0 μg/ml. The definitions of the multidrug resistance were that of the commercial test kit (BD BACTEC MGIT-960 SIRE).

Study design and statistical analysis. This study was conducted as a retrospective clinical study. Data analysis was performed using SPSS 20.0 software pack (SPSS Inc., USA).

Results

In 278 (3.7%) of 7,480 clinical specimens from patients with suspected tuberculosis, one type of *Mycobacterium* species was isolated. Of the patients with *Mycobacterium* species, 123 (44.2%) were female, 155 (55.8%) were male.

The type of specimens from which MTBC's were isolated was as follows: 198 respiratory tract samples (sputum, BAL and tracheal aspirate), 29 tissue specimens (lymph node biopsy, etc.), 22 sterile body fluids (pleura, peritoneum, CSF), 11 fasting gastric fluid, 11 abscesses, and seven urine samples.

In our study, the AFB positivity was 1.4% (104/7,480), and the culture positivity (LJ and/or MGIT-960) was 3.7% (278/7,480) in the clinical samples of patients with suspected tuberculosis. The culture positivity was 3.4% for LJ (254/7,480) and 3.7% for MGIT-960 (278/7,480). The contamination rate in cultures was 9% (675/7,480) for LJ and 7% (525/7,480) for MGIT-960. In the study, all strains identified as MBTC or NTMs were identified as the same species by both methods.

During the study period, PCR assay was performed for 24 patients' samples upon request from the ordering clinics. A commercial automated Real-time PCR assay (QIAGEN Benelux B.V. The Netherlands) was used at a reference laboratory. Out of these 24 samples, five (20.8%) were positive. PCR positive samples were also positive in liquid (MGIT-960) and solid (LJ) culture methods as studied in house, but only three were positive by AFB. One of the samples negative by PCR (19 patients) was positive by the AFB staining, and 17 out of these 19 specimens were positive on solid media (LJ); all 19 were positive in liquid (MGIT-960) culture.

Two hundred thirty-three (MTBC) and 45 (NTMs) strains were positive by liquid (MGIT-960) or solid (LJ) culture methods. NTMs distribution was as follows: 11 (24.5%) isolates were of *Mycobacterium fortuitum* group, eight (17.8%) of *Mycobacterium abscessus* complex, five (11.1%) of *Mycobacterium simiae*, five (11.1%) of *Mycobacterium lentifilavum*, four (8.9%) of *Mycobacterium chelonae*, four (8.9%) of *Mycobacterium intracellulare*, three (6.7%) of *Mycobacterium gordonae*, two (4.4%) of *Mycobacterium avium* spp., two (4.4%) of *Mycobacterium kansasii*, and one (2.2%) of *Mycobacterium heckeshornense*.

The most MTBC isolates were from respiratory specimens; 120 from sputum, 35 from BALs, and four from tracheal aspirates. The remaining MTBC were recovered from different specimen types. Of the total 45 isolated NTMs strains, 37 were isolated from sputum samples. The number and the types of specimens from which mycobacteria were isolated are presented in Table I.

In the study, the AFB was observed in 98 respiratory patient samples. We performed AFS for the patient respiratory samples as well as the growing microorganisms in the culture. However, 198 respiratory samples grew *Mycobacterium* species that were confirmed as acid-fast organisms by staining.

In all 104 patients, the AFB positive samples (respiratory, tissue, sterile body fluid), at least one type of *Mycobacterium* species was isolated on either solid or in liquid culture methods. Sixty-six (63.5%) of the AFB positive samples were obtained from male subjects, 38 (36.5%) were from females, and the mean age was 43.16 years old (females, mean age 37.55, males – 46.4 years old).

When the age distribution of the patients was examined, a bi-modal distribution was observed. The

Table I
Number, species, AFB positivity and distribution of Mycobacterial strains according to clinical samples.

		AFB	MTBC	NTMs
Respiratory	198	98	159	39
Sputum	157	89	120	37
Bronchoalveolar lavage	37	7	35	2
Tracheal aspirate	4	2	4	–
Tissue	22	3	21	1
Lymph Node Biopsy	12	2	12	–
Other Tissues	10	1	9	1
Sterile body fluid	22	–	22	–
Pleura	13	–	13	–
BOS	6	–	6	–
Peritoneum	3	–	3	–
Abscess	18	3	17	1
Fasting gastric fluid	11	–	9	2
Urine	7	–	5	2
Total	278	104	233	45

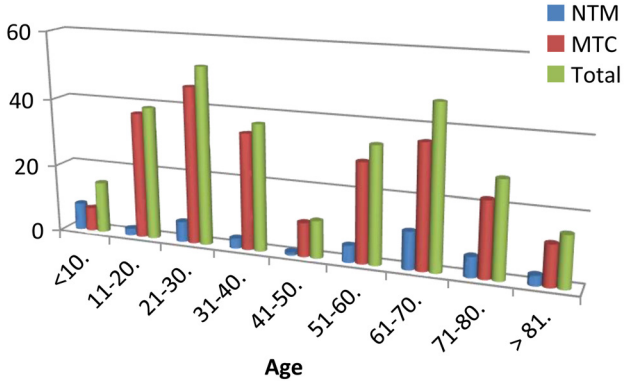

Age range	MTC	NTM	Total
1–10	7	8	15
11–20	37	2	39
21–30	46	6	52
31–40	34	3	37
41–50	10	1	11
51–60	29	5	34
61–70	36	11	47
71–80	22	6	28
>81	12	3	15

$p < 0.05$

Fig. 1. Distribution of *Mycobacterial* strains according to age groups.

number of patients diagnosed with tuberculosis peaked twice between the ages of 20–31 and 60–71. Similarly, isolations of MTBC peaked twice in the patients of 20–31 and 60–71 age range. The isolation of NTMs species was also prominent in the 0–11 age range. The distribution of Mycobacterial strains according to age groups is presented in Fig. 1.

Of the 233 MTBC strains isolated in the study, 182 (78.1%) were susceptible to all 1st-line anti-tuberculosis drugs, while 51 isolates (21.9%) were resistant to at least one of the 1st-line anti-tuberculosis drugs tested (Table II). Total drug resistance rates for INH, SM, RIF, and ETM were 16.7% (n = 39), 14.6% (n = 34), 3% (n = 7), and 0.8% (n = 2), respectively. The highest rates of resistance were observed to the pair of INH + SM (n: 22, 9.4%), and the highest rates of resistance to three drugs were against INH + SM + RIF (n = 73%). Seven rifampin-resistant strains were also resistant to INH and SM. One of the strains was resistant to four 1st-line anti-tuberculosis drugs. In our study, the rate of MDR-TB was 13.7% (7/51) among resistant strains and 3% (7/233) among all strains isolated.

In the present study, 21.4% of MTBC isolates in 2015, 6.7% in 2016, 25.8% in 2017, 21.8% in 2017, 36.7% in 2018, and 36.7% in 2017 were tested against 1st-line anti-tuberculosis drugs. As the number of strains isolated in 2017 and 2018 increased, so did the number of resistant strains. However, this increase was not statistically significant ($p < 0.05$). The number and ratio of isolated resistant MTBC strains by years are presented in Table II.

The number of *M. tuberculosis* isolates at different age groups was presented in Fig. 1. Accordingly, the numbers of TB isolated at different age groups demonstrated a bi-model distribution peaking at third and seventh decade of life. Possible differences between various age groups were analyzed by the Chi-square test, and in both decades, the rates of *M. tuberculosis* isolations were significantly different.

Discussion

TB remains a major public health problem throughout the world. According to the 2018 report of the World Health Organization, it was estimated that in 2017 approximately 10 million people suffered from TB, and approximately 1.5 million people have died (WHO 2019). The determination of the presence of the etiological agent and correct identifications are important to prevent the spread of tuberculosis. Therefore, it is necessary to isolate, determine the type, and to

Table II
Number and proportion of resistant MTBC strains by years.

	2015 (n:14)	2016 (n:45)	2017 (n:66)	2018 (n:78)	2019 (n:30)	Total (n:233, %)	
Sensitive to all drugs	11	42	49	61	19	182	(78.1)
INH	2	3	13	12	9	39	(16.7)
SM	2	1	11	12	8	34	(14.6)
RIF	1	–	2	2	2	7	(3)
EMB	–	–	–	1	1	2	(0.8)
İNH + SM	2	1	8	7	5	23	(9.9)
INH + RIF + SM (MDR-TB)	1		2	2	2	7	(3)

AFB – Acid-fast bacilli; MTC – *Mycobacterium tuberculosis* complex; NTMs – Non-tuberculosis mycobacteria

assess the drug resistance of *Mycobacterium* species (Kurtoglu et al. 2011).

Direct microscopic examination of smears is rapid and relatively practical and, therefore, is preferred despite low rates of sensitivity in detecting bacilli (Kurtoglu et al. 2011). Patients positive on direct microscopic examination are considered to be both more contagious and exhibit a fast progression to clinical disease. Consequently, a direct microscopic examination is recommended, especially in patients with pulmonary tuberculosis (Tarylan et al. 2015).

In our study, the AFB positivity was 1.4% (104/7,480), and culture positivity (LJ and/or MGIT-960) was 3.7% (278/7,480) in patients with suspected tuberculosis. Overall, MTBC detection rate was 3.1% (233/7,480). Similarly, MTBC detection rate was between 2.1% and 11% in many studies (Baylan et al. 2002; Dundar et al. 2009; Kurtoglu et al. 2011).

Today, culture is the standard gold method for the detection of mycobacteria (Kunduracioglu et al. 2013). World Health Organization recommends the use of liquid media for *M. tuberculosis* culture (WHO 2007). In other studies, it has been reported that the liquid medium was superior in recovering mycobacteria over solid media (Hwang et al. 2014; Kwak et al. 2017). In the current investigation, mycobacteria were detected in 3.7% (278/7,480) liquid cultures (MGIT-960) and 3.4% (254/7,480) solid (LJ) cultures.

Age distribution of TB patients is an important parameter reflecting the control of TB in the community. While the disease peaks in advanced ages in populations that implement effective TB control programs, in populations where the control programs are lax, the disease peaks at younger ages (Karatas et al. 2019). In some studies, the TB is seen mostly in advanced ages (Coffman et al. 2017); however, in an earlier Turkish study (Karatas et al. 2019), it was reported two peaks of the TB prevalence in the age group 15–24 and over 65 years old. Similarly, we noticed that the number of patients diagnosed with tuberculosis peaked twice between the ages of 20–31 and 60–71 years. These results suggest that the Turkish population is composed of mixed communities where both loose and effective TB control efforts are exerted.

The isolation rate of mycobacteria (NTMs) other than the *M. tuberculosis* complex is increasing throughout the world (Mbeha et al. 2014). To date, more than 160 NTMs species have been identified, and approximately one third is associated with diseases in humans. It has been shown to cause serious clinical consequences, especially in people with immunodeficiency (Liu et al. 2016). It has been reported that the distribution of NTMs species varies according to geographical regions and demographic characteristics of affected patients (Spaulding et al. 2017).

In our study, NTMs were isolated from 45 patients. Among NTMs, *M. fortuitum* group (11 isolates), and *M. abscessus* complex (eight isolates) were the most common mycobacteria. In the US study, Spaulding et al. (Spaulding et al. 2017) reported that other than MAC, *M. abscessus*/*M. chelonae*, and *M. fortuitum* were the most common isolated NTMs species. In other investigations, the frequencies among NTMs species varied significantly according to geographical regions. In a study conducted in China, Liu et al. (2016) found that more than half (59.66%) of 523 NTMs isolates were *M. avium*, and *M. intracellulare*. In this study, rapid growers such as *M. abscessus* and *M. fortuitum* were more frequent. The number MAC isolates were not as high as the others (Liu et al. 2016; Spaulding et al. 2017). Many factors could be accounted for this difference. The discrepancies in the number of people with immunodeficiency could be one factor since immunodeficiency seems to be an underlying risk factor for MAC infection. TB is a disease that should be treated with proper drug regimens to be administered to patients. The increased drug resistance complicates the treatment and impairs control of the disease. In many studies, resistance rates to commonly used 1st-line anti-tuberculosis drugs have been reported to be between 10–25% for INH, 3–16% for RIF, 0.7–19% for SM, and 0.7–10% for ETM (Karadag et al. 2004; Saral et al. 2007; Dundar et al. 2009; Aydin et al. 2011; Perincek et al. 2011). Similarly, in this report, resistances to 1st-line anti-tuberculosis drugs of INH, SM, RIF and ETM were 16.7%, 14.6%, 3%, and 0.8%, respectively. These data argue that the rate of resistance in this country follows trends not unlike those of other countries.

In many studies, it has been reported that resistance to INH and RIF are often, but resistance to other anti-tuberculosis drugs may also develop (Dheda et al. 2014; Pienar et al. 2018). However, in some studies, similar to our study, resistance to INH and SM was higher, and RIF and ETM resistances were reduced. In these studies, there were significant differences between the resistance rates by region, and the primary anti-tuberculosis drugs with the highest resistance rates were INH and SM (Kurtoglu et al. 2011; Linger et al. 2014; Sani et al. 2015; Stagg et al. 2017). It is thought that higher rates of INH and SM resistance compared to other primary anti-tuberculosis drugs may be related to the more frequent use of these drugs in both prophylaxis and treatment. Similar arguments could be put forth for this country.

The Report of the Turkish Association of Anti-TB Campaign published in 2018 indicated that in 2016, the drug susceptibility test results were surveyed for 6,037 MTC, and resistance to at least one drug was detected in 19.2% isolates. According to this report,

3.3% of the patients who underwent drug susceptibility testing were found to have MDR-TB, and the rate of multidrug resistance was 2.1% in new patients and 14.2% in previously treated patients (Saglik Bakanligi T.C. 2018). According to WHO 2018 data, MDR-TB ratio is 3.5% of new TB cases and 18% of previously treated cases globally (WHO 2019). The rates of MDR-TB in the studies made in different regions of Turkey vary between 2.2–14.7% (Saral et al. 2007; Dundar et al. 2009; Aydin et al. 2011; Kurtoglu et al. 2011). In our study, resistance to more than one drug was detected in 51 (21.88%) isolates. MDR-TB ratio was 13.7% (7/51) among resistant strains and 3% (7/233) among all strains isolated, and this rate was consistent with other studies.

Today, the number of patients with tuberculosis has increased, possibly due to changes in recent years such as social and economic turmoil, increased number of migrant patients, changes in the practices healthcare system, and drug-resistant *Mycobacterium* isolates. Therefore, a correct and rapid diagnosis and supervised treatment concepts should be reviewed and applied to prevent susceptible strains from gaining resistance and stopping the further spread of resistant strains. Our data indicate that NTMs species will probably be more frequently encountered in the future. Furthermore, we can speculate that drug resistance will continue to be an important problem in patients with tuberculosis.

One of the limitations of this study was that the patients and the isolates were selected from a single centre albeit it was a large tertiary care centre. This might have influenced the information gathered. However, it should also be stated that the medical centre where the study is conducted is located in the heart of the old city of Istanbul, where the immigrants are concentrated.

Data from this study indicate that the frequency of isolations of *M. tuberculosis* complex in the population seems to form a bimodal distribution, one in the third decade of life and the other in the 7th. Obviously, our study is not designed to address this particular demographic aspect of *M. tuberculosis* infection in detail. However, we judge that providing such data would be a useful addition to a study aiming to capture a current picture of *Mycobacterium* species in an endemic country.

In conclusion, this investigation demonstrates that tuberculosis is still a growing public health threat in Istanbul, Turkey. We do not know how much of this increase is the result of the recent high immigration rates. The drug resistance rates also seem to be on the rise. Therefore, rapid and accurate laboratory services are imperative in combatting such a growing public health menace. Our study demonstrates that the liquid culture is superior to the solid media for the recovery of *Mycobacterium* species and, hence, should be included in the routine mycobacteriology laboratory procedures. Collectively, these results underscore the need for the marshaling preventive public health efforts on this age-old concern.

ORCID

Bilge Sumbul https://orcid.org/0002-8768-3777

Mehmet Ziya Doymaz https://orcid.org/0000-0003-2066-0252

Conflict of interest

The authors do not report any financial or personal connections with other persons or organizations, which might negatively affect the contents of this publication and/or claim authorship rights to this publication.

Literature

Aydın F, Kaklıkkaya N, Bayramoğlu G, Ozkul G, Buruk K, Dinç U, Köse T, Dede R. [Resistance rates of *Mycobacterium tuberculosis* complex strains isolated from clinical specimens] (Turkish). Mikrobiyol Bul. 2011 Jan;45(1):36–42.

Bañuls AL, Sanou A, Van Anh NT, Godreuil S. *Mycobacterium tuberculosis*: ecology and evolution of a human bacterium. J Med Microbiol. 2015 Nov 01;64(11):1261–1269. https://doi.org/10.1099/jmm.0.000171

Baylan O, Kısa O, Albay A, Dogancı L. *Mycobacterium tuberculosis* Complex (MTC) strains isolated from tuberculosis cases in our mycobacteriology laboratory and their anti-tuberculosis drug susceptibilities in 2002. Gulhane Tip Derg. 2003;45(3):256–262.

Churchyard G, Kim P, Shah NS, Rustomjee R, Gandhi N, Mathema B, Dowdy D, Kasmar A, Cardenas V. What we know about tuberculosis transmission: an overview. J Infect Dis. 2017; 216(suppl_6):S629-S635. https://doi.org/10.1093/infdis/jix362

Coffman J, Chanda-Kapata P, Marais BJ, Kapata N, Zumla A, Negin J. Tuberculosis among older adults in Zambia: burden and characteristics among a neglected group. BMC Public Health. 2017 Dec;17(1):804. https://doi.org/10.1186/s12889-017-4836-0

Dheda K, Gumbo T, Gandhi NR, Murray M, Theron G, Udwadia Z, Migliori GB, Warren R. Global control of tuberculosis: from extensively drug-resistant to untreatable tuberculosis. Lancet Respir Med. 2014 Apr;2(4):321–338. https://doi.org/10.1016/S2213-2600(14)70031-1

Dundar D, Sonmez Tamer G. Resistance Rates of *Mycobacterium tuberculosis* isolates to primary antituberculous agents. Klimik Derg. 2009;22(2):52–54.

Hwang SM, Hwang KC, Hong YJ, Lee HR, Kim TS, Park KU, Song J, Lee JH, Kim EC. Improving antitubercular drug susceptibility testing with liquid media. Ann Clin Lab Sci. 2014 Spring; 44(2):123–130.

Karadag A, Tokac M, Guvenli A, Sunbul M, Gunaydin M, Sanic A. Resistance ratio to major anti-tuberculosis drugs of tuberculosis complex bacilli isolated from clinical samples. ANKEM Derg. 2004;18(4):189–192.

Karataş M, Kuyucu T, Sevim T. Evaluation of 1753 patients treated with the diagnosis of tuberculosis. Cumhuriyet Med J. 2019 Mar 27;41(1):34–41. https://doi.org/10.7197/223.vi.543017

Kunduracioğlu A, Karasu I, Bïçmen C, Özsöz A, Erbaycu AE. [Comparison of the performances of MTD Gene-Probe® test, BACTEC 960™ system and Löwenstein-Jensen culture methods in the diagnosis of smear-negative tuberculosis cases] (Turkish). Mikrobiyol Bul. 2013 Jul 29;47(3):417–431. https://doi.org/10.5578/mb.5728

Kurtoglu MG, Kesli R, Terzi Y, Baykan M. Investigation of the Susceptibilities of *Mycobacterium tuberculosıs* Complex strains to major anti-tuberculosis drugs with BACTEC MGIT 960 System. Nobel Med. 2011;7(1):42–48.

Kurtoğlu MG, Ozdemir M, Keşli R, Ozkalp B, Baysal B. [Isolation rate of *Mycobacterium tuberculosis* complex from patients with suspected tuberculosis and identification of the strains with BACTEC™ NAP and immunochromatographic TB Ag MPT64 Rapid™ Tests] (Turkish). Mikrobiyol Bul. 2011 Apr;45(2):266–273.

Kwak M, Lee WK, Lim YJ, Lee SH, Ryoo S. Systematic review and meta-analysis of the nitrate reductase assay for drug susceptibility testing of *Mycobacterium tuberculosis* and the detection limits in liquid medium. J Microbiol Methods. 2017 Oct;141:1–9. https://doi.org/10.1016/j.mimet.2017.07.001

Linger Y, Kukhtin A, Golova J, Perov A, Lambarqui A, Bryant L, Rudy GB, Dionne K, Fisher SL, Parrish N, et al. Simplified microarray system for simultaneously detecting rifampin, isoniazid, ethambutol, and streptomycin resistance markers in *Mycobacterium tuberculosis.* J Clin Microbiol. 2014 Jun 01;52(6):2100–2107. https://doi.org/10.1128/JCM.00238-14

Liu H, Lian L, Jiang Y, Huang M, Tan Y, Zhao X, Zhang J, Yu Q, Liu J, Dong H, et al. Identification of species of nontuberculous mycobacteria clinical isolates from 8 provinces of China. BioMed Res Int. 2016;2016:1–10. https://doi.org/10.1155/2016/2153910

Mbeha B, Mine M, Motswaledi MS, Dewar J. Nontuberculous mycobacteria, Botswana, 2011–2014. Emerg Infect Dis. 2019 Jul; 25(7):1401–1403. https://doi.org/10.3201/eid2507.181440

Miotto P, Zhang Y, Cirillo DM, Yam WC. Drug resistance mechanisms and drug susceptibility testing for tuberculosis. Respirology. 2018 Dec;23(12):1098–1113. https://doi.org/10.1111/resp.13393

Ozmen E, Aslan A, Ucar M, Aydin H, Yilmaz A. Resistance ratios of *Mycobacterium tuberculosis* Complex strains isolated in Erzurum Regional Tuberculosis Laboratory against major anti-tuberculosis drugs. ANKEM Derg. 2017;31(2):53–58.

Perincek G, Tabakoglu E, Otkun M, Ozdemir L, Ozdemir B. Resistance ratesofAnti-tuberculosisdrugsinpulmonarytuberculosis patients producing *Mycobacterium Tuberculosis.* Turk Thorac J. 2011 Sep 1;12(3):111–113. https://doi.org/10.5152/ttd.2011.25

Pienaar E, Linderman JJ, Kirschner DE. Emergence and selection of isoniazid and rifampin resistance in tuberculosis granulomas. PLoS One. 2018 May 10;13(5):e0196322. https://doi.org/10.1371/journal.pone.0196322

Saglik Bakanligi T.C. Turkiyede Verem Savaşi 2018 Raporu. Ankara (Turkey): Sağlık Bakanlığı Yayın; 2018.

Şamlı A, İlki A. Comparison of MALDI-TOF MS, nucleic acid hybridization and the MPT64 immunochromatographic test for the identification of *Mycobacterium tuberculosis* and non-tuberculosis *Mycobacterium* species. New Microbiol. 2016 Oct;39(4):259–263.

Saral OB, Sucu N, Boz GA, Erdem M, Koksal İ. Evaluation of combined drug resistance with Bactec method in 442 *Mycobacterium tuberculosis* strains. Turk Thorac J. 2007;8(3):174–178.

Spaulding AB, Lai YL, Zelazny AM, Olivier KN, Kadri SS, Prevots DR, Adjemian J. Geographic distribution of nontuberculous mycobacterial species identified among clinical isolates in the United States, 2009–2013. Ann Am Thorac Soc. 2017 Nov;14(11): 1655–1661. https://doi.org/10.1513/AnnalsATS.201611-860OC

Stagg HR, Lipman MC, McHugh TD, Jenkins HE. Isoniazid-resistant tuberculosis: a cause for concern? Int J Tuberc Lung Dis. 2017 Feb 01;21(2):129–139. https://doi.org/10.5588/ijtld.16.0716

Tavanaee Sani A, Shakiba A, Salehi M, Bahrami Taghanaki HR, Ayati Fard SF, Ghazvini K. Epidemiological characterization of drug resistance among *Mycobacterium tuberculosis* isolated from patients in Northeast of Iran during 2012–2013. BioMed Res Int. 2015;2015:1–6. https://doi.org/10.1155/2015/747085

Taylan M, Yilmaz S, Kaya H, Demir M, Selimoglu-Sen H, Sezgi C, Abakay O, Tanrıkulu AC, Abakay A. Tuberculosis control status of Diyarbakir province between the years 2005–2010. Dicle Med J. 2015;42(2):227–234.

Waters V, Ratjen F. Antibiotic treatment for nontuberculous mycobacteria lung infection in people with cystic fibrosis. Cochrane Database Syst Rev. 2016;12:CD010004. https://doi.org/10.1002/14651858.CD010004.pub4

WHO. Global tuberculosis report 2019. Geneva (Switzerland): World Health Organization; 2019.

WHO. The use of liquid medium for culture and DST [Internet]. Geneva (Switzerland): World Health Organization; 2007 [cited 2019 Dec 16]. Available from: https://www.who.int/tb/laboratory/policy_liquid_medium_for_culture_dst/en/

Polish Journal of Microbiology
2020, Vol. 69, No 2, 193–203
https://doi.org/10.33073/pjm-2020-022

ORIGINAL PAPER

Luffa cylindrica Immobilized with *Aspergillus terreus* QMS-1: an Efficient and Cost-Effective Strategy for the Removal of Congo Red using Stirred Tank Reactor

QANDEEL LARAIB[1, 2], MARYAM SHAFIQUE[2, 3]*, NUSRAT JABEEN[1, 3], SEHAR AFSHAN NAZ[3], HAFIZ RUB NAWAZ[4], BARKAT SOLANGI[4], ARIF ZUBAIR[5] and MUHAMMAD SOHAIL[1]

[1] Department of Microbiology, University of Karachi, Karachi, Sindh, Pakistan
[2] Department of Bioscience, Mohammad Ali Jinnah University, Karachi, Sindh, Pakistan
[3] Department of Microbiology, Federal Urdu University of Arts, Science and Technology, Gulshan-e-Iqbal, Karachi, Sindh, Pakistan
[4] PCSIR, Leather Research Centre, SITE, South Avenue, Karachi, Sindh, Pakistan
[5] Department of Environmental Sciences, Federal Urdu University of Arts, Science and Technology, Gulshan-e-Iqbal, Karachi, Sindh, Pakistan

Submitted 1 February 2020, revised 28 March 2020, accepted 19 April 2020

Abstract

Microbial populations within the rhizosphere have been considered as prosperous repositories with respect to bioremediation aptitude. Among various environmental contaminants, effluent from textile industries holds a huge amount of noxious colored materials having high chemical oxygen demand concentrations causing ecological disturbances. The study was aimed to explore the promising mycobiome of rhizospheric soil for the degradation of azo dyes to develop an efficient system for the exclusion of toxic recalcitrants. An effluent sample from the textile industry and soil samples from the rhizospheric region of *Musa acuminata* and *Azadirachta indica* were screened for indigenous fungi to decolorize Congo red, a carcinogenic diazo dye, particularly known for its health hazards to the community. To develop a bio-treatment process, *Aspergillus terreus* QMS-1 was immobilized on pieces of *Luffa cylindrica* and exploited in stirred tank bioreactor under aerobic and optimized environment. Quantitative estimation of Congo red decolorization was carried out using UV-Visible spectrophotometer. The effects of fungal immobilization and biosorption on the native structure of *Luffa cylindrica* were evaluated using a scanning electron microscope. *A. terreus* QMS-1 can remove (92%) of the dye at 100 ppm within 24 h in the presence of 1% glucose and 1% ammonium sulphate at pH 5.0. The operation of the bioreactor in a continuous flow for 12 h with 100 ppm of Congo red dye in simulated textile effluent resulted in 97% decolorization. The stirred tank bioreactor was found to be a dynamic, well maintained, no sludge producing approach for the treatment of textile effluents by *A. terreus* QMS-1 of the significant potential for decolorization of Congo red.

Key words: *Aspergillus terreus*, biodegradation, Congo red, immobilization, stirred tank bioreactor, textile industry

Introduction

The microbiome of the rhizospheric area is generally viewed as a treasure trove to scrutinize the indigenous microbial communities in search of natural detoxification of xenobiotics and other biotechnological perspective. It is estimated that one gram of this enriched soil comprises approximately 10 billion microorganisms, while only 1% of soil microbial population has been explored (Kakirde et al. 2010), which is widely reported for deterioration of organic polymers and pollutants.

Among numerous ventures, textile materials are directly associated with ecological angles to be unequivocally considered. With 10–15% of the share, the textile industry ranks on the top among all the dye consuming sectors utilizing 100,000 different synthetic coloring agents for various processes (Daassi et al. 2014). Discharge of dye-contaminated waste to receiving water bodies may cause immense ecological threats due to disturbances in photosynthetic activities of aquatic life, creating adverse effects on the amphibian territory (Husseiny 2008). It has been estimated that there are

* Corresponding author: S. Maryam, Department of Microbiology, Federal Urdu University of Arts, Science and Technology, Gulshan-e-Iqbal, Karachi, Sindh, Pakistan; **e-mail: maryamshafique@yahoo.com**

more than 670 textile industries in Pakistan, and almost all are dumping their hued mechanical waste into natural water bodies without embracing the essential treatment strategies (Andleeb et al. 2010). Although the worldwide figure demonstrates 280,000 tons discharge of textile dyes and colored pigments into water bodies, per annum (Maas and Chaudhari 2005), this situation can be mulled over to comprehend the gravity of the matter. Azo dyes representing 60–70% of the commonly used dyes are characterized by the presence of one or more chromogenic azo groups. Separate chromophore (N=N, C=C, C=O) and the auxochrome (−OH, $-NH_2$, $-NR_2$) are present in these dyes. These are intended to oppose the chemical and microbial assaults and stay stable in light and washing systems. A considerable lot of these dyes are cancer-causing and may trigger allergic reactions in human beings (Adedayo et al. 2004). Therefore, industrial wastes carrying azo dyes must be pretreated prior to its disposal to the environment.

The physical and chemical effluent-treatment strategies, for example, adsorption, synthetic precipitation, and flocculation, are inefficient because of the prerequisite of strong foundation, high cost, and generation of secondary-sludge (McMullan et al. 2001). Given the disadvantages of chemical treatments, microbial remediation procedures have gained strong consideration during recent decades. Fungi turned out to be the most reasonable species for the treatment of textile-effluents for the evacuation of toxic colors. Numerous fungal strains either in free-living or in the immobilized state have been utilized for the decolorization of various dyes (Prachi and Anushree 2009). The ability of fungi to decolorize dyes relies on three mechanisms, namely biosorption (Fu and Viraraghavan 2001), biodegradation (Conneely et al. 1999), and enzymatic mineralization (Wesenberg et al. 2003; Rojek et al. 2004). Bioreactors operated with immobilized fungal cells have shown enhanced productivity, and permit expanded process strength and resistance to shock loadings in comparison to free fungal cells for decolorization of dyes (Hao et al. 2000).

The reported potential of mycobiota of rhizospheric soil for bioremediation and ecological effect of azo dyes envisaged the current study to isolate fungal species and to evaluate their ability to develop an efficient system for removal of hazardous and toxic recalcitrants in stirred tank reactor.

Experimental

Materials and Methods

The chemicals used in the study include Congo red (Sigma-Aldrich), Sabouraud's Dextrose Broth (Oxoid) as a fungal growth medium, Technical Agar (Oxoid), and 0.05% Tween 80 solution for the preparation of the spore suspension. Composition of Minimal Salt Media was [per l, $Na_2HPO_4 \cdot 2H_2O$: 7.8 g; KH_2PO_4: 6.8 g; $MgSO_4 \cdot 7H_2O$: 0.2 g; $NaNO_3$: 0.085 g; $Ca(NO_3)_2 \cdot 4H_2O$: 0.050 g; $C_6H_8FeNO_7$: 0.01 g; trace elements solution: 10 ml]. Simulated textile effluent (STE) was formulated as [per l, acetic acid (99.9%): 0.15 ml; $(NH_4)_2Cl$: 108.0 mg; KH_2PO_4: 67.0 mg; $NaHCO_3$: 840.0 mg; $MgSO_4 \cdot 7H_2O$: 38.0 mg; $CaCl_2$: 21.0 mg; $FeCl_3 \cdot 6H_2O$: 7.0 mg; glucose: 860 mg].

Sampling and isolation of fungi. The rhizospheric soil samples of *Musa acuminata* (banana plant) and *Azadirachta indica* (neem tree) were collected from the garden area of Federal Urdu University of Arts, Science and Technology, Gulshan-e-Iqbal Campus, Karachi, Pakistan. The textile effluent sample was collected from local textile industry in Karachi. The spread plate technique was adopted for the isolation of fungi from soil samples. Each soil sample (1 g) was serially diluted 10^4 times in sterile distilled water (10 ml), and 0.1 ml of the diluted sample was spread on Sabouraud dextrose agar (SDA) plates followed by incubation at 28°C for seven days. Fungal strains were also isolated from the sampled textile effluent by adopting a similar procedure. The fungal isolates were identified based on microscopic and colonial characteristics on SDA (Larone 1995).

Qualitative screening of fungal isolates for bioremoval of Congo red. All the fungal isolates were screened qualitatively for removal of dye using SDA supplemented with 0.01% Congo red. Fungal discs (1 cm) were cut from the periphery of each colony, inoculated on center of the modified SDA, and incubated for seven days at 28°C. The formation of the clear transparent zone around the fungal colony indicated the degradation of Congo red by fungi.

Quantitative screening of fungal isolates for bioremoval of Congo red. Fungal isolates were screened quantitatively for removal of Congo red using SDB supplemented with 0.01% Congo red (modified SDB) through shake flask experiments. Fungal discs (1 cm) from SDA plates were cut from the periphery of each colony inoculated into the flask containing 20 ml of modified SDB and incubated at 28°C for three days on an orbital shaker at 150 rpm. The uninoculated flasks of the same medium served as controls in each case. A 4-ml sample was drawn aseptically from each flask after 72 h, filtered to separate biomass, and centrifuged at 5,000 rpm for 15 minutes. The degree of decolorization of Congo red by each fungal strain was determined in terms of percentage, measuring the absorbance of the cell-free culture supernatant (CFCS) spectrophotometrically at 498 nm (Mahbub et al. 2012).

Development of inoculum. The promising fungal strain, *A. terreus* QMS-1 was revived on the SDA plate

for a week at 28°C. The spores of *A. terreus* QMS-1 were harvested using a wire loop and shifted to the flask containing 50 ml of sterile distilled water with 0.05% Tween 80 (v/v). Following 30 minutes of vigorous shaking, 10 µl of the spore suspension was utilized for spore count. This inoculum was immediately used for further experimentation or stored in a refrigerator at 4°C for one week.

Optimization of physicochemical parameters for degradation of Congo red. The effect of agitation on biodegradation efficiency was studied by using SDB supplemented with 0.01% Congo red. Test flasks were inoculated with 1 ml spore suspension of *A. terreus* QMS-1, whereas uninoculated flasks served as control. One set of test and control flasks was incubated at room temperature in an orbital shaker at 100 rpm, while another set was incubated without shaking. Likewise, keeping shaking as constant, the effect of concentration of Congo red on biodegradation efficiency was investigated using 50 ml of Minimal Salt Medium (MSM) supplemented with different concentrations of Congo red (from 100–500 ppm) as described previously (Ali et al. 2008a). Similarly, the effect of carbon source in the medium on the ability of *A. terreus* QMS-1 to reduce Congo red was studied with different carbon sources like glucose, fructose, lactose, maltose, sucrose and starch in MSM containing a 100-ppm dye. When determining an optimum nitrogen source, the previously known factors were kept constant, and nitrogen source present in MSM (peptone, yeast extract, ammonium sulfate, and ammonium nitrate) was varied. The effect of pH was also investigated in a similar way by maintaining pH to 5.0, 7.0, and 9.0 with 1 M HCl or 1 M NaOH keeping other parameters unchanged.

In all the experiments, each test flask was inoculated with 1 ml spore suspension of *A. terreus* QMS-1, whereas uninoculated flasks served as controls. A 4-ml sample from each flask was taken aseptically after every 24 h up till 120 h, filtered and centrifuged at 5,000 rpm for 15 minutes, and used as cell-free culture supernatant (CFCS) to check the percent decolorization.

Immobilization of *A. terreus* QMS-1 on carrier materials. Seventeen natural and synthetic carrier materials were selected for fungal immobilization based on their stability and cost effectiveness, including polyethene polymer, sand, gravels, natural loofah sponge, corn cob, used steel wool, orange peels, banana skins, nylon net, polyurethane foam (PUF), coconut bagasse, sugarcane bagasse, water beads, scouring pad, sandpaper, pistachio shells, and sunflower seed shells. All the supports were washed thoroughly with distilled water. Flasks containing 200 ml of SDB and 12–15 pieces of carrier material were autoclaved, inoculated with 10 ml of spore suspension of *A. terreus* QMS-1, and kept on a rotary shaker at room temperature for 15 days.

Degradation of Congo red by immobilized cells in the stirred tank bioreactor. A benchtop stirred tank bioreactor (STR) comprised of an overhead impeller, and a vessel body (2 l volume) was used. The reactor was run at room temperature, pH 5.0, with a working volume of 1 l of simulated textile effluent (STE) containing 100 ppm of Congo red. The medium was inoculated separately with different carrier materials with immobilized *A. terreus* QMS-1. The hydraulic retention time was 12–120 h. The effluent samples were taken intermittently after every 12 h and analyzed for percent degradation of dye. When investigating the dye adsorption on the carrier materials, similar experiments were performed using carrier supports without immobilized cells.

Recycling of immobilized *A. terreus* QMS-1. In another experiment using the same procedure, STR was run and fed with immobilized carrier material yielding maximum decolorization of STE. The matrix with immobilized cells was checked for repeated use by reusing the previously withdrawn immobilized carrier supports from the reactor tank to fresh STE.

Quantitative estimation of decolorization. Decolorization was determined using a method described by Mahbub et al. (2012), measuring the absorbance of the CFCS at 498 nm by UV-Visible spectrophotometer. The extent of dye degradation was calculated in terms of percentage, using the following equation:

$$\% \text{ decolorization} = \frac{\text{initial obsorbance} - \text{final absorbance}}{\text{initial obsorbance}} \times 100$$

where, initial absorbance is the absorbance taken at 0 h after the inoculation, and final absorbance is the absorbance taken at after every 12–24 h.

Physico-chemical characterization of treated and untreated effluent samples under STR conditions. Treated and untreated STE samples were tested by using standard methods of Biological Oxygen Demand (APHA 5210 B), Chemical Oxygen Demand (APHA 5220 C), Total Dissolved Solids (APHA 2540 C), and Total Suspended Solids (APHA 2450 D).

Scanning electron microscope analysis. The surface morphology of the best carrier material (natural loofah sponge) before and after the immobilization and biosorption was investigated using scanning electron microscope (SEM) analysis (JEOL, Model number: JSM-6380A).

Statistical analysis. All the experimental attempts were executed in triplicate, and the findings were declared as mean ± standard deviation. Experimental data were analyzed by the one-way and two-way analysis of variance (ANOVA) using GraphPad Prism (version 6.0).

Results and Discussion

Based on the environmental impact of azo dyes as well as reported bioremediation potential of fungi, the present study was aimed to isolate and screen indigenous mycobiota for developing a process of bioremediation. For this purpose, 56 fungal strains isolated from different samples of soil and textile effluent were identified by standard mycological protocols (Table I). The identified fungal strains included *Alternaria* sp., *A. flavus*, *A. niger*, *A. terreus*, *Cladosporium* sp., *Curvularia* sp., *Fusarium* sp., *Helimenthosporium* sp., *Mucor* sp., *Penicillium* sp., and *Rhizopus* sp.

This data also revealed that most of the fungal strains belonged to the genus *Aspergillus.* Amongst Aspergilli, *A. flavus* was found most frequent (19%) as compared to the other fungal strains isolated from different soil and textile effluent samples followed by *A. niger* (13.4%), *A. terreus* (13.4%), *Mucor* sp. (11.5%), *Penicillium* sp. (11.5%), *Rhizopus* sp. (9.6%), *Curvularia* sp. (7.69%), *Cladosporium* sp. (5.7%), *Fusarium* sp. (5.7%), *Helimenthosporium* sp. (5.7%), and *Alternaria* sp. (3.8%). Earlier, Cardoso Duarte and Costa-Ferreira (1994) have reported the abundance of *Aspergillus* in soil, whereas, Sohail et al. (2009) found *Aspergillus* as the predominant genus of the hydrolytic-enzyme producing fungi in soil.

Out of 56 fungal isolates, 42 strains showed decolorization of Congo red in the qualitative screening method. The ability of the fungi tested to remove dye was confirmed by the appearance of clear zones around the fungal colonies whereas, 14 strains were found unable to decolorize the Congo red, forming no zones of

Table I
Identification and screening of fungal isolates for biodegradation potential of Congo red.

Fungal isolate number	The fungi identified	Qualitative screening for Congo red dye	Quantitative screening for Congo red dye (%)
01	*Alternaria* sp QMS-1	–	–
02	*Alternaria* sp QMS-2	+	66
03	*Aspergillus flavus* QMS-1	+	60
04	*Aspergillus flavus* QMS-2	+	55
05	*Aspergillus flavus* QMS-3	+	80
06	*Aspergillus flavus* QMS-4	+	17
07	*Aspergillus flavus* QMS-5	+	80
08	*Aspergillus flavus* QMS-6	–	–
09	*Aspergillus flavus* QMS-7	–	–
10	*Aspergillus flavus* QMS-8	+	26
11	*Aspergillus flavus* QMS-9	+	42
12	*Aspergillus flavus* QMS-10	+	28
13	*Aspergillus niger* QMS-1	–	–
14	*Aspergillus niger* QMS-2	+	54
15	*Aspergillus niger* QMS-3	+	26
16	*Aspergillus niger* QMS-4	+	53
17	*Aspergillus niger* QMS-5	+	18
18	*Aspergillus niger* QMS-6	+	89
19	*Aspergillus niger* QMS-7	+	54
20	*Aspergillus terreus* QMS-1	+	92
21	*Aspergillus terreus* QMS-2	+	35
22	*Aspergillus terreus* QMS-3	+	12
23	*Aspergillus terreus* QMS-4	–	–
24	*Aspergillus terreus* QMS-5	+	12
25	*Aspergillus terreus* QMS-6	+	31
26	*Aspergillus terreus* QMS-7	+	79
27	*Cladosporium* sp QMS-1	+	65
28	*Cladosporium* sp QMS-2	+	66
29	*Cladosporium* sp QMS-3	+	62
30	*Curvularia* sp QMS-1	–	–
31	*Curvularia* sp QMS-2	+	56
32	*Curvularia* sp QMS-3	–	–
33	*Curularia* sp QMS-4	–	–
34	*Fusarium* spQMS-1	+	43
35	*Fusarium* sp QMS-2	+	66
36	*Fusarium* sp QMS-3	+	81
37	*Helimenthosporium* sp QMS-1	+	74
38	*Helimenthosporium* sp QMS-2	+	62
39	*Helimenthosporium* sp QMS-3	+	54
40	*Mucor* sp QMS-1	+	31
41	*Mucor* sp QMS-2	–	–
42	*Mucor* sp QMS-3	+	62
43	*Mucor* sp QMS-4	–	–
44	*Mucor* sp QMS-5	–	–
45	*Mucor* sp QMS-6	+	82
46	*Penicillium* sp QMS-1	_	_
47	*Penicillium* sp QMS-2	+	43
48	*Penicillium* sp QMS-3	+	83
49	*Penicillium* sp QMS-4	+	79
50	*Penicillium* sp QMS-5	+	65
51	*Penicillium* sp QMS-6	–	–
52	*Rhizopus sp* QMS-1	+	11
53	*Rhizopus* spQMS-2	+	25
54	*Rhizopus* sp QMS-3	–	–
55	*Rhizopus* sp QMS-4	+	56
56	*Rhizopus* sp QMS-5	+	43

(+) – it indicates the zone of Congo red decolorization around the fungi
(–) – it indicates no zone of Congo red decolorization around the fungi

decolorization. Since the screening was mainly carried out using SDA that supports the growth of fungi and, therefore, growth-linked removal of the dye was investigated. The absence of zones around 14 strains may be linked with the inhibitory effect of the dye on the growth rate of fungi due to which degradation of dye proceeded more slowly as compared to radial growth of fungi; consequently, zone of decolorization did not appear around the fungal mycelia (Machado et al. 2006).

The findings of quantitative screening assay showed that fungal isolates namely *A. flavus* QMS-3, *A. flavus* QMS-5, *A. niger* QMS-6, *Fusarium* sp. QMS-3, *Mucor* sp. QMS-6, *Penicillium* sp. QMS-3 and *A. terreus* QMS-1 were found to possess excellent dye removal potential. However, amongst all the outstanding dye degraders, the strain QMS-1 of *A. terreus* exhibited promising potential for degradation of Congo red (92%) as compared to other fungal strains (Table I).

The dye removal ability of fungi is attributed to different phenomena such as bio-sorption/ bio-adsorption followed by bio-degradation (Knapp and Newby 1995; Fu and Viraraghavan 2000; Sumathi and Manju 2000; Ali et al. 2008b). Bio-sorption is regarded as the primary process of dye removal, which enables the fungi to bind with molecules of dyes in the vicinity of fungal biomass due to electrostatic attraction between the positively charged cell walls and negatively charged dye molecules (Aksu and Tezer 2000). Bio-degradation enables the fungi to break down the dye molecule enzymatically into various products (Saranraj et al. 2010). It has been reported that some species belong to genus *Aspergillus* can produce enzymes like laccase, lignin peroxidases, and manganese peroxidases (Kanayama et al. 2002). In this context, it may be suggested that high electrostatic attractions due to the increased number of positively charged receptors on the cell wall of *A. terreus* QMS-1 were responsible for the efficient removal of Congo red in comparison with other fungal strains.

The strain *A. terreus* QMS-1 was found capable of exhibiting maximum degradation of Congo red (95%) under shaking (100 rpm) conditions after 24 h of cultivation, although degradation was increased to 96% when cultivation was extended to 48 h. In contrast, the cultivation of *A. terreus* QMS-1 under static conditions caused a decrease in decolorization, and only 62% and 63% reduction was noted in 24 h and 48 h, respectively (Fig. 1). The aeration has its recognizable effect on the growth and metabolic activities of all the obligate aerobes including fungi by expanding oxygenation and dissemination of nutrients in the medium that lead to the increased fungal mass and might be heightened expression of oxidative enzymes for the biotransformation of dye (Rani et al. 2014). However, static cultural medium causes a reduction in decolorization potential of the fungal strains by limiting oxygen just

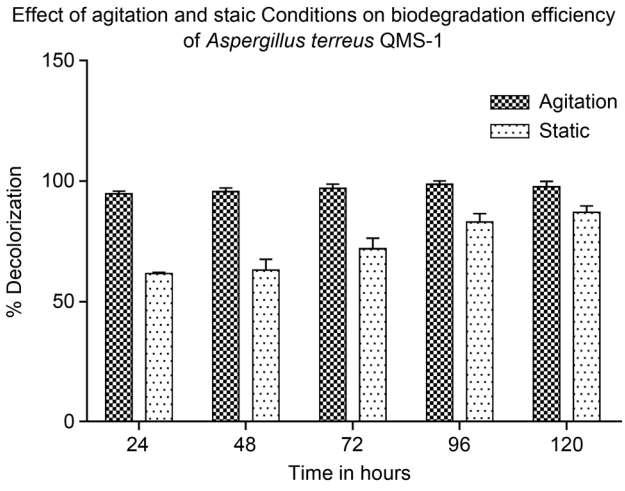

Fig. 1. Effect of agitation and static conditions on biodegradation efficiency of *Aspergillus terreus* QMS-1.

in inward layers of fungal mycelia triggering suppression of oxidative enzymes and considerable reduction in biodegradation activities.

The concentration of dye has a marked impact on the dye removal efficiency as a higher concentration may inhibit fungal growth. The strain was found capable of degrading the dye at all concentrations after 72 h; however, maximum degradation (95%) was observed with 100 ppm of dye followed by 84%, 78.6%, 70%, and 76% at 200, 300, 400, and 500 ppm, respectively (Fig. 2). Hence, it could be stated that the decolorization ability of *A. terreus* QMS-1 decreased with the increasing concentration of dye, which may be attributed to the toxicity of Congo red at higher concentrations as reported for some other fungi (Sponza and Isik 2005; Siddiqui et al. 2009). Nonetheless, the dye at a concentration equal to 90 ppm was being removed within 24 h regardless of the initial concentration used. In the studies by Gharbani et al. (2008), 60 ppm of Congo red was used as 'simulated loaded textile wastewater' implicating the importance of dye removal ability by *A. terreus* QMS-1 and its possible application for *in situ* dye removal.

The strain, *A. terreus* QMS-1 showed maximum degradation of Congo red in the presence of 1% glucose (95.2%) followed by maltose (90.3%), fructose (76%), sucrose (73%), lactose (66.6%), and starch (56.70%) after 24 h of cultivation under shaking conditions in the medium containing 100 ppm of Congo red (Fig. 3). These findings showed that glucose was the most suitable catabolisable carbon source for *A. terreus* QMS-1 that accelerated the decolorization of Congo red. Nevertheless, monosaccharides like glucose are decomposed readily as compared to the disaccharides or polysaccharides. Earlier research findings suggested that 5.0 g l^{-1} glucose was sufficient to achieve maximum decolorization of Congo red as a further increase in

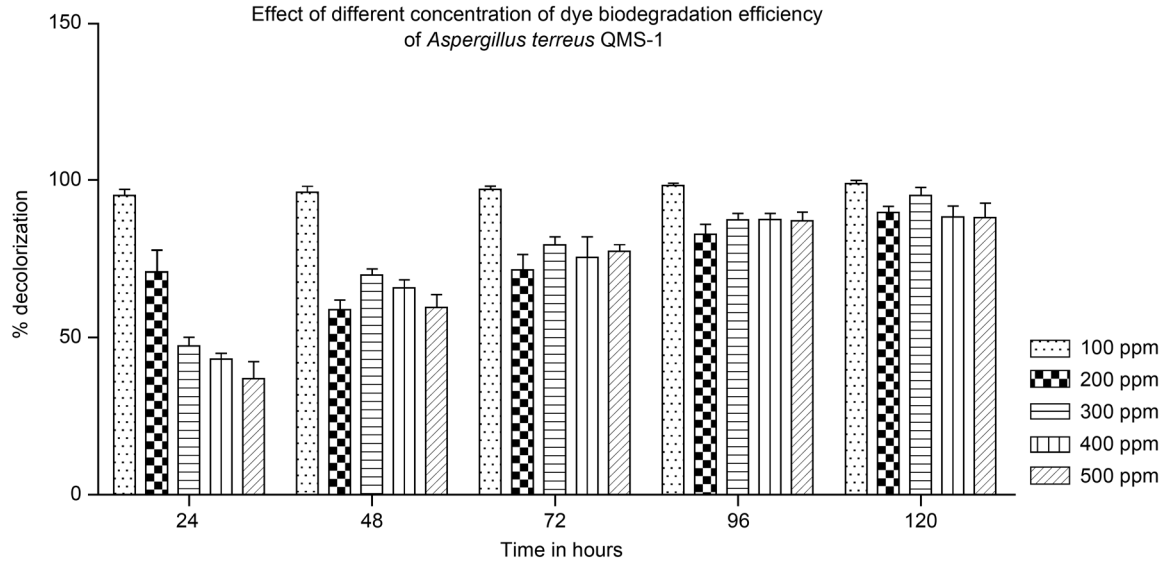

Fig. 2. Effect of different concentration of dye on biodegradation efficiency of *Aspergillus terreus* QMS-1.

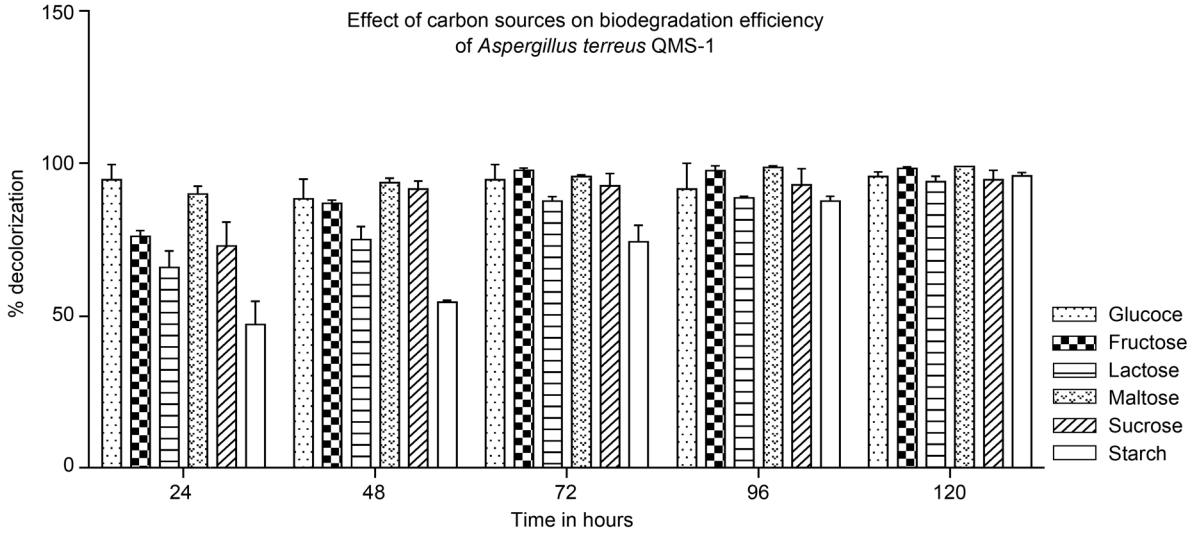

Fig. 3. Effect of carbon sources on biodegradation efficiency of *Aspergillus terreus* QMS-1.

glucose concentration resulted in a decline in the rate of dye decolorization (Radha et al. 2005). Furthermore, it is also reported that polysaccharides such as starch, cellulose, and its derivatives did not support the dye decolorization process by fungi (Vaidyanathan et al. 2011).

The strain, *A. terreus* QMS-1, exhibited maximum dye removal, i.e., 92.3% and 91% in the presence of ammonium nitrate and ammonium sulfate after 24 h of cultivation, respectively. However, a noticeable decline in the removal of dye was observed, i.e., 55.2% and 39.2% in the presence of organic sources of nitrogen, i.e., peptone and yeast extract, respectively (Fig. 4). The results obtained are in agreement with those of Kashif et al. (2011) who reported the maximum decolorization of dye, Sollar Golden Yellow R by *Pleurotus osttreatus* species in the presence of ammonium sulfate that facilitated in the regeneration of NADH in the medium as electron donor, causing reduction of the dye.

A. terreus QMS-1 showed maximum mineralization of Congo red at pH 5.0, i.e., 95% and 99% after 24 h and 48 h, respectively. In contrast, an increase in pH (alkaline pH) proved to have an undesirable effect on the biodegradation potential of *A. terreus* QMS-1, and decolorization was decreased considerably to 39% (Fig. 5). In this regard, it was reported that the effective dye biotransformation/decolorization process and fungal growth usually required pH between 3 and 6 (Mansur et al. 2003; Baldrian 2004). Low pH enables the fungi to show maximum dye removal potential by providing an increased number of H^+ ions located on the fungal cell wall and facilitating the uptake of negatively charged dye molecule (Won et al. 2009). It has

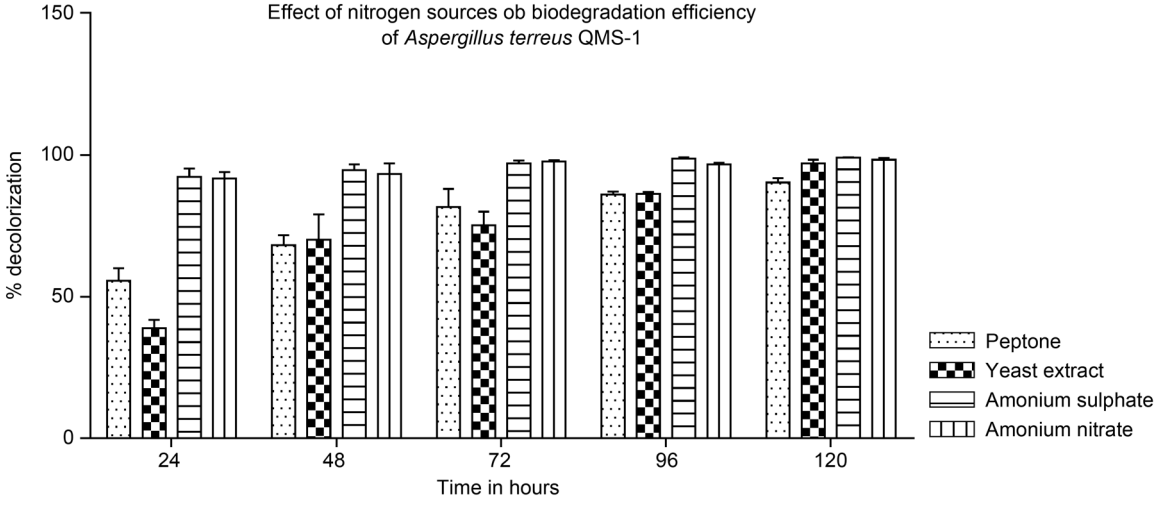

Fig. 4. Effect of nitrogen sources on biodegradation efficiency of *Aspergillus terreus* QMS-1.

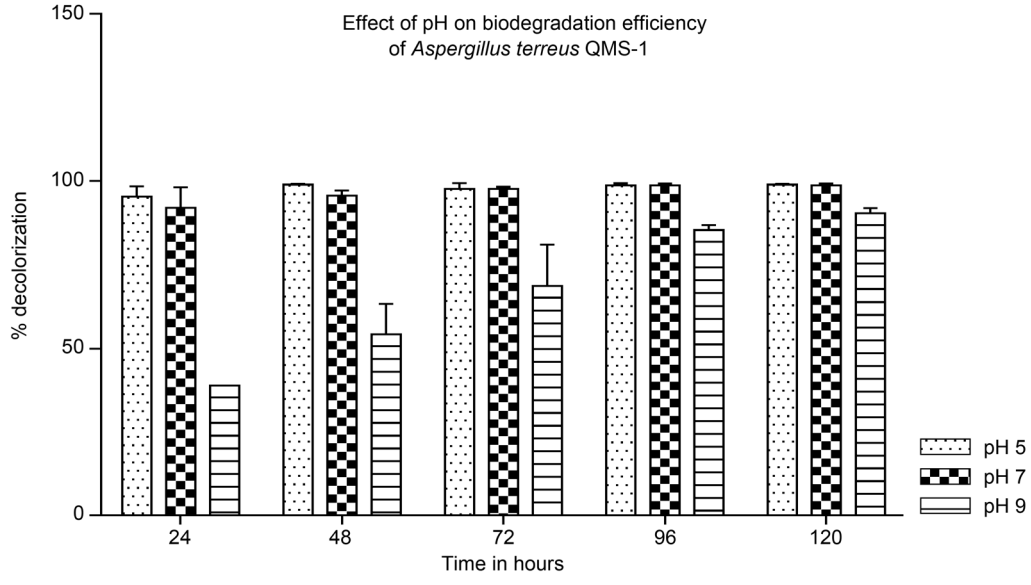

Fig. 5. Effect of pH on biodegradation efficiency of *Aspergillus terreus* QMS-1.

also been observed and suggested that a further increase in pH greater than 5.0 leads to the disintegration of fungal mycelia and reduction in fungal growth, therefore, the dye removal process decreases.

Using the STR system, the effect of various natural and synthetic immobilization support matrices on Congo red removal efficiency was investigated. *A. terreus* QMS-1 was immobilized over 17 different support matrices to select the one best for decolorization/degradation of dye. The selection of support matrices was based on high porosity, inert nature, easy availability, and low cost. It was found that *A. terreus* QMS-1 immobilized over natural loofah sponge showed maximum removal of Congo red, i.e., 97%, followed by polyethene polymer (92%), sugarcane bagasse (86.3%), nylon net (83%), used steel wool (83%), orange peels (81%), scouring pad (80%), sand (77.3%), coconut bagasse (77.3%), polyurethane foam (74.87%), banana skins (67.8%), water beads (63%), corn cob (62%), sand paper (62%), pistachio shells (65%), sunflower seed shells (55.5%) and gravels (48.9%) at a hydraulic retention time of 12 h under STR conditions. However, complete decolorization, i.e., 100% removal of Congo red dye, was achieved at a hydraulic retention time of 48 h by employing *A. terreus* QMS-1 immobilized over natural loofah sponge (Fig. 6). The results of removal of Congo red dye (100 mg/l) under STR conditions revealed the superiority of natural loofah sponge as an immobilization support matrix for *A. terreus* QMS-1, as compared to the other immobilization supports (Fig. 7), in terms of decolorization of dye and reduction in the treatment time. Natural loofah sponge is derived from the vegetable fibre of *Luffa cylindrica* or *Luffa aegyptiaca.* The spatial structure of natural loofah sponge is formed

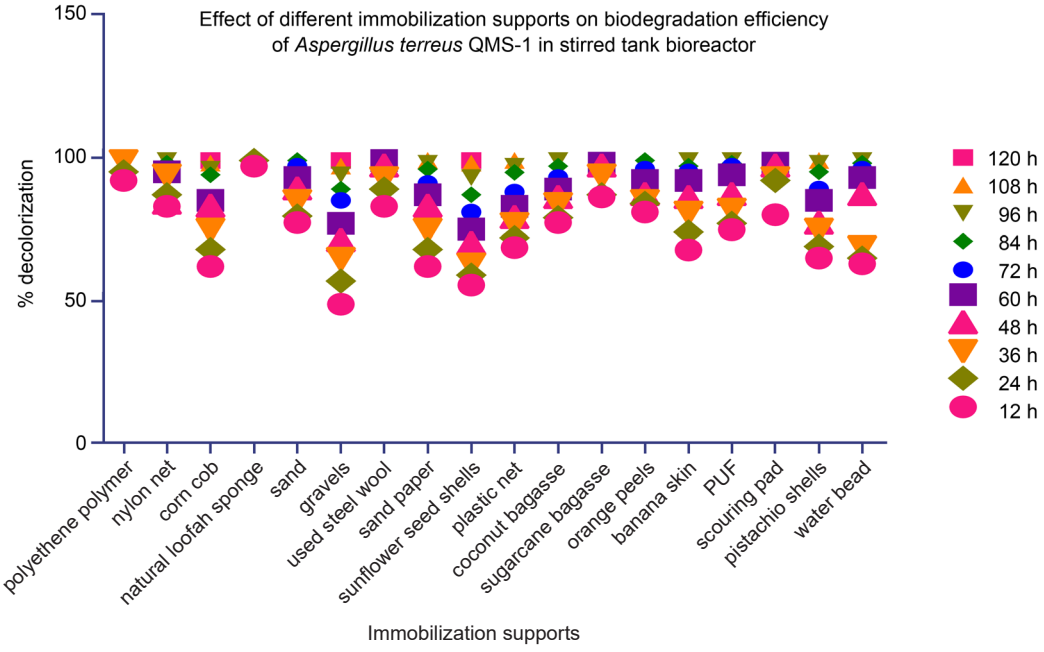

Fig. 6. Effect of different immobilization supports on biodegradation efficiency of *Aspergillus terreus* QMS-1 in the stirred tank bioreactor.

by the parallel and antiparallel arrangement of fibres, thereby creating open and free spaces for the exchange of nutrients. Moreover, it provides enough space for the diffusion of oxygen and contains sites for the physical confinement or localization of fungal hyphae. Other advantages of this carrier include its high porosity (85–95%) with simultaneous low density (0.018–0.05 g/cm^3) and mechanical strength. Previously, natural loofah sponge has been applied as a Microalgal-luffa sponge immobilized discs for biosorption of nickel (Akhtar et al. 2003). Furthermore, due to the robustness, stability, and regenerating capability of this matrix, the immobilized culture can be recycled for at least seven times. Besides, loofah sponge is also used as a nutrient source for white-rot fungi providing carbon and energy contributing towards long-term bioremediation (Mazmanci et al. 2005).

The decolorization of Congo red dye in simulated textile effluent was also investigated in the bioreactor with entire pieces of natural loofah sponge without fungal cells to determine the physical adsorption capacity of the support matrix. It was found that removal of

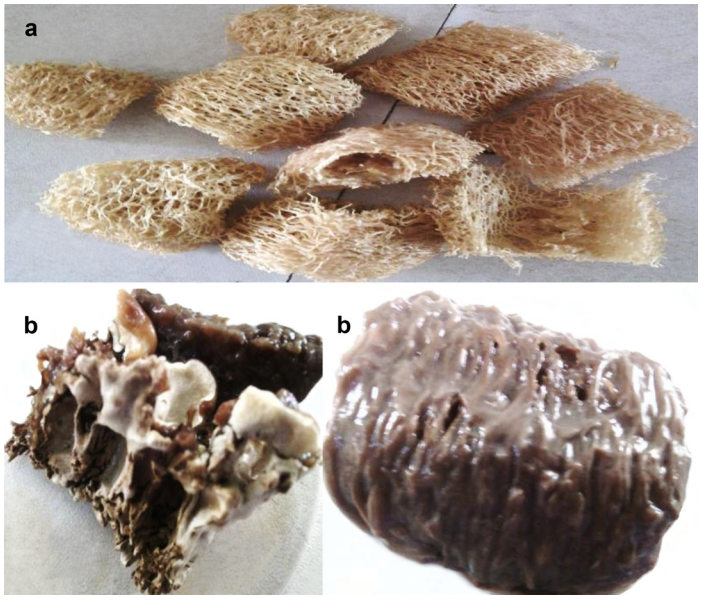

Fig. 7. *Luffa cylindrica* (a) before and (b) after with immobilization of *Aspergillus terreus* QMS-1.

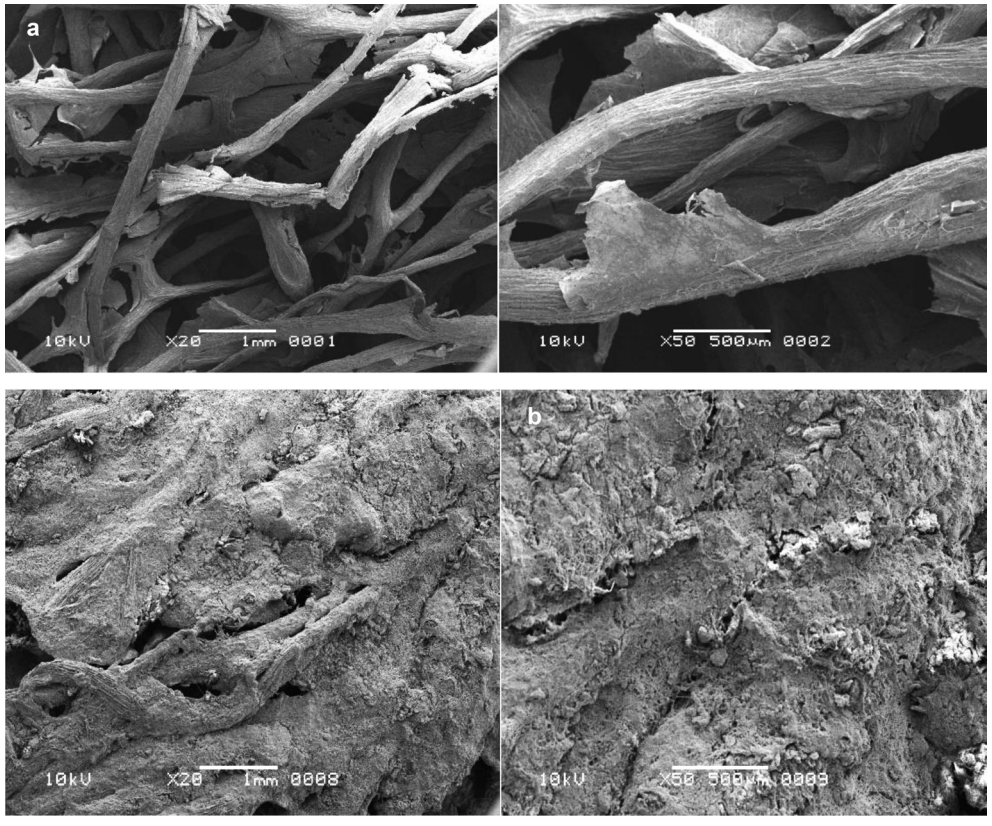

Fig. 8. SEM micrographs of *Luffa cylindrica*, a) before and b) after immobilization of *Aspergillus terreus* QMS-1.

Congo red from simulated textile effluent by the intact pieces of natural loofah sponge was not significant, and hence the dye removal was not because of adsorption by the natural loofah sponge.

These experimental findings suggested that natural loofah sponge possessed all the required characteristics to be utilized as an ideal bio-support. Therefore, it was further subjected to SEM analysis at various magnifications (×20 and ×50) to observe the morphological changes before and after the immobilization of *A. terreus* QMS-1, and was later applied in STR system. SEM micrographs of intact natural loofah sponge indicated porous, hollow, and rough topography with a greater number of interstitial voids and inner channels (Fig. 8a). This was converted into a compact, tighter, and smooth material as fungal mycelia covered interstitial voids, inner channels, and superficial surfaces (Fig. 8b). The channeled structure has an identifiable effect as it allows respiratory gases and essential elements effectively through fungal mycelial mass, increasing metabolic efficiency of the strain. Therefore, immobilized fungi are viewed as more proficiently than suspended mycelia in many frameworks (Villena et al. 2010).

Effect of repeated use of *A. terreus* QMS-1 immobilized over the most promising carrier matrix (natural loofah sponge) on decolorization of Congo red dye in STE was also evaluated to make the use of bioreactor more affordable and economical. Moreover, it was found that loofah sponge was an extremely stable carrier and can be reused for at least eight times with the same rate of decolorization, i.e., 97% (12 h). However, further recycling for more than eight cycles resulted in a gradual reduction in the rate of decolorization by the immobilized *A. terreus* QMS-1. In this regard, several factors including higher molecular mass, structural complexity, a saturation of receptors on fungal cells, and the presence of inhibitory functional groups may cause desorption or removal of dye from fungal cells, especially at the long contact time, thereby declining the recyclability of immobilized fungus and affecting the process of decolorization (Ali and Muhammad 2008b).

Although microbes can remove color-producing recalcitrant compounds by a wide variety of mechanisms, it has also been indicated by several research studies that detoxification of reactive group of azo dyes leads to the generation of robust and even more lethal intermediates during biodegradation processes (Gottlieb et al. 2003). Therefore, Biological Oxygen Demand (BOD), Chemical Oxygen Demand (COD), Total Dissolved Solids (TDS), and Total Suspended Solids (TSS) analysis of the dye-containing effluent samples (before and after treatment under STR) were carried out to evaluate and confirm the extent of degradation of Congo red dye by *A. terreus* QMS-1 through

quantifying and comparing their organic loads. In case of STR treatment system, the BOD, COD, TDS and TSS values decreased from 1,260, 2,657, 3,000, and 500 mg/l to 300, 1,180, 2,160, and 160 mg/l at HRT of 12 h respectively, showing the acceptable values according to National Environmental Quality Standards (NEQs) range. The drastic reduction of BOD, COD, TDS, and TSS values suggests the significance of STR treatment technology, even though it is crucially imperative to explore final residues of dye mineralization to render this system as an ecologically perfect and economical alternative to conventional treatment methods.

Conclusions

This research study proclaimed the excellent attempt of immobilized *A. terreus* QMS-1 under STR conditions for the reduction of Congo red, i.e., 97% decolorization within 12 h, reinforcing its potential for a safer environment by reducing the hazardous effects of textile dyes and proposing this technology as an adaptable, proficient and sustainable way for dealing with textile effluents.

Acknowledgments

The authors acknowledge Dean Faculty science research grant, Federal Urdu University of Arts, Science and Technology, Gulshan-e-Iqbal Campus, Karachi, Pakistan, for providing financial support to conduct this study.

Conflict of interest

The authors do not report any financial or personal connections with other persons or organizations, which might negatively affect the contents of this publication and/or claim authorship rights to this publication.

Literature

Adedayo O, Javadpour S, Taylor C, Anderson WA, Moo-Young M. Decolorization and detoxification of methyl red by aerobic bacteria from a wastewater treatment plant. World J Microbiol Biotechnol. 2004;20(6):545–550. https://doi.org/10.1023/B:WIBI.0000043150.37318.5f

Akhtar N, Iqbal J, Iqbal M. Microalgal-luffa sponge immobilized disc: a new efficient biosorbent for the removal of Ni(II) from aqueous solution. Lett Appl Microbiol. 2003 Aug;37(2):149–153. https://doi.org/10.1046/j.1472-765X.2003.01366.x

Aksu Z, Tezer S. Equilibrium and kinetic modelling of biosorption of Remazol Black B by *Rhizopus arrhizus* in a batch system: effect of temperature. Process Biochem. 2000 Dec;36(5):431–439. https://doi.org/10.1016/S0032-9592(00)00233-8

Ali H, Muhammad SK. Biodecolorization of acid violet 19 by *Alternaria solani*. Afr J Biotechnol. 2008b;7:831–833.

Ali N, Ikramullah, Lutfullah G, Hameed A, Ahmed S. Decolorization of Acid red 151 by *Aspergillus niger* SA1 under different physicochemical conditions. World J Microbiol Biotechnol. 2008a Jul;24(7):1099–1105. https://doi.org/10.1007/s11274-007-9581-6

Andleeb S, Atiq N, Ali MI, Razi-Ul-Hussnain R, Shafique M, Ahmad B, Ghumro PB, Hussain M, Hameed A, Ahmed S. Biological treatment of textile effluent in stirred tank bioreactor. Int J Agric Biol. 2010;12:256–260.

Baldrian P. Purification and characterization of laccase from the white-rot fungus *Daedalea quercina* and decolorization of synthetic dyes by the enzyme. Appl Microbiol Biotechnol. 2004 May 1;63(5): 560–563. https://doi.org/10.1007/s00253-003-1434-0

Cardoso Duarte JÃ, Costa-Ferreira M. Aspergilli and lignocellulosics: enzymology and biotechnological applications. FEMS Microbiol Rev. 1994 Mar;13(2–3):377–386. https://doi.org/10.1111/j.1574-6976.1994.tb00057.x

Conneely A, Smyth WF, McMullan G. Metabolism of the phthalocyanine textile dye remazol turquoise blue by *Phanerochaete chrysosporium*. FEMS Microbiol Lett. 1999 Oct;179(2):333–337. https://doi.org/10.1111/j.1574-6968.1999.tb08746.x

Daâssi D, Rodríguez-Couto S, Nasri M, Mechichi T. Biodegradation of textile dyes by immobilized laccase from *Coriolopsis gallica* into Ca-alginate beads. Int Biodeterior Biodegradation. 2014 May;90:71–78. https://doi.org/10.1016/j.ibiod.2014.02.006

Fu Y, Viraraghavan T. Fungal decolorization of dye wastewaters: a review. Bioresour Technol. 2001 Sep;79(3):251–262. https://doi.org/10.1016/S0960-8524(01)00028-1

Fu YZ, Viraraghavan T. Removal of a dye from an aqueous solution by the fungus *Aspergillus niger*. Water Qual Res J Can. 2000;35:95–111.

Gharbani P, Tabatabaii SM, Mehrizad A. Removal of Congo red from textile wastewater by ozonation. Int J Environ Sci Technol. 2008 Sep;5(4):495–500. https://doi.org/10.1007/BF03326046

Gottlieb A, Shaw C, Smith A, Wheatley A, Forsythe S. The toxicity of textile reactive azo dyes after hydrolysis and decolourisation. J Biotechnol. 2003 Feb;101(1):49–56. https://doi.org/10.1016/S0168-1656(02)00302-4

Hao OJ, Kim H, Chiang PC. Decolorization of wastewater. Crit Rev Environ Sci Technol. 2000 Oct;30(4):449–505. https://doi.org/10.1080/10643380091184237

Husseiny M. Biodegradation of the reactive and direct dyes using Egyptian isolates. J Appl Sci Res. 2008;4:599–606.

Kakirde KS, Parsley LC, Liles MR. Size does matter: application-driven approaches for soil metagenomics. Soil Biol Biochem. 2010 Nov;42(11):1911–1923. https://doi.org/10.1016/j.soilbio.2010.07.021

Kanayama N, Tohru S, Keiichi K. Purification and characterization of an alkaline manganese peroxidase from *Aspergillus terreus* LD-1. J Biosci Bioeng. 2002 Apr;93(4):405–410. https://doi.org/10.1016/S1389-1723(02)80075-5

Kashif J, Muhammad A, Haq NB, Zahid M. Shake flask decolorization of direct dye solar golden yellow R by *Pleurotus ostreatus*. J Chem Soc Pak. 2011;33:209–214.

Knapp JS, Newby PS. The microbiological decolorization of an industrial effluent containing a diazo-linked chromophore. Water Res. 1995 Jul;29(7):1807–1809. https://doi.org/10.1016/0043-1354(94)00341-4

Kumar Praveen GN, Bhat SK. Fungal Degradation of Azo Dye-Red 3BN and optimization of physico-chemical parameters. ISCA Res. J.Biol. Sci. 2012;1:17–24.

Larone DH. Medically Important Fungi. A Guide to Identification. Washington (USA): ASM Press; 1995.

Maas R, Chaudhari S. Adsorption and biological decolourization of azo dye Reactive Red 2 in semicontinuous anaerobic reactors. Process Biochem. 2005 Feb;40(2):699–705. https://doi.org/10.1016/j.procbio.2004.01.038

Machado KMG, Compart LCA, Morais RO, Rosa LH, Santos MH. Biodegradation of reactive textile dyes by basidiomycetous fungi from Brazilian ecosystems. Braz J Microbiol. 2006 Dec;37(4): 481–487. https://doi.org/10.1590/S1517-83822006000400015

Mahbub KR, Mohammad A, Ahmed MM, Begum S. Decolourisation of synthetic dyes using bacteria isolated from textile industry effluent. Asian J Biotechnol. 2012 Mar 1;4(3):129–136. https://doi.org/10.3923/ajbkr.2012.129.136

Mansur M, Arias ME, Copa-Patiño JL, Flärdh M, González AE. The white-rot fungus *Pleurotus ostreatus* secretes laccase isozymes with different substrate specificities. Mycologia. 2003 Nov;95(6): 1013–1020. https://doi.org/10.1080/15572536.2004.11833017

Mazmanci MA, Ünyayar A. Decolourisation of Reactive Black 5 by *Funalia trogii* immobilised on *Luffa cylindrica* sponge. Process Biochem. 2005 Jan;40(1):337–342. https://doi.org/10.1016/j.procbio.2004.01.007

McMullan G, Meehan C, Conneely A, Kirby N, Robinson T, Nigam P, Banat IM, Marchant R, Smyth WF. Microbial decolourisation and degradation of textile dyes. Appl Microbiol Biotechnol. 2001 Jul 1;56(1–2):81–87. https://doi.org/10.1007/s002530000587

Prachi K, Anushree M. Effect of the nutrient composition on dye decolourization and extra cellular enzyme production by *Lentinus edodeson* solid medium. Enzyme Microb Technol. 2009;30:381–386.

Radha KV, Regupathi I, Arunagiri A, Murugesan T. Decolorization studies of synthetic dyes using *Phanerochaete chrysosporium* and their kinetics. Process Biochem. 2005 Oct;40(10):3337–3345. https://doi.org/10.1016/j.procbio.2005.03.033

Ramya, M.B., S. Anusha, Kalavathy and S. Devilaksmi. Biodecolorization and biodegradation of Reactive Blue by *Aspergillus* spp. Afr J Biotechnol. 2007;6:1441–1445.

Rani B, Kumar V, Singh J, Bisht S, Teotia P, Sharma S, Kela R. Bioremediation of dyes by fungi isolated from contaminated dye effluent sites for bio-usability. Braz J Microbiol. 2014 Sep;45(3):1055–1063. https://doi.org/10.1590/S1517-83822014000300039

Saranraj P, Sumathi V, Reetha D, Stella D. Fungal decolourization of direct azo dyes and biodegradation of textile dye effluent. J. Ecobiotechnol. 2010;2:12–16.

Siddiqui MS, Andleeb S, Ali N, Ghumro PB, Ahmed S. Up-flow immobilized fungal column reactor for the treatment of Anthraquinone dye Drimarene Blue K2RL. Afr J Biotechnol. 2009; 8: 5570–5577.

Sohail M, Naseeb S, Sherwani SK, Sultana S, Aftab S, Shahzad S, Ahmad A, Khan SA. Distribution of hydrolytic enzymes among native Fungi: aspergillus the pre-dominant genus of hydrolase producer. Pak J Bot. 2009;41:2567–2582.

Sponza DT, Işık M. Reactor performances and fate of aromatic amines through decolorization of Direct Black 38 dye under anaerobic/aerobic sequentials. Process Biochem. 2005 Jan;40(1): 35–44. https://doi.org/10.1016/j.procbio.2003.11.030

Sumathi S, Manju BS. Uptake of reactive textile dyes by *Aspergillus foetidus*. Enzyme Microb Technol. 2000 Sep;27(6):347–355. https://doi.org/10.1016/S0141-0229(00)00234-9

Vaidyanathan VK, Selvaraj DK, Premkumar P, Subramanian S. Screening and induction of laccase activity in fungal species and its application in dye decolorization. Afr J Microbiol Res. 2011 Jun 04;5(11):1261–1267. https://doi.org/10.5897/AJMR10.894

Villena GK, Fujikawa T, Tsuyumu S, Gutiérrez-Correa M. Structural analysis of biofilms and pellets of *Aspergillus niger* by confocal laser scanning microscopy and cryo scanning electron microscopy. Bioresour Technol. 2010 Mar;101(6):1920–1926. https://doi.org/10.1016/j.biortech.2009.10.036

Wesenberg D, Buchon F, Agathos SN. Degradation of dye containing textile effluents by the agaric white-rot fungus *Clitocybula dusenii*. J Biotechnol. 2002;24:989–993.

Won SW, Vijayaraghavan K, Mao J, Kim S, Yun YS. Reinforcement of carboxyl groups in the surface of *Corynebacterium glutamicum* biomass for effective removal of basic dyes. Bioresour Technol. 2009 Dec;100(24):6301–6306. https://doi.org/10.1016/j.biortech.2009.07.063

Polish Journal of Microbiology
2020, Vol. 69, No 2, 205–215
https://doi.org/10.33073/pjm-2020-024

ORIGINAL PAPER

Lactobacillus fermentum JX306 Restrain D-galactose-induced Oxidative Stress of Mice through its Antioxidant Activity

DI ZHANG[&], CHUANG LI[&], RUIRUI SHI, FENGCHUN ZHAO* and ZHENGYOU YANG*

Department of Microbiology, College of Life Science, Key Laboratory for Agriculture Microbiology, Shandong Agricultural University, Taian, China

Submitted 14 February 2020, revised 5 April 2020, accepted 21 April 2020

Abstract

Oxidative stress-induced series of related degenerative diseases have received widespread attention. To screen new lactic acid bacteria (LAB) strains to resist oxidative stress, traditional Chinese fermented vegetables were used as a resource library to screen of LAB. The *Lactobacillus fermentum* JX306 strain, which showed high scavenging activity of DPPH free radical and hydrogen radical, and a strong lipid peroxidation inhibition rate *in vitro* was selected. *L. fermentum* JX306 was also examined for its antioxidant capacity in D-galactose-induced aging mice. The results showed that *L. fermentum* JX306 could significantly decrease malondialdehyde (MDA) levels and improve the activity of glutathione peroxidase (GSH-Px), and total antioxygenic capacity (TOC) in the serum, kidney, and liver. Meanwhile, the strain could remarkably upregulate the transcriptional level of the antioxidant-related enzyme genes, such as peroxiredoxin1 (Prdx1), glutathione reductase (Gsr), glutathione peroxidase (Gpx1), and thioredoxin reductase (TR3) encoding genes in the liver. Besides, histopathological observation proves that this probiotic strain could effectively inhibit oxidative damage to the liver and kidney in aging mice. Therefore, this unique antioxidant strain may have a high application value in the functional food industry and medicine industry.

Key words: lactic acid bacteria, antioxidant activity, *Lactobacillus fermentum*, traditional Chinese fermented vegetables, D-galactose-induced aging mice

Introduction

Oxidative stress refers to an imbalance, which is caused by high levels of reactive oxygen species (ROS) and low levels of antioxidant activity (Preiser 2012). The excessive ROS can damage enzymes, fatty acids, proteins, nucleic acids, and other physiological substances of cells, which leads to structure and function disorders (Dizdaroglu et al. 1992; Wu et al. 2014). The oxidative stress can cause various diseases, including amyotrophic lateral sclerosis, asthma, allergies, and diabetes as well as further accelerate aging (Nyström 2003; Kurien et al. 2006; Lin and Beal 2006). When the entire antioxidant defense system cannot protect all biological macromolecules from the effects of oxidative damage, it is necessary to increase the defense capacity of the antioxidant system in order to protect human health (Wang et al. 2017). In recent years, LAB have received increasing attention because of their long history of safe use and their potential health benefits, such as improving stool consistency, immune modulation, and antagonism towards the pathogens. Another attractive feature of the LAB is their antioxidant capacity. Increasing experimental evidence indicates that probiotic LAB exerts beneficial antioxidative effects by ROS scavenging, chelating transition metal ions, and activating certain enzyme activities. Therefore, using LAB to scavenge the excess of free radicals, inhibit oxidative damage, and prevent the related restrictive diseases can be a potential treatment option (Mishra et al. 2015; Wang et al. 2017; Lin et al. 2018a).

The most studied probiotics are *Lactobacillus* and *Bifidobacterium*. Compared with other probiotic strains such as *L. rhamnosus*, *L. casei*, and *L. plantarum*, the

[&] These authors contributed equally to this work.

* Corresponding authors: Z.Y. Yang, Department of Microbiology, College of Life Science, Key Laboratory for Agriculture Microbiology, Shandong Agricultural University, Taian, China; **e-mail: zhyou21cn@sdau.edu.cn**
F.C. Zhao, Department of Microbiology, College of Life Science, Key Laboratory for Agriculture Microbiology, Shandong Agricultural University, Taian, China; **e-mail: zhaofengchun@126.com**

study on *L. fermentum* is one of the less-studied potential probiotic strain and still in a developing stage (Lin et al. 2017). *L. fermentum* has beneficial effects on the cholesterol level, effectiveness of the immune response, and reduction of the gastrointestinal and upper respiratory tract infections in infants (Wang et al. 2009; Pan et al. 2011; Maldonado et al. 2012; Russo et al. 2015). It is worth noting that the antioxidant properties of *L. fermentum* have received extensive attention. Using the oxygen radical absorbance capacity (ORAC) method, a significant *in vitro* antioxidant capacity of *L. fermentum* LF31 has been shown (Persichetti et al. 2014). *L. fermentum* ME-3, as a well-known anti-oxidant probiotic strain, inhibited oxidative damage to the body and reduced the risk of intestinal infection in patients (Mikelsaar and Zilmer 2009). *L. fermentum* Suo could eliminate the chain reaction of oxygen free radicals and lipid peroxidation as well as inhibit HCl/ethanol-induced oxidative damage in the gastric tissue (Suo et al. 2016). *L. fermentum* MTCC589 could improve antioxidant enzyme activity, resist the reinfection of *Escherichia coli*, and reduce the immune aging of mice (Sharma et al. 2014).

In this study, 481 of LAB strains from Chinese traditional fermented vegetables were screened to isolate the probiotic strains with antioxidant activity. After the characterization of the antioxidant properties of the LAB strains *in vitro*, *L. fermentum* strain JX306 with high antioxidant activity was selected, and these properties were further studied *in vivo* using a D-galactose-induced aging mice model.

Experimental

Materials and Methods

Bacterial strains and culture conditions. A total of 481 isolates (Table SI) were used in this study, which were obtained from 35 Chinese traditional fermented vegetable samples collected from different areas of China. They were identified using the methods described earlier (Wu et al. 2009). All the strains were stored at −80°C in MRS broth with 20% glycerol. For all subsequent experiments, the strains were incubated in MRS broth at 37°C for 18 h. The intact cells were obtained by centrifugation (8,000 g for 10 min at 4°C) and then washed with sterilized isotonic saline (0.85%) three times. The final concentration of intact cells was adjusted to 4.0×10^8 CFU/ml.

***In vitro* determination of antioxidant activity of LAB strains. Primary screening of LAB with antioxidant capacity.** The scavenging capacity against DPPH· of 481 LAB strains was evaluated based on the method described by Wang et al. (2017) with some modification. Briefly, 1.0 ml of LAB suspension was added to 2.0 ml of DPPH· solution (0.2 mM in ethanolic) and shaken well before incubation for 30 min in the dark at room temperature. In the control group, LAB suspension was replaced by sterile saline, and the DPPH free radical solution was replaced with ethanol solution in the blank group. After centrifugation at 8,000 g for 10 min, the absorbance of the supernatants was measured at 517 nm. The specific method for measuring DPPH· free radical scavenging capacity was as follows:

$$\text{Scavenging activity (\%)} = [1 - (A_{sample} - A_{blank})/A_{control}] \times 100$$

Hydroxyl radical scavenging. The method for the measurement of hydroxyl radical scavenging ability of the preliminarily screened LAB strains was based on Lin's test method (Lin et al. 2018a) with some modifications. Briefly, 1 ml of the LAB suspension was added to 2.5 ml mixture containing 0.5 ml of O-phenanthroline (2.5 mM), 1.0 ml of PBS (10 mM, pH = 7.4), 0.5 ml of $FeSO_4$ (2.5 mM), and 0.5 ml of H_2O_2 (20 mM). The mixture was shaken well and incubated in a water bath at 37°C for 1.5 h. The control group used sterile saline instead of LAB suspension. After centrifugation at 8,000 g for 10 minutes, the absorbance of the supernatant was measured at 510 nm. The specific details of the measurement of hydroxyl radical scavenging ability of LAB cells were as follows:

$$\text{Scavenging activity (\%)} = [(A_{sample} - A_{control}) / (A_{blank} - A_{control})] \times 100$$

Lipid peroxidation inhibition rate. The lipid peroxidation inhibition rate of the primary screening LAB strains was determined based on a Kullisaar's test method (Kullisaar et al. 2003) with some modifications. Briefly, 1.0 ml of the LAB suspension was added to a solution containing 0.5 ml of deionized water, 0.2 ml of $FeSO_4$ (0.01%, w/v), 0.02 ml of ascorbic acid (0.01%, w/v), and 1.0 ml of linoleic acid emulsion (20 ml linoleic acid emulsion includes 0.2 ml of tween 20, 0.1 ml of linoleic acid, and 19.7 ml of sterile saline). The mixture was incubated at 37°C for 12 h. Then, 0.2 ml of 4% TCA, 2 ml of thiobarbituric acid (TBA, 0.8%), and 0.2 ml of butylated hydroxytoluene (BHT, 0.4%) were added to the mixture and shaken well. After reaction in a heated water bath at 100°C for 30 min, the solution was rapidly cooled by using an ice bath and extracted by 2 ml butyl alcohol. The supernatant was obtained by centrifugation at 8,000 g for 10 min, and the absorbance at 532 nm was determined as A_{sample}. The absorbance of the mixture without the LAB cells was determined as $A_{control}$. The specific calculation method of the lipid peroxidation inhibition rate was as follows:

$$\text{Lipid peroxidation inhibition capacity (\%)} = [(A_{control} - A_{sample})/A_{control}] \times 100$$

Tolerance of the selected strains to simulated bile. The tolerance of the six LAB strains to simulated bile

was evaluated based on the test method described by Argyri et al. (2013). LAB cells (4×10^8 CFU/ml) were collected and resuspended into 1 ml simulated bile (a sterile saline solution containing 1 mg/ml pancreatic enzymes, and 0.5% (w/v) of bile salt. The LAB cells were incubated at 37°C for 1 h, and then the samples were diluted and plated on MRS solid plates. After 48 h of incubation at 37°C, the survival rate (SR) of cells was determined by a plate count method. The survival rate was determined as follows:

$$SR\ (\%) = S_2 / S_1 \times 100$$

where, S_1 is the initial number of cells, S_2 is the final number of cells.

Tolerance of the selected strains to simulated gastric and intestinal fluids. Tolerance of the selected six strains to simulated gastric and intestinal fluids was tested based on the method described by Huang and Adams (2004). Briefly, LAB cells (4×10^8 CFU/ml) were collected and resuspended into 1 ml of the simulated gastric fluid or intestinal fluid. The simulated gastric and intestinal fluids were made in the same way as in the previous study (Huang and Adams 2004). LAB strains in the simulated gastric fluid were incubated at 37°C for 3 h, and LAB strains in the simulated intestinal fluid were incubated at 37°C for 24 h. Then, LAB strains were diluted and spread on MRS plates. After 48 h of incubation at 37°C respectively, the survival rate was determined as shown above for the SR(%) equation.

Assay antioxidant activity of *L. fermentum* JX306 *in vivo* using the D-galactose-induced aging mice model. Animal experiment designs. Sixty male KM mice (20 ± 2 g), purchased from Jinan Pengyue Animal Experimental Center (Jinan, China), were randomly divided into six groups after one-week adaptation: the normal control group (NC), model control group (MC), positive control group (PC), low-dose group (LD), middle-dose group (MD), and high-dose group (HD). The treatments of each group were shown in Table I. After feeding for eight weeks, mice were sacrificed. The specific methods and details of animal experiments have been approved by the Ethics Committee of Shandong Agriculture University and comply with relevant guidelines in the European Union (Directive 2010/63/EU).

Determination of serum, liver, and kidney antioxidative parameters. Blood samples of each group were obtained by moving mice eyeballs after 12 h of the final administration. Subsequently, the samples were centrifuged (8,000 g, 10 min at 4°C) to obtain the serum samples. The serum samples were stored at – 80°C for further analysis. The liver and kidney samples of each mouse (0.1 g) were added to 0.9 ml of sterile saline and fully homogenized. After centrifugation at 8,000 g for 10 min at 4°C, the supernatants of each group were gathered for further analysis. Four oxidative stress products, including malondialdehyde (MDA), superoxide dismutase (SOD), glutathione peroxidase (GSH-Px), and total antioxidant capacity (T-AOC) were determined in the serum, liver, and kidney samples according to the details in the kit (Nanjing Jiancheng Bioengineering Institute, China).

Changes of the antioxidant-related genes' transcription in the liver. The total RNA of liver tissue in each group was extracted according to the specific details in the RNAiso Plus (Takara, China). The purity and quality of total RNA were determined by OD_{260}/OD_{280} and agar gel electrophoresis. Then, the reversed transcription to synthesize cDNA was performed according to the details in the PrimeScriptII First Strand cDNA Synthesis Kit (Takara, China), and considering the needs of the next experiment, the cDNA was placed at –20°C. The 7500 Fast Real-Time PCR System (ABI, USA) and SYBR Green PCR Kit (TransGen, China) were used for operating the RT-PCR. The PCR procedure contained a denaturation step at 94°C for 10 min, followed by 40 cycles of denaturation at 94°C for 5 s, annealing, and extension at 60°C for 30 s.

The primers (Table SII) for the amplification of the genes encoding for peroxiredoxin-1 (Prdx1), glutathione peroxidase (Gsr), glutathione peroxidase (Gpx), and thioredoxin reductase (TR3), used for quantitative-PCR, were as described previously (Zhao et al. 2018). The gene encoding for β-actin was considered as a reference gene. The transcriptional levels of

Table I
Groups of experimental animals.

Group	Number	Experimental treatments	
		Oral administration	Intraperitoneal injection
NC	10	Normal saline (0.85%, 20 ml/kg BW)	Normal saline (0.85%, 20 ml/kg BW)
MC	10	Normal saline (0.85%, 20 ml/kg BW)	D-galactose (30 g/l, 200 mg/kg BW)
PC	10	Vitamin C (30 g/l, 200 mg/kg BW)	D-galactose (30 g/l, 200 mg/kg BW)
LD	10	*L. fermentum* JX306 (10^8 CFU/day)	D-galactose (30 g/l, 200 mg/kg BW)
MD	10	*L. fermentum* JX306 (10^9 CFU/day)	D-galactose (30 g/l, 200 mg/kg BW)
HD	10	*L. fermentum* JX306 (10^{10} CFU/day)	D-galactose (30 g/l, 200 mg/kg BW)

four genes encoding antioxidant enzymes Prdx1, Gsr, Gpx, and TR3 in the liver were evaluated according to the standard curve of quantitative analysis. The specific result of the relative expression of the gene is expressed by the formula $2^{-\Delta\Delta CT}$.

Histological analysis. Liver and kidney tissues were fixed with 10% formalin for 24 h and then embedded in conventional paraffin. For each paraffin block, thin sections (4–5 μm thickness) were gained, and then HE stained, and professional pathologists were invited to interpret the section results. Subsequently, these sections were used for light microscopic evaluation.

Statistical analysis. The software SPSS 20 was used to perform the statistical evaluation. Mean ± standard deviations were used to interpret the data. One-way ANOVA was operated to analyze the data. Significant differences between experimental groups were determined using LSD's and Tukey's tests. The data are significantly different with $p < 0.05$.

Results

Screening of antioxidant LAB strains. In this study, 481 strains isolated from Chinese traditional fermented vegetable samples were firstly screened for their DPPH free radical scavenging ability. As shown in Table II, six LAB strains were selected based on their high DPPH radical scavenging capacity. The strongest scavenging effects on the DPPH radical scavenging capacity were found for *L. fermentum* 306 (37.29%).

The antioxidant activity of the strains selected was further evaluated by HO· scavenging ability, and the lipid peroxidation inhibition rate. As shown in Table II, among the strains selected, *L. fermentum* JX306 exhibited the highest HO· scavenging capability, and the strongest lipid peroxidation inhibition activity with the HO· scavenging rate of 37.29%, and lipid peroxidation inhibition rate of 37.9%.

Tolerance to bile salts and the simulated gastric and intestinal fluids. Prerequisites for the application of LAB strains for commercial use include resistance to bile salt-mediated growth inhibition (Jamalifar et al. 2010), and their survival in an acidic, alkaline gastrointestinal environment. Oral lactic acid bacteria must overcome these adverse conditions to live to the intestines and, therefore, play a beneficial health effect. Thus, the tolerance of the strains selected for simulated bile, gastric fluid, and intestinal fluid was determined, as shown in Table III, *L. fermentum* JX306 showed the highest survival rates after incubation in these three simulated solutions. The survival rates were 78.28% for simulated bile, 53.05% for simulated gastric fluid, and 42.07% for simulated intestinal fluid, respectively.

Table II
The selected LAB strains with high antioxidant activity.

Strains	DPPH scavenging rate (%)	Hydrogen radicals scavenging rate (%)	Inhibition rate of lipid peroxidation (%)
L. fermentum JX306	37.29 ± 1.75^{a}	37.90 ± 0.29^{a}	28.14 ± 2.97^{a}
L. fermentum GZ394	34.92 ± 3.57^{a}	35.02 ± 1.70^{b}	23.89 ± 1.60^{b}
L. plantarum SC34	23.09 ± 4.00^{c}	34.50 ± 1.44^{b}	12.69 ± 0.23^{d}
L. plantarum GZ328	27.83 ± 2.25^{b}	29.21 ± 1.60^{c}	20.85 ± 2.07^{bc}
Pediococcus pentosaceus GZ430	16.22 ± 0.89^{d}	23.32 ± 1.62^{d}	18.01 ± 2.09^{c}
Leuconostoc mesenteroides YN295	15.26 ± 0.67^{d}	34.31 ± 1.18^{b}	14.43 ± 1.29^{d}

[a-d] An average value within a list with different superscript alphabets differ ($p < 0.05$)
Data are shown as means ± SD from triplicate results

Table III
The survival rate (%) of LAB in simulated bile, gastric fluid, and intestinal fluid.

Strains	Simulated bile	Simulated gastric fluid	Simulated intestinal fluid
L. fermentum JX306	78.28 ± 0.18^{a}	53.05 ± 1.75^{a}	42.07 ± 6.52^{a}
L. fermentum GZ394	74.61 ± 4.67^{a}	30.57 ± 3.68^{b}	27.26 ± 4.95^{b}
L. plantarum SC34	65.09 ± 6.33^{b}	5.34 ± 1.92^{c}	12.23 ± 1.85^{e}
L. splantarum GZ328	74.48 ± 1.79^{a}	1.51 ± 0.22^{e}	9.75 ± 0.45^{f}
*Pediococcus pentosaceus GZ*430	22.99 ± 3.12^{d}	3.62 ± 1.11^{d}	15.26 ± 2.34^{d}
Leuconostoc mesenteroides YN295	33.89 ± 0.96^{c}	5.34 ± 0.79^{c}	17.28 ± 0.56^{c}

[a-f] Average value within a list with different superscript alphabets differ ($p < 0.05$)
Data are shown as means ± SD from triplicate results

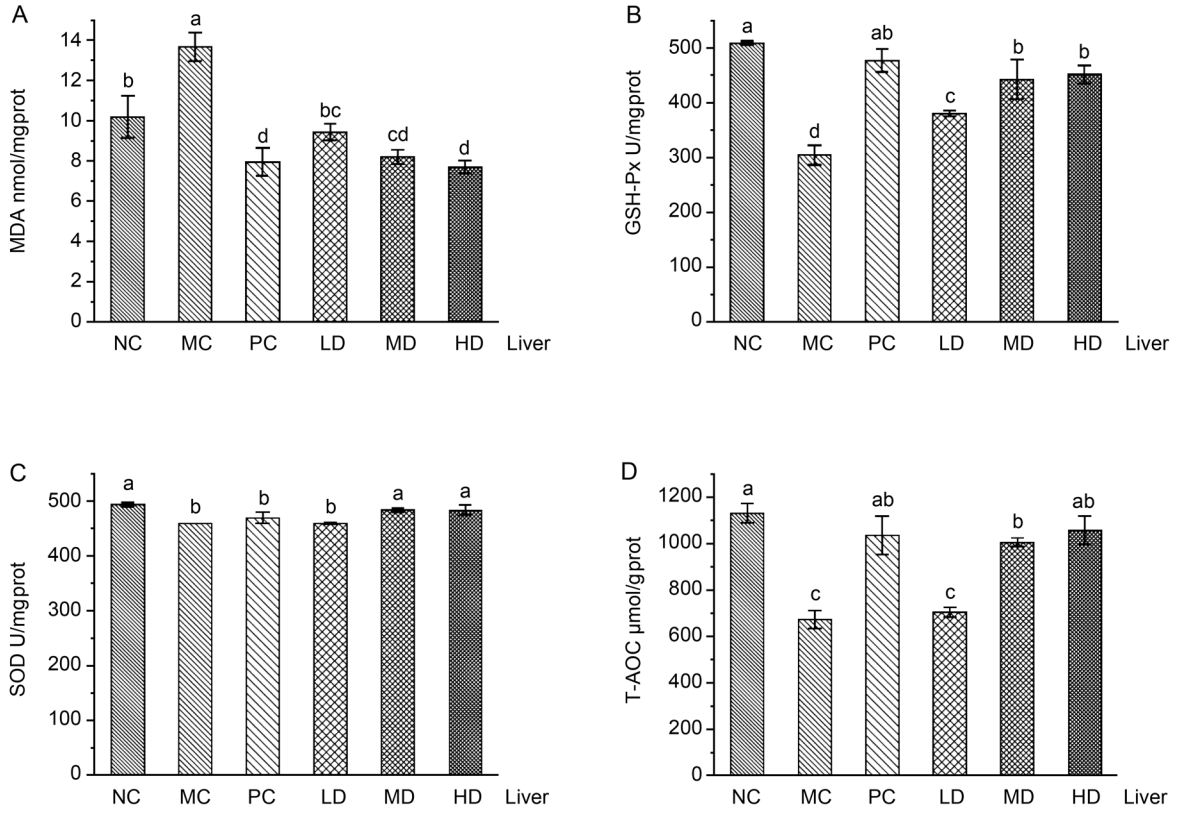

Fig. 1. Effect of *L. fermentum* JX306 on GSH-Px, SOD, T-AOC activities, and MDA concentration in the liver of mice with oxidative stress induced by D-galactose. (A) MDA; (B) GSH-Px; (C) SOD; (D) T-AOC. All data are presented as mean ± SD (n = 3). Bars with different letters were significantly different ($p < 0.05$).

Therefore, based on the antioxidant activities and the survival responses of the strains selected to the simulated conditions in the human gastrointestinal tract, the strain of *L. fermentum* JX306 was finally selected for *in vivo* assay to examine their antioxidant profiles in the D-galactose-induced aging mice model.

Antioxidant activities of *L. fermentum* JX306 in the D-galactose-induced aging mice model. High levels of ROS lead to oxidative damage. D-galactose has low toxicity and slow action and could stimulate the body to produce a large number of free radicals. It has been used as a mature model to simulate the body's oxidative stress process. In this study, the antioxidant activities of *L. fermentum* JX306 were verified *in vivo* in the D-galactose-caused oxidative damaged mice. After intraperitoneal injection of D-galactose for eight weeks, compared with the NC group, the MC group exhibited obvious signs of aging. The skin color of the mice was dull, the skin elasticity was poor, and worse emotions such as irritability and lethargy appeared. It is worth noting that no mouse death occurred during the entire test. The weight of the mice was analyzed in detail without statistical differences in all groups ($p > 0.05$) (data not shown).

The level of antioxidant products in the D-galactose-induced aging mice liver. Compared with the NC group, the levels of GSH-Px and T-AOC antioxidant products in the MC group showed a significant downward trend, while the activity of MDA showed an upward trend. ($p < 0.05$, Fig. 1). Oral treatment with *L. fermentum* JX306 strain could change significantly adverse effects, which were caused by the three oxidative stress products (Fig. 1). The MDA levels decreased with the increase of LAB dose, and it reached 9.43 nmol/mg protein, 8.19 nmol/mg protein, and 7.70 nmol/mg protein in the LD, MD, and HD group, respectively, which were 31.01%, 40.03%, and 43.65% lower than the results in MC group. It should be noted that the MDA levels in a high-dose group were significantly decreased compared to the normal control group, and comparable to the PC group. In the LAB groups, the GSH-Px and T-AOC levels increased with the increase of LAB dose, and it reached 451.80 U/mgprot, and 1057.13 μmol/gprot in a HD group respectively, which were 48.40% and 57.13% higher than the results in MC group. As shown in Fig. 1, the hepatic SOD activity was not significantly influenced by D-gal, vitamin C or *L. fermentum* JX306 strain application.

The level of antioxidant products in the D-galactose-induced aging mice kidney. When compared with the NC group, the injection of D-galactose to mice from the MC group generated a lot of free radicals. The

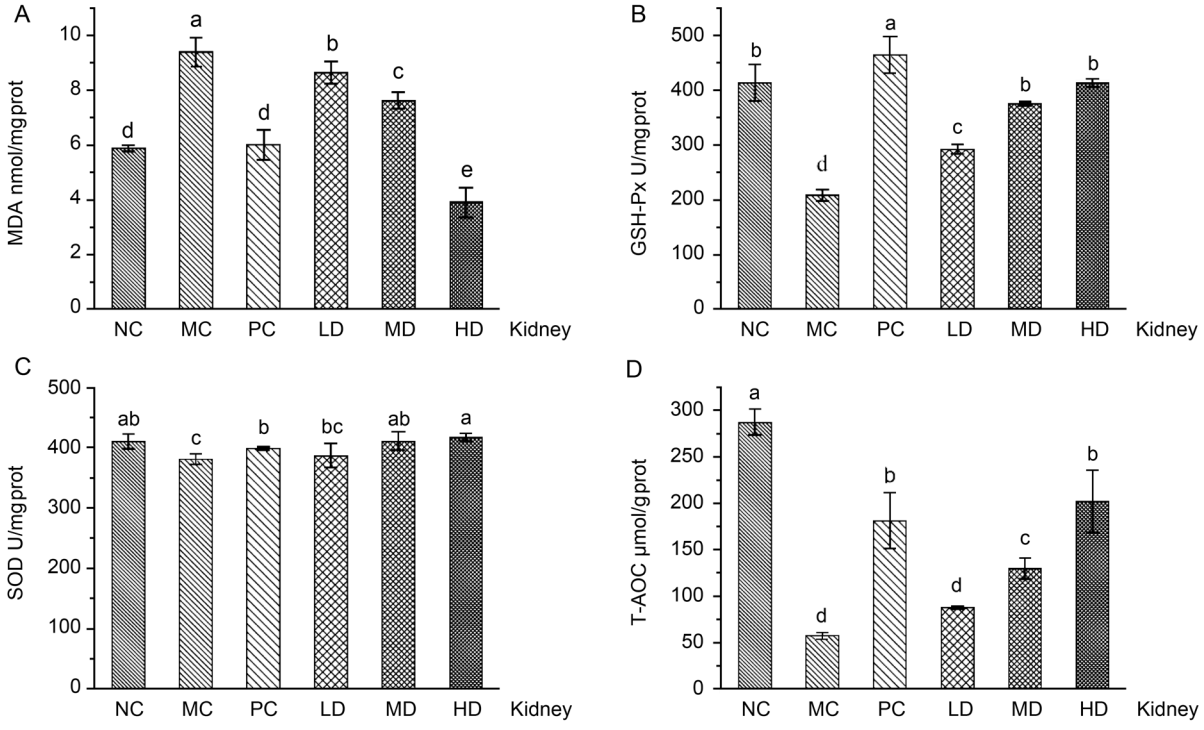

Fig. 2. Effect of *L. fermentum* JX306 on GSH-Px, SOD, T-AOC activities, and MDA concentration in the kidney of mice with oxidative stress induced by D-galactose. (A) MDA; (B) GSH-Px; (C) SOD; (D) T-AOC. All data are presented as mean ± SD (n = 3). Bars with different letters were significantly different ($p < 0.05$).

excessive radicals hurt all biological macromolecules and cause oxidative damage to tissues and cells; thus, they led to the decrease of GSH-Px and T-AOC activities and the increase of MDA levels ($p < 0.05$, Fig. 2). The administration of *L. fermentum* JX306 could effectively reverse the adverse changes, which were caused by D-galactose ($p < 0.05$). The T-AOC levels boosted with the increase of the LAB dose and reached 87.80 μmol/g protein, 129.80 μmol/g protein, and 202.27 μmol/g protein in the LD, MD, and HD group respectively. These levels were 53.12%, 126.34%, and 252.76% higher than the results demonstrated for the MC group. It is worth mentioning that the activity of GSH-Px with high-dose of *L. fermentum* JX306 was higher, and there was no statistically significant difference when compared to the NC group. This result showed that the high-dose of *L. fermentum* JX306 had the most significant effect in inhibiting oxidative damage, which was caused by excessive free radicals. The MDA levels decreased with the increase of the LAB dose, and reached 8.64 nmol/mg protein, 7.62 nmol/mg protein, and 3.91 nmol/mg protein in the LD, MD, and HD group, respectively. These levels were 7.92%, 18.79%, and 58.32% lower when compared to the MC group. It should be noted that the MDA levels in the high-dose group were significantly decreased in comparison to the normal control group and PC group. The administration of *L. fermentum* JX306 did not significantly affect SOD activity in the kidney when compared to that of the MC group.

Effect of antioxidant products in the serum from the D-galactose-induced aging mice. As shown in Fig. 3, a significant decrease of T-AOC activities and an increase of MDA levels were observed in the serum of the D-galactose induced aging mice's control group when compared to those of the normal control group. *L. fermentum* JX306 administration reversed the changes in T-AOC and MDA levels. The T-AOC levels enlarged with the increase of the LAB dose and reached 641.25 μmol/g protein, 772.53 μmol/g protein, and 793.53 μmol/g protein in the LD, MD, and HD group, respectively. These values were 4.45%, 25.83%, and 29.25% higher than the results in the MC group. The MDA levels decreased with the increase of LAB dose, and reached 1.92 nmol/mg protein in the HD group, and were 35.75%, 27.64%, and 20.44% lower than the results in the MC group, NC, and PC group, respectively. The GSH-Px levers in sera of *L. fermentum* JX306 administration mice showed only a slight increase. The serum SOD activities were not significantly influenced by D-galactose, vitamin C or *L. fermentum* JX306.

Effect of *L. fermentum* JX306 on the relative gene expression in the liver of D-galactose-induced aging mice. In order to further explore the related antioxidant mechanism of *L. fermentum* JX306 at the gene level, we have completed a quantitative analysis of the relative expression of the key antioxidant genes in the thioredox system (TRX) and the glutathione system (GSH). As shown in Fig. 4, when compared with the normal group,

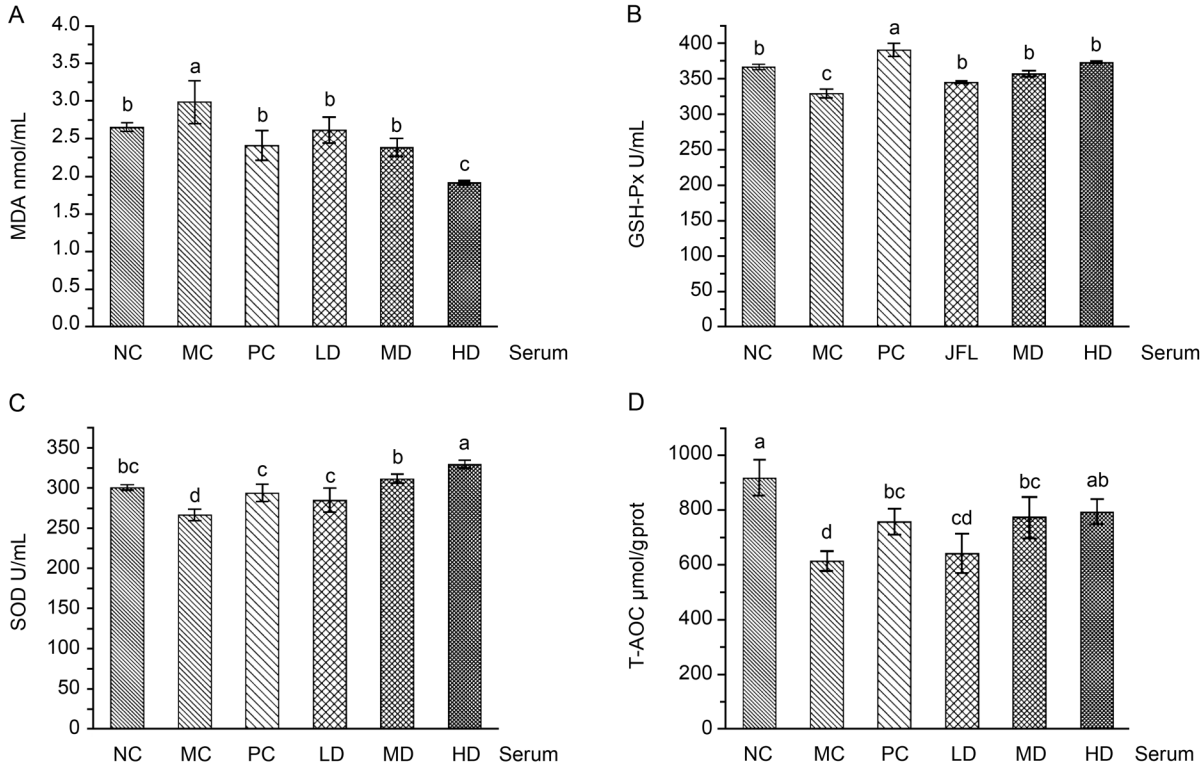

Fig. 3. Effect of *L. fermentum* JX306 on GSH-Px, SOD, T-AOC activities and MDA concentration in the serum of mice with oxidative stress induced by D-galactose. (A) MDA; (B) GSH-Px; (C) SOD; (D) T-AOC. All data are presented as mean ± SD (n = 3). Bars with different letters were significantly different ($p < 0.05$).

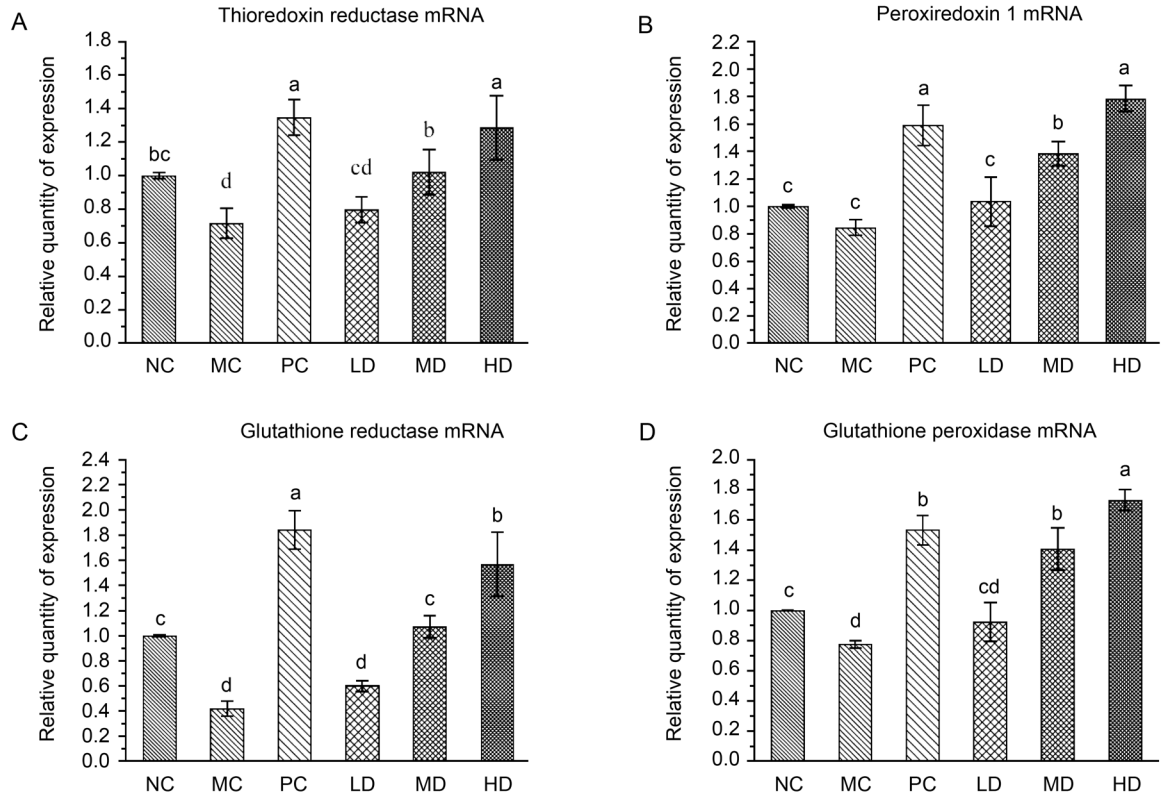

Fig. 4. Effect of *L. fermentum* JX306 on the expression of the genes encoding for peroxiredoxin-1 (Prdx1), glutathione peroxidase (Gsr), glutathione peroxidase (Gpx), and thioredoxin reductase (TR3) in the liver of D-galactose induced aging mice. (A) Thioredoxin reductase mRNA; (B) Peroxiredoxin1 mRNA; (C) Glutathione reductase mRNA; (D) Glutathione peroxidase mRNA. All data are presented as mean ± SD (n = 3). Bars with different letters were significantly different ($p < 0.05$).

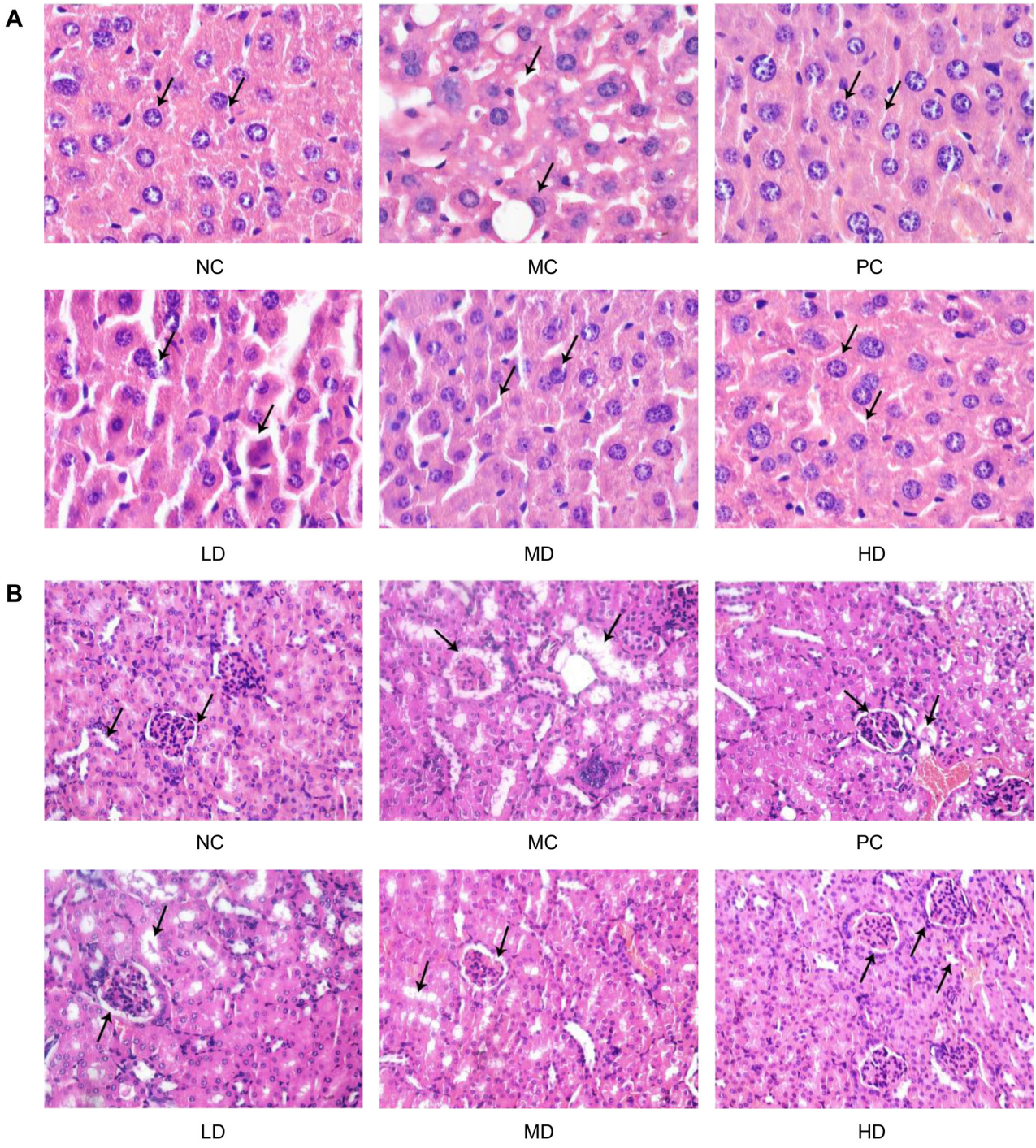

Fig. 5. Effects of *L. fermentum* JX306 treatment on organic damages in the liver (A), and the kidney (B) of D-galactose induced aging mice.

D-galactose treatment significantly reduced the relative gene expression levels of Prdx1, Gsr, Gpx, and TR3 ($p < 0.05$). However, it is worth noting that this phenomenon was significantly alleviated by *L. fermentum* JX306 intervention, and the relative gene expression levels of Prdx1, Gsr, Gpx, and TR3 were all significantly increased. Therefore, oral treatment with *L. fermentum* JX306 strain could significantly increase the transcription level of antioxidant genes in the liver and could play a key role in inhibiting oxidative damage.

Histopathological changes in mice livers and kidneys. As shown in Fig. 5, the HE sections showed that *L. fermentum* JX306 had an inhibitory effect on the oxidative damage caused by D-galactose in liver and kidney tissues. In the NC group, cells in the liver indicated large and round cell nucleus, nucleoli conspicuous, and entire cytoplasm (Fig. 5A). The renal tubules and glomerulus of the kidney showed an intact morphological structure (Fig. 5B). While for the MC group, the histological picture of the kidney indicated that glo-

meruli were severely damaged, as did tubulointerstitial lesions. A loss of brush borders and vacuolation of renal tubules were also observed. A histological picture of the liver showed necrotic spots, edema degeneration, and vacuoles degeneration. However, analysis of the three groups treated with *L. fermentum* JX306 indicated that D-galactose-induced pathologic changes could be alleviated with a dose-related effect. As especially observed in the HD group, the severe oxidative damages caused by D-galactose were strikingly improved to the level of the normal group.

Discussion

In recent years, due to long history of safe use and potential therapeutic benefits (Mokoena 2017; Garcia-Castillo et al. 2019; Zhao et al. 2019) for human health of probiotics, the antioxidative activity of LAB has attracted more and more attention (Amaretti et al. 2013; Tang et al. 2016; Zhao et al. 2018). Traditional Chinese fermented vegetables contain abundant LABs. In this study, for isolation of new LAB strains with high antioxidant activity, the variety of fermented vegetable samples from different areas of China were collected, and 481 LAB strains were isolated from these samples (Table SI). A DPPH free radical scavenging method can directly and rapidly reflect the antioxidant capacity of lactic acid bacteria and has been widely used to evaluate this activity (Antolovich et al. 2002; Ding et al. 2017; Lin et al. 2018b). After screening of the antioxidant activity of 481 LAB strains with a DPPH free radical scavenging method, six strains with a high DPPH radical scavenging rate were selected. It should be noted that these six strains were isolated from the fermented vegetable samples, which were collected from southwestern China. The *L. fermentum* JX306, isolated from Chinese sauerkraut in Jiangxi Province, showed the highest scavenging ability of DPPH radicals at a density of 10^8 CFU/ml (37.29%). Additionally, the strains of *L. plantarum* GZ328 and *L. fermentum* GZ394 (Table II), which showed high DPPH radical scavenging ability, were also isolated from Chinese sauerkraut. Therefore, the sauerkraut from southwestern China is a good source for the isolation of LAB with high antioxidant activity.

A D-galactose-induced oxidative stress model is a very mature model in many animal experiments (Ho et al. 2003) In this study, the antioxidant activities of *L. fermentum* JX306 were verified *in vivo* in a D-galactose-induced aging mice model. MDA is considered one of the by-products of the lipid peroxidation process, and its concentration is one of the most commonly used biomarkers to reflect the lipid peroxidation level (Nielsen et al. 1997). It was reported that *L. plantarum* CCFM10, *L. plantarum* AR501, and *L. delbrueckii subsp. bulgaricus* F17 can decrease the level of MDA and inhibit the generation of an excess of free radicals (Ding et al. 2017; Lin et al. 2018b; Zhao et al. 2018). A comprehensive analysis of the literature and our results shows that lactic acid bacteria could indeed relieve the D-galactose-induced oxidative damage. After oral administration of *L. fermentum* JX306 for eight weeks, the MDA levels in serum, liver, and kidney were significantly lower when compared to the MD group. It is worth emphasizing that MDA levels in the high-dose group were also significantly lower than those in the NC group. Therefore, *L. fermentum* JX306 has high lipid antioxidant activity.

Generally, excess of free radicals is mainly eliminated by redox systems in the body, such as the sulfur oxygen reduction (TRX) system and the glutathione (GSH) system, which can reduce and control the occurrence of the oxidative stress-related diseases (Yu et al. 2015; Lin et al. 2018a). GSH-Px is the most important antioxidant factor in the glutathione (GSH) system, which could directly scavenge free radicals and prevent cell damage (Esposito et al. 2000; Ding et al. 2017). The oral treatment with *L. fermentum* JX306 strain could significantly increase the antioxidant enzymatic activity of GSH-Px in the liver and kidney of mice. SOD is the key enzyme for hastening the reaction of superoxide anions to H_2O_2 (Nordberg and Arnér 2001). However, almost no difference was observed in SOD levels among these groups. Our results were supported by previous research (Zhao et al. 2018), and the low toxicity and slow action of D-galactose may be the reason that no significant differences in SOD levels among these groups were observed (Zhao et al. 2018). Total antioxidant capacity (T-AOC) represents the ability of non-enzymatic antioxidant systems to scavenge an excess of free radicals (Zhang et al. 2013). After intragastric administration of *L. fermentum* JX306, T-AOC levels showed an upward trend in the serum, liver, and kidney. Similar to our findings, the previous researches reported that intragastric administration of *L. fermentum* JX306, *L. plantarum* AR501 (Lin et al. 2018a), *L. plantarum* CCFM10, and *L. plantarum* RS15-3 (Zhao et al. 2019) significantly increased T-AOC in the liver.

Normal dose of D-galactose can be metabolized into glucose through the liver enzymatic hydrolysis, and excessive concentration of D-galactose will induce the production of reactive oxygen radicals, causing oxidative damage to liver tissues. To further elucidate the antioxidant mechanism, the changes in the relative level of mRNA encoding Prdx1, Gsr, Gpx, and TR3 in the liver were determined. GSH serves as the most abundant cellular thiol resource and provides a buffer system to maintain the cellular redox status. Prdx1, Gsr, and Gpx are all part of a glutathione peroxidase/glutathione/glutathione reductase antioxidant pathway

(Wu et al. 2019). TR3 is a component of the TRX system (Arnér and Holmgren 2000). TRX can directly remove intracellular ROS, such as hydrogen peroxide and oxygen free radicals, and regulate intracellular oxidation-reduction balance (Nordberg and Arnér 2000). This test proved that D-galactose harms all body's biological macromolecules, generates excessive free radicals, and causes oxidative damage. After oral administration of *L. fermentum* JX306, the expression of the genes encoding Prdx1, Gsr, Gpx, and TR3 was increased (Fig. 4), thus alleviating the D-galactose-induced liver injury in mice, and delaying the oxidative damage process. This was supported in this study by the histopathological analysis results. A high dose of *L. fermentum* JX306 was able to significantly improve the consequences of severe oxidative damage caused by D-galactose in the liver and kidney tissue.

In this study, *L. fermentum* JX306 with high antioxidant activities was isolated from traditional Chinese fermented vegetable samples. The strain not only showed excellent antioxidant activities *in vitro*, but also effectively restrained the oxidative damage in D-galactose-induced aging mice. While administered orally, the strain could significantly decrease the MDA levels and improve activities of SOD, GSH-Px. and TOC in the serum, liver, and kidney. It could also markedly up-regulate the transcription levels of the genes encoding for antioxidant-related enzymes in the livers of D-galactose-induced aging mice. Besides, the strain could improve the D-galactose-induced histological lesions, and a dose-effect relationship was observed in this case. Thus, *L. fermentum* JX306 could be regarded as a potential strain for further exploiting antioxidant functional products to treat the oxidative-stress-related restrictive disease.

Acknowledgments

This experiment was supported by the National Natural Science Foundation of China (31772060) and Shandong Provincial Key Laboratory of Agricultural Microbiology Open Fund (SDKL2017015).

Conflict of interest

The authors do not report any financial or personal connections with other persons or organizations, which might negatively affect the contents of this publication and/or claim authorship rights to this publication.

Literature

Amaretti A, Di Nunzio M, Pompei A, Raimondi S, Rossi M, Bordoni A. Antioxidant properties of potentially probiotic bacteria: *in vitro* and *in vivo* activities. Appl Microbiol Biot. 2013; 97(2): 809–817. https://doi.org/10.1007/s00253-012-4241-7

Antolovich M, Prenzler PD, Patsalides E, McDonald S, Robards K. Methods for testing antioxidant activity. Analyst (Lond). 2002 Jan 10;127(1):183–198. https://doi.org/10.1039/b009171p

Argyri AA, Zoumpopoulou G, Karatzas KAG, Tsakalidou E, Nychas GJE, Panagou EZ, Tassou CC. Selection of potential probiotic lactic acid bacteria from fermented olives by *in vitro* tests. Food Microbiol. 2013 Apr;33(2):282–291. https://doi.org/10.1016/j.fm.2012.10.005

Arnér ESJ, Holmgren A. Physiological functions of thioredoxin and thioredoxin reductase. Eur J Biochem. 2000 Oct; 267(20): 6102–6109. https://doi.org/10.1046/j.1432-1327.2000.01701.x

Chaplin AV, Shkoporov AN, Efimov BA, Pikina AP, Borisova OY, Gladko IA, Postnikova EA, Lordkipanidze AE, Kafarskaia LI. Draft genome sequence of Lactobacillus fermentum NB-22. Genome Announc. 2015 Aug 27;3(4):e00896-15. https://doi.org/10.1128/genomeA.00896-15

Ding W, Wang L, Zhang J, Ke W, Zhou J, Zhu J, Guo X, Long R. Characterization of antioxidant properties of lactic acid bacteria isolated from spontaneously fermented yak milk in the Tibetan Plateau. J Funct Foods. 2017 Aug;35:481–488. https://doi.org/10.1016/j.jff.2017.06.008

Dizdaroglu M. Oxidative damage to DNA in mammalian chromatin. Mutation Research/DNAging. 1992 Sep;275(3–6):331–342. https://doi.org/10.1016/0921-8734(92)90036-O

Esposito LA, Kokoszka JE, Waymire KG, Cottrell B, MacGregor GR, Wallace DC. Mitochondrial oxidative stress in mice lacking the glutathione peroxidase-1 gene. Free Radic Biol Med. 2000 Mar; 28(5):754–766. https://doi.org/10.1016/S0891-5849(00)00161-1

Garcia-Castillo V, Komatsu R, Clua P, Indo Y, Takagi M, Salva S, Islam MA, Alvarez S, Takahashi H, Garcia-Cancino A, et al. Evaluation of the immunomodulatory activities of the probiotic strain *Lactobacillus fermentum* UCO-979C. Front Immunol. 2019 Jun 13;10:1376. https://doi.org/10.3389/fimmu.2019.01376

Ho SC, Liu JH, Wu RY. Establishment of the mimetic aging effect in mice caused by D-galactose. Biogerontology. 2003;4(1):15–18. https://doi.org/10.1023/A:1022417102206

Huang Y, Adams MC. *In vitro* assessment of the upper gastrointestinal tolerance of potential probiotic dairy propionibacteria. Int J Food Microbiol. 2004 Mar;91(3):253–260. https://doi.org/10.1016/j.ijfoodmicro.2003.07.001

Jamalifar H, Bigdeli B, Nowroozi J, Zolfaghari HS, Fazeli MR. Selection for autochthonous bifidobacteial isolates adapted to simulated gastrointestinal fluid. Daru. 2010;18(1):57–66.

Kant R, Blom J, Palva A, Siezen RJ, de Vos WM. Comparative genomics of *Lactobacillus*. Microb Biotechnol. 2011 May;4(3):323–332. https://doi.org/10.1111/j.1751-7915.2010.00215.x

Kullisaar T, Songisepp E, Mikelsaar M, Zilmer K, Vihalemm T, Zilmer M. Antioxidative probiotic fermented goats' milk decreases oxidative stress-mediated atherogenicity in human subjects. Br J Nutr. 2003 Aug;90(2):449–456. https://doi.org/10.1079/BJN2003896

Kurien BT, Hensley K, Bachmann M, Scofield RH. Oxidatively modified autoantigens in autoimmune diseases. Free Radic Biol Med. 2006 Aug 15;41(4):549–556. https://doi.org/10.1016/j.freeradbiomed.2006.05.020

Lin MT, Beal MF. Mitochondrial dysfunction and oxidative stress in neurodegenerative diseases. Nature. 2006 Oct;443(7113):787–795. https://doi.org/10.1038/nature05292

Lin Q, Li D, Qin H. Molecular cloning, expression, and immobilization of glutamate decarboxylase from *Lactobacillus fermentum* YS2. Electron J Biotechnol. 2017 May;27:8–13. https://doi.org/10.1016/j.ejbt.2017.03.002

Lin X, Xia Y, Wang G, Xiong Z, Zhang H, Lai F, Ai L. *Lactobacillus plantarum* AR501 alleviates the oxidative stress of D-galactose-induced oxidative stress model liver by upregulation of Nrf2-mediated antioxidant enzyme expression. J Food Sci. 2018a;83(7): 1990–1998. https://doi.org/10.1111/1750-3841.14200

Lin X, Xia Y, Wang G, Yang Y, Xiong Z, Lv F, Zhou W, Ai L. Lactic acid bacteria with antioxidant activities alleviating oxidized oil

induced hepatic injury in mice. Front Microbiol. 2018b Nov 6;9: 2684. https://doi.org/10.3389/fmicb.2018.02684

Maldonado J, Cañabate F, Sempere L, Vela F, Sánchez AR, Narbona E, López-Huertas E, Geerlings A, Valero AD, Olivares M, et al. Human milk probiotic *Lactobacillus fermentum* CECT5716 reduces the incidence of gastrointestinal and upper respiratory tract infections in infants. J Pediatr Gastroenterol Nutr. 2012 Jan;54(1):55–61.
https://doi.org/10.1097/MPG.0b013e3182333f18

Mikelsaar M, Zilmer M. *Lactobacillus fermentum* ME-3 – an antimicrobial and antioxidative probiotic. Microb Ecol Health Dis. 2009 Apr;21(1):1–27.

Mishra V, Shah C, Mokashe N, Chavan R, Yadav H, Prajapati J. Probiotics as potential antioxidants: a systematic review. J Agric Food Chem. 2015 Apr 15;63(14):3615–3626.
https://doi.org/10.1021/jf506326t

Mokoena MP. Lactic acid bacteria and their bacteriocins: classification, biosynthesis and applications against uropathogens: A mini-review. Molecules. 2017 Jul 26;22(8):1255.
https://doi.org/10.3390/molecules22081255

Nielsen F, Mikkelsen BB, Nielsen JB, Andersen HR, Grandjean P. Plasma malondialdehyde as biomarker for oxidative stress: reference interval and effects of life-style factors. Clin Chem. 1997 Jul 01; 43(7):1209–1214.
https://doi.org/10.1093/clinchem/43.7.1209

Nordberg J, Arnér ESJ. Reactive oxygen species, antioxidants, and the mammalian thioredoxin system. Free Radic Biol Med. 2001 Dec;31(11):1287–1312.
https://doi.org/10.1016/S0891-5849(01)00724-9

Nyström T. The free-radical hypothesis of aging goes prokaryotic. Cell Mol Life Sci. 2003;60(7):1333–1341.
https://doi.org/10.1007/s00018-003-2310-X

Pan DD, Zeng XQ, Yan YT. Characterisation of *Lactobacillus fermentum* SM-7 isolated from koumiss, a potential probiotic bacterium with cholesterol-lowering effects. J Sci Food Agric. 2011 Feb;91(3):512–518. https://doi.org/10.1002/jsfa.4214

Persichetti E, De Michele A, Codini M, Traina G. Antioxidative capacity of *Lactobacillus fermentum* LF31 evaluated *in vitro* by oxygen radical absorbance capacity assay. Nutrition. 2014 Jul;30 (7–8):936–938. https://doi.org/10.1016/j.nut.2013.12.009

Preiser JC. Oxidative stress. J pen-Parenter Enter. 2012;36(2):147–154.

Russo P, Iturria I, Mohedano ML, Caggianiello G, Rainieri S, Fiocco D, Spano G. Zebrafish gut colonization by mCherry-labelled lactic acid bacteria. Appl Microbiol Biot. 2015 Apr;99(8):3479–3490.
https://doi.org/10.1007/s00253-014-6351-x

Sharma R, Kapila R, Kapasiya M, Saliganti V, Dass G, Kapila S. Dietary supplementation of milk fermented with probiotic *Lactobacillus fermentum* enhances systemic immune response and antioxidant capacity in aging mice. Nutr Res. 2014 Nov;34(11):968–981.
https://doi.org/10.1016/j.nutres.2014.09.006

Suo H, Zhao X, Qian Y, Sun P, Zhu K, Li J, Sun B. *Lactobacillus fermentum* Suo attenuates HCl/ethanol induced gastric injury in mice through its antioxidant effects. Nutrients. 2016 Mar 10;8(3): 155. https://doi.org/10.3390/nu8030155

Tang W, Xing Z, Hu W, Li C, Wang J, Wang Y. Antioxidative effects *in vivo* and colonization of *Lactobacillus plantarum* MA2 in the murine intestinal tract. Appl Microbiol Biotechnol. 2016 Aug; 100(16): 7193–7202. https://doi.org/10.1007/s00253-016-7581-x

Tang W, Xing Z, Li C, Wang J, Wang Y. Molecular mechanisms and *in vitro* antioxidant effects of *Lactobacillus plantarum* MA2. Food Chem. 2017 Apr;221:1642–1649.
https://doi.org/10.1016/j.foodchem.2016.10.124

Wafula EN, Brinks E, Becker B, Huch M, Trierweiler B, Mathara JM, Oguntoyinbo FA, Cho GS, Franz CMAP. Draft genome sequence of *Lactobacillus fermentum* BFE 6620, a potential starter culture for African vegetable foods, isolated from fermented cassava. Genome Announc. 2017 Aug 17;5(33):e00801-17.
https://doi.org/10.1128/genomeA.00801-17

Wang A, Yu H, Gao X, Li X, Qiao S. Influence of *Lactobacillus fermentum* I5007 on the intestinal and systemic immune responses of healthy and *E. coli* challenged piglets. Antonie van Leeuwenhoek. 2009 Jun;96(1):89–98. https://doi.org/10.1007/s10482-009-9339-2

Wang Y, Wu Y, Wang Y, Xu H, Mei X, Yu D, Wang Y, Li W. Antioxidant properties of probiotic bacteria. Nutrients. 2017 May 19;9(5):521. https://doi.org/10.3390/nu9050521

Wu KC, Cui JY, Liu J, Lu H, Zhong X, Klaassen CD. RNA-Seq provides new insights on the relative mRNA abundance of antioxidant components during mouse liver development. Free Radic Biol Med. 2019 Apr;134:335–342.
https://doi.org/10.1016/j.freeradbiomed.2019.01.017

Wu R, Wang L, Wang J, Li H, Menghe B, Wu J, Guo M, Zhang H. Isolation and preliminary probiotic selection of lactobacilli from koumiss in Inner Mongolia. J Basic Microbiol. 2009 Jun;49(3): 318–326. https://doi.org/10.1002/jobm.200800047

Wu Y, Tang L, Chen B. Oxidative stress: implications for the development of diabetic retinopathy and antioxidant therapeutic perspectives. Oxid Med Cell Longev. 2014;2014:1–12.
https://doi.org/10.1155/2014/752387

Yu Y, Bai F, Liu Y, Yang Y, Yuan Q, Zou D, Qu S, Tian G, Song L, Zhang T, et al. Fibroblast growth factor (FGF21) protects mouse liver against d-galactose-induced oxidative stress and apoptosis via activating Nrf2 and PI3K/Akt pathways. Mol Cell Biochem. 2015 May; 403(1–2):287–299.
https://doi.org/10.1007/s11010-015-2358-6

Zhang L, Liu C, Li D, Zhao Y, Zhang X, Zeng X, Li S. Antioxidant activity of an exopolysaccharide isolated from *Lactobacillus plantarum* C88. Int J Biol Macromol. 2013 Mar;54:270–275.
https://doi.org/10.1016/j.ijbiomac.2012.12.037

Zhao J, Tian F, Yan S, Zhai Q, Zhang H, Chen W. *Lactobacillus plantarum* CCFM10 alleviating oxidative stress and restoring the gut microbiota in D-galactose-induced oxidative stress model. Food Funct. 2018 Feb 21;9(2):917-924.
https://doi.org/10.1039/c7fo0174g

Zhao Y, Hong K, Zhao J, Zhang H, Zhai Q, Chen W. *Lactobacillus fermentum* and its potential immunomodulatory properties. J Funct Foods. 2019 May;56:21–32.
https://doi.org/10.1016/j.jff.2019.02.044

Supplementary materials are available on the journal's website.

Polish Journal of Microbiology
2020, Vol. 69, No 2, 217–222
https://doi.org/10.33073/pjm-2020-025

ORIGINAL PAPER

Performance Evaluation of Different Commercial Serological Kits for Diagnosis of Acute Hepatitis E Viral Infection

QIANG ZHANG[1]*, XIAOLONG ZONG[2], DONGMING LI[3], JING LIN[1] and LIHUA LI[1]

[1] Department of Clinical Laboratory, Branch of Tianjin Third Central Hospital, Tianjin, China
[2] Department of Clinical Laboratory, The Second Hospital of Tianjin Medical University, Tianjin, China
[3] Department of Clinical Laboratory, Tianjin Third Central Hospital, Tianjin, China

Submitted 7 March 2020, revised 4 May 2020, accepted 9 May 2020

Abstract

Clinical diagnosis of hepatitis E viral (HEV) infection mainly relies on serological assays, and the current status of misdiagnoses regarding HEV infection is uncertain. In this study, patients with acute HEV infection were tested for anti-HEV IgM and IgG, a HEV antigen (Ag), and viral loads (HEV RNA). Serology was performed using four commercial HEV ELISA kits: Wantai, Kehua, Lizhu, and Genelabs IgM and IgG. The HEV RNA was detected using RT-PCR assays. The sensitivities of different kits for anti-HEV IgM ranged from 82.6% to 86%. Each kit for anti-HEV IgM was highly specific (97.8–100%). The sensitivities of all kits to detect anti-HEV IgG with (87.2–91.9%) had a substantial agreement, but the Kehua and Genelabs tests were more specific than the Wantai and Lizhu tests. The Wantai tests for the HEV Ag and HEV RNA were also important for acute HEV infections (Kappa = 0.787). Furthermore, a total of 6.98% of HEV infections were positive for HEV RNA but negative for both the HEV Ag and anti-HEV antibodies of IgM and IgG classes. Our findings demonstrate that the diagnosis of hepatitis E may be missed if only serological assays are used. Thus, a combination of serological and nucleic acid testing provides the optimal sensitivity and specificity to the diagnostic process.

Key words: hepatitis E virus, serological markers, diagnostic performance, enzyme-linked immunosorbent assay, misdiagnosis

Introduction

Hepatitis E is the infection of the liver caused by a virus known as the hepatitis E virus (HEV) and has posed severe public health hazards around the world. HEV has four major genotypes (1–4) that are globally distributed into different epidemiological patterns based on socioeconomic factors and ecology (Lu et al. 2006). HEV genotypes 1 and 2 infect humans solely (Ahmad et al. 2011). Generally, genotype 1 accounts for the epidemics in some parts of Asia, while genotype 2 is more prevalent in Africa, Mexico, and other developing countries (Colson et al. 2012). Genotypes 3 and 4 are zoonotic with an expanded host range (Okamoto 2007), while there have been noted chronic HEV infections in immunosuppressed patients (Honer zu Siederdissen et al. 2014). Genotype 3 is prevalent worldwide, while genotype 4 is mainly present in Asia. Besides, genotypes 5 and 6, which primarily infect wild boar, have been found in Japan (Sato et al. 2011; Takahashi et al. 2011). Recently, new genotypes, known as HEV-7 and HEV-8, were also found to infect camels and humans (Al-Sadeq et al. 2017).

Currently, HEV's diagnosis depends on specific serological and nucleic acid tests, as the clinical manifestations and routine laboratory measures of HEV are similar to those of other acute hepatitis (Zhang et al. 2019). There are four major methods for diagnosing hepatitis E, including the detection of anti-HEV IgM and IgG antibodies, the antigen (Ag), and HEV RNA. Presently, the clinical diagnosis of acute hepatitis E cases mainly depends on the serological detection of anti-HEV antibodies (Dreier and Juhl 2014). However, equivalence, sensitivity, and specificity in the results of the HEV Enzyme-linked Immunosorbent Assay (ELISA) kits tend to differ between manufacturers, leading to discrepancies in the rates of anti-HEV antibodies among different populations (Herremans et al. 2007; Drobeniuc et al. 2010), together with the HEV genome heterogeneity, and the different antigenic structure

* Corresponding author: Q. Zhang, Department of Clinical Laboratory, Branch of Tianjin Third Central Hospital, Tianjin, China; **e-mail: zhangqiang_tj@hotmail.com**

of HEV proteins. Moreover, cross-reactions of anti-HEV IgM with the Epstein-Barr virus (EBV) and cytomegalovirus (CMV) antibodies have been reported, which cause false-positive results (Hyams et al. 2014). Currently, the development of the HEV RNA assay kits is in the early stages in China and has not yet been widespread. Thus, the clinical diagnosis of HEV infection still mainly relies on serological assays with a few reports of hepatitis E misdiagnoses occurring in China.

In the present study, the performance of four commercial serological assays and PCR assay for the detection of HEV infection was evaluated, and the possibility of misdiagnosing of this infection using serological detection alone was determined.

Experimental

Materials and Methods

Samples. From March 2014 to March 2018, 364 serum samples were collected from Tianjin Third Central Hospital and Tianjin Medical University General Hospital. A total of 86 cases were diagnosed with acute viral hepatitis E (Kamar et al. 2014; European Association for the Study of the Liver 2018), 91 cases with rheumatic diseases (RD) including systemic lupus erythematosus (SLE) and rheumatoid arthritis (RA), and 91 cases with viral hepatitis by CMV or EBV according to the diagnostic guidelines of each disease. Meanwhile, 96 healthy volunteers were included in this study. Five milliliters of venous blood was collected and agglutinated for 10 min at 37°C, and subsequently centrifuged at 3,000 × g for 15 min at 4°C. The serum was taken and stored at −80°C before analysis. This study received approval from the Branch of Tianjin Third Central Hospital Ethics Committee (2019028). Our study was non-interventional and did not involve any specific sampling or addition to the usual procedures. An anonymized database provided analytical support. Therefore, the ethics committee waived the need for patient consent.

HEV serological assays. The commercially available HEV ELISA kits were selected with Wantai (Beijing, China), Kehua (Shanghai, China), Lizhu (Zhuhai, China), and Genelabs (Singapore, Singapore) for the detection of both IgM and IgG antibodies. For the HEV Ag assay, the Wantai was the only available commercial provider for the ELISA kit in China. All the experimental operations were performed according to the instructions recommended by manufacturers. Results of the ELISA tests were listed as ratios (s/co), and interpretations were made as advised in the instructions.

The HEV RNA assay. One-step reverse transcription-quantitative polymerase chain reaction (RT-qPCR) assay was set up by our research team and had been approved for clinical use. Primers and probes were designed based on a multiple sequence alignment of the HEV genome sequences in the ORF3 region, and synthesized by the Sangon Biotech Company (Shanghai, China): forward primer, 5'-GGTGGTTTCTGGGGTGAC-3' (T_m = 61.2°C); reverse primer, 5'-AGGGGTTGGTTGGATGAA-3' (T_m = 61.2°C); probe, 5'-TGATTCTCAGCCCTTCGC-3' (T_m = 62.5°C). NCBI-Primer-BLAST searches for the primers and probe showed that the genetic sequences of the different HEV genotypes 1–4 were highly conserved in the ORF3 region. Firstly, the target fragment of 70 bp was amplified from the strain of HEV genotype 4 (CHNXJ-SW13) by the forward and reverse primers mentioned above, and then inserted the fragment into Promega T-easy Vector (3105 bp) to obtain the standard plasmid. Serial dilutions plasmids of $5 \times 10^0 \sim 5 \times 10^9$ copies/2 µl were obtained by 10-fold dilution, and the standard curve was established. Total RNA was extracted from 140 µl serum using TIANamp Virus RNA Kit (Tiangen, Beijing, China). The One-Step PrimeScript' RT-PCR Kit (Takara, Dalian, China) enabled the performance of RT-qPCR in a total 20-µl reaction system, including 10 µl GoTaq Probe qPCR Master Mix (1×), 0.4 µl GoScript RT Mix for one-step RT-qPCR (1×), 1 µl forward primer (500 mM), 1 µl reverse primer (500 mM), 0.5 µl probe (250 nM), 5.1 µl RNase-Free H_2O and 2 µl RNA template or standard plasmid of HEV. Subsequently, the reaction was conducted with the MX3000P Real-Time QPCR System (Aligent, California, USA). The conditions for PCR amplification involved the following: 1 cycle at 45°C for 30 min, 1 cycle at 95°C for 15 min, followed by 45 cycles at 95°C for 10 sec, at 55°C for 20 sec and at 72°C for 15 sec. The expression of the HEV RNA was calculated according to the standard curve established by plasmids with different dilutions.

Data analysis. Commercially available software was used for all the statistical analyses (MedCalc, version 18.2, Belgium). The receiver operating characteristic (ROC) curve was used to analyze the diagnostic performances for anti-HEV IgG and IgM assays. Agreements between different kits were assessed by the Kappa statistic. The level of agreement was defined by the Kappa coefficient as excellent (> 0.8), substantial (0.6–0.8), moderate (0.4–0.6), fair (0.2–0.4), and poor (< 0.2) (Nogues-Sabate et al. 2018). A p-value of less than 0.05 was considered statistically significant. Additionally, two-sided 95% confidence intervals (CI) were calculated.

Results

Performance of anti-HEV IgM assays. The diagnostic performance characteristic of each anti-HEV IgM kit was determined by the ROC curve. As shown

Table I
Diagnostic performance of anti-HEV IgM assays.

Commercial tests	% Sensitivity (95% CI)	% Specificity (95% CI)	% PPV (95% CI)	% NPV (95% CI)	AUC (95% CI)	*p*	% Specificity with RD (95% CI)	% Specificity with CMV/EBV (95% CI)	% Specificity with healthy (95% CI)
Wantai	84.9 (75.5–91.7)	100 (98.7–100)	100 (100–100)	95.5 (92.8–97.2)	0.924 (0.892–0.949)	< 0.01	100 (100–100)	100 (100–100)	100 (100–100)
Kehua	86.0 (76.9–92.6)	100 (98.7–100)	100 (100–100)	95.9 (93.2–97.5)	0.930 (0.899–0.954)	< 0.01	100 (100–100)	100 (100–100)	100 (100–100)
Lizhu	83.7 (74.2–90.8)	100 (98.7–100)	100 (100–100)	95.2 (92.5–97.0)	0.919 (0.886–0.945)	< 0.01	100 (100–100)	100 (100–100)	100 (100–100)
Genelabs	82.6 (72.9–89.9)	99.3 (97.4–99.9)	97.3 (89.9–99.3)	94.8 (92.1–96.7)	0.909 (0.875–0.937)	< 0.01	97.8 (94.8–100)	100 (100–100)	100 (100–100)

in Table I, the area under the curve (AUC) value of the ELISA kits ranged from 0.909 to 0.93. The sensitivity among the 86 acute HEV infections ranged from 82.6% to 86% (Table I), suggesting an excellent agreement (Kappa: 0.819–1) in anti-HEV IgM antibody detection between the ELISA kits (Table II). All the anti-HEV IgM assays evaluated demonstrated good specificities (97.8–100%), except for two false-positive results obtained from the RD cases detected by the Genelabs ELISA kit. No positive results were shown in CMV/EBV infected patients by all the assays (Table I), which demonstrated that there were no cross-reactions of IgM against CMV and EBV.

Table II
Concordance for anti-HEV IgM assays in the diagnosis of the acute HEV infections.

Commercial tests	% Concordance	Kappa (95% CI)
Wantai		
Kehua	98.8	0.950 (0.852–1.000)
Lizhu	98.8	0.953 (0.862–1.000)
Genelabs	95.3	0.819 (0.648–0.990)
Kehua		
Lizhu	97.7	0.903 (0.771–1.000)
Genelabs	96.5	0.860 (0.706–1.000)
Lizhu		
Genelabs	96.5	0.868 (0.722–1.000)

Performance of anti-HEV IgG assays. The AUC value (0.827–0.929) of the four distinct anti-HEV IgG kits are shown in Table III. The sensitivity among the acute HEV infection patients ranged from 87.2% to 91.9% and showed a substantial agreement with Kappa coefficients from 0.752 to 0.927 between each different ELISA kit (Table III and IV). However, the specificities of anti-HEV IgG among the non-HEV population showed significant inconsistency between each ELISA kit (Table IV). The specificity of the Kehua (96.9–98.9%) and Genelab (96.7–98.9%) tests were significantly higher when compared with the Wantai (64.6–81.3%) and Lizhu assays (69.8–83.5%) (Table III).

The HEV Ag and HEV RNA assays. A total of 36 acute HEV patients were positive for the HEV Ag

Table III
Diagnostic performance of anti-HEV IgG assays.

Commercial tests	% Sensitivity (95% CI)	% Specificity (95% CI)	% PPV (95% CI)	% NPV (95% CI)	AUC (95% CI)	*p*	% Specificity with RD (95% CI)	% Specificity with CMV/EBV (95% CI)	% Specificity with healthy (95% CI)
Wantai	91.9 (83.9–96.7)	74.8 (69.3–79.8)	53.0 (47.7–58.3)	96.7 (93.6–98.4)	0.833 (0.791–0.870)	< 0.01	79.2 (71.0–87.3)	81.3 (73.3–89.3)	64.6 (55.0–74.1)
Kehua	87.2 (78.3–93.4)	97.5 (94.9–99.0)	91.5 (83.7–95.7)	96.1 (93.4–97.7)	0.923 (0.891–0.949)	< 0.01	98.9 (96.6–100)	97.8 (94.8–100)	96.9 (93.4–100)
Lizhu	89.5 (81.1–95.1)	75.9 (70.4–80.8)	53.5 (48.0–58.9)	95.9 (92.6–97.8)	0.827 (0.784–0.865)	< 0.01	83.5 (75.9–91.1)	74.7 (65.8–83.6)	69.8 (60.6–79.0)
Genelabs	88.4 (79.7–94.3)	97.5 (94.9–99.0)	91.6 (83.9–95.8)	96.4 (93.8–98.0)	0.929 (0.898–0.953)	< 0.01	98.9 (96.6–100)	96.7 (93.0–100)	97.9 (95.0–100)

Table IV
Concordance for anti-HEV IgG assays.

Commercial tests	Concordance of HEV		Concordance of RD		Concordance of CMV/EBV		Concordance of healthy	
	%	Kappa (95% CI)	%	Kappa (95% CI)	%	Kappa (95% CI)	%	Kappa (95% CI)
Wantai								
Kehua	95.3	0.753 (0.524–0.982)	80.2	0.081 (–0.069–0.231)	81.3	0.069 (–0.102–0.239)	68.8	0.147 (0.015–0.279)
Lizhu	98.8	0.927 (0.785–1.000)	91.2	0.712 (0.525–0.898)	88.5	0.809 (0.664–0.954)	94.8	0.882 (0.782–0.982)
Genelabs	96.5	0.805 (0.592–1.000)	80.2	0.081 (–0.069–0.231)	82.4	0.153 (–0.064–0.369)	67.7	0.111 (–0.007–0.229)
Kehua								
Lizhu	96.5	0.823 (0.629–1.000)	84.6	0.107 (–0.087–0.300)	76.9	0.125 (–0.034–0.283)	74.0	0.183 (0.238–0.341)
Genelabs	96.5	0.837 (0.658–1.000)	100	1.000 (1.000–1.000)	98.9	0.795 (0.403–1.000)	99.0	0.852 (0.566–1.000)
Lizhu								
Genelabs	95.3	0.752 (0.520–0.984)	84.6	0.107 (–0.087–0.300)	78.0	0.183 (0.001–0.366)	72.9	0.139 (–0.005–0.282)

Table V
Consistency for HEV Ag and HEV RNA assays in the diagnosis of the acute HEV infections.

	HEV RNA +, n (%)	HEV RNA –, n (%)	Total, n (%)
HEV Ag +, n (%)	36 (41.86)	0 (0)	36 (41.86)
HEV Ag –, n (%)	8 (9.3)	42 (48.84)	50 (58.14)
Total, n (%)	44 (51.16)	42 (48.84)	86 (100)

using the Wantai ELISA kit, with no positive cases found among the non-HEV infection patients. A total of 44 acute HEV infection patients were positive for HEV RNA. The consistency rate between the HEV Ag and RNA was 90.7% (78/86), as shown in Table V. The two methods had a substantial agreement with a Kappa coefficient of 0.787 (0.656–0.918). Furthermore, six of the 86 samples were positive for HEV RNA but negative for anti-HEV IgM and IgG antibodies, and the HEV Ag by all ELISA kits (Fig. 1).

Discussion

To date, the identification of serological markers in HEV infections using accurate diagnostic assays remain a challenge. There are a plethora of issues regarding the specificity and sensitivity of HEV serological assays in epidemiological and clinical settings that require urgent attention. In this present study, we evaluated four dominant, commercially available anti-HEV IgM and IgG assays, as well as the HEV Ag and HEV RNA to investigate the misdiagnosis's current status rely on the current measurements.

Anti-HEV IgM appears in the early phase of acute hepatitis E. The antibodies can be detected as early as four days after the onset of jaundice and last up to five months (Kuniholm et al. 2009). There are two main methods in anti-HEV IgM serological assays: the capture method with anti-human IgM μ chain (Wantai, Kehua and Lizhu), and the indirect method (Genelabs). The sensitivity and specificity of different meth-

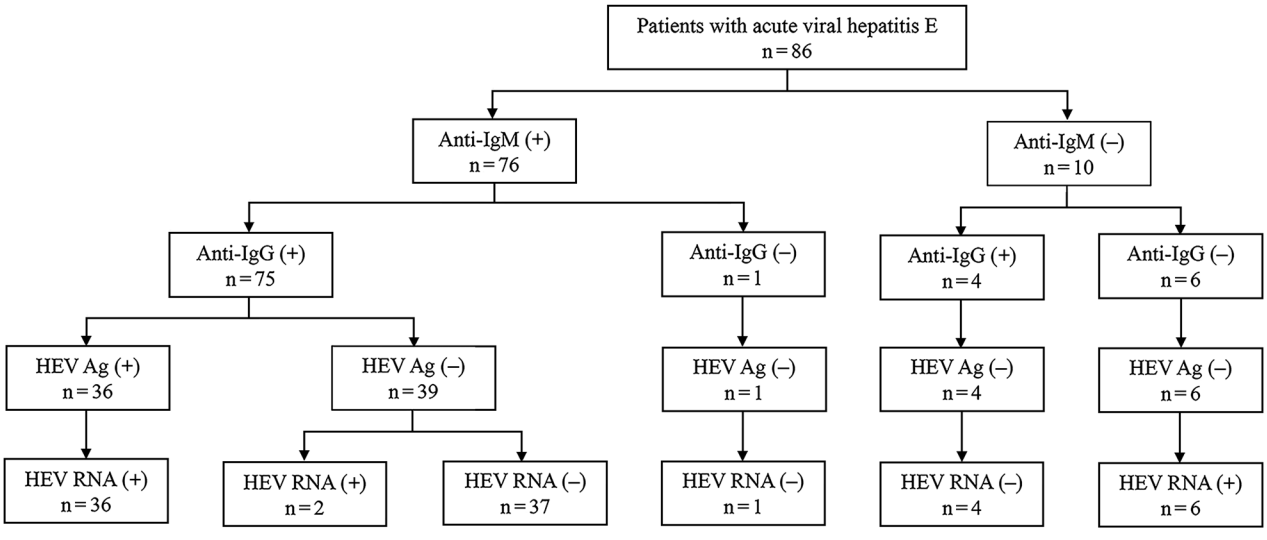

Fig.1. Flow diagram for patients with acute viral hepatitis E.

ods present variations in anti-HEV IgM assays with a recent study demonstrating a high cross-reactivity of HEV IgM compared to EBV and CMV (Drobeniuc et al. 2010). However, in the present study, no false-positive results due to cross-reaction with EBV- or CMV-infected patients were observed, indicating the highly specific nature of the anti-HEV IgM assays. Moreover, these findings were found to be consistent with those of the other groups, including immunocompromised patients (Abravanel et al. 2013) and infections with HEV genotype 3 (Legrand-Abravanel et al. 2009). The Genelabs ELISA kit detected two false-positive results obtained from patients with RD. This finding supports the opinion that the capture method using the anti-human IgM μ chain is more specific than the indirect method using the anti-HEV IgM assay.

In general, the detection of anti-HEV IgG is usually used as an indicator of past infection. However, the appearance of the anti-HEV IgG antibody is early, which could be used in the clinical diagnosis of acute HEV infection (Aggarwal and Jameel 2011). The Qatar research group found that Wantai HEV-IgG assays revealed high sensitivity and specificity with excellent Kappa concordance using different enzyme immunoassays in assessing seroprevalence of HEV antibodies (Al-Absi et al. 2018). However, a significant discrepancy in anti-HEV IgG results between different assay kits in the non-HEV population was found in our study. The positive rates were significantly higher by the Wantai and Lizhu kits than those of Kehua and Genelabs. A Korean research compared anti-HEV IgG antibody results using the Genelabs and Wantai ELISA kits to estimate HEV serum prevalence in the Korean population (Park et al. 2012). They found a significant inconsistency in the results between the two assays, which was also observed in our study. Therefore, epidemiological investigations of HEV in the population may lead to significant inconsistencies when different kits are used. The Kehua and Genelabs IgG assays had high specificities in the non-HEV population and could be used in the clinical diagnosis of HEV. On the other hand, the Wantai and Lizhu IgG assays were more suitable for epidemiological investigations because the positive rates in the non-HEV population were too high to distinguish the acute HEV infection from the previous disease.

In this study, all four anti-HEV IgG serological assays used the indirect method. There are two major types of antigens coated on the plates for binding of anti-HEV IgG antibodies, including synthetic peptides and recombinant proteins (Innis et al. 2002; Ulanova et al. 2008). The use of the recombinant ORF2-encoded protein in numerous serological studies has revealed its significant efficacy in the identification of antibodies against various HEV strains (Christensen et al. 2008; Kuniholm et al. 2009). Since recombinant proteins can replicate the HEV neutralizing epitope better than the synthetic peptides, the results in the Wantai anti-HEV IgG assay were more sensitive. A French research group also substantiated that the Wantai IgG assay was the most sensitive amongst all other eight commercial ELISA kits used to detect HEV of genotypes 1 and 3 (Abravanel et al. 2013). The results suggested that the anti-HEV IgM assay was superior in the diagnosis of acute HEV infection due to its good specificity when paired with the Wantai anti-HEV IgG assay, which could improve the accuracy of diagnosis.

The latest reports have indicated that this novel HEV Ag is a resourceful serum marker to detect the acute HEV infection and has a good consistency with HEV RNA (Zhang et al. 2006; Zhao et al. 2015; Fraga et al. 2018; Zhang et al. 2019). Our findings in this study also supported this view. However, all the HEV Ag positive samples showed positive anti-HEV IgM results (Fig. 1), which provided no direct evidence to support that Ag detection could improve diagnostic efficiency. Furthermore, six samples were only positive for HEV RNA but negative for anti-HEV IgM and IgG, as well as Ag in all ELISA kits employed, which showed that 6.98% of acute HEV infection patients have a chance to be misdiagnosed if reliant on serological assays detection alone. It indirectly indicates that HEV RNA detection can improve diagnostic efficiency. However, despite the highly specific and sensitive capability of some PCR assays for the detection of HEV RNA, their utility has been restricted due to the short period of HEV viremia detection. Therefore, the incidence of acute HEV infection cannot be completely ruled out by a negative HEV PCR result.

In conclusion, for the successful diagnosis of acute viral hepatitis E, a combination of nucleic acid and serological tests is imperative to provide excellent specificity and sensitivity to the diagnosis. However, we also observed significant inconsistencies between the serological and HEV RNA assays; thereby, caution is warranted while interpreting the results of both serological and molecular tests in HEV diagnosis.

Acknowledgments

This project was supported by the Tianjin Science and Technology Program of China (No. 17ZXHLSY00020).

Conflict of interest

The authors do not report any financial or personal connections with other persons or organizations, which might negatively affect the contents of this publication and/or claim authorship rights to this publication.

Literature

Abravanel F, Chapuy-Regaud S, Lhomme S, Miedougé M, Peron JM, Alric L, Rostaing L, Kamar N, Izopet J. Performance of anti-HEV assays for diagnosing acute hepatitis E in immunocompromised patients. J Clin Virol. 2013 Dec;58(4):624–628. https://doi.org/10.1016/j.jcv.2013.10.003

Aggarwal R, Jameel S. Hepatitis E. Hepatology. 2011 Dec;54(6): 2218–2226. https://doi.org/10.1002/hep.24674

Ahmad I, Holla RP, Jameel S. Molecular virology of hepatitis E virus. Virus Res. 2011 Oct;161(1):47–58. https://doi.org/10.1016/j.virusres.2011.02.011

Al-Absi ES, Al- Sadeq DW, Younis MH, Yassine HM, Abdalla OM, Mesleh AG, Hadwan TA, Amimo JO, Thalib L, Nasrallah GK. Performance evaluation of five commercial assays in assessing seroprevalence of HEV antibodies among blood donors. J Med Microbiol. 2018 Sep 01;67(9):1302–1309. https://doi.org/10.1099/jmm.0.000807

Al-Sadeq DW, Majdalawieh AF, Nasrallah GK. Seroprevalence and incidence of hepatitis E virus among blood donors: A review. Rev Med Virol. 2017 Sep;27(5):e1937. https://doi.org/10.1002/rmv.1937

Christensen PB, Engle RE, Hjort C, Homburg KM, Vach W, Georgsen J, Purcell RH. Time trend of the prevalence of hepatitis E antibodies among farmers and blood donors: a potential zoonosis in Denmark. Clin Infect Dis. 2008 Oct 15;47(8):1026–1031. https://doi.org/10.1086/591970

Colson P, Romanet P, Moal V, Borentain P, Purgus R, Benezech A, Motte A, Gérolami R. Autochthonous infections with hepatitis E virus genotype 4, France. Emerg Infect Dis. 2012 Aug;18(8): 1361–1364. https://doi.org/10.3201/eid1808.111827

Dreier J, Juhl D. Autochthonous hepatitis e virus infections: a new transfusion-associated risk? Transfus Med Hemother. 2014; 41(1):29–39. https://doi.org/10.1159/000357098

Drobeniuc J, Meng J, Reuter G, Greene-Montfort T, Khudyakova N, Dimitrova Z, Kamili S, Teo CG. Serologic assays specific to immunoglobulin M antibodies against hepatitis E virus: pangenotypic evaluation of performances. Clin Infect Dis. 2010 Aug; 51(3):e24–e27. https://doi.org/10.1086/654801

European Association for the Study of the Liver. EASL Clinical Practice Guidelines on hepatitis E virus infection. J Hepatol. 2018 Jun;68(6):1256–1271. https://doi.org/10.1016/j.jhep.2018.03.005

Fraga M, Doerig C, Moulin H, Bihl F, Brunner F, Müllhaupt B, Ripellino P, Semela D, Stickel F, Terziroli Beretta-Piccoli B, et al. Hepatitis E virus as a cause of acute hepatitis acquired in Switzerland. Liver Int. 2018 Apr;38(4):619–626. https://doi.org/10.1111/liv.13557

Herremans M, Bakker J, Duizer E, Vennema H, Koopmans MPG. Use of serological assays for diagnosis of hepatitis E virus genotype 1 and 3 infections in a setting of low endemicity. Clin Vaccine Immunol. 2007 May;14(5):562–568. https://doi.org/10.1128/CVI.00231-06

Höner zu Siederdissen C, Pischke S, Schlue J, Deterding K, Hellms T, Schuler-Lüttmann S, Schwarz A, Manns MP, Cornberg M, Wedemeyer H. Chronic hepatitis E virus infection beyond transplantation or human immunodeficiency virus infection. Hepatology. 2014 Sep;60(3):1112–1113. https://doi.org/10.1002/hep.26987

Hyams C, Mabayoje DA, Copping R, Maranao D, Patel M, Labbett W, Haque T, Webster DP. Serological cross reactivity to CMV and EBV causes problems in the diagnosis of acute hepatitis E virus infection. J Med Virol. 2014 Mar;86(3):478–483. https://doi.org/10.1002/jmv.23827

Innis BL, Seriwatana J, Robinson RA, Shrestha MP, Yarbough PO, Longer CF, Scott RM, Vaughn DW, Myint KS. Quantitation of immunoglobulin to hepatitis E virus by enzyme immunoassay. Clin Diagn Lab Immunol. 2002 May;9(3):639–648.

Kamar N, Dalton HR, Abravanel F, Izopet J. Hepatitis E virus infection. Clin Microbiol Rev. 2014 Jan 01;27(1):116–138. https://doi.org/10.1128/CMR.00057-13

Kuniholm MH, Purcell RH, McQuillan GM, Engle RE, Wasley A, Nelson KE. Epidemiology of hepatitis E virus in the united states: results from the third national health and nutrition examination survey, 1988–1994. J Infect Dis. 2009 Jul;200(1):48–56. https://doi.org/10.1086/599319

Legrand-Abravanel F, Thevenet I, Mansuy JM, Saune K, Vischi F, Peron JM, Kamar N, Rostaing L, Izopet J. Good performance of immunoglobulin M assays in diagnosing genotype 3 hepatitis E virus infections. Clin Vaccine Immunol. 2009 May;16(5):772–774. https://doi.org/10.1128/CVI.00438-08

Lu L, Li C, Hagedorn CH. Phylogenetic analysis of global hepatitis E virus sequences: genetic diversity, subtypes and zoonosis. Rev Med Virol. 2006 Jan;16(1):5–36. https://doi.org/10.1002/rmv.482

Nogués-Sabaté A, Aviles-Jurado FX, Ruiz-Sevilla L, Lehrer E, Santamaría-Gadea A, Valls-Mateus M, Vilaseca I. Intra and inter-observer agreement of narrow band imaging for the detection of head and neck tumors. Eur Arch Otorhinolaryngol. 2018 Sep; 275(9):2349–2354. https://doi.org/10.1007/s00405-018-5063-8

Okamoto H. Genetic variability and evolution of hepatitis E virus. Virus Res. 2007 Aug;127(2):216–228. https://doi.org/10.1016/j.virusres.2007.02.002

Park HK, Jeong SH, Kim JW, Woo BH, Lee DH, Kim HY, Ahn S. Seroprevalence of anti-hepatitis E virus (HEV) in a Korean population: comparison of two commercial anti-HEV assays. BMC Infect Dis. 2012 Dec;12(1):142. https://doi.org/10.1186/1471-2334-12-142

Sato Y, Sato H, Naka K, Furuya S, Tsukiji H, Kitagawa K, Sonoda Y, Usui T, Sakamoto H, Yoshino S, et al. A nationwide survey of hepatitis E virus (HEV) infection in wild boars in Japan: identification of boar HEV strains of genotypes 3 and 4 and unrecognized genotypes. Arch Virol. 2011 Aug;156(8):1345–1358. https://doi.org/10.1007/s00705-011-0988-x

Takahashi M, Nishizawa T, Sato H, Sato Y, Jirintai, Nagashima S, Okamoto H. Analysis of the full-length genome of a hepatitis E virus isolate obtained from a wild boar in Japan that is classifiable into a novel genotype. J Gen Virol. 2011 Apr 01;92(4):902–908. https://doi.org/10.1099/vir.0.029470-0

Ulanova TI, Obriadina AP, Talekar G, Burkov AN, Fields HA, Khudyakov YE. A new artificial antigen of the hepatitis E virus. J Immunoassay Immunochem. 2008 Dec 31;30(1):18–39. https://doi.org/10.1080/15321810802570269

Zhang F, Li X, Li Z, Harrison TJ, Chong H, Qiao S, Huang W, Zhang H, Zhuang H, Wang Y. Detection of HEV antigen as a novel marker for the diagnosis of hepatitis E. J Med Virol. 2006 Nov; 78(11):1441–1448. https://doi.org/10.1002/jmv.20717

Zhang H, Rao H, Wang Y, Wang J, Kong X, Ji Y, Zhu L, Liu Y, Fang J, Yang M, et al. Evaluation of an antigen assay for diagnosing acute and chronic hepatitis E genotype 4 infection. J Gastroenterol Hepatol. 2019 Feb;34(2):458–465. https://doi.org/10.1111/jgh.14405

Zhao C, Geng Y, Harrison TJ, Huang W, Song A, Wang Y. Evaluation of an antigen-capture EIA for the diagnosis of hepatitis E virus infection. J Viral Hepat. 2015 Nov;22(11):957–963. https://doi.org/10.1111/jvh.12397

Supplementary materials are available on the journal's website.

Polish Journal of Microbiology
2020, Vol. 69, No 2, 223–229
https://doi.org/10.33073/pjm-2020-026

ORIGINAL PAPER

N-acetylcysteine (NAC) Attenuating Apoptosis and Autophagy in RAW264.7 Cells in Response to Incubation with Mycolic Acid from Bovine *Mycobacterium tuberculosis* Complex

XUE LIN[1, 2#], MENGMENG WEI[1, 2#], FUYANG SONG[1, 2], DI XUE[1, 2*] and YUJIONG WANG[1, 2*]

[1] Key Laboratory of Ministry of Education for Conservation and Utilization of Special Biological Resources in the Western, Ningxia University, Yinchuan, Ningxia, China
[2] College of Life Science, Ningxia University, Yinchuan, Ningxia, China

Submitted 17 March 2020, revised 10 May 2020, accepted 10 May 2020

Abstract

Bovine tuberculosis is an airborne infectious disease caused by organisms of the *Mycobacterium tuberculosis* (MTB) complex. Mycolic acid (MA) is the main lipid component of the cell membrane of MTB. It is non-enzymatically reduced by NAD(P)H and further produces reactive oxygen species (ROS), which can cause oxidative stress in human cells. N-acetylcysteine (NAC) is a synthetic precursor of glutathione (GSH) and exhibits anti-ROS activity. However, the underlying mechanisms of its protective properties remain uncertain. Herein, after pre-incubation of RAW264.7 cells with NAC, the factors associated with apoptosis and autophagy were measured. Mechanistically, NAC could reduce MA-induced expression of pro-apoptotic and pro-autophagy proteins. At the mRNA level, NAC can inhibit AMPK and activate mTOR expression. The results indicate that NAC might regulate autophagy in RAW264.7 cells through the AMPK/mTOR pathway. To further prove the effect of NAC on MA, ICR mice were used to evaluate the lung injury. Hematoxylin-eosin (HE) staining was performed on the lung. The results show that NAC could reduce cell injury induced by MA. In conclusion, our research showed that NAC attenuates apoptosis and autophagy in response to incubation with mycolic acid.

Key words: N-acetylcysteine, mycolic acid, apoptosis, autophagy

Introduction

Bovine tuberculosis is an airborne infectious disease caused by organisms of the MTB complex (Baker et al. 2019). MTB complex often colonizes immunocompromised hosts, then induces inflammation, and disrupts the host immune response. MTB can produce many substances to exert its virulence to mammalian cells. One of them is mycolic acid (MA). MA is a unique lipid component of the MTB cell wall and plays an essential role in the process of binding MTB to macrophages (Lehmann et al. 2018). Previous studies have shown that MTB lacking MA is less pathogenic *in vivo*, suggesting that MA plays an important role in MTB's infection (Slama et al. 2016). Furthermore, MTB promotes bacterial survival by inducing oxidative stress in macrophages (Mohanty et al. 2016). Therefore, the strategy to alleviate the virulence of MTB is to inhibit the biosynthesis of MA, neutralize the oxidative stress produced by MA, and reduce the damage of ROS to intracellular substances.

N-acetylcysteine (NAC) is a synthetic precursor of intracellular cysteine and glutathione (GSH) (Aldini et al. 2018), and its anti-ROS activity is attributed to the ability to react with oxygen ions. Some researchers believe that inhaled GSH or NAC can increase the level of GSH and reduce the oxidative damage that MTB causes to the host (Amaral et al. 2016). Several reports show that NAC protects against oxidative stress-induced cell death (Wang et al. 2014). The self-protective mechanism of intracellular MTB produces free radicals, which increases the toxicity to cells, so whether antioxidants are beneficial for MTB infection is still under investigation. As a marker of MTB cell

# These are co-first authors who contributed equally to this work.

* Corresponding authors: Y. Wang, College of Life Science, Ningxia University Yinchuan, Ningxia, China; **e-mail: wyj@nxu.edu.cn**
D. Xue, College of Life Science, Ningxia University, Yinchuan, Ningxia, China; **e-mail: xue_di@yeah.net**

envelope (Lederer et al. 1975), does MA affect cells? Although a large body of literature has elucidated the structural mechanism of MA (Marrakchi et al. 2014), it is unclear whether NAC affects autophagy and apoptosis of MA-incubated RAW cells.

In this study, RAW264.7 macrophages were used to explore further the immunological response and cell damage of host cells after incubation with MA. Animal experiments were performed to investigate the role of NAC in antagonizing the effects of MA in the induction of apoptosis and autophagy.

Experimental

Materials and Methods

Animals. Male ICR (Institute of Cancer Research) mice aged six weeks were purchased from the Chinese Academy of Sciences (Shanghai, China). The Ethics Committee approved all experimental procedures for Laboratory Animals at the Ningxia University. Mice were kept under conditions of a pathogen-free facility and given free access to food and tap water. After the mice were acclimated for one week, the mice were divided into the following four treatment groups: 1) the control group (administered 50 µl, 0.9% saline by intranasal route for 7 days); 2) the MA group (received 50 µl MA [50 µg/ml] for 7 days); 3) the MA + NAC group (received 50 µl MA [50 µg/ml] by intranasal route 3 hours post NAC protection for 7 days); and 4) the NAC group (received intranasal NAC for 7 days).

Histological evaluation. Mice were sacrificed by cervical dislocation at indicated time points. Lungs were extracted from mice, washed once with PBS, fixed in 4% paraformaldehyde for 24 hours, and stained with hematoxylin and eosin. The fixed tissue was embedded in paraffin and cut into 4-µm-thick sections using a microtome.

Cell culture. The RAW264.7 cell line was cultured in DMEM medium supplemented with 10% FBS and incubated at 37°C and 5% CO_2. Tissue-culture plasticware was acquired from Corning (Tewksbury, MA, USA). Before incubation, the cell line was seeded at a density of 1×10^6 cells per well in 6-well plates. The total cell number was determined with an automated vision-based cell counter.

Assessment of cell viability. To assess the viability rate of cells, we used the MTT assay (Sigma-Aldrich, Saint Louis, MO, USA). The RAW264.7 cells were seeded at a density of 5×10^3 cells per well in 96-well plates. They were subsequently treated with MA (50 µg/ml) for 0, 6, 12, and 24 hours. Another cells were pretreated with NAC at a concentration of 600 mg/ml for 2 hours before treatment with MA. After 2 hours, the culture supernatant was replaced with fresh DMEM. MA (50 µg/ml) was added to a culture medium. After 6, 12, and 24 hours of incubation, the MTT solution (50 µl) was added to each well. The plates were transferred to the incubator at 37°C and 5% CO_2 for 4 hours. After the incubation, the DMSO solution (200 µl) was added to each well. The absorbance was measured at 560 nm with a microplate reader (Bio-Rad Laboratories Inc, Hercules, CA, USA). The reading was converted to the percentage of the controls.

Quantification of IL-6 levels by ELISA. The RAW264.7 cell culture supernatant in each group was collected for the measurement of pro-inflammatory cytokine IL-6 levels. According to the manufacturer's instructions, the IL-6 levels were assayed by the cytokine ELISA (Wuhan Boster Biological, Wuhan, China).

Real-time quantitative PCR analysis. The total RNA was extracted using the MiniBEST Universal RNA Extraction Kit (Takara Biotechnology, Dalian, China). RNA was reverse transcribed into cDNA according to the experimental procedure of the high-capacity cDNA Archive Kit (Applied Biosystems, Foster City, CA, USA). The reverse transcription products were used as templates and subjected to quantitative PCR (Q-PCR). The obtained cDNA was subjected to PCR amplification in an ABI 7500 Fast thermocycler (Applied Biosystems, USA) using a SYBR-Green PCR Kit (Takara Biotechnology, Dalian, China). A two-step PCR cycle procedure was used: 95°C for 30 seconds, then 40 cycles for 5 seconds at 95°C, followed by an annealing and extension step at 60°C for 15 seconds. After completion of PCR amplification, DNA melting curve analysis was performed. The primers were synthesized by Shanghai Sango Company (Shanghai, China). Specific primer sequences for each gene are shown in Table I.

Table I
Primer sequences.

Gene name	Forward primer	Reverse primer
TNF-α	CGCTGAGGTCAATCTGC	GGCTGGGTAGAGAATGGA
Caspase-9	AGCGATTCTGCCTTTCAC	TGGAGATTTTGTGGTCAGC
mTOR	CTGGGGCTGCTTTCTGT	ACGGTTTTCTGCCTCTTGT
AMPK	CATCCCCAAACCTGTCC	ACAAGCCCCGAACAAAA

Western blot analysis. Total protein was extracted from the different treatment groups using the M-PER Mammalian Protein Extraction Reagent (Pierce, Rockford, IL, USA). The protein sample (20 μg) was mixed with 6* loading buffer and baked for 5 minutes. The proteins from each treatment group at the equal concentrations were separated by electrophoresis on 10% SDS-PAGE and then transferred to a nitrocellulose membrane (Mini-PROTEAN Tetra Cell, Bio Rad, Hercules, CA, USA). Membranes were blocked in 5% milk, immersed in the primary antibody solution, and incubated overnight at 4°C. It was thoroughly washed six times with 0.5% TBS-Tween, for 5 minutes each time. Then, the membrane was incubated with the secondary antibody for 1 hour at room temperature. Protein bands were displayed using a chemiluminescence (ECL) kit (UVP, Upland, CA, USA). β-actin was used as an internal control. The band intensity of the protein was quantified by using the ImageJ program. Antibodies used for blotting were BAX, LC3, and beclin-1 (at the dilution of 1:2000).

Statistics. Results are expressed as mean ± standard deviation. One-way ANOVA using the Student's t-test was used for multiple comparisons in SPSS 16.0 software. $P < 0.05$ was considered to represent a statistically significant difference.

Results

NAC decreases RAW264.7 cell viability during incubation with MA. The viability of RAW264.7 macrophages incubated with MA was determined with the MTT assay. The cells were treated with MA (50 μg/ml) for 0, 6, 12, and 24 hours. Other groups of cells were pretreated with NAC at a concentration of 600 mg/ml. The results showed a significant reduction of the RAW264.7 viability after treatment with MA when compared to the control after 6 hours of incubation, and the survival rate of the cells incubated with MA continued to decline within 36 hours (Fig. 1A). Pretreatment with NAC provided a significant increase in viability when compared to the MA-treated cells.

The IL-6 level in the supernatant was measured with an ELISA to elucidate further the cytokine level in the MA-induced cell damage and the effect of NAC on RAW264.7 macrophages. The results confirmed that MA could reduce the secretion of IL-6 compared with the control group (Fig. 1B). In contrast to the MA-treated cells, the treatment with NAC reduced the secretion of IL-6 significantly.

NAC reduces MA-induced apoptosis in RAW264.7 macrophages *in vivo*. To determine whether NAC regulates the apoptosis of RAW264.7 cells exposed to MA, the Western blot was used to analyze the relative expression of the BAX gene, which encodes an important protein for the regulation of apoptosis. As shown in Fig. 2B, MA induced a decrease in the BAX level compared with the control. Combined treatment of NAC further exaggerated this effect, indicating that NAC reduced apoptosis in RAW264.7 cells treated with MA.

Then, the caspase-9 mRNA level was pronouncedly decreased when compared to MA in the MA + NAC group (Fig. 2D). The level of TNF-α mRNA was found to decrease when compared to MA (Fig. 2C). This observation further proved the protective effect of NAC on RAW364.7 cells.

NAC reduces MA-induced autophagy in RAW264.7 cells via the AMPK/mTOR signaling pathway. To further explore the upstream events that

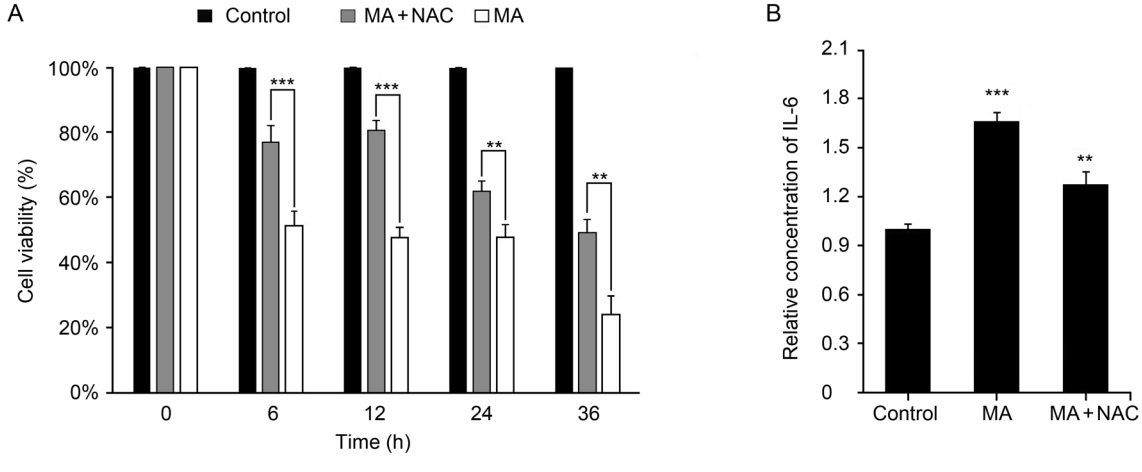

Fig. 1. Effect of NAC on the viability and cytokine levels of RAW264.7 cells during incubation with MA.

(A) Different groups of RAW264.7 cells were treated with MA (50 μg/ml) for 6, 12, 24, and 36 h and then analyzed for viability with MTT. Changes in the optical density (OD) values at 560 nm were recorded with a microplate reader. (B) The cell culture supernatants were collected after 24 h in the MA group and NAC + MA group; the levels of secreted cytokines in the samples were quantified. The graphical representation shows the relative concentration of the secreted IL-6. (Mean ± standard deviation, n = 3 experiments, $*p < 0.05$, $**p < 0.01$, $***p < 0.001$ by Student's t-test).

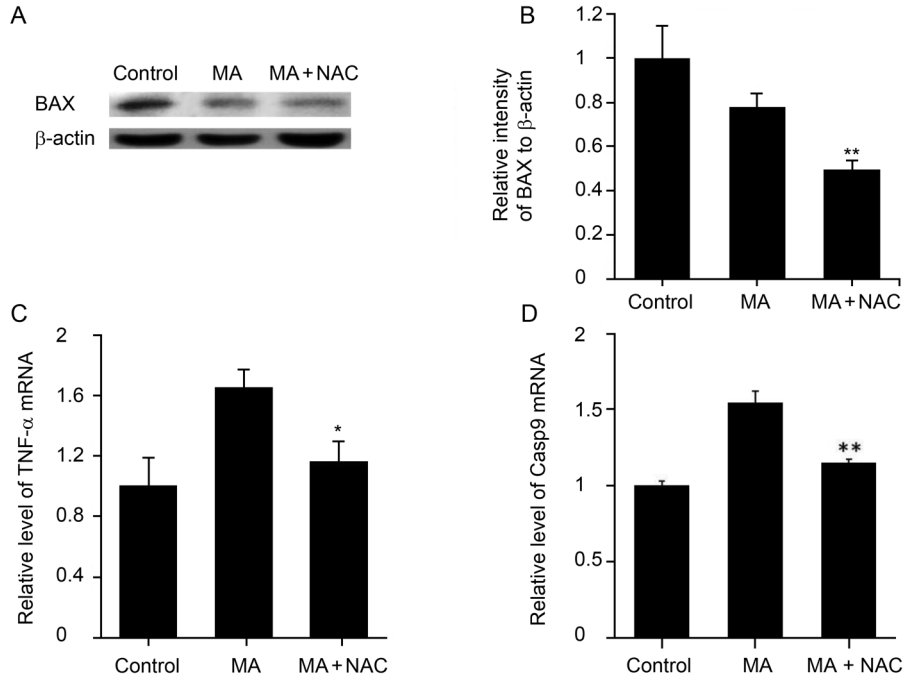

Fig. 2. Effects of NAC on apoptosis-related factors in RAW264.7 cells during incubation with MA.

The MA group was treated with MA (50 μg/ml) for 24 h. MA + NAC group was pre-treated with NAC at a concentration of 600 mg/ml for 2 h before treatment with MA. The results are representative of three separate experiments. (A) Representative Western blot of BAX in RAW264.7 treated with MA or MA + NAC (n = 3 experiments, $*p < 0.05$, $**p < 0.01$ by image J). (B) Quantification of BAX levels, as represented in A it was quantified by densitometry and standardized to the β-actin level. (C, D) The levels of TNF-α and Casp9 mRNA was standardized by the double delta CT method. (Mean ± standard deviation, n = 3 experiments, $*p < 0.05$, $**p < 0.01$ by Student's t-test).

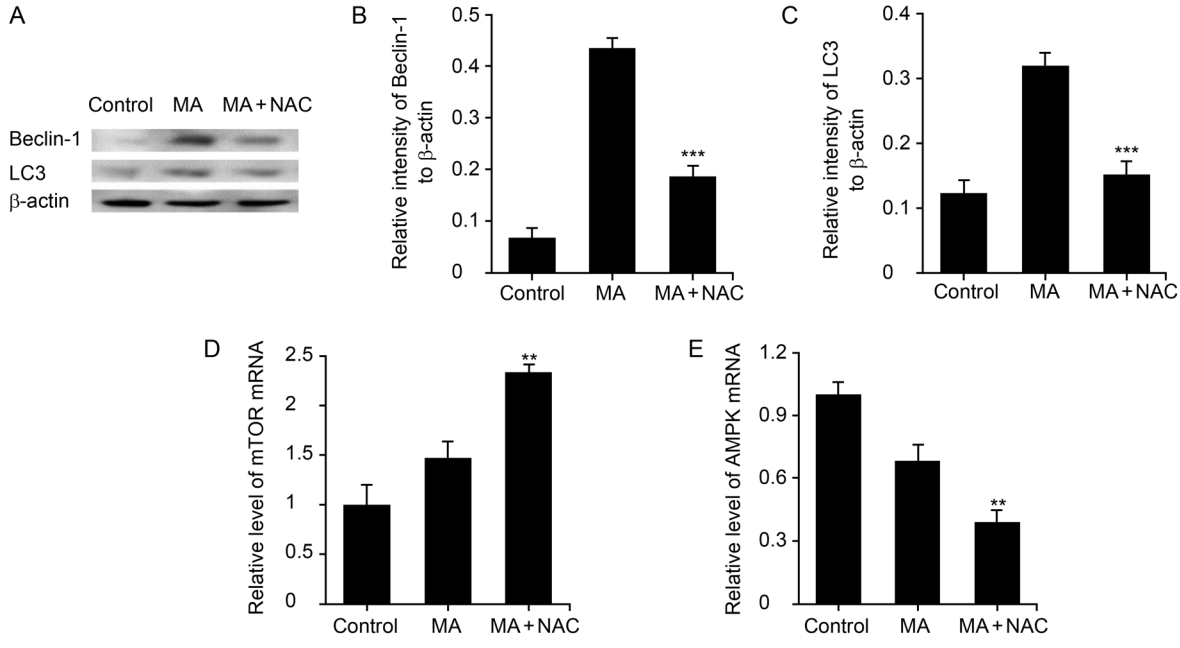

Fig. 3. Effects of NAC on autophagy-related factors in RAW264.7 cells during incubation with MA.

The MA group was treated with MA (50 μg/ml) for 24 h. MA + NAC group was pre-treated with NAC at a concentration of 600 mg/ml for 2 h before treatment with MA. (A) Representative Western blot of beclin-1 and LC3 in RAW264.7 macrophages treated with MA or MA + NAC (n = 3 experiments). (B, C) Quantification of beclin-1(b) and LC3(c) levels, as represented in A. (D, E) The levels of mTOR and AMPK mRNA was quantified by densitometry, and standardized to the β-actin level. (Mean ± standard deviation, n = 3 experiments, $*p < 0.05$, $**p < 0.01$ by Student's t-test).

were induced by the combination of MA and NAC, we measured the expression of autophagy-related factors. LC3 and beclin-1 are essential cytokines involved in the regulation of autophagy. As shown in Fig. 3A and B, pretreatment with NAC significantly suppressed the expression of LC3 and beclin-1 under MA treatment. This result indicates that NAC decreased autophagy in MA-treated RAW264.7 cells (Fig. 3A-C).

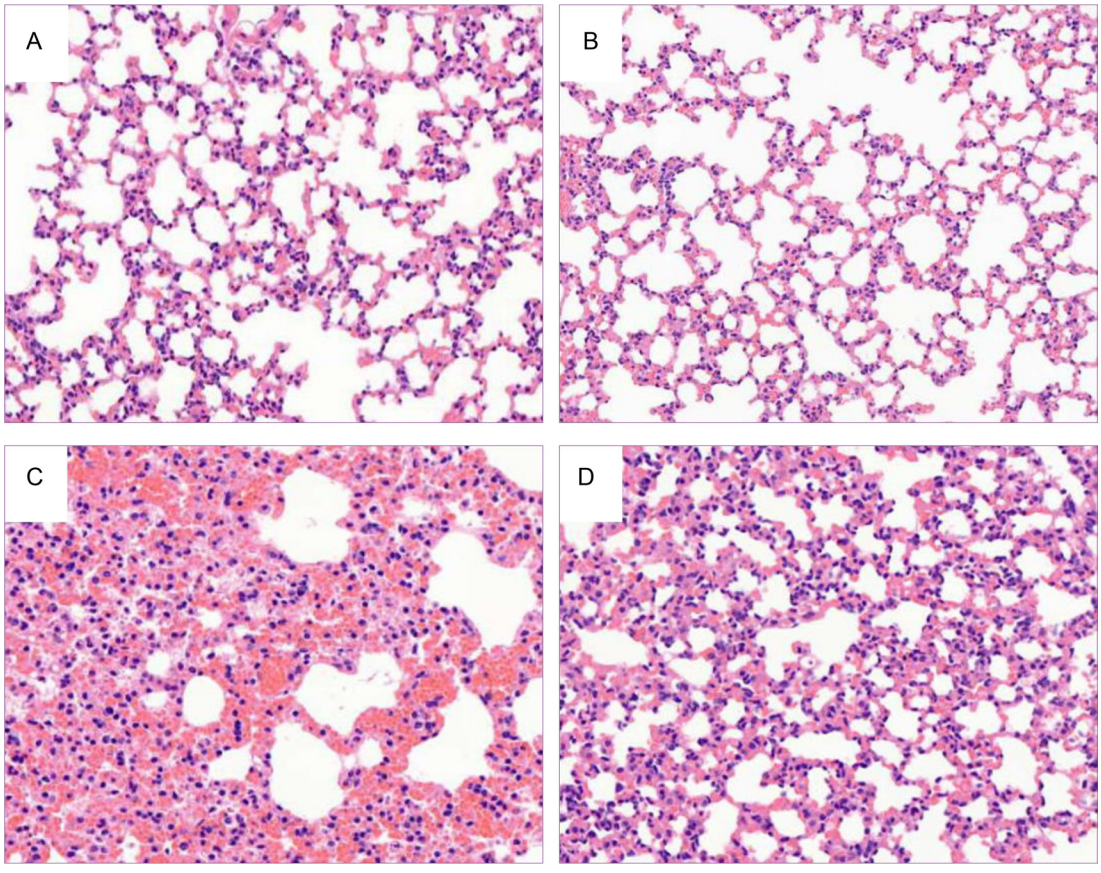

Fig. 4. Morphological changes in the lung tissue (H&E staining) in ICR mice treated with MA and induced by NAC. Representative photomicrographs illustrated characteristic lesions in 8 week-old C57BL/6 mice. The lung tissues, which had not been lavaged, were fixed with 4% paraformaldehyde solution and routinely processed for pathological slices. The morphological change of the lung tissue was observed after H&E staining. (A) The control group. (B) The NAC group. (C) The MA group. (D) The MA + NAC group. (Scale bar 50 μm).

Next we sought to examine AMPK and mTOR, important components in autophagy. The results indicated that NAC induced an increase in the level of mTOR mRNA when compared with MA only (Fig. 3D). As shown in Fig. 3E, NAC induced a decrease in the level of AMPK mRNA when compared to the MA group.

NAC reduces lung damage caused by MA. Finally, to confirm the immune suppression function of MA and NAC's protection, we examined the histological changes in the lungs of mice after their treatment by the intranasal route with NAC and MA. Lung tissues of mice were analyzed by hematoxylin-eosin (HE) staining. Lung tissue sections from the control group and NAC group displayed normal structure and no pathologic changes under the light microscope; no inflammatory cell infiltration was observed (Fig. 4A, B). In the MA group, the lung tissue of the mice was obviously damaged, the interstitial lung was congested, and apparent inflammatory cell infiltration was observed (Fig. 4C). In the MA + NAC group, the degree of alveolar wall damage was reduced compared with the MA group, and the infiltrating inflammatory cells were also significantly reduced (Fig. 4D).

Discussion

Bovine MTB complex is the primary causative agent of bronchiectasis and chronic and recurrent lung infections in patients. MA is a key compound of MTB infection and a significant contributor to lung injury in chronic MTB infection (Liu and Nikaido 1999). Early studies have shown that MA damage is primarily mediated by the generation of ROS and the destruction of host antioxidant defense mechanisms (Li et al. 2015). Consistent with previously published studies, we show here that RAW264.7 cells in response to incubation with MA reduce the relative expression of protein engaged in apoptosis and autophagy.

In the current study, RAW264.7 cells were first treated with NAC for 2 hours and then treated with MA for 24 hours. Here, we firstly showed that pretreatment with NAC significantly attenuated the changes in the level of the cell apoptosis protein BAX that were induced by the MA treatment. Compared with the MA group, the expression of the BAX gene was obviously reduced in the NAC + MA group. In addition, the mRNA levels of TNF-α and caspase-9 were also decreased.

BAX protein is known to be pro-apoptotic by regulating the permeability of the mitochondrial outer membrane (Lin et al. 2019). Caspase-9 cleaves the inactive pro-forms of effector caspases in apoptosis (Liu et al. 2014). When the mitochondrial membrane permeability changes, it promotes caspase-9 activation to induce apoptosis through TNF-α. The data obtained in the present study showed that NAC resulted in the simultaneous downregulation of caspase-9 and TNF-a, and the subsequent translocation of BAX to mitochondria. These results supported the hypothesis that NAC reduced MA-induced cell apoptosis of RAW264.7 cells, and it was mediated by the intrinsic mitochondrial pathway.

Under certain stress conditions (such as oxidative damage), autophagy plays a vital role in cell survival by scavenging proteins and damaged organelles to maintain cell homeostasis and integrity (Gutierrez et al. 2004). We examined the gene and protein expression of autophagy through quantitative real-time PCR and Western blot analysis. Besides, IL-6 concentration was evaluated with ELISA. From a mechanistic standpoint, LC3 can specifically accumulate in neonatal autophagosomes, so it is the most extensive and useful specific marker of autophagy. In contrast to the marker LC3, which forms the final autophagosome, beclin-1 is involved in the early stages of autophagy, releasing phosphorylated beclin-1, synthesizing autophagic vesicles, and recruiting proteins (Menon and Dhamija 2018). They are widely monitored as autophagy-related proteins. Our results show that incubation with MA increased the expression of autophagy-related protein. Remarkably, NAC inhibited the expression of the LC3 and beclin-1-encoding genes.

Furthermore, there are many signaling cascades involved in autophagy regulation in response to different stimuli. AMPK is the primary sensor of energy stress and is normally activated in response to various intracellular and extracellular stresses (Hardie 2014). It can also be activated by intracellular oxidative stress. The AMPK/mTOR signaling pathway is a classical upstream pathway regulating autophagy. Indeed, the reduction in ROS inhibits AMPK, thereby activating mTOR, the negative regulator of autophagy, and subsequently inhibiting autophagy (Cerni et al. 2019). Our results demonstrate that NAC might inhibit the expression of the autophagy-related LC3 and beclin-encoding genes via the reduction of intracellular ROS production.

In conclusion, our research showed that NAC attenuated the expression of the genes encoding for proteins of apoptosis and autophagy in RAW264.7 cells in response to incubation with MA. Mechanistically, an infection of MTB induced intracellular ROS production and subsequently promoted cell apoptosis. NAC attenuated MA-induced suppression of the activation of BAX and the production of IL-6. At the genetic level, NAC inhibits the expression of the TNF-α and caspase-9 genes and reduces the translation of apoptotic proteins. On the other hand, to investigate its possible autophagy mechanism, some autophagy-related proteins were measured. Our current study demonstrated that MA-induced the reduction of the cell autophagy-relative protein LC3, beclin-1, and the cell apoptosis-relative protein BAX. However, NAC could efficiently inhibit this reduction.

ORCID
Di Xue https://orcid.org/0000-0003-4376-5014

Acknowledgments
This study was funded by the National Natural Science Foundation of China (No. 31772710), Key Project of Research and Development of Ningxia Hui Autonomous Region of China (No. 2017BN04, No. 2020BEG03019, No. 2019BBF02005), Institution of Higher Education Projects of Building First-class Discipline Construction in Ningxia Region (Biology, NXYLXK2017B05), CAS "Light of West China" Program (XAB2017AW08).

Conflict of interest
The authors do not report any financial or personal connections with other persons or organizations, which might negatively affect the contents of this publication and/or claim authorship rights to this publication.

Literature

Aldini G, Altomare A, Baron G, Vistoli G, Carini M, Borsani L, Sergio F. N-acetylcysteine as an antioxidant and disulphide breaking agent: The reasons why. Free Radic Res. 2018 Jul;52(7):751–762. https://doi.org/10.1080/10715762.2018.1468564

Amaral EP, Conceição EL, Costa DL, Rocha MS, Marinho JM, Cordeiro-Santos M, D'Império-Lima MR, Barbosa T, Sher A, Andrade BB. N-acetyl-cysteine exhibits potent anti-mycobacterial activity in addition to its known anti-oxidative functions. BMC Microbiol. 2016 Oct 28;16(1):251. https://doi.org/10.1186/s12866-016-0872-7

Baker JJ, Dechow SJ, Abramovitch RB. Acid fasting: modulation of *Mycobacterium tuberculosis* metabolism at acidic pH. Trends Microbiol. 2019 Nov;27(11):942–953. https://doi.org/10.1016/j.tim.2019.06.005

Cerni S, Shafer D, To K, Venketaraman V. *Mycobacterium tuberculosis* investigating the role of everolimus in mtor inhibition and autophagy promotion as a potential host-directed therapeutic target in infection. J Clin Med. 2019 Feb 11;8(2):232. https://doi.org/10.3390/jcm8020232

Gutierrez MG, Master SS, Singh SB, Taylor GA, Colombo MI, Deretic V. Autophagy is a defense mechanism inhibiting BCG and *Mycobacterium tuberculosis* survival in infected macrophages. Cell. 2004 Dec 17;119(6):753–766. https://doi.org/10.1016/j.cell.2004.11.038

Hardie DG. AMPK-sensing energy while talking to other signaling pathways. Cell Metab. 2014 Dec 2;20(6):939–952. https://doi.org/10.1016/j.cmet.2014.09.013

Lederer E, Adam A, Ciorbaru R, Petit JF, Wietzerbin J. Cell walls of Mycobacteria and related organisms; chemistry and immunostimulant properties. Mol Cell Biochem. 1975 May 30; 7(2): 87–104. https://doi.org/10.1007/bf01792076

Lehmann J, Cheng T-Y, Aggarwal A, Park AS, Zeiler E, Raju RM, Akopian T, Kandror O, Sacchettini JC, Moody DB et al. An antibacterial β-lactone kills *Mycobacterium tuberculosis* by disrupting mycolic acid biosynthesis. Angew Chem Int Ed Engl. 2018 Jan 2; 57(1):348–353. https://doi.org/10.1002/anie.201709365

Li G, Liu G, Song N, Kong C, Huang Q, Su H, Bi A, Luo L, Zhu L, Xu Y et al. A novel recombinant BCG-expressing pro-apoptotic protein BAX enhances Th1 protective immune responses in mice. Mol Immunol. 2015 Aug;66(2):346–356. https://doi.org/10.1016/j.molimm.2015.04.003

Lin J, Chang Q, Dai X, Liu D, Jiang Y, Dai Y. Early secreted antigenic target of 6-kDa of *Mycobacterium tuberculosis* promotes caspase-9/caspase-3-mediated apoptosis in macrophages. Mol Cell Biochem. 2019 Jul;457(1–2):179–189. https://doi.org/10.1007/s11010-019-03522-x

Liu J, Nikaido H. A mutant of *Mycobacterium smegmatis* defective in the biosynthesis of mycolic acids accumulates meromycolates. Proc Natl Acad Sci USA. 1999 Mar 30;96(7):4011–4016. https://doi.org/10.1073/pnas.96.7.4011

Liu L, Yim H, Choi JH, Kim S-T, Jin Y, Lee SK. ATM kinase promotes both caspase-8 and caspase-9 activation during TNF-α – induced apoptosis of HeLa cells. FEBS Lett. 2014 Mar 18;588(6): 929–935. https://doi.org/10.1016/j.febslet.2014.01.050

Marrakchi H, Lanéelle M-A, Daffé M. Mycolic acids: structures, biosynthesis, and beyond. Chem Biol. 2014 Jan 16;21(1):67–85. https://doi.org/10.1016/j.chembiol.2013.11.011

Menon MB, Dhamija S. Beclin 1 phosphorylation – at the center of autophagy regulation. Front Cell Dev Biol. 2018 Oct 12;6:137. https://doi.org/10.3389/fcell.2018.00137

Mohanty S, Dal Molin M, Ganguli G, Padhi A, Jena P, Selchow P, Sengupta S, Meuli M, Sander P, Sonawane A. *Mycobacterium tuberculosis* EsxO (Rv2346c) promotes bacillary survival by inducing oxidative stress mediated genomic instability in macrophages. Tuberculosis (Edinb). 2016 Jan;96:44–57. https://doi.org/10.1016/j.tube.2015.11.006

Slama N, Jamet S, Frigui W, Pawlik A, Bottai D, Laval F, Constant P, Lemassu A, Cam K, Daffé M et al. The changes in mycolic acid structures caused by hadc mutation have a dramatic effect on the virulence of *Mycobacterium tuberculosis*. Mol Microbiol. 2016 Feb; 99(4):794–807. https://doi.org/10.1111/mmi.13266

Wang C, Chen K, Xia Y, Dai W, Wang F, Shen M, Cheng P, Wang J, Lu J, Zhang Y et al. N-acetylcysteine attenuates ischemia-reperfusion-induced apoptosis and autophagy in mouse liver via regulation of the ROS/JNK/Bcl-2 pathway. PLoS ONE. 2014 Sep 29;9(9):e108855. https://doi.org/10.1371/journal.pone.0108855

Polish Journal of Microbiology
2020, Vol. 69, No 2, 231–234
https://doi.org/10.33073/pjm-2020-017

SHORT COMMUNICATION

Extensively Drug-resistant *Acinetobacter baumannii* Belonging to International Clone II from A Pet Cat with Urinary Tract Infection; The First Report from Pakistan

ZEESHAN TAJ[1, 2], MUHAMMAD HIDAYAT RASOOL[1], AHMAD ALMATROUDI[3], MUHAMMAD SAQALEIN[1, 2] and MOHSIN KHURSHID[1*]

[1] Department of Microbiology, Government College University Faisalabad, Pakistan
[2] Pet Care Clinic, Faisalabad, Pakistan
[3] Department of Medical Laboratories, College of Applied Medical Sciences, Qassim University, Qassim, Saudi Arabia

Submitted 30 December 2019, revised 26 March 2020, accepted 29 March 2020

Abstract

The carbapenem-resistant *Acinetobacter baumannii* (CRAB) has got global attention as a notorious nosocomial pathogen. This study describes a case of urinary tract infection in a 2-years old pet female cat infected with *A. baumannii*. The susceptibility profiling, screening for the resistance determinants, and the multilocus sequence typing was performed. The *A. baumannii* isolate was found to harbor the *bla*OXA23-like gene and corresponded to International clone II that has been widely reported to be involved in human infections. The study proposes that the pets may contribute towards the spread of clinically relevant antimicrobial-resistant pathogens.

K e y w o r d s: MLST, sequence types, carbapenemases, *Acinetobacter baumannii*, companion animals

Acinetobacter baumannii is the most prevalent species of genus Acinetobacter that caused various nosocomial infections in clinical settings. *A. baumannii* is quite ubiquitous and has been found in water, air, and soil. Although the studies related to the animal infections caused by *A. baumannii* are limited, the reports have highlighted the involvement of *Acinetobacter* species in respiratory, urinary, bloodstream, and wound infections with an attributable mortality of 47% in pets (Pomba et al. 2017). The therapeutic management of carbapenem-resistant *A. baumannii* (CRAB) is challenging in clinical medicine (Sohail et al. 2016; Khurshid et al. 2017). The emergence of multidrug-resistant CRAB isolates has been increasingly reported and is mainly associated with the acquisition of the *bla*NDM gene and overexpression of the *bla*OXA-23 gene in bovines and equines (Poirel et al. 2012; Smet et al. 2012; Zhang et al. 2013). However, the majority of carbapenem-resistant phenotypes in *A. baumannii* isolates from the pets are mainly linked with the increased expression of the intrinsic genes (Ewers et al. 2017).

The data regarding the mechanisms underlying the antimicrobial resistance and molecular epidemiology of *Acinetobacter* species from the veterinary origin are limited compared to the *A. baumannii* strains from humans. However, the studies have revealed that the *A. baumannii* isolates from veterinary sources may harbor identical antimicrobial resistant determinants as well as share the identical clonal lineages as human strains suggesting a common source of infection (Zordan et al. 2011; Puntener-Simmen et al. 2019). Here, we have described a CRAB isolate harboring the *bla*OXA-23 gene from a pet cat suffering from urinary tract infection.

A two-years-old pet cat was brought to our pet clinic with dysuria and hematuria. The urine sample was aseptically collected, which showed significant bacteriuria, and *A. baumannii* was solely obtained. The cat was having a history of persistent fever, pyuria, anorexia, weight loss, postural changes, and mood disorders from the last three months, which were previously attempted to treat with multiple courses of antimicrobial agents empirically. Initially, the oral amoxicillin-clavulanate

* Corresponding author: M. Khurshid, Department of Microbiology, Government College University Faisalabad, Pakistan; **e-mails: mohsin.mic@gmail.com, mohsinkhurshid@gcuf.edu.pk**

Table I
Resistance genes detected in the *A. baumannii* strain isolated in a urine sample from the urinary tract infection suffering cat.

Antibiotic category	Mechanism	Resistance associated gene	Resistance phenotypes
Aminoglycosides	16S rRNA methyltransferase genes	*armA*	Amikacin[a], Gentamicin[b], Tobramycin[b]
	Aminoglycoside modifying enzymes	*aphA6*, *aadB*, and *aacC1*	
Carbapenems	Oxacillinases	*blaOXA-23*	Imipenem[c], Meropenem[d], Ceftazidime[e], Cefotaxime[e], Ceftriaxone[e], Cefepime[f], Piperacillin-tazobactam[g], Ampicillin-sulbactam[h]
Fluoroquinolones	Quinolones Resistance Determining Region (QRDR)	*gyrA* gene mutation (Ser83Leu)	Ciprofloxacin[i]
Sulfonamides	Dihydropteroate synthase	*Sul2*	Sulfamethoxazole-Trimethoprim[j]
Tetracyclines	Tetracycline efflux MFS transporter	*tetB*	Doxycycline[k]

[a] MIC 1024 µg/ml, [b] MIC 512 µg/ml, [c] MIC 16 µg/ml, [d] MIC 32 µg/ml, [e] MIC 64 µg/ml, [f] MIC 32 µg/ml, [g] MIC 128/4 µg/ml, [h] MIC 64/32 µg/ml, [i] MIC 16 µg/ml, [j] MIC 16/304 µg/ml, [k] MIC 128 µg/ml

suspension was administered at a dose rate of 62.5 mg/cat PO twice daily for 14 days, followed by ciprofloxacin at a dose rate of 6 mg/kg PO q12h for 10 days.

The *A. baumannii* isolate was identified by amplification of the *recA* gene and ITS region in a multiplex PCR as described previously, as well as the amplification of the *bla*OXA-51 gene (Khurshid et al. 2017; Khurshid et al. 2020). The broth microdilution method was used to determine the minimum inhibitory concentrations (MICs) according to the CLSI guidelines (CLSI 2015). The genes encoding the carbapenem resistance and the presence of insertion element i.e., IS*Aba1*, were detected using PCR as described previously using specific primers (Khurshid et al. 2017). The PCR was performed to detect the presence of 16S rRNA methyltransferase genes (*arm*A, *rmt*A, *rmt*B, *rmt*C, *rmt*D, and *rmt*E) and aminoglycoside modifying enzymes (AMEs) i.e., *aphA1*, *aphA6*, *aadB*, *aadA1,* and *aacC1* and tetracycline and sulfonamide resistant genes including *tetA*, *tetB*, *sul1*, *sul2*, and *sul3* genes (Khurshid et al. 2019). The isolates were also screened for plasmid-mediated quinolone resistance genes (*qnrA*, *qnrB*, and *qnrS*) as well as mutations in the quinolone resistance-determining region by sequencing *gyrA* and *parC* gene (Gu et al. 2015). The multi-locus sequence typing (MLST) was performed using primers recommended by the MLST database for *A. baumannii* following the Pasteur scheme.

The strain was susceptible only to colistin (MIC 0.5 µg/ml), and tigecycline (MIC 1 µg/ml). The higher MICs of imipenem (MIC 16 µg/ml), meropenem (MIC 32 µg/ml), ceftazidime, cefotaxime, ceftriaxone (MIC 64 µg/ml), cefepime (MIC 32 µg/ml), piperacillin-tazobactam (MIC 128/4 µg/ml), and ampicillin-sulbactam (MIC 64/32 µg/ml) were linked with the production of *bla*OXA-23 (Opazo et al. 2012; Khurshid et al. 2017). The resistance to aminoglycoside i.e., MICs of amikacin (MIC 1024 µg/ml), gentamicin, and tobramycin (MIC 512 µg/ml) was attributed to the presence of 16S rRNA methyltransferase genes i.e., the *armA* gene as well as AMEs i.e., *aphA6*, *aadB*, and *aacC1*. Moreover, the MIC of trimethoprim-sulfamethoxazole was 16/304 µg/ml attributed to the presence of the *sul2* gene. The *A. baumannii* isolates showed resistance to tetracycline/doxycycline with a doxycycline MIC equal to 128 µg/ml, and it was related to the presence of the *tetB* gene. The strain was found resistant to ciprofloxacin (MIC 16 µg/ml), which was attributed to the mutation (Ser83Leu) in the *gyrA* gene. The genes conferring resistance to different antimicrobial agents that were found in the *A. baumannii* strain are summarized in Table I. The IS*Aba1* was found upstream to the *bla*OXA-51 and *bla*OXA-23 genes.

The concerns related to the possible threats of the *bla*OXA-23 harboring CRAB among the pets and other farm animals have been increasing (Ewers et al. 2017). The information on *A. baumannii* in veterinary settings is, however, limited, and data related to the comparison of strains isolated from the humans and veterinary sources are quite inadequate (van der Kolk et al. 2019). From Pakistan, this is the very first report of extensively drug-resistant (XDR) CRAB isolates harboring the acquired the *bla*-OXA-23 and *armA* genes from an infected pet cat, which drives the attention towards the possible transmission of these XDR pathogens from the companion animals to humans.

The *bla*OXA-23 gene is a major cause of carbapenem resistance throughout the world; therefore, it can be considered a virulence marker and is located on the chromosome as well as on the plasmids. Moreover, the studies have found a strong correlation between the occurrence of the *bla*OXA-23 gene and multidrug-resistant phenotypes (Pomba et al. 2014; Zowawi et al. 2015; Khurshid et al. 2017).

The MLST has shown that the *A. baumannii* strain belonged to the sequence type 2 (ST2), and the eBURST analysis has revealed that it corresponded to the inter-

national clonal lineage 2. The study conducted by Tada and his colleagues concluded that there is worldwide dissemination of this clone also harboring the *bla*OXA-23 and *armA* genes but does not suggest the human-to animal transmission (Tada et al. 2015). Notably, the *A. baumannii* ST2 has been extensively isolated from humans, while some of the recent reports have also indicated the presence of ST2 in pets (Puntener-Simmen et al. 2019). The carbapenem-resistant isolates in these studies were found to possess the intrinsic *bla*OXA-51 gene solely or accompanied by the acquired the *bla*OXA-23-like genes. Interestingly, the *A. baumannii* isolates were reported among the pets living in the community (Lupo et al. 2017). Although the data is quite limited regarding the carriage of *Acinetobacter* species beyond the veterinary clinical settings, more than a few studies during the recent few years have detected the *A. baumannii* isolates in the community among domestic birds, dogs, livestock, and other large animals. These studies specify that the incidence of *A. baumannii* infections among animals is increasing and these animals may serve as a reservoir for *A. baumannii*, particularly carbapenem-resistant strains, due to their selective advantage compared to the susceptible strains (Pomba et al. 2014; van der Kolk et al. 2019).

This study has reported an extensively drug-resistant *A. baumannii*, harboring the *bla*OXA-23 gene and other resistant associated genes isolated from a companion animal previously treated with multiple empirical antimicrobial courses. The infected pets may contribute to the pool of multidrug-resistant clinically relevant bacteria and their interaction with the human may transmit these pathogens to humans. The extensive epidemiological studies are essential for a better understanding of the extent of distribution, risk factors, and the directions of transmission of these multidrug-resistant strains.

ORCID

Mohsin Khurshid https://orcid.org/0000-0002-3196-2857

Funding

This work was supported by the Higher Education Commission (HEC), Pakistan grant number 5679/Punjab/NRPU/R&D/HEC/2016.

Conflict of interest

The authors do not report any financial or personal connections with other persons or organizations, which might negatively affect the contents of this publication and/or claim authorship rights to this publication.

Literature

CLSI. Performance standards for antimicrobial susceptibility testing. Twenty-Fifth Informational Supplement. Wayne (USA): Clinical and Laboratory Standard Institute; 2015.

Ewers C, Klotz P, Leidner U, Stamm I, Prenger-Berninghoff E, Göttig S, Semmler T, Scheufen S. OXA-23 and IS *Aba1* – OXA-66 class D β-lactamases in *Acinetobacter baumannii* isolates from companion animals. Int J Antimicrob Agents. 2017 Jan;49(1):37–44. https://doi.org/10.1016/j.ijantimicag.2016.09.033

Gu D, Hu Y, Zhou H, Zhang R, Chen GX. Substitutions of Ser83Leu in GyrA and Ser80Leu in ParC associated with quinolone resistance in *Acinetobacter pittii*. Microb Drug Resist. 2015 Jun; 21(3):345–351. https://doi.org/10.1089/mdr.2014.0057

Khurshid M, Rasool MH, Ashfaq UA, Aslam B, Waseem M, Xu Q, Zhang X, Guo Q, & Wang M. Dissemination of bla_{OXA-23} harboring carbapenem-resistant *Acinetobacter baumannii* clones in Pakistan. J Glob Antimicrob Resist. 2020;S2213-7165(2220):30002–30003.

Khurshid M, Rasool MH, Ashfaq UA, Aslam B, Waseem M. Emergence of IS *Aba1* harboring carbapenem-resistant *Acinetobacter baumannii* isolates in Pakistan. Future Microbiol. 2017 Nov; 12(14):1261–1269. https://doi.org/10.2217/fmb-2017-0080

Khurshid M, Rasool MH, Siddique MH, Azeem F, Naeem M, Sohail M, Sarfraz M, Saqalein M, Taj Z, Nisar MA, et al. Molecular mechanisms of antibiotic co-resistance among carbapenem resistant *Acinetobacter baumannii*. J Infect Dev Ctries. 2019 Oct 31;13(10): 899–905. https://doi.org/10.3855/jidc.11410

Lupo A, Châtre P, Ponsin C, Saras E, Boulouis HJ, Keck N, Haenni M, Madec JY. Clonal spread of Acinetobacter baumannii sequence type 25 carrying bla_{OXA-23} in companion animals in France. Antimicrob Agents Chemother. 2017 Jan;61(1):e01881–16. https://doi.org/10.1128/AAC.01881-16

Opazo A, Domínguez M, Bello H, Amyes SGB, González-Rocha G. OXA-type carbapenemases in *Acinetobacter baumannii* in South America. J Infect Dev Ctries. 2011 Dec 24;6(04):311–316. https://doi.org/10.3855/jidc.2310

Poirel L, Berçot B, Millemann Y, Bonnin RA, Pannaux G, Nordmann P. Carbapenemase-producing *Acinetobacter* spp. in cattle, France. Emerg Infect Dis. 2012 Mar;18(3):523–525. https://doi.org/10.3201/eid1803.111330

Pomba C, Endimiani A, Rossano A, Saial D, Couto N, Perreten V. First report of OXA-23-mediated carbapenem resistance in sequence type 2 multidrug-resistant *Acinetobacter baumannii* associated with urinary tract infection in a cat. Antimicrob Agents Chemother. 2014 Feb;58(2):1267–1268. https://doi.org/10.1128/AAC.02527-13

Pomba C, Rantala M, Greko C, Baptiste KE, Catry B, van Duijkeren E, Mateus A, Moreno MA, Pyörälä S, Ružauskas M, et al. Public health risk of antimicrobial resistance transfer from companion animals. J Antimicrob Chemother. 2017 Apr 1;72(4):957–968.

Püntener-Simmen S, Zurfluh K, Schmitt S, Stephan R, Nüesch-Inderbinen M. Phenotypic and genotypic characterization of clinical isolates belonging to the *Acinetobacter calcoaceticus-Acinetobacter baumannii* (ACB) complex isolated from animals treated at a veterinary hospital in Switzerland. Front Vet Sci. 2019 Feb 5;6:17. https://doi.org/10.3389/fvets.2019.00017

Smet A, Boyen F, Pasmans F, Butaye P, Martens A, Nemec A, Deschaght P, Vaneechoutte M, Haesebrouck F. OXA-23-producing *Acinetobacter* species from horses: a public health hazard? J Antimicrob Chemother. 2012 Dec 01;67(12):3009–3010. https://doi.org/10.1093/jac/dks311

Sohail M, Rashid A, Aslam B, Waseem M, Shahid M, Akram M, Khurshid M, Rasool MH. Antimicrobial susceptibility of *Acinetobacter* clinical isolates and emerging antibiogram trends for nosocomial infection management. Rev Soc Bras Med Trop. 2016 Jun;49(3):300–304. https://doi.org/10.1590/0037-8682-0111-2016

Tada T, Miyoshi-Akiyama T, Shimada K, Nga TTT, Thu LTA, Son NT, Ohmagari N, Kirikae T. Dissemination of clonal complex 2 *Acinetobacter baumannii* strains co-producing carbapenemases

and 16S rRNA methylase ArmA in Vietnam. BMC Infect Dis. 2015 Dec;15(1):433. https://doi.org/10.1186/s12879-015-1171-x

van der Kolk JH, Endimiani A, Graubner C, Gerber V, Perreten V. *Acinetobacter* in veterinary medicine, with an emphasis on *Acinetobacter baumannii*. J Glob Antimicrob Resist. 2019 Mar; 16:59–71. https://doi.org/10.1016/j.jgar.2018.08.011

Zhang WJ, Lu Z, Schwarz S, Zhang RM, Wang XM, Si W, Yu S, Chen L, Liu S. Complete sequence of the bla_{NDM-1}-carrying plasmid pNDM-AB from *Acinetobacter baumannii* of food animal origin. J Antimicrob Chemother. 2013 Jul;68(7):1681–1682. https://doi.org/10.1093/jac/dkt066

Zordan S, Prenger-Berninghoff E, Weiss R, van der Reijden T, van den Broek P, Baljer G, Dijkshoorn L. Multidrug-resistant *Acinetobacter baumannii* in veterinary clinics, Germany. Emerg Infect Dis. 2011 Sep;17(9):1751–1754. https://doi.org/10.3201/eid1709.101931

Zowawi HM, Sartor AL, Sidjabat HE, Balkhy HH, Walsh TR, Al Johani SM, AlJindan RY, Alfaresi M, Ibrahim E, Al-Jardani A, et al. Molecular epidemiology of carbapenem-resistant *Acinetobacter baumannii* isolates in the Gulf Cooperation Council States: dominance of OXA-23-type producers. J Clin Microbiol. 2015 Mar;53(3):896–903. https://doi.org/10.1128/JCM.02784-14

Polish Journal of Microbiology
2020, Vol. 69, No 2, 235–238
https://doi.org/10.33073/pjm-2020-023

SHORT COMMUNICATION

Effect of *Chlorella vulgaris* on Growth and Photosynthetic Pigment Content in Swiss Chard (*Beta vulgaris L.* subsp. *cicla*)

TIMEA HAJNAL-JAFARI*, VLADIMIRA SEMAN, DRAGANA STAMENOV and SIMONIDA ĐURIĆ

Department of Field and Vegetable Crops, Faculty of Agriculture, University of Novi Sad, Novi Sad, Serbia

Submitted 6 March 2020, revised 10 April 2020, accepted 19 April 2020

Abstract

Microalgae application in agriculture is an alternative measure that could be highly beneficial to plants. The application of microalgae *Chlorella vulgaris* S45 and its effect on plant growth and pigment content in Swiss chard were investigated. In the treatments, 5% and 10% algal suspensions were applied by spraying on plants and in soil, respectively. *C. vulgaris* S45 affected the initial growth of Swiss chard and the content of photosynthetic pigments positively. The correlation analysis proved the existence of statistically significant interdependency between chlorophyll a (Chl *a*) content and leaf number ($r = 0.876$ at $p < 0.05$), and chlorophyll b (Chl *b*) content and fresh leaf weight ($r = 0.783$ at $p < 0.05$).

Key words: Swiss chard, soil microalgae, foliar spraying, growth parameters, pigment content

One of the challenges of modern agriculture is to organize production sustainably, applying all the means that are available to farmers in order to minimize the negative influences of agrochemicals on plants and soil. Microbial formulations containing effective microorganisms (EM) with the biofertilizer or biostimulator properties could be an alternative to chemical substances used in agriculture. Many positive effects are attributed to EM. Stimulated plant growth (Ku et al. 2018), and improved plant quality (Khalid et al. 2017) have been reported. Microalgae and their positive effects on plants are getting more attention in recent years because of their multifunctionality. Green algae species (*Chlorella vulgaris, Chlorella sorokiniana,* and *Chlorella pyredoinosa*) are rich sources of proteins, lipids, carbohydrates, pigments, and other metabolites with different antimicrobial, antioxidant, and antitumor properties (Panahi et al. 2019). Moreover, microalgae are used as animal feed and human food. The application of green algae in vegetable production is also well documented (Hajnal-Jafari et al. 2016; Kim et al. 2018). Live algal cells or cell extracts are applied mostly as a soil amendment but also through seed priming or by foliar spraying (Barone et al. 2018). When applied foliarly, a thin algal biofilm is formed on the plant surface, which enables faster nutrients uptake, reduces evapotranspiration, and provides additional protection against pathogenic microorganisms and parasites (Ortiz-Moreno et al. 2019). Swiss chard (*Beta vulgaris* L. subsp. *cicla*) is a leafy vegetable very rich in vitamins K, A, and C but also in fatty acids, phospholipids, glycolipids, polysaccharides, ascorbic acid, folic acid, pectins, saponins, flavonoids, phenolic acids, and betalains (Gao et al. 2009). Swiss chard leaves contain high amounts of photosynthetic pigments such as chlorophylls and carotenoids. Their content in the plant can be enhanced through varying agricultural management practices (Barickman and Kopsell 2016). Although few pieces of researches focused on the investigation of EM application in Swiss chard (Daiss et al. 2008; Mouhamad et al. 2017), there is no information about green microalgae utilization in Swiss chard production for yield enhancement and/or quality improvement. Therefore, the aim of this research was to investigate the application of microalgae *C. vulgaris* and its effect on initial plant growth and photosynthetic pigment content in Swiss chard leaves.

The microalga *C. vulgaris* S45 (Algae Collection, Faculty of Agriculture, University of Novi Sad, Serbia), isolated from soil (Vojvodina, Serbia), was used in the research. It was cultured in liquid BG11 medium

* Corresponding author: T. Hajnal-Jafari, Department of Field and Vegetable Crops, Faculty of Agriculture, University of Novi Sad, Novi Sad, Serbia; **e-mail: mikrobiologija@polj.uns.ac.rs**

(1.5 g $NaNO_3$, 0.04 g K_2HPO_4, 0.075 g $MgSO_4 \cdot 7H_2O$, 0.036 g $CaCl_2 \cdot 2H_2O$, 0.006 g Citric acid, 0.006 g Ferric ammonium citrate, 0.001 g EDTA, 0.02 g Na_2CO_3 and 1 ml Trace metal solution) at 24°C on an orbital shaker (90 rpm) under two cold white lamps (2 × 950 Lm) and a photoperiod of 12 h light/12 h dark for two weeks. An algal culture containing 14×10^6 CFU/ml was used to prepare the treatments for the seed germination and plant fertilization experiments. The treatments were set as follows: 1) control (BG11 medium without algae – 10% (v/v) water solution); 2) 5% (v/v) algal suspension (applied by spraying on plants); 3) 10% (v/v) algal suspension (applied by spraying on plants); 4) 10% (v/v) algal suspension (applied in soil).

Swiss chard seedlings were grown on humus/sand (3:1) mixture under the controlled condition at room temperature (25 ± 2°C) and natural daylight photoperiod for two weeks. The seedlings were transplanted in pots (800 ml) with the same humus/sand (3:1) mixture. Each treatment contained four repetitions. The first application of microalgae was made one week after seedlings transplantation following the experiment scheme. The second application was performed 30 days later. Each time, 15 ml of algal inoculums were sprayed on plants or added to the soil. Seven days after the second application the plant material was collected for pigments quantification. Leaves number, leaf (stalk + leaf) length and weight, root length, and weight were counted and measured. Chlorophyll a (Chl *a*), chlorophyll b (Chl *b*), and carotenoids contents in leaves were calculated according to von Wettstein (1957). Plant samples (0.2 g) were grounded with 25 ml of 80% acetone in combination with 0.1% $CaCO_3$ to prevent chlorophyllase activity. After grinding, the samples were filtered, and the final volume (25 ml) was transferred to graduate tubes. The absorbance was read at 662, 644, and 440 nm, respectively, according to von Wettstein (1957) and Holm (1954) (Unicam SP600 spectrophotometer Series 2, Cambridge England). The pigment concentrations were calculated using von Wettstein's formula as following: Chl $a = 9.784 \times A662 - 0.99 \times A644$ Chl $b = 21.426 \times A644 - 4.65 \times A662$; Carotenoids $= 4.695 \times A440 - 0.268 \times$ (Chl $a + b$). The concentration of pigments was expressed in mg/g of fresh weight of leaves according to the following formula: mg/g = (mg/l × dilution) / (sample weight × 1,000). All the assays were performed in triplicate. The software Statistica, version 13.3 (TIBCO Software Inc.) was used for statistical analysis. The least significant difference test (Fisher LSD) and the Spearman correlation analysis were performed to compare the results between treatments.

Foliar and soil application of *C. vulgaris* S45 influenced the initial growth parameters of Swiss chard (Table I). The number of leaves per plant increased in both foliar treatments and treatment with soil application in comparison to the control. The highest number was achieved after the treatment with a 10% suspension applied foliarly. Leaf length and weight also differed significantly in treatments where algae were applied. The highest leaf length was obtained when *C. vulgaris* S45 was applied in the soil. The inoculated plants had bigger roots with an increased weight. Root length was not affected significantly by treatments.

Table II
Effect of *Chlorella vulgaris* S45 on pigment content in Swiss chard leaf (mg/g).

Treatments	Chlorophyll a	Chlorophyll b	Carotenoids
Control	0.0012^{b*}	0.3949^{c}	0.0563^{b}
5% foliar	0.0149^{c}	0.3491^{b}	0.0311^{d}
10% foliar	0.0326^{a}	0.5354^{a}	0.1033^{a}
10% soil	0.0126^{c}	0.4000^{c}	0.0488^{c}

* Different letters in subscripts indicate statistically significant difference according to the Fisher LSD test ($p < 0.05$)

C. vulgaris S45 affected the initial growth of Swiss chard positively, which is in accordance with the results of Faheed and Fattah (2008), who studied the effect of green algae on lettuce (*Lactuca sativa*) growth parameters (fresh and dry weight and shoot and root length).

The best results were achieved in treatments where *C. vulgaris* S45 were applied foliarly, particularly after the use of the 10% algal suspension. Microalgae contain different nutrients; produce secondary metabolites like hormones, enzymes, vitamins and/or pigments that could lead to significant increases in crop growth parameters, yield quantity, and its quality. When applied via foliar spraying, plants usually respond more rapidly since foliar uptake and translocation of nutrients and solutes are faster. Our results correlate with the results of Dias et al. (2016), who found positive effects of microalgae products (*Spirulina platensis*) applied on leaves of eggplant. The tomato fertilization with *Nannochloris* sp. 424 leads to better plant development and growth (Oancea et al. 2013). The authors found an increase in the plant height by more than 10% when compared to the control, also better development of root length (108.08% control), leaf number (120.31% control), and leaf area (105.16% control). The weight of fresh lettuce increased by 56.34% after foliar treatment with *C. vulgaris* (Hajnal-Jafari et al. 2016).

The soil application of *C. vulgaris* S45 affected positively the leaf length (24.76 cm) and fresh leaf weight (11.33 g/plant) as well as root length (8.46 cm) and fresh root weight (0.33 g/plant), though the increase was not statistically significant. Microalgae as soil additives can promote plant nutrition, which in turn enhances all physiological reactions that lead to enhanced growth (Faheed and Fattah 2008). In transplanted vegetable crops such as Swiss chard, the application of microalgae

Table I
Effect of *Chlorella vulgaris* S45 on the plant growth parameters.

Treatments	Leaf number	Leaf length cm	Root length cm	Fresh root weight g/plant	Fresh leaf weight g/plant
Control	5^{c*}	16.66^{c}	6.75^{ab}	8.46^{b}	0.17^{b}
5% foliar	7^{bc}	18.43^{bc}	5.36^{b}	6.87^{b}	0.14^{ba}
10% foliar	9^{a}	21.96^{ab}	7.60^{a}	13.04^{a}	0.37^{a}
10% soil	7^{bc}	24.76^{a}	8.46^{a}	11.33^{a}	0.33^{ab}

* Different letters in subscripts indicate statistically significant difference according to the Fisher LSD test ($p < 0.05$)

has particular importance since plants go through a very stressful period. The root system, after transplantation, must be provided with a sufficient supply of nutrients in order to plant development proceeds normally. Barone et al. (2019) found that soil treatment with *C. vulgaris* and their extract increased soil enzymatic activity as well as the growth of tomato plants in treated soil. The soil application of *Acutodesmus dimorphus* biomass (50 and 100 g of dry biomass per 28-cm pot) on tomato seedlings, three weeks before the seedling transplantation resulted in the increased plant growth (higher numbers of branches and flowers), compared to the non-treated control (Garcia-Gonzalez and Sommerfeld 2016).

According to the results (Table II), in Swiss chard leaves, Chl *a* content ranged from 0.0012 mg/g to 0.0326 mg/g. The highest concentration of *C. vulgaris* S45 as foliar treatment led to the highest content of Chl *a* and Chl *b* (0,0326 mg/g and 0.5354 mg/g, respectively). Our results showed higher content of Chl *b* after all treatments when compared to Chl *a* content. It could be because during the plant experiment, although conducted in controlled conditions with natural daylight photoperiod, plants were not exposed to direct sunlight. Goncalves et al. (2001) also found higher Chl *b* concentrations in tonka beans and mahogany grown in the shade. Foliar treatment with 10% algal suspension showed a significant increase in carotenoids content (0.1033 mg/g) compared to the control.

The correlation analysis proved the existence of statistically significant interdependency between Chl *a* content and leaf number ($r = 0.876$ at $p < 0.05$). High correlations were observed between Chl *b* content and leaf fresh weight leaf ($r = 0.783$ at $p < 0.05$). Carotenoids content and fresh leaf weight also correlated positively ($r = 0.720$ at $p < 0.05$)

Plant pigment content is an important quality indicator, which has a great impact on consumer selection. Chlorophylls and carotenoids accumulation is influenced not only by plant physiological, biochemical, and genetic attributes, but also by environmental factors, such as light, temperature, and fertilization (Barickman et al. 2016). Application of fresh microalgal cells increased the pigmentation (Chl *a*, Chl *b*, and carotenoids content) in Swiss chard. The results of this study comply with other studies related to biostimulants application and pigments accumulation in tomato and watermelon (Abdel-Mowgoud et al. 2010; Djuric et al. 2014). Coppens et al. (2016) recorded an increased carotenoid concentration in tomato fruits treated with dry biomass of *Nannochloropsis* spp., *Ulothrix* spp., and *Klebsormidium* spp. Seed soaking and plant treatment with different microbial consortia containing algae led to increased accumulation of chlorophylls and carotenoids in plants (Dineshkumar et al. 2018). The improved photosynthetic activity resulted in an improved yield quality. The stimulation of chlorophyll and carotenoid biosynthesis was associated with enhanced plant growth in the study with lettuce inoculated with *C. vulgaris* (Faheed and Fattah 2008). The correlation analysis showed that higher pigment content could positively influence plant growth and final yield development. The high interdependency between cotton chlorophyll content and yield parameters was also found in the research conducted by Boggs et al. (2003). Blackmer and Schepers (1995) also found a higher correlation between chlorophyll content and the maize grain yield in a later stage of development. On the other hand, Güler and Özcelik (2007) argued that lower leaf chlorophyll values in the early developmental stage of dry bean (38 days after emergence) did not mean that the final yield could be lower.

In conclusion, the results indicated that *C. vulgaris* S45 might be used as an alternative foliar fertilizer that could enhance and improve the growth of Swiss chard, especially after the use of the 10% algal suspension. The application of an appropriate microalgae formulation could be an important measure to achieve a more sustainable and eco-friendly food production.

Acknowledgments

This work was supported by the Ministry of Education, Science, and Technological Development of the Republic of Serbia (Project III 43002).

Conflict of interest

The authors do not report any financial or personal connections with other persons or organizations, which might negatively affect the contents of this publication and/or claim authorship rights to this publication.

Literature

Abdel-Mawgoud AS, Hafez MM, Habib AM. Seaweed extract improves growth, yield and quality of different watermelon hybrids. Res J Agric Biol Sci. 2010;6(2):161–168.

Barickman TC, Kopsell DA, Sams CE. Abscisic acid impacts tomato carotenoids, soluble sugars, and organic acids. HortScience. 2016 Apr;51(4):370–376. https://doi.org/10.21273/HORTSCI.51.4.370

Barickman TC, Kopsell DA. Nitrogen form and ratio impact Swiss chard (*Beta vulgaris* subsp. *cicla*) shoot tissue carotenoid and chlorophyll concentrations. Sci Hortic (Amsterdam). 2016 Jun; 204:99–105. https://doi.org/10.1016/j.scienta.2016.04.007

Barone V, Baglieri A, Stevanato P, Broccanello C, Bertoldo G, Bertaggia M, Cagnin M, Pizzeghello D, Moliterni VMC, Mandolino G, et al. Root morphological and molecular responses induced by microalgae extracts in sugar beet (*Beta vulgaris* L.). J Appl Phycol. 2018 Apr;30(2):1061–1071. https://doi.org/10.1007/s10811-017-1283-3

Barone V, Puglisi I, Fragalà F, Stevanato P, Baglieri A. Effect of living cells of microalgae or their extracts on soil enzyme activities. Arch Agron Soil Sci. 2019 Apr 16;65(5):712–726. https://doi.org/10.1080/03650340.2018.1521513

Blackmer TM, Schepers JS. Use of chlorophyll meter to monitor nitrogen status and schedule fertigation for corn. J Prod Agric. 1995;8(1):56–60. https://doi.org/10.2134/jpa1995.0056

Boggs JL, Tsegaye TD, Coleman TL, Reddy KC, Fahsi A. Relationship between hyperspectral reflectance, soil nitrate-nitrogen, cotton leaf chlorophyll and cotton yield: a step toward precision agriculture. J Sustain Agric. 2003 Jul 17;22(3):5–16. https://doi.org/10.1300/J064v22n03_03

Coppens J, Grunert O, Van Den Hende S, Vanhoutte I, Boon N, Haesaert G, De Gelder L. The use of microalgae as a high-value organic slow-release fertilizer results in tomatoes with increased carotenoid and sugar levels. J Appl Phycol. 2016 Aug;28(4):2367–2377. https://doi.org/10.1007/s10811-015-0775-2

Daiss N, Lobo MG, Socorro AR, Brückner U, Heller J, Gonzalez M. The effect of three organic pre-harvest treatments on Swiss chard (*Beta vulgaris* L. var. *cycla* L.) quality. Eur Food Res Technol. 2008 Jan;226(3):345–353. https://doi.org/10.1007/s00217-006-0543-2

Dias GA, Rocha RHC, Araújo JL, Lima JF, Guedes WA. Growth, yield, and postharvest quality in eggplant produced under different foliar fertilizer (*Spirulina platensis*) treatments. Semin Cienc Agrar. 2016 Dec 14;37(6):3893–3902. https://doi.org/10.5433/1679-0359.2016v37n6p3893

Dineshkumar R, Subramanian J, Arumugam A, Ahamed Rasheeq A, Sampathkumar P. Exploring the microalgae biofertilizer effect on onion cultivation by field experiment. Waste Biomass Valor. 2018;11:77–87. https://doi.org/10.1007/s12649-018-0466-8

Djuric M, Mladenovic J, Pavlovic R, Zdravkovic J. Application of bio-stimulator biocomplex 900 in producing tomato (*Lycopersicon Essculentum* Mill.) seedling. Acta Agric Serb. 2014;19(38):97–103. https://doi.org/10.5937/AASer1438097D

Faheed FA, Fattah ZA. Effect of *Chlorella vulgaris* as bio-fertilizer on growth parameters and metabolic aspects of lettuce plant. J Agri Soc Sci. 2008;4:165–169.

Gao ZJ, Han XH, Xiao XG. Purification and characterisation of polyphenol oxidase from red Swiss chard (*Beta vulgaris* subspecies *cicla*) leaves. Food Chem. 2009 Nov;117(2):342–348. https://doi.org/10.1016/j.foodchem.2009.04.013

Garcia-Gonzalez J, Sommerfeld M. Biofertilizer and biostimulant properties of the microalga *Acutodesmus dimorphus*. J Appl Phycol. 2016 Apr;28(2):1051–1061. https://doi.org/10.1007/s10811-015-0625-2

Gonçalves JFDC, Marenco RA, Vieira G. Concentration of photosynthetic pigments and chlorophyll fluorescence of mahogany and tonka bean under two light environments. Rev Bras Fisiol Vegetal. 2001;13(2):149–157. https://doi.org/10.1590/S0103-31312001000200004

Güler S, Özcelik H. Relationships between leaf chlorophyll and yield related characters of dry bean (*Phaseolus vulgaris* L.). Asian J Plant Sci. 2007 Apr 1;6(4):700–703. https://doi.org/10.3923/ajps.2007.700.703

Hajnal-Jafari T, Djuric S, Stamenov D. Influence of green algae *Chlorella vulgaris* on initial growth of different agricultural crops. Zb Matice Srp Prir Nauke. 2016;130(130):29–33. https://doi.org/10.2298/ZMSPN1630029H

Holm G. Chlorophyll mutations in barley. Acta Agriculturae Scandinavica. 1954 Jan;4(1):457–471. https://doi.org/10.1080/00015125409439955

Khalid M, Hassani D, Bilal M, Asad F, Huang D. Influence of biofertilizer containing beneficial fungi and rhizospheric bacteria on health promoting compounds and antioxidant activity of *Spinacia oleracea* L. Bot Stud (Taipei, Taiwan). 2017 Dec;58(1):35. https://doi.org/10.1186/s40529-017-0189-3

Kim MJ, Shim CK, Kim YK, Ko BG, Park JH, Hwang SG, Kim BH. Effect of biostimulator *Chlorella fusca* on improving growth and qualities of Chinese chives and spinach in organic farm. Plant Pathol J. 2018 Dec;34(6):567–574

Ku Y, Xu G, Tian X, Xie H, Yang X, Cao C, Chen Y. Correction: root colonization and growth promotion of soybean, wheat and Chinese cabbage by *Bacillus cereus* YL6. PLoS One. 2018 Nov 21; 13(11):e0200181. https://doi.org/10.1371/journal.pone.0200181

Mouhamad RS, Fadhel AS, Yousir ShA, Razaq IB, Iqbal M, Ayub S, Younas U. Impact of effective microorganisms actuate (EMa) on development of barley, corn and chard plants. Curr Sci Perspect. 2017;3:60–66.

Oancea F, Velea S, Fătu V, Mincea C, Ilie L. Micro-algae based plant biostimulant and its effect on water stressed tomato plants. Rom J Plant Prot. 2013;6:104–117.

Ortiz-Moreno ML, Sandoval-Parra KX, Solarte-Murillo LV. Chlorella, a potential biofertilizer? Orinoquia (Univ Tecnol Llanos Orient). 2019 Dec 16;23(2):71–78. https://doi.org/10.22579/20112629.582

Panahi Y, Yari Khosroushahi A, Sahebkar A, Heidari HR. Impact of cultivation condition and media content on *Chlorella vulgaris* composition. Adv Pharm Bull. 2019 Jun 01;9(2):182–194. https://doi.org/10.15171/apb.2019.022

von Wettstein D. Chlorophyll letale und der sub-mikroskopishe formweschselder plastiden (in German). Exp Cell Res. 1957 Jun; 12(3):427–506. https://doi.org/10.1016/0014-4827(57)90165-9

Polish Journal of Microbiology
2020, Vol. 69, No 2, 239–245

INFORMACJE Z POLSKIEGO TOWARZYSTWA MIKROBIOLOGÓW

Od ostatniej informacji o działalności Zarządu Głównego Polskiego Towarzystwa Mikrobiologów, zamieszczonej w zeszytach nr 1 z 2020 r. kwartalników *Advancements of Microbiology – Postępy Mikrobiologii* i *Polish Journal of Microbiology*, ZG PTM zajmował się następującymi sprawami:

I. Zgodnie ze Statutem PTM raz w roku odbywa się zebranie członków ZG PTM, które było planowane na 30.03.2020 r. w Warszawie. Jednakże ze względu na panującą pandemię COVID-19 zdecydowano się na przeprowadzenie Zebrania ZG PTM w formie elektronicznej. Ankietę z pytaniem dotyczącym tej formy Zebrania dostarczono e-mailowo do członków ZG PTM. Wszyscy wyrazili zgodę na zaproponowaną formę zebrania. W **Uchwale 8-2020** z dnia 13.03.2020 r. podjęto decyzję w tej sprawie.
Odbyło się pierwsze w historii PTM zebranie internetowe Zarządu Głównego PTM. Przygotowane materiały w postaci plików zostały rozesłane w 19 e-mailach do wszystkich członków ZG PTM w piątek 27.03.2020. Przyjęcie Uchwał ustalono na dzień 30.03.2020 r. Podczas Zebrania ZG PTM w formie elektronicznej poruszano następujące zagadnienia:

1. Przedstawiono informację o działalności Prezydium PTM od 25.03.2019 r. do 27.03.2020 r.
Podjęto **Uchwałę 9-2020** w sprawie akceptacji działalności Prezydium ZG PTM za oceniany okres.

2. Przedstawiono informację o Konkursie o Nagrodę Naukową Polskiego Towarzystwa Mikrobiologów im. prof. Edmunda Mikulaszka, edycja 2020. Tylko dwie osoby zgłosiły się do Konkursu: Pani mgr Karolina Furtak z Zakładu Mikrobiologii Rolniczej Instytutu Uprawy Nawożenia i Gleboznawstwa Państwowy Instytut Badawczy z Puław, która zgłosiła cykl trzech publikacji oraz Pan dr inż. Łukasz Łopusiewicz z Centrum Bioimmobilizacji i Innowacyjnych Materiałów Opatrunkowych Wydział Nauk o Żywności i Rybactwa Zachodniopomorski Uniwersytet Technologiczny w Szczecinie, który zgłosił jedną publikację. Materiały dotarły do Komisji powołanej pod przewodnictwem Pani prof. dr hab. Stefanii Giedrys-Kalemby. Zgodnie z Uchwałą 4-2020 Komisja do dnia 30.04.2020 powinna przedstawić wyniki konkursu. Szkoda, że konkurs cieszy się tak małym zainteresowaniem młodych adeptów nauki. Może mieć na to wpływ opracowany nowy Regulamin konkursu, w którym zastrzeżone jest, że konkurs dotyczy tylko członków PTM – to są nasze środki finansowe. Celowe byłoby informowanie na Zebraniach Oddziałów o Konkursie i nagrodach.

3. Podjęto **Uchwałę 10-2020** w sprawie uporządkowania listy członków zwyczajnych PTM i usunięcia z niej osób niepłacących składek członkowskich w statutowo przewidzianym terminie. W porównaniu z ubiegłym rokiem podobna jest liczba osób nieopłacających składki członkowskiej za rok 2019 r. (w 2018 r. z PTM usunięto 78 osób), pomimo przypominania o tym podstawowym obowiązku członka PTM przez OT PTM w styczniu 2020 r. i następnie dwukrotnie przez sekretariat ZG PTM w lutym i marcu b.r. Imienne listy osób usuwanych z poszczególnych Oddziałów zestawiono w załączniku do Uchwały 10-2020.

4. Podjęto **Uchwałę 11-2020** w sprawie przyjęcia nowych członków zwyczajnych. Zebrała się grupa 53 osób chętnych do przystąpienia do PTM, duża część to kandydaci do nowego Oddziału Terenowego PTM w Rzeszowie.

5. Spotykamy się z sytuacją, że osoby zaakceptowane Uchwałami PTM jako członkowie zwyczajni nie opłacają pierwszej składki członkowskiej, pomimo wyraźnej informacji, że trzeba spełnić oba warunki, aby być przyjętym do PTM. Przyjęto **Uchwałę 12-2020**, w której określono, że **deklaracja członka zwyczajnego**, zaakceptowana Uchwałą ZG PTM, której nie będzie towarzyszyć opłata składki członkowskiej wniesionej w ciągu 6 miesięcy od daty tej Uchwały, o której zawiadamiany jest kandydat na członka, **zostanie usunięta z archiwum PTM, a decyzja ZG PTM o akceptacji przyjęcia członka do PTM anulowana**. Osoba zostanie o tym fakcie poinformowana drogą elektroniczną. Wprowadzony zostanie odpowiedni zapis w formularzu.

6. Zgodnie z uchwalonym Regulaminem wydatkowania i rozliczania środków pieniężnych przez Oddziały Terenowe PTM, została przekazana informacja o udostępnianiu Oddziałom Terenowym PTM od stycznia 2019 r., na pokrycie kosztów prowadzenia działalności statutowej przez ten Oddział, 10% kwoty uzyskanej z tytułu składek członkowskich oraz 50% kwoty uzyskanej z tytułu pozyskania sponsora, Członka Wspierającego PTM, darowizny, lub innej dodatkowej kwoty, na rzecz PTM, przez dany Oddział. Przedstawiono Tabelę dotyczącą liczby członków w Oddziałach oraz Tabelę przyznanych Oddziałom środków finansowych w 2020 r. oraz w roku poprzednim.
Jednocześnie zauważamy pojawiający się problem kumulacji środków niewykorzystywanych przez Oddziały. Musimy tę sprawę uregulować, ponieważ za kilka lat może pojawić się problem, że w jednym roku kilka Oddziałów będzie chciało wykorzystać swoje nagromadzone fundusze, a wtedy budżet PTM tego może nie udźwignąć. Poprosiliśmy wszystkich członków ZG PTM o zastanowienie się nad rozwiązaniem tego problemu, przekazaniem swoich uwag i ewentualne propozycje aneksu do Regulaminu. Sprawa ta powinna zostać uregulowana w najbliższym czasie.

7. Przekazano informację o stanie finansowym PTM. Załączono bilans PTM za 2019 r. przygotowany przez Panią księgową PTM oraz Uchwałę Głównej Komisji Rewizyjnej (GKR) o zatwierdzeniu sprawozdania finansowego PTM za okres 2019 r. Sytuacja finansowa Towarzystwa jest stabilna.

8. Zgodnie ze Statutem PTM Główna Komisja Rewizyjna PTM powinna działać na podstawie swojego Regulaminu. Regulaminu takiego nie było. Członkowie GKR PTM opracowali roboczą wersję Regulaminu działalności GKR, tekst został oceniony przez członków Prezydium PTM oraz Kancelarię Prawną. **Uchwałą 13-2020** ZG PTM zaakceptował Regulaminu GKR do stosowania od 2020 r. Ostateczne zatwierdzenie Regulaminu GKR odbędzie się na Walnym Zgromadzeniu Delegatów PTM podczas XXIX Zjazdu PTM.

9. Dosyć bolesna dla Towarzystwa jest sprawa likwidacji Oddziału Terenowego PTM w Puławach. Liczba członków w Oddziale znacząco spadła, Zarząd Oddziału nie jest kompletny. Pan prof. Grzegorz Woźniakowski Przewodniczący Oddziału PTM w Puławach nie widzi możliwości funkcjonowania Oddziału zgodnie ze Statutem PTM i przekazał pismo, z prośbą o likwidację Oddziału. Członkowie Oddziału w Puławach, zgodnie z pismem Zarządu OT PTM, zostaną włączeni do Oddziału w Lublinie.
Podjęto **Uchwałę 14-2020** o rozwiązaniu Oddziału Terenowego w Puławach.

10. Mamy także bardzo pozytywną informację. Pan dr Mariusz Worek z Klinicznego Szpitala Wojewódzkiego Nr 1 im. Fryderyka Chopina w Rzeszowie, Podkarpackie Centrum Chorób Płuc, Kliniczny Zakład Diagnostyki Laboratoryjnej, Regionalne Referencyjne Laboratorium Prątka Gruźlicy w województwie podkarpackim, zwrócił się do ZG PTM z prośbą o powołanie Oddziału Terenowego PTM w Rzeszowie. Pan doktor przekazał deklaracje członkowskie około 50 osób, które wyraziły chęć przystąpienia do nowego Oddziału Terenowego PTM. Z bardzo dużym zadowoleniem witamy tą cenną inicjatywę i życzymy powodzenia i sukcesów w działalności nowego Oddziału Terenowego PTM w Rzeszowie. Przyjęto **Uchwałę 15-2020** o powołaniu Oddziału Terenowego PTM w Rzeszowie.

11. Przedstawiono sprawozdania Zarządów Oddziałów Terenowych za okres od 25.03.2019 r. do 27.03.2020 r. oraz informacje o czynionych staraniach w celu pozyskania środków finansowych na XXIX Zjazd PTM, a także o planach Oddziałów na przyszłość.

12. Przedstawiono sprawę organizacji XXIX Zjazdu PTM w Warszawie, 15–18 wrzesień 2020 r. Została otwarta strona Zjazdu: www.zjazdptm2020.pl. Uruchomiony został również system rejestracyjny i system zgłaszania wykładów, doniesień ustnych, plakatów. Utworzono plan ramowy Zjazdu i określono sesje tematyczne z przyporządkowanymi osobami odpowiedzialnymi za organizacje tych sesji. Wszyscy członkowie ZG PTM oraz kilka osób zaproszonych, członków PTM, będzie pełniło funkcje przewodniczących i wiceprzewodniczących Sesji. Oczekujemy aktywnego włączenia się Oddziałów zarówno w organizacje Sesji, jak i poszukiwanie sponsorów i wystawców na Zjazd. Planujemy wykładowców do sesji plenarnych, którymi chcielibyśmy, aby byli Członkowie Honorowi PTM oraz laureaci dwóch konkursów o Nagrodę Naukową Polskiego Towarzystwa Mikrobiologów im. prof. Edmunda Mikulaszka, edycje 2018 i 2020. Zwracamy uwagę na fakt, że Ogólnopolski Zjazd PTM jest organizowany co 4 lata i jest to największe wydarzenie w tym okresie związane z mikrobiologią. Obecny Zjazd organizowany jest po raz pierwszy przez członków ZG PTM i wszyscy powinni być zaangażowani w to wydarzenie. Prosimy się zastanowić, nad ewentualnymi kandydatami na nowych Członków Honorowych PTM. Najlepiej aby kandydatury członków PTM zasłużonych dla mikrobiologii i naszego Towarzystwa ustalić przed Zjazdem. Można będzie wtedy przy-

gotować dyplomy i wręczyć je na Zjeździe. Na razie zakładamy, że nasz Zjazd odbędzie się w określonym miejscu i terminie, dlatego też działamy przy jego organizacji. Nie wiemy jednak jak rozwinie się pandemia COVID-19 i czy Zjazd się odbędzie. Wiele osób zwłaszcza diagnostów laboratoryjnych i osób pracujących w laboratoriach medycznych zaangażowanych jest obecnie w walkę z koronawirusem SARS-CoV-2 i nie ma czasu, aby zajmować się Zjazdem – prowadzić badania, przygotowywać streszczenia zjazdowe. Mamy też poważne trudności z pozyskaniem środków finansowych na Zjazd, bo wiele firm walczy o przetrwanie w tym trudnym dla siebie okresie.
Bierzemy pod uwagę możliwość przełożenia Zjazdu na wrzesień 2021 r., a także odpowiednie przedłużenie kadencji obecnych władz PTM zarówno ZG jak i Oddziałów oraz kadencji wybranych Delegatów PTM na WZD PTM.
Rzeczywistość przekroczyła nasze wyobrażenie jakie mieliśmy przygotowując Statut PTM i nie przewidziano takiej nadzwyczajnej sytuacji jak pandemia COVID-19.
Będziemy Państwa informować o ewentualnej decyzji o przesunięciu daty organizacji Ogólnopolskiego XXIX Zjazdu PTM.

13. Przekazano informacje z FEMS i IUMS. Federacja FEMS przyznała dofinansowanie do: XXIX Zjazdu PTM 2020 w wysokości 3 000 Euro oraz do I Polish Yeast Conference w wysokości 2 000 Euro. Ponadto FEMS przyznała granty na realizację projektów
* „Siderophores and biosurfactants produced by Antarctic psychrotolerant bacteria as new bioproducts for cold-active biotechnologies – identification and characterisation of novel secondary metabolites" złożonego przez Pana Michała Styczyńskiego z Wydziału Biologii UW;
* „Susceptibility profiling of Mycobacterium tuberculosis isolates from Poland and Lithuania", złożonego przez Panią Zofię Bakułę z Wydziału Biologii UW.
W przyszłym roku FEMS organizuje 9th Congress of European Microbiologists w dniach 11–15 lipca 2021 w Hamburgu, Niemcy (https://fems2021.org/).
* Federacja IUMS organizuje kongres IUMS w dniach 12–16 października 2020 r. w Daejon w Korei Południowej (https://www.iums2020.org/).

14. Omówiono sprawę nadawania punktów edukacyjnych na zebraniach Oddziałów PTM w stanowisku Komisji PTM, do określania zasad przyznawania punktów edukacyjnych za uczestnictwo w zebraniach i seminariach organizowanych przez Oddziały PTM, powołanej Uchwałą 10-2019. Polskie Towarzystwo Mikrobiologów, jako Towarzystwo Naukowe, zgodnie z Rozporządzeniem Ministra Zdrowia z dnia 24 lipca 2017, może przyznać diagnostom laboratoryjnym za udział w spotkaniach naukowo-szkoleniowych co najwyżej 2 miękkie punkty edukacyjne, za wygłoszenie wykładu – 10 punktów edukacyjnych (miękkich). Możliwość przyznania tzw. punktów twardych za udział w spotkaniach organizowanych przez Towarzystwo wymaga nawiązania współpracy PTM z akredytowanymi jednostkami szkolącymi oraz poniesienia przez diagnostów laboratoryjnych dodatkowych kosztów wskazanych przez te jednostki. Zarząd Główny Polskiego Towarzystwa Mikrobiologów sposób przydzielania punktów edukacyjnych pozostawia w gestii Oddziałów Terenowych.

15. Na zeszłorocznym zebraniu ZG PTM przedstawiono sprawę nieetycznego postępowania, członka zwyczajnego PTM, samodzielnego pracownika nauki i nauczyciela akademickiego, kierownika Zakładu na Warszawskim Uniwersytecie Medycznym, polegającego na przepisywaniu materiałów z 11 prac magisterskich do 21 publikacji współautorstwa opiekunki tych prac magisterskich, bez jakiegokolwiek zaznaczenia udziału magistranta w publikacjach. Najwyższa rangą w naszym kraju Komisja ds. Etyki w Nauce PAN, uznała takie postępowanie za niedopuszczalne i naganne. **Zgodnie z zapisem w Statucie PTM par. 15, ust. 1, p. 4 , za „czyny nie licujące z godnością członka Towarzystwa" można wykluczyć członka PTM z Towarzystwa.** Po dyskusji na ubiegłorocznym zebraniu ZG PTM, zdecydowano, aby wobec braku Komisji Dyscyplinarnej w Statucie PTM, powołać Uchwałą 12-2019 specjalną Komisję ds. etyki członków PTM, która będzie wydawała opinie do podejmowanych Uchwał przez ZG PTM w zgłaszanych sprawach. Z Komisji został wyłoniony zespół do oceny obecnej sprawy, który pod przewodnictwem Pani prof. dr hab. Stefanii Giedrys-Kalemby ze Szczecina przygotował opinię w oparciu o dostarczone materiały. Na podstawie przygotowanej opinii Komisji ds. etyki członków PTM oraz 13 załączników w tym opinii prawnej, **Uchwałą 16-2020** wykluczono członka zwyczajnego Oddziału Terenowego PTM w Warszawie z Polskiego Towarzystwa Mikrobiologów **za czyny nie licujące z godnością członka Towarzystwa**".
Skala nieetycznego postępowania pracownika naukowego i nauczyciela akademickiego, członka PTM, jak i podjęta Uchwała 16-2020 mają charakter bezprecedensowy.

16. Sprawa zmiany sekretarki w biurze ZG PTM. Ze względu na zaawansowaną już ciążę i zwolnienie lekarskie Pani Karoliny Pawłowskiej, dotychczasowej sekretarki biura PTM, zaproponowano, aby od kwietnia br. obowiązki sekretarki przejęła Pani Monika Kucharska, która już pełniła tę funkcje na początku naszej kadencji w latach 2016–2017. Przyjęto **Uchwałę 17-2020** w tej sprawie.

17. Przedstawiono pomysł Przewodniczącego Zarządu Oddziału PTM w Warszawie dotyczący tworzenia logotypów i osobnych stron internetowych Oddziałów Terenowych PTM. Zbieramy opinie w tej sprawie.

18. Zamieszczono informacje Redakcji o wydawanych czasopismach PTM – *Advancements of Microbiology – Postępy Mikrobiologii* i *Polish Journal of Microbiology.*
Prosiliśmy o zastanowienie się członków ZG PTM nad kierunkiem rozwoju i sposobem wydawania kwartalnika PTM *Postępy Mikrobiologii* w przyszłości i przedstawienie swoich opinii.

Naświetlenie sytuacji

Jak informowano na zebraniach ZG PTM w 2017 i 2018 r., a także w 2019 r., wydawanie czasopism PM i PJM przynosi Towarzystwu istotne straty finansowe.
Aby temu zaradzić w pierwszym etapie zdecydowano znacznie ograniczyć wydawanie papierowej edycji zeszytów czasopism oraz ich wysyłkę do członków PTM.
W drugim etapie rozważano możliwości upublicznienia i umiędzynarodowienia obu czasopism, co miało zaowocować zwiększeniem cytowalności (przez autorów zagranicznych), tym samym zwiększeniem wartości współczynników IF i MNiSW (opartych na cytowalności), a w końcowym efekcie możliwości podniesienia opłat za publikacje artykułów w czasopismach, tak aby osiągnąć samofinansowanie się czasopism. Ta polityka wydaje się sprawdzać w przypadku czasopisma PJM.
Poczynając od 2017 r. gdy wygasła umowa z firmą wydawniczą Index Copernicus, członkowie Prezydium ZG PTM z Warszawy wraz z członkami redakcji PM i PJM starali się wypracować optymalne rozwiązanie dla poprawienia sytuacji finansowej czasopism. W ciągu dwóch lat nastąpiły zmiany członków redakcji PJM. Obecnie w celu ograniczenia kosztów redakcja PJM pracuje w dwu osobowym składzie. Nawiązano kontakt z firmą Exeley z Nowego Jorku, która obiecywała duże wsparcie w wydawaniu i upublicznianiu czasopism, co miało podnieść ich pozycje w rankingach. Podpisano umowy trzyletnie dotyczące wydawania PJM od 2018 r. oraz wydawania PM od 2019 r. na platformie Exeley. Wdrożenie nowej formy wydawniczej wiązało się z bardzo dużą pracą zespołów redakcyjnych. Zwłaszcza opanowanie systemu wydawniczego Editorial Manager i przygotowanie go do obecnej funkcjonalności przez dwu osobowy zespół PJM, wymagało dużego zaangażowania i czasu. Również współpraca z firmą Exeley nie jest idealna i nie spełniła wszystkich naszych oczekiwań.
Towarzystwo realizując zamiar podniesienia rangi czasopism wydawanych przez PTM wystąpiło w 2017 r. do MNiSW z wnioskiem o dofinansowanie wydawania obydwu czasopism i tłumaczenia artykułów na język angielski w PM. Otrzymaliśmy dwuletnie dofinansowanie (2018–2019), które skończyło się w ubiegłym roku, ale zaowocowało wydaniem kilku zeszytów PM w dwóch wersjach językowych polskiej i angielskiej. Skorygowano tytuł PM, tak aby był rozpoznawalny za granicą – *Advancements of Microbiology.* Było to spowodowane przekonaniem, że żaden autor zagraniczny nie będzie wysyłał manuskryptu do czasopisma o polskim tytule. Rozpropagowywano informacje o możliwości publikowania artykułów przez autorów zagranicznych w PM, a także starano się pozyskiwać recenzentów zagranicznych. Taki proces jest długotrwały, zanim zacznie przynosić efekty. Jak podaje Redakcja PM dopiero teraz zaczęły docierać artykuły zagranicznych autorów. Zróżnicowano opłaty za publikowanie manuskryptów w PM tylko w języku polskim (wyższa cena) i angielskim lub w wersji dwujęzycznej (niższa cena), co ma zdopingować autorów do tekstów angielskojęzycznych. Tylko zwiększając krąg czytelników można zwiększyć cytowalność artykułów, a to przekłada się na ocenę czasopisma.
Ze względu na wydawanie artykułów w języku polskim i niską cytowalność PM w ubiegłym roku został wykluczony z bazy Scopus. Zmniejszenie liczby artykułów w języku angielskim może w końcowym efekcie spowodować obniżenie oceny PM i utratę współczynnika IF, co skończy się fatalnie, bo niewiele osób będzie wtedy chciało publikować w PM. Z taką sytuacją obecnie boryka się kwartalnik *Medycyna Doświadczalna i Mikrobiologia*, który choć przyjmuje artykuły eksperymentalne i przeglądowe w języku angielskim, to niewiele osób chce w nim publikować ze względu na brak współczynnika IF, chociaż czasopismo ma 20 punktów MNiSW. W ubiegłym roku ukazały się tylko 2 zeszyty MDiM.

Nieźle sobie chyba radzi kwartalnik *Postępy Higieny i Medycyny Doświadczalnej*, publikujący w podobny sposób jak MDiM, ale będąc wyżej notowanym w rankingach i posiadając współczynnik IF, może pozwolić sobie na pobieranie opłaty 1100 zł + VAT. Podobna opłata dla członków PTM (350 USD + VAT) dotyczy artykułów zamieszczanych w PJM. Ale dla autorów nie należących do PTM, publikujących w PJM to już 700 USD + VAT, co pozwala na znaczne obniżenie kosztów wydawania czasopisma. Na brak manuskryptów redakcja PJM nie narzeka. Mamy nadzieję, że w przyszłym roku PJM będzie już czasopismem samofinansującym się.

Redakcja PM oraz Zarząd Oddziału Warszawskiego PTM skierowały pisma do ZG PTM w trosce o przyszłość PM i rozważenia „wiodącej, jeśli nie wyłącznej roli języka polskiego w publikacjach czasopisma *Postępy Mikrobiologii*". Członkowie PTM muszą się nad tą sprawą zastanowić. Będziemy zbierać opinie na ten temat, ale wydaje się jednak, że konieczne jest czynienie dużych wysiłków w celu upublicznienia i umiędzynarodowienia czasopisma, co mogłoby w pewnej perspektywie przynieść korzyści w postaci podniesienia pozycji PM w rankingach i zmniejszenia strat ponoszonych przez PTM.

II. W związku z trwającą pandemią COVID-19, brakiem możliwości przewidzenia jej przebiegu w tym roku oraz niebezpieczeństwem zakażenia, związanym ze zgromadzeniem dużej liczby osób, a także zaangażowaniem osób pracujących w laboratoriach diagnostycznych, mikrobiologicznych, zespołach naukowych oraz firmach działających w obszarze mikrobiologicznym na walkę z SARS-CoV-2, niezbędne wydaje się podjęcie decyzji o przesunięciu terminu naszego Ogólnopolskiego XXIX Zjazdu PTM na wrzesień 2021 r. Zmiana terminu dotyczy również Walnego Zgromadzenia Delegatów PTM oraz wyborów nowych Władz PTM. W związku z powyższym przedłużeniu do września 2021 r. ulega kadencja Władz PTM na wszystkich szczeblach, tj. Prezesa PTM razem z Prezydium PTM i Zarządem Głównym PTM, Głównej Komisji Rewizyjnej PTM, Zarządów Oddziałów Terenowych PTM, Komisji Rewizyjnych OT PTM, oraz Delegatów poszczególnych OT PTM wybranych na kadencję 2016–2020.

W dniu 20.04.2020 r w drodze elektronicznej Zarząd Główny PTM podjął **Uchwałę 18-2020** w sprawie przesunięcia terminu Ogólnopolskiego XXIX Zjazdu PTM na wrzesień 2021 r. oraz przedłużenia o rok kadencji Władz PTM na wszystkich szczeblach, a także kadencji Delegatów PTM na Walne Zgromadzenie Delegatów PTM.

III. Prezydium ZG PTM podjęło **Uchwałę 19-2020 w sprawie przyznania Nagród Naukowych PTM im. Prof. Edmunda Mikulaszka za prace opublikowane w latach 2018–2019.** Do Nagrody Naukowej PTM im. prof. Edmunda Mikulaszka zgłosiło się dwoje kandydatów. Komisja Konkursowa pod przewodnictwem Pani prof. dr hab. Stefanii Giedrys-Kalemby postanowiła przyznać:

- **nagrodę I stopnia (5.000 zł) dla mgr biot. Karoliny Furtak** za cykl 3 prac: (**1). Furtak K.**, Grządziel J., Gałązka A., Niedźwiecki J. (2020): Prevalence of unclassified bacteria in the soil bacterial community from floodplain meadows (fluvisols) under simulated flood conditions revealed by a metataxonomic approach. Catena, 188, 104448; doi: 10.1016/j.catena.2019.104448 (IF = 3,851; 140 pkt. MNiSW); (**2). Furtak K.,** Grządziel J., Gałązka A., Niedźwiecki J. (2019): Analysis of soil properties, bacterial community composition, and metabolic diversity in fluvisols of a floodplain area. Sustainability, 11, 14, 3929; doi:10.3390/su11143929 (IF = 2,592; 70 pkt. MNiSW); (**3). Furtak K.**, Gałązka A., Niedźwiecki J. (2020): Changes in soil enzymatic activity caused by hydric stress. Polish Journal of Environmental Studies, 29, 4, 1–8; ISSN 1230-1485; doi: https://doi.org/10.15244/pjoes/112896 (IF = 1,186; 40 pkt. MNiSW);
- **nagrodę II stopnia (3.000 zł) dla dr inż. Łukasza Łopusiewicza** za pracę: **Ł. Łopusiewicz**, E. Drozłowska, P. Siedlecka, M. Mężyńska, A. Bartkowiak, M. Sienkiewicz, H. Zielińska-Bliźniewska, P. Kwiatkowski (2019) Development, characterization, and bioactivity of non-dairy kefir-like fermented beverage based on flaxseed oil cake. Food, 8, 554 (IF = 3,011; 70 pkt. MNiSW).

Gratulujemy laureatom, którzy przedstawią swoje prace na XXIX Zjeździe PTM.
Zachęcamy młodych adeptów nauki do bardziej licznego starania się o Nagrodę Naukową PTM im. Prof. Edmunda Mikulaszka za prace opublikowane w latach 2020–2021.

IV. Prezydium ZG PTM w dniu 08.05.2020 r. podjęło **Uchwałę 20-2020** o organizacji **Ogólnopolskiego XXIX Zjazdu PTM w terminie 14–17 września 2021 r. w Sangate Airport Hotel w Warszawie.** Mamy nadzieję, że do tak odległego terminu, pandemia COVID-19 zostanie opanowana i będzie wystarczająco czasu aby przygotować prezentacje na Zjazd oraz pozyskać środki finansowe na jego organizację.

V. PTM podpisało umowę „Agreeement for Full Participation of *Polish Journal of Microbiology* in NIH PubMed Central Archive" dotyczącą indeksowania PJM w bazie PubMed, co jest bardzo ważne dla wizualizacji i indeksacji naszego kwartalnika.
Dnia 05.06.2020 r. otrzymaliśmy wiadomość, że **Polish Journal of Microbiology** znalazł się w bazie PubMed Central po adresem: https://www.ncbi.nlm.nih.gov/pmc/journals/3847/

VI. Członkowie ZG PTM w stanowisku z dnia 22.04.2020 r. nie zaakceptowali pomysłu Przewodniczącego Oddziału Terenowego PTM w Warszawie, aby Oddziały utworzyły swoje osobne strony internetowe i opracowały swoje logotypy, wychodząc z założenia, że PTM jest jednolitym stowarzyszeniem posiadającym swoją stronę internetową i podstrony dla wszystkich Oddziałów oraz logotyp PTM wyłoniony w konkursie zorganizowanym kilka lat temu.

VII. Polskie Towarzystwo Mikrobiologów wyrażało swoje opinie dla Krajowej Rady Diagnostów Laboratoryjnych w sprawie testów genetycznych służących do wykrywania wirusa SARS CoV-2 i testów serologicznych do wykrywania przeciwciał dla tego wirusa.

VIII. Organizatorzy kongresu IUMS, 12–16 października 2020 r. w Daejon w Korei Południowej przesunęli terminy: przesłania abstraktów – do 30.06.2020 r. oraz wczesnej rejestracji – do 31.07.2020 r.

IX. Zmieniono formę dorocznego spotkania przedstawicieli europejskich towarzystw mikrobiologicznych FEMS Council 2020. Odbędzie się ono 04.09.2020 r. (13:00-15:00) on-line.

X. W dniu 08.06.2020 r. odbyło się wirtualne spotkanie członków Komitetu Organizacyjnego XXIX Zjazdu PTM. Omawiano sprawy:
1) pozyskiwania środków finansowych (zdecydowano podpisać umowę z MNiSW dotyczącą dofinansowania organizacji Zjazdu na kwotę 70 000 zł – występowaliśmy o 300 000 zł),
2) zaangażowania firm mogących wspierać logistycznie organizację Zjazdu,
3) zdecydowano popierać i udzielać patronatu konferencjom mikrobiologicznym organizowanym w 2021 r. w innym terminie niż XXIX Zjazd PTM. Jednocześnie prosimy wszystkie Zarządy OT PTM oraz wszystkich członków PTM o nieorganizowanie konferencji mikrobiologicznych w planowany terminie naszego Zjazdu PTM, to jest 14–17.09.2021.

XI. Zwróciliśmy się do kancelarii prawnej w sprawie opinii na temat poprawności Uchwały ZG PTM nr 18-2020 dotyczącej przesunięcia terminu Ogólnopolskiego XXIX Zjazdu PTM na wrzesień 2021 r. oraz przedłużenia o rok kadencji Władz PTM na wszystkich szczeblach, a także kadencji Delegatów PTM na Walne Zgromadzenie Delegatów PTM. O ile sprawa przesunięcia terminu Zjazdu jest poprawna pod względem prawnym, to „przedłużenie o rok kadencji Władz PTM na wszystkich szczeblach, a także kadencji Delegatów PTM na Walne Zgromadzenie Delegatów PTM" wymaga innego niż Uchwala ZG PTM trybu postępowania. Zgodnie z opinią prawną, kadencja władz wszystkich stowarzyszeń w Polsce, w tym PTM, zostaje wydłużona w drodze Ustawy z dnia 04.06.2020 r. (Czwarta Tarcza), a nie decyzją ZG PTM. Według tej Ustawy wybór władz stowarzyszenia na nową kadencję musi być dokonany w terminie do 60 dni od dnia odwołania stanu zagrożenia epidemicznego lub stanu epidemii.

XII. Na dzień 1 maja 2020 r. nasze Towarzystwo liczy 924 członków. Najliczniejsze oddziały terenowe, grupujące ponad 100 członków, to OT Warszawa i OT Kraków.

Warszawa, 10.06.2020 r.

SEKRETARZ
Polskiego Towarzystwa Mikrobiologów
dr hab. n. farm. Agnieszka E. Laudy

PREZES
Polskiego Towarzystwa Mikrobiologów
prof. dr hab. Stefan Tyski

CZŁONKOWIE WSPIERAJĄCY PTM

Członek Wspierający PTM – Złoty
od 27.03.2017 r.

HCS Europe – Hygiene & Cleaning Solutions
ul. Warszawska 9a, 32-086 Węgrzce k. Krakowa
tel. (12) 414 00 60, 506 184 673, fax (12) 414 00 66
www.hcseurope.pl

Firma projektuje profesjonalne systemy utrzymania czystości i higieny dla klientów o szczególnych wymaganiach higienicznych, m.in. kompleksowe systemy mycia, dezynfekcji, osuszania rąk dla pracowników służby zdrowia, preparaty do dezynfekcji powierzchni dla służby zdrowia, systemy sterylizacji narzędzi.

Członek Wspierający PTM – Srebrny
od 12.09.2017 r.

Firma Ecolab Sp. z o.o. zapewnia: najlepszą ochronę środowiska pracy przed patogenami powodującymi zakażenia podczas leczenia pacjentów, bezpieczeństwo i wygodę personelu, funkcjonalność posiadanego sprzętu i urządzeń.
Firma jest partnerem dla przemysłów farmaceutycznego, biotechnologicznego i kosmetycznego.

Członek Wspierający PTM – Zwyczajny
od 12.09.2017 r.

Firma Merck Sp. z o.o. jest częścią międzynarodowej grupy Merck KGaA z siedzibą w Darmstadt, Niemcy i dostarcza na rynek polski od roku 1992 wysokiej jakości produkty farmaceutyczne i chemiczne, w tym podłoża mikrobiologiczne.

Członek Wspierający PTM – Zwyczajny
od 06.06.2019 r.

Firma BART jest producentem i dystrybutorem surowców oraz dodatków dla przemysłu spożywczego i farmaceutycznego.
Specjalizujemy się w probiotykach oraz surowcach uzyskiwanych metodami biotechnologicznymi.
Współpracujemy z renomowanymi producentami: Probiotical, Gnosis, Lesaffre.